L4018/GWM I

Groundwater Modelling

September 2000 G.H.P. Oude Essink

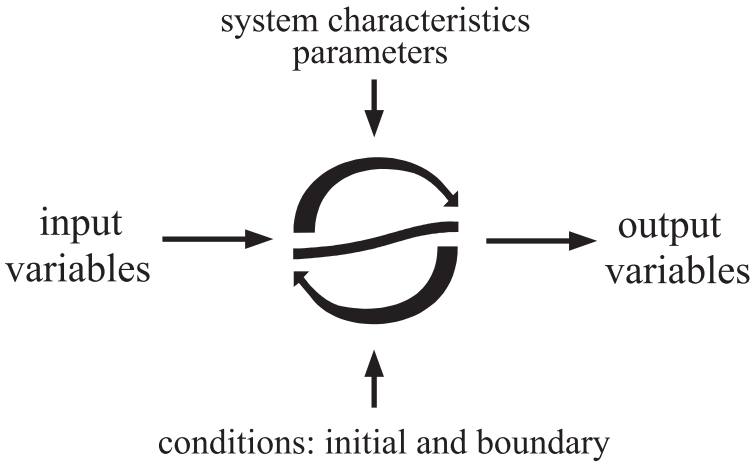

Utrecht University
Interfaculty Centre of Hydrology Utrecht
Institute of Earth Sciences
Department of Geophysics

f. 15,-

Contents

General introduction

The development of models has been the direct outcome of the need to integrate our existing theories with all physical and measured data. The key factor in this development is the (still ongoing) breakthrough in computation technologies, because it is the digital computer which is capable to store, to manipulate data and to execute complex calculations beyond the physical ability of man, yet within his mental capacity. In order to avoid that you, as a hydrogeologist-in-spe, will get stranded in the fine art of modelling, these lecture notes[1] are written to show you some ropes in the fantastic, tempting, and yet creepy world of groundwater modelling.

The presence course, which comes under the ICHU[2], is called Groundwater Modelling I. The aim of this course is to gain more insight in the behaviour of groundwater processes, quantitatively as well as qualitatively, by means of numerical modelling. These lecture notes are divided into two parts:

I. Modelling protocol
: in this part, the procedure of modelling hydrologic processes is described. A hydrogeologist should advance this procedure, from coping with a hydrological problem towards solving the problem by means of (numerical) modelling, while skipping all kinds of traps on the track; and

II. Groundwater modelling
: in this part, features of groundwater flow and solute transport are considered and numerical solution techniques of partial differential equations are discussed. Moreover, some groundwater computer codes will be treated.

During the computer practicals, attention will be paid to the modelling of standard problems by means of the codes MODFLOW and MOC(3D). Primarily knowledge should comprise basic knowledge on hydrogeologic processes such as the Darcy equation and stationary groundwater flow; as well as basic knowledge on discretisation techniques such as Taylor series and simple numerical solution techniques. For students of the Department of Physical Geography, it is strongly recommended to have followed Groundwaterhydrology (HYDB). For all students, the lectures Hydrological Transport Processes (L3041/KHTP) are also recommended.

Gualbert Oude Essink, September 2000
g.oude.essink@geo.uu.nl

[1] Parts of these lecture notes are based on the lecture notes Hydrological models (f15D) of the Delft University of Technology (Oude Essink, G.H.P., Rientjes, T. & R.H. Boekelman, 1996).

[2] The Interfacultair Centrum voor Hydrologie Utrecht (ICHU) is a centre which provides a so-called study-path Hydrologie to students from the Faculty of Earth Sciences and Department of Physical Geography.

æ

Part I

Modelling Protocol

Chapter 1

Introduction

1.1 Historical developments towards hydrologic modelling

The science of hydrology began with the conceptualisation of the hydrologic cycle. Much of the speculations of the Greek philosophers was scientifically unsound. Nonetheless, some of them correctly described some aspects of the hydrologic cycle. For example, Anaxagoras of Clazomenae (500-428 B.C.) formed a primitive version of the hydrologic cycle (e.g. the sun lifts water from the sea into the atmosphere). Another Greek philosopher, Theophrastus (circa 372-287 B.C.) gave a sound explanation of the formation of precipitation by condensation and freezing. Meanwhile, independent thinking occurred in ancient Chinese, Indian and Persian civilizations.

During the Renaissance, a gradual change occurred from purely philosophical concepts of hydrology toward observational science, e.g. by Leonardo da Vinci (1452-1519). Hydraulic measurements and experiments flourished during the eighteenth century, when Bernoulli's equation and Chezy's formula were discovered. Hydrology advanced more rapidly during the nineteenth century, when Darcy developed his law of porous media flow in 1856 and Manning proposed his open-channel flow formula (1891).

However, quantitative hydrology was still immature at the beginning of the twentieth century. Gradually, empiricism was replaced with rational analysis of observed data. For example, Sherman devised the unit hydrograph method to transform effective rainfall to direct runoff (1932) and Gumbel proposed the extreme value law for hydrological studies (1941). Like many sciences, hydrology was recognized only recently as a separate discipline (e.g. in 1965, the US Civil Service Commission recognized a hydrologist as a job classification).

Over the last decades, the subject of interest from society to hydrology gradually changed. Some two decades ago, the main subject was of a quantitative nature: how much water is available, how much can be extracted, what are the effects on piezometric heads, etc. Nowadays, also the qualitative aspect of water becomes more and more important, such as pollution of surface water and groundwater by acid rain (e.g. due to agricultural and industrial activities).

The spectacular boom in computer possibilities during recent times (viz. decades and especially the last years) makes hydrologic analysis possible on a larger scale. Figure 1.1 shows that the improvements of desktop computer systems are outstanding. As a result, hydrologists have analysed problems in more detail and with shorter computation intervals than before. Complex theories describing hydrologic processes have been applied using computer simulations. Also interactions between surface water systems and groundwater

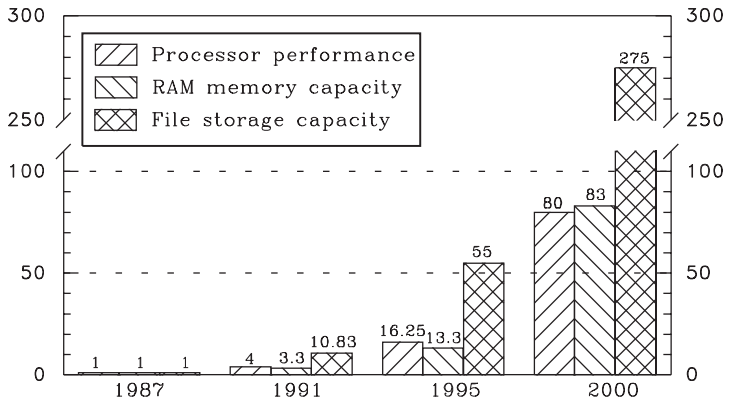

Figure 1.1: *Relative performance improvements of a 6000 US$ computer as a function of three moments in time relative to 1987 (no parallel processing) [after Cutaia, 1990].*

systems in terms of quality and quantity became within the reach of the hydrologist. Vast quantities of observed data have easily been processed for statistical analysis. Moreover, during the past decade, developments in electronics and data transmission have made possible to retrieve instantaneous data from remote recorders (e.g. satellites), which lead to the development of real-time programmes for water management (e.g. flood forecasting for the river Maas).

1.2 Why modelling ?

Hydrology is a subject of great importance for people and their environment. Practical applications of hydrology are found in tasks such as water supply (both surface and groundwater), wastewater treatment, irrigation, drainage, flood control, erosion and sediment control, salinity control, pollution reduction, and flora and fauna protection.

Mankind has always been anxious to comprehend and subsequently control the processes of the hydrologic cycle. Many hydrologic phenomena are extremely complex, and thus, they may never be fully understood. However, the one that knows the hydrologic processes best is you, the hydrogeologist.

During the past, the processes of the hydrologic cycle were only conceptualised, and causes and effects were just described in relatively simple relations. For example, ancient Roman times, water courses were constructed without preceding sound (theoretical) scientific research, yet the construction lasted for ages. Nowadays, however, the state of technology makes it possible to even understand rather complex processes of the hydrologic cycle by means of executing a *model* on the computer.

Some definitions of a model are given here:

> *"a model is a simplified representation of a complex system."*
> or:
> "*a model is any device that represents an approximation of a field situation*"
> [Anderson & Woessner, 1992].

or:
"a model is a part of the reality for the benefit of a specific purpose."
or:
"a model is a computer code filled up with variables and parameters of the specific system."

The purpose of a model is:

"*to replace reality, enabling measuring and experimenting in a cheap and quick way, when real experiments are impossible, too expensive, or too time-consuming*" [Eppink, 1993].

Modelling (also called *simulation* or *imitation*) of specific elements of the real world could help you, as a hydrologist, considerably in understanding the hydrological problem. It is an excellent way to help you organise and synthesize field data. Modelling should contribute to the perception of the reality, yet applied on the right way. In fact, hydrological models should ónly be applied to help the user with the analysis of a problem, nothing more, nothing less. Remember that it is only part of the way to understand or percept a hydrological process.

1.3 Some drawbacks in modelling

Microcomputers now provide many hydrologists new computational convenience and power. The evolution of hydrological knowledge and methods brings about continual improvement in the accuracy of solutions to hydrological problems. However, the continuous supply of hydrological models and their sophisticated graphical modules makes it very easy that the primary function of modelling ("*only to help the user with the analysis of a problem*") might be in danger of being overlooked. Formulating of and simulating with a hydrological model can be accomplished rather easily, however, checking the correctness of the model description, the applied concept of the model, the applied schematisation of the process involved, the applied simplifications, the applied parameters and the accuracy of the results may be very complex. Therefore, a critical view upon the application of computers in hydrology is very useful, especially on relative new topics such as modelling of acid rain, nitrification and NAPL's[1].

Unfortunately, models have been applied by just anybody, sometimes without really awareness of its potentials and impossibilities. This might lead to serious errors in the conclusions. It is very tempting to overestimate the predictive and interpretive potential of models, in particular if sophisticated graphical modules make the simulations realistic and reliable. Note that even a wrong concept may well produce a reasonable prediction. Knowing this, it's a logic phrase, that "*models which reproduce results that exactly fits available historical records should be treated with suspicion.*"

Another reason for scepticism is the data availability. A well-known statement concerning data applied in models is:

garbage in, garbage out !

[1] nonaqueous phase liquids (NAPL's) are complex dissolved substances which contaminate porous media.

It may occur that data are inadequate, e.g. due to poor quality, to support modelling results. Not taking into account the uncertainty of the model parameter during the calibration phase would inevitably lead to inaccurate results. Therefore, results and conclusions of modelling are rather disputable when the reliability of the results is not given at the same time. As today's computer codes and graphics packages can easily produce impressive results, one might be misled to model anyway, while it should be ethically sound to advice against modelling. Hence, a responsibility rests upon the hydrologist to provide the best analysis that knowledge and data will permit. Yet, an element of risk is always present, e.g. a more extreme event than any historically known can occur at any time.

1.4 Definitions

Before going on, some keywords (on an alphabetical order), applied in these lecture notes, are defined here:

- Computer code
  A computer code (or computer programme) describes and solves (partial differential) equations by means of numerical methods on a digital computer.

- Hydrologic system
  "*a set of physical, chemical and/or biological processes acting upon an input variable or variables, to convert it (them) into an output variable (or variables)*" [Dooge, 1968]. See figure 1.2.

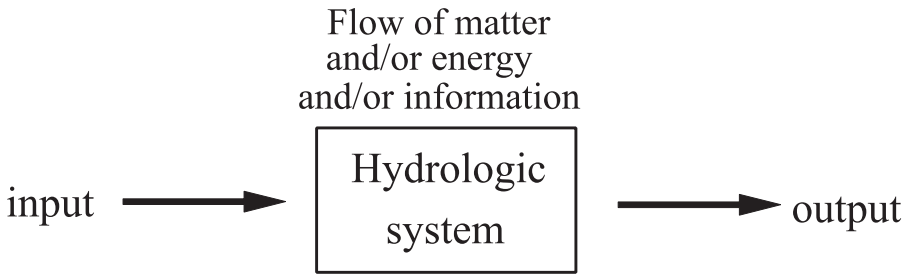

Figure 1.2: *Schematic representation of a hydrologic system [after Domenico, 1972].*

  or:
  "*a structure or volume in space, surrounded by a boundary, that accepts water and other inputs, operates on them internally, and produces them as output*" [Ven Te Chow, Maidment & Mays, 1988].

- Hydrology
  "*Hydrology is the science of the occurrence, the behaviour and the chemical and physical properties of water in all its phases on and under the surface of the earth, with the exception of water in the seas and oceans.*" [CHO-TNO, 1986].

- Parameter
  a quantity characterising a hydrologic system and which remains constant in time.

For example, the area of a hydrogeologic system is a parameter characterising the system. This definition is distinguished from the erroneous definition that any measurable characteristic of a hydrologic system is a parameter, whether time-variant or time-invariant.

- Variable or variate
  a characteristic of a system which is measured, and which assumes different values measured at different times.

In addition, here follows an outline of the disciplines involved (in Dutch !) [OCV, 1997]:

- Fysische geografie
  omvat de studie van het terrestrische deel van het aardoppervlak. Dit aardoppervlak wordt in deze discipline opgevat als een samenhangend geheel van abiotische en biotische elementen: een geo-ecologisch systeem. In dit systeem zijn geomorfologisch, bodemkundige en biologische componenten nauw verweven.

- Geochemie
  omvat de studie van het vóórkomen, en de verspreiding (verdeling) van de chemische elementen en verbindingen in de lithosfeer, de hydrosfeer en de atmosfeer alsmede van de chemische omzettingen en processen die in deze sferen plaats vinden. De relatie tot de biosfeer is daarin begrepen. Veelal worden subdisciplines onderscheiden: bijv. anorganische en organische geochemie, isotopengeochemie, hydrogeochemie, biogeochemie en mariene geochemie.

- Geofysica
  omvat de studie van de processen en de structuur van de vaste aarde met nadruk op de observatie van fysische processen en velden en hun kwantitatieve (mathematisch-fysische) modellering. De geofysica kent de subdisciplines: theoretische geofysica, seismologie, tectonofysica, en paleo/geo-magnetische die gericht zijn op de planetaire fysica en in het bijzonder op processen in de korst, lithosfeer en mantel, en de exploratie geofysica welke gericht is op de opsporingsmethoden voor aardgas, olie, water, ertsen en andere verrijkingen/verontreinigingen van de ondiepe ondergrond.

- Geologie
  omvat de studie van de huidige gesteldheid van en de processen op en in de aarde en betreft de reconstructie van hun veranderend verleden door analyse van het gesteentearchief waarin de geschiedenis van het gehele aarde systeem en de evolutie van het leven besloten ligt. De geologie kent traditioneel de volgende subdisciplines: mineralogie, petrologie, vulcanologie, structurele geologie, tectoniek, stratigrafie, paleontologie en sedimentologie. Afgeleide subdisciplines zoals exploratie-geologie en milieu-geologie richten zich op respectievelijk de opsporing van delfstoffen en de paleoklimatologie/-oceanografie/-geografie alsmede het terrestrische en marine milieubeheer.

- Hydrologie (somewhat different as defined above)
  houdt zich bezig met de opslag en transport van water, over en onder het aardoppervlak. De landfase van de hydrologische cyclus in al zijn onderdelen vormt het weten-

schapsgebied. De Hydrologie heeft duidelijke relaties met de bodemkunde, fysische geografie en meteorologie/klimatologie.

- Geohydrologie
  houdt zich bezig met het voorkomen, de ruimtelijke verdeling, de verplaatsing en het beheer van water onder het aardoppervlak

- Hydrogeologie
  idem als geohydrologie, alleen grotere nadruk op de geologie

Many other keywords, such as deterministic, lumped and distributed, are defined separately in the following chapter.

Chapter 2

Classification of mathematical models

2.1 Introduction

In general, three main classes of models can be distinguished: I. a *physical model* or *scale model*, being a scaled-down duplicate of a full-scale prototype; II. an *analogue model*[1], being a physical process which is translated to the hydrologic process involved, such as electric models (conduction of heat in solids[2]); and III. a *mathematical model*.

In these lecture notes, the third main class is described intensively, as nowadays, most models are of that kind. Various definitions of a mathematical model exist, as subject to the concept of the model and the field of application. Before going on, two commonly applied definitions are given:

- "*A mathematical model is a model in which the behaviour of the system is represented by a set of equations, perhaps together with logical statements, expressing relations between variables and parameters*" [Clarke, 1973]. See also figure 2.1.

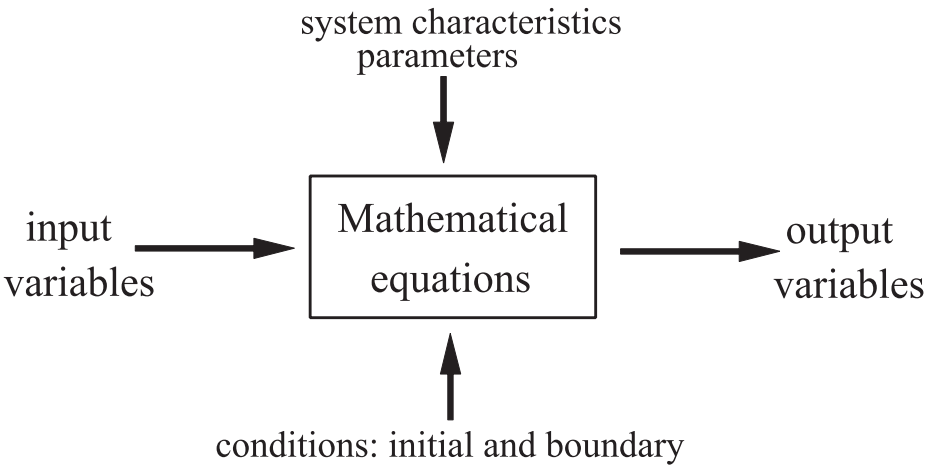

Figure 2.1: *Parts of a mathematical model.*

[1]This main class is often subdivided under *physical models*.

[2]Note that the mathematical similarity between conduction of heat in solids and groundwater flow through porous media has been discovered several decades ago. Analytical (exact) solutions for heat problems have been applied in (equivalent) groundwater flow problems, after conversion of parameters.

- "*A mathematical model simulates groundwater flow indirectly by means of a governing equation thought to represent the physical processes that occur in the system, together with equations that describe heads or flows along the boundaries of the model*" [Anderson & Woessner, 1992]. As you can read, this definition is specific for groundwater flow.

In order to gain an overview of the types of mathematical models, they are classified on the basis of various characteristics. As can be seen in the following sections, various classifications of mathematical models are possible. The terms applied in the classifications are just global indications. In the procedure of selecting the most suitable mathematical model, proper use of these terms should guide you when the characteristics of available mathematical models are quickly compared.

2.2 Based on the design of the mathematical model

This classification is based on the way the mathematical model is designed, e.g. how the model domain or problem area is schematised; what the characteristics of the data are (variables and/or parameters) and how they are utilised in the model.

Analytical model versus numerical model

An *analytical model* is a model that is based on (e.g. Laplace) transformations and the hodograph method (conformal mapping). In a *numerical model*, the partial differential equations are replaced by a set of algebraic equations written in terms of discrete values. A numerical model is often based on computer codes. At this moment, numerical models are available in great numbers.

Deterministic model versus stochastic model

A model is regarded *deterministic*, if all variables are regarded as free from random variation, or, if the chance of occurrence of the variables involved in such a process is ignored and the model is considered to follow a definite law of certainty and thus not any law of probability. A deterministic model is one that is defined by cause-and-effect relations. A deterministic model treats the hydrologic processes in a physical way.

A model is regarded *stochastic*, if any of the variables are regarded as random variables, having distributions in probability. Early stochastic approaches concentrated on linear or multiple correlation and regression techniques to relate the *dependent* variables (e.g. discharge out of an aquifer) to the *independent* variables (e.g. rainfall). With modern computer abilities, methods to represent random variations in processes by means of the probability laws became possible. Note that stochastic is a more general word than statistical, to emphasize the spatial and time-dependence of the hydrologic variables related in the model.

Bear in mind that neither model always stands alone as a practical approach. For example, the input of a deterministic model for determining the water balance in an aquifer is usually based on measurements of rainfall and evaporation. Where this information is limited, stochastic models can be employed to develop synthetic rainfall records, e.g. using

the Monte Carlo simulation. Consequently, in this example, the output from the deterministic model is stochastic as the input is stochastic as well. Nonetheless, the structure of the model itself remains deterministic.

Lumped model versus distributed model

A *lumped model* neglects the spatial distribution in the input variables and the parameters in the model domain. A lumped model is a system with a particular quantity of matter, whereas a *distributed model* is a system with a specified regions of space. For example, a lumped model treats variables, such as natural groundwater recharge, in the area of a catchment surface as a single (1D) unit, whereas a distributed model calculates the variables from one point in the area to another point (2D or 3D). A *semi-distributed model* still follows some physiographic characteristics of the area. Figure 2.2 shows three discretisations of a rainfall-runoff process in a catchment. The application of the terms lumped, semi-distributed and distributed are only useful in case methods of modelling, each describing the same physical process in a different way, are compared with each other. It appears that most terms mentioned here are applied for surface water models.

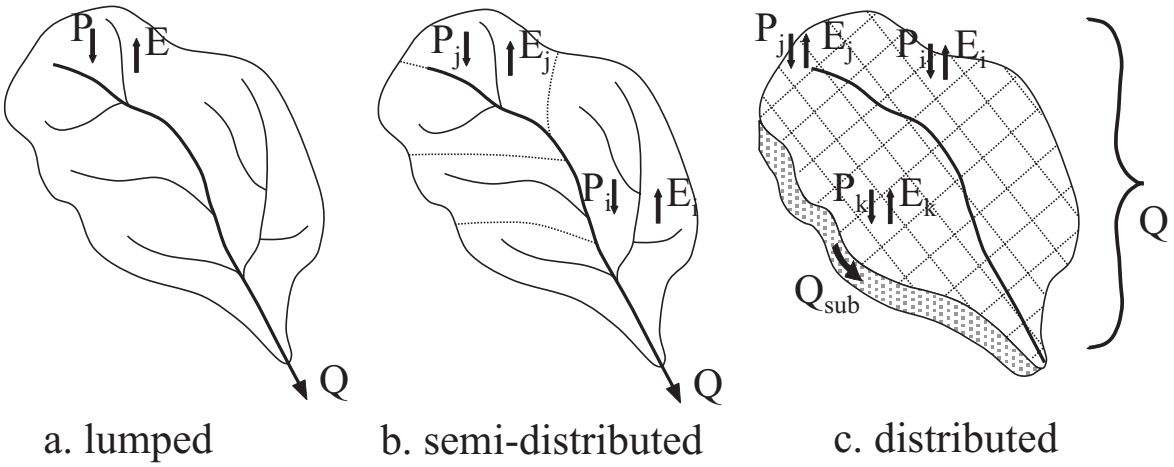

Figure 2.2: *Comparison between a lumped, a semi-distributed and a distributed model: discretisation of precipitation and evaporation.*

Black box model versus white box model

A *black box model* is a term often used for a lumped-parameter model in which inputs and outputs of a hydrologic system can be measured or estimated though the processes which interrelate them are not often observable. The distinctive feature of a black box problem is that a space coordinate system is not required in problem formulation and solution. As such, the time aspect is an important feature in the modelling process.

For example, a water table rise in wells over a certain time interval, a so-called response variable, may be converted to natural groundwater recharge without any regard to the

location of wells in the field or to their spacing or even to the amount of rainfall. For example, the hydrologic cycle itself is often presented as a black box system of lumped elements.

By contrast, a *white box model*, which is by the way not a frequently used term, is regarded as a distributed-parameter model of which the distinctive feature is that the internal space of the hydrologic system is described by a distribution of points, each of which requires information. The model domain is partitioned which results in a grid with elements. For a mathematical solution, the model input data must include not only the values of the properties at all elements within the system, but also the location and the values of the model boundaries. A space coordinate system comprises a necessary part of the problem formulation and solution, when the mathematical model applies partial differential equations. In literature, a grey box model is synonymous for a conceptual model.

Empirical model versus conceptual model versus physically based model

An *empirical model* is based on observation and experiment, not on physically sound theory. In the empirical approach, physical laws are not taken into account. These models are often applied in inaccessible (ungauged) areas, where only little is known about the area involved. The models are based on regression analysis : for example, $\sum Q_{x,t} = \alpha + \beta P_t + \epsilon_t$. This means that the coefficients in the function are determined through calibration with the output data of the hydrologic phenomena involved. As such, a calibrated model is not universal, as each area has its own relation. For example, the discharge at a specific moment in time can be a function of discharges and precipitations at previous moments in time and a few extra parameters: $Q_{x,t} = f(Q_{x,t-1}, Q_{x,t-2}, ..., Q_{y,t}, Q_{y,t-1}, ..., P_{m,t}, P_{m,t-1}, ..., P_{n,t}, P_{n,t-1}, ..., a_1, a_2) + \epsilon_t$. In addition, it is also possible that empirical models are based on physiographic characteristics of the system. Note that the dimensions of the different parameters do not have to be equal !

A model is regarded as a *conceptual model*, if physical processes are considered which are acting upon the input variables to produce output variables. In the conceptual approach, an attempt is made to add physical relevance to the variables and parameters used in the mathematical function which represent the interactions between all the processes that affect the system. An example of simple conceptual models is the formulation of Darcy (law of porous media flow). Conceptual models are widely applied, as they are easy to use, apply limited input data, and can always be calibrated.

A *physically based model* is based on the understanding of the physics of the processes involved. They describe the system by incorporating equations grounded on the laws of conservation of mass, momentum and energy. The parameters of a physically based model are identical with or related to the respective prototype characteristics (e.g. storage capacities, transmissivities). Physically based models often apply deterministic and distributed input data. They can be applied in measured as well as unmeasured systems. Physically based models have the advantage that they have universal applications. The measured or estimated model parameters and hydrologic stresses (e.g. differences in natural groundwater recharge, human impacts such as groundwater extractions) can be adjusted in the input data file, so that the model is geographically and climatically transferable to any other area. Because of this reason, recent activities in hydrogeology are mostly focused on physically

based modelling. On the other hand, these models are limited due to presuppositions of the theoretical background (as such, there is a fundamental deficiency of similarity between theoretical model and reality), huge amounts of input data and restricted computer capacity. Moreover, model development is labour-intensive. Physically based computer codes for groundwater problems are MODFLOW (section 9.2) and MOC (section 9.5).

Table 2.1 shows the differences between the three models in terms of discretisation and application of complex hydrological problems. An empirical model is often called a black box model, a conceptual model a so-called grey box model and a physically based model a white box model.

Table 2.1: *Model types and applied space discretisations: differences between empirical, conceptual and physically based models.*

Model type		Spatial discretisation			System dimension		
		distributed	semi-distributed	lumped	1-D	2-D	3-D
Empirical	(Black box)	-	-	+	+	-	-
Conceptual	(Grey box)	(+)	+	+	+	+	-
Physically based	(White box)	+	(+)	-	+	+	+

In a way, a conceptual model has some degree of empiricism, since its (lumped) parameters do not depend on direct measurements. In fact, the distinction between conceptual and empirical is almost artificial. Historically, the treatment of hydrological theory and calculation has been restricted due to computational facilities. Subsequently, individual and component processes were considered, such as evaporation and runoff. For example, Darcy's law is a latter of observation, and hence, it is empirical by strict definition. With the advent of the digital computer, the component processes could be integrated and time and space variables could be represented, which lead to a physically based approach. For example, models apparently firmly based on physics may contain empirical components.

Transient model versus steady state model

A model is called a *transient* model (other synonyms are *dynamic*, *unsteady*, *non-steady state*, *non-stationary*) when a time variable is present in the partial differential equation and a time variable is calculated for every time step. In a transient model, the initial situation must be known. Obviously, in a *steady state* model, the time variable is set to infinite. As such, the partial derivative of the time variable is zero.

Note that the so-called *quasi-transient* situation is the succession of steady state situations. As such, the result seems to be a transient situation.

It is important to recognise whether or not the hydrologic process you want to model is steady state or transient. For example, you will not retrieve correct results when you are modelling the effect of the tide on a coastal groundwater system when you are applying a steady state model (see figure 2.3).

Linear model versus nonlinear model

A linear term is a first degree in the dependent variables and their derivatives. A linear differential equation consists of a sum of linear terms. The most important feature of a

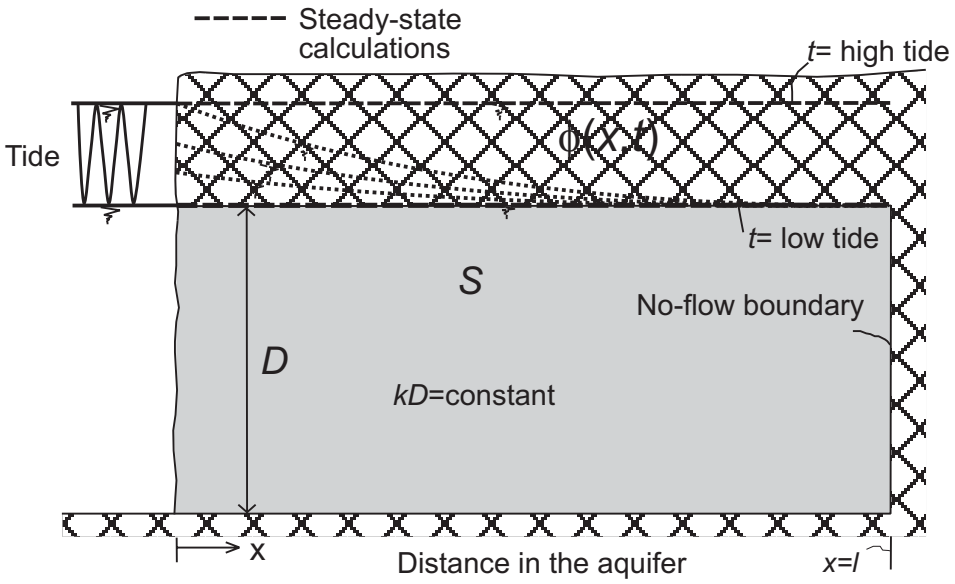

Figure 2.3: *Attempt to simulate the tidal effect on the coastal groundwater system with a steady state model will not give satisfying results.*

linear model is that linearity in differential equations is synonymous with the *principle of superposition*, meaning that the derivative of a sum of terms is equal to the sum of the derivatives of the individual terms. Moreover, linear representation of the relationship between processes means that, when the processes are plotted against each other, the relationship would be a straight line, whereas for a nonlinear model a curve would exist.

For example, expressed in terms of the response of the hydrologic system, the total effect resulting from several stresses acting simultaneously is equal to the sum of the effects caused by each of the stresses acting separately.

Unfortunately, most hydrologic processes are nonlinear, though often the processes are linearised to simplify the mathematics. For example, the variation of infiltration rate with time for a uniform rainfall intensity is nonlinear. Note that it requires various skills to recognise a system being in fact a linear system.

If the model is linear, it is possible to use *linear programming* for optimizing a hydrologic process to meet a given goal. For example, a well-known groundwater flow problem is the extraction of groundwater from wells: through maximising the extraction (which is limited by physical circumstances), combined with maximising the economic return from the extraction and minimising the pumping costs, the result of the optimization is the location of the optimal wells within the possible locations and the optimal extraction rate in these wells.

Note that in fact, many groundwater processes, such as solute transport in groundwater flow, control of salt water intrusion, flow of heat or cold groundwater, are nonlinear. This is because the groundwater flow equation and advection-dispersion equation are interconnected with each other, e.g. through the dispersion coefficients as a function of the velocity (see section 6.2, equations 6.70 to 6.74, page 88). As such, these processes cannot

be subjected to linear programming optimization.

Space dimensionality of the model: viz. 0D, 1D, 2D, 3D, quasi, radial, axial-symmetric

Though the term dimension is difficult to define, it can be applied to qualify the characteristic of the partial differential equations in the mathematical model. The number of dimensions of a mathematical model is related to the number of independent space-variables in the applied partial differential equation. As such, the so-called quasi-2D and quasi-3D models drop out, as mostly the term 'quasi' only comprehends a trick to interpret the results of respectively a 1D model and a 2D model in an extra dimension. For example, the position of an interface between fresh and saline groundwater in a horizontal 2D-plane gives a 3D-presentation of the results.

Based on this definition, so-called 0D-models are possible, when in the equations no space-variables occur. For example, the lumped-parameter model of figure 2.2 is such a 0D-model. However, there are always dubious cases. For example, the dimension of a model, which consist so-called linked reservoirs (viz. each reservoir does not contain a space-variable), is difficult to give: 0D or 1D. Such a model is a model for a sewage system of a city, containing several reservoirs with both water flow and silt transport for each district [Heikens, 1992]. And what will be the answer (0D or 1D) if the length between the districts is taken into account to determine only the flow friction in the channel ?

2.3 Based on the processes in the hydrologic cycle

This classification is based on the processes in the hydrologic cycle described with the model. Figure 2.4 shows a schematic representation of the hydrologic cycle. Note that, obviously, not every process is represented. Most models simulate a few hydrologic processes at the same time. Table 2.2 shows some hydrologic processes which can be described by models.

2.4 Based on the application of the model

This classification is based on the purpose the model is applied. The models should provide the user more (quantitative) information on the hydrologic processes involved. The use of models can be subdivided into three classes:

I. process models, applied from a scientific point of view,
in order to promote a better description of hydrologic phenomena, through research and investigation of the hydrologic processes involved. Science is interested in determining certain relations between processes.

II. design models, applied from an engineering point of view,
in order to achieve certain objectives. Engineering is interested in hydrologic processes only to the extent that they achieve some utility or purpose. Thus, the engineer is concerned with the relations between processes discovered by science to simulate performance, reliability, cost of development, maintainability, or life expectancy.

A further subdivision is in:

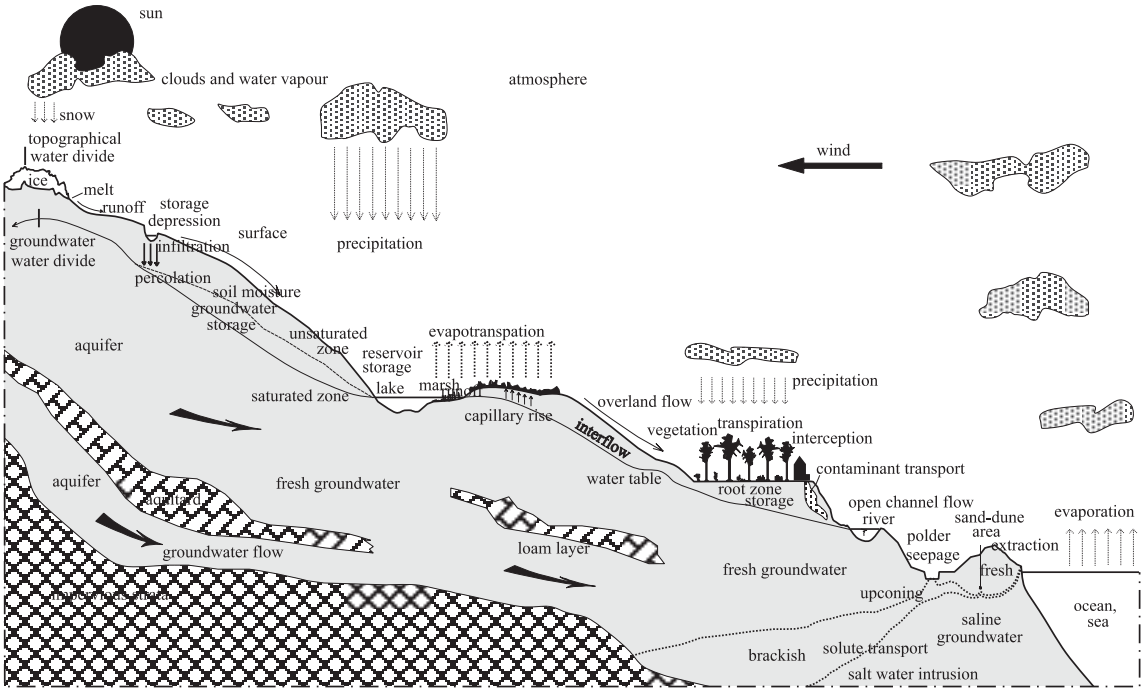

Figure 2.4: *A schematic representation of the hydrologic cycle. Surface water processes are not taken into account in these lectures.*

a. assessive or interpretive models,
   which try to assess the present state of a system to gain more insight and understanding into the controlling parameters in a site-specific setting. For example, to improve understanding in regional groundwater flow systems, more quantitative information should be provided on the magnitude, quality, distribution (and timing) of available water. These interpretive models are also useful for design purposes.

b. predictive models,
   which try to extend the knowledge of the assessive models to predict the future effect of any physical alteration on a system, such as direct and indirect influence of human actions (e.g. urbanisation, intensification of agricultural and forestry land use, higher rates of groundwater extraction for future water supply, climate change, sea level rise). Most modelling efforts are aimed at predicting the consequences of a proposed action.

Note that predictive models require a calibration phase (see also section 3.5), whereas the assessive models do not necessarily require such a phase.

III. management models applied from a point of view of management and planning,
in order to control a certain system by decision variables. Management is interested in the establishment of: (a) output models that describe the consequences if

Table 2.2: *Processes in the hydrologic cycle.*

Groundwater/Subsurface
-Occurrence, origin, movement, quality, recovery, use
-Solute transport: chloride, pesticides, hydrochemical constituents
-Density differences: fresh-salt interface, non-uniform density distributions
-Pumping discharges, water table variations (transient or steady state)
-Biochemical processes
-Waterbalances
-Subsidence of the ground surface due to compaction, shrinkage and oxidation of peat
Surface water
-Rainfall-runoff† (the most often described hydrologic process)
-Precipitation, evaporation, infiltration
-Thermal surface water transport (power plants, energy)
-Solute transport (pesticides, hydrochemical constituents
-Open channel flow (hydraulic)
-Soil erosion (sediment transport)
Interaction groundwater-surface water
-Rainfall-runoff, base-flow
-Saturated-unsaturated zone (agricultural device and purposes, crop yield)
-Water management of polder areas
-Infiltration-percolation, interflow
† = another term of rainfall-runoff is precipitation-discharge.

a system is developed in an unregulated manner, and (b) intervention models that describe the probable result of intervention. These models are useful for operational management (e.g. decision techniques). The planners and decision makers also apply information from class II. Examples of management processes are: water yield assessment (rain, snow and/or groundwater); agricultural crop yield management (unsaturated zone); flood and drought forecasting (rainfall-runoff, water distribution, design and frequency); drinking water supply from groundwater (extraction, upconing fresh groundwater); water quality assessment; control of soil contamination and soil erosion assessment; use management.

For the (recently) more complicated multi-objective and multi-constraint problems, the decision making process is a complex process, and thus, system analyses have been required (e.g. flood and drought forecasting; river basin management; reservoir control; see the PAWN-study (Policy Analysis for the Watermanagement of the Netherlands) [Pulles, 1985]). For example, for the problem of water resources assessment, conflicting water requirements (which form the objectives) as well as the water availability are considered. Moreover, a number of constraints should also be taken into account (see table 2.3).

æ

Table 2.3: *Example of the aspects involving a water resources assessment.*

Water resources assessment		
Water requirements	Water availability	Constraints
-agriculture -water supply: domestic & industrial -flood regulation -pollution control -power plants -environment	-surface water: snow melt, precipitation -groundwater: fossil, sustainable, mining -desalinisated water	-min./max. allowable flows -quality -water level -velocities

Chapter 3

Methodology of modelling

In this main chapter of part I, the methodology of modelling will pass in review, based on the steps in the diagram in figure 3.1. It is very tempting to pass over some steps, for example, verification of the computer code for your specific problem is not a very popular activity,

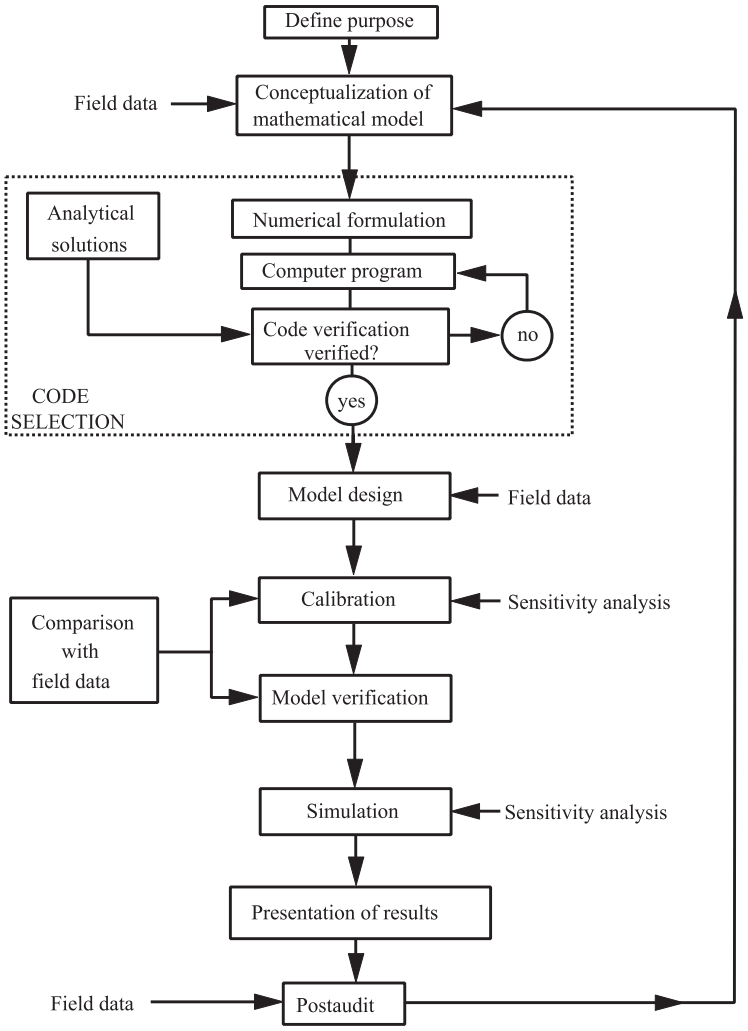

Figure 3.1: *Steps in the protocol for model application [adapted from Anderson & Woessner, 1992].*

and therefore, it is often skipped over too fast. As can be seen, several steps precede the total simulation phase. Though not always every step should be treated equally intensive, you should always at least glance through all steps.

3.1 Define purpose of the modelling effort

Obviously, it is essential to identify the purpose of the modelling effort before going on. Therefore, in order to help yourself in the way of modelling, you should ask yourself the following questions:

- What is the application of the model (from a scientific, engineering or management point of view, see section 2.4) ?
- What do you want to learn from the model ?
- What questions do you want the model to answer ?
- Is a modelling exercise the best way to answer the question ?
- Do we really need a mathematical model ? Can an analytical model provide the answer or must a numerical model be constructed ? In a number of case studies, an analytical model is adequate enough and a numerical model only lead to overkill.

The responses of these questions will lead you in determining the modelling effort: analytical or numerical, lumped or distributed, transient or steady state, etc. Note that, once again, modelling is only one component in the process of solving the hydrological problem, and not an end in itself. It is recommended to use only models when it is really necessary and, if possible, to use already existing standardized programme code.

3.2 Conceptualisation of a mathematical model

In general, it is not possible to include all processes of a hydrologic system in one model, as the 'real-world' situation is too complex. Therefore, you have to select those processes you want to model for sure, and you have to define which processes can be left out of consideration. The conceptualisation of the model consists of two modules: (a.) a schematisation of the hydrological problem and (b.) a concept of the mathematical model.

ad a. Schematisation of the hydrological problem

The first step towards the conceptualisation of the mathematical model is to set up a schematised or pictorial representation of the hydrological problem you want to model. Simplification is necessary because a complete reconstruction of the hydrologic system is not feasible. For example, figure 3.2 shows the schematisation of the subsoil of the groundwater flow system in the low-lying western part of the Netherlands. In general, schematisations in groundwater problems are focussed on [Hemker, handouts, 1994]: the composition of the subsoil (layered system, number of aquifers); the type of groundwater flow (steady state, 1D or 2D); the properties of groundwater (density, temperature, fresh-saline interface,

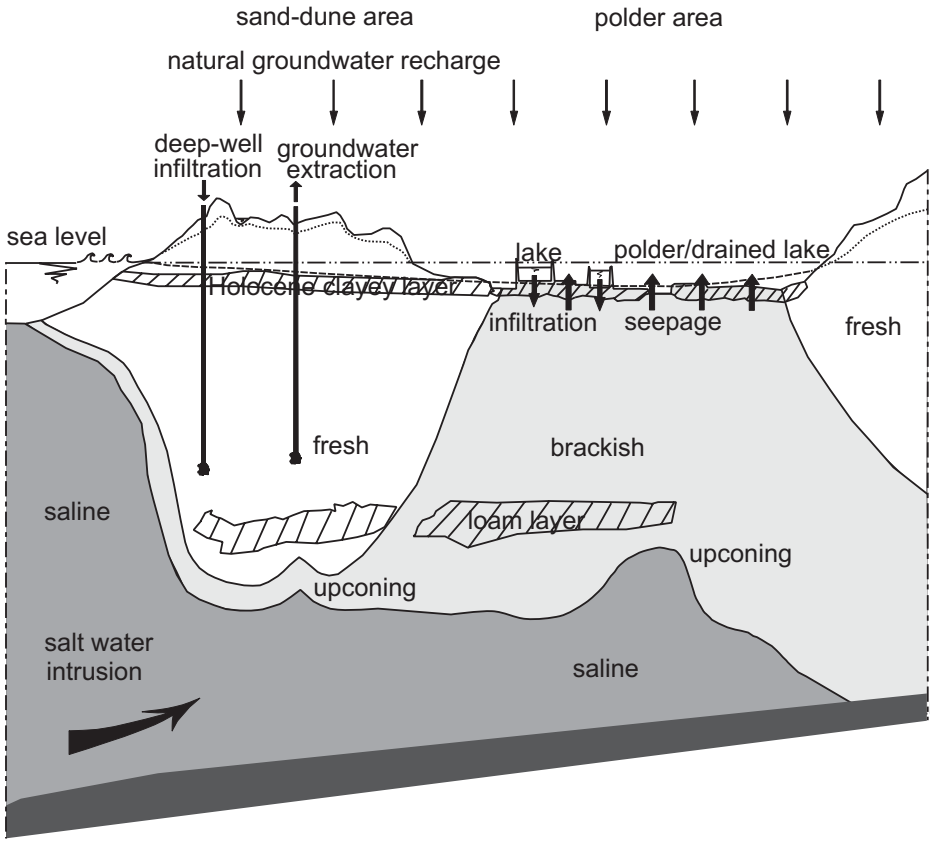

Figure 3.2: *A schematisation of the groundwater flow system in the low-lying western part of the Netherlands: the system is divided up into a fresh, brackish and saline part.*

fresh/saline, dissolved solutes); the boundaries of the study area (location of the boundary, type of boundary condition); and the use of averaged values (piezometric head, polder level, thickness of layers, porosity, groundwater extraction).

ad b. Concept of the mathematical model

Based on the schematisation of the hydrologic problem, the *concept* of the mathematical model is built. The purpose to building a concept is to simplify the field problem in order to make the schematisation suitable for numerical modelling. In other words, you have to simplify the system you are interested in to a large extent. In addition, the building of a concept organises the associated field data so that the hydrologic system can be analysed more easily. A concept is set up to define system characteristics, processes and interactions. For example, figure 3.3 shows the concept of the mathematical model of the groundwater flow system in the low-lying western part of the Netherlands (the property of groundwater is not shown in this figure). This concept is based on the schematisation in figure 3.2 and is suitable for numerical modelling.

Note that this step of the modelling protocol is obviously a very important one. You

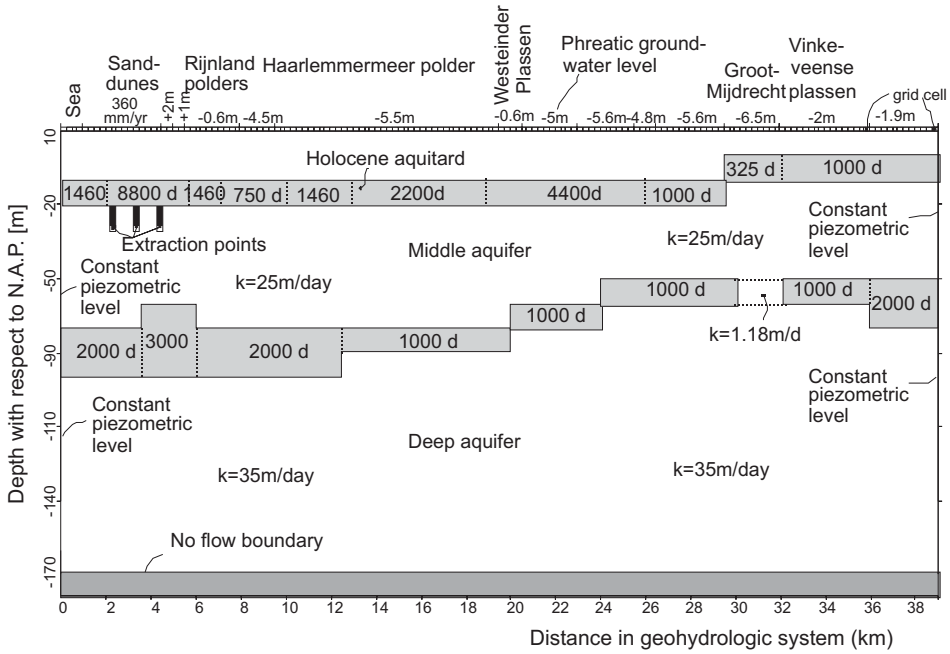

Figure 3.3: *A concept of the mathematical model of the groundwater flow system in the low-lying western part of the Netherlands.*

have to know what detail can be neglected, what will be the time scale and space scale (the number of model dimensions), what will be the relation between the scale of the system itself and the model, etc. In the end, the nature of the concept determines the dimensions of the numerical model and the spatial and temporal discretisations. In addition, the concept determines what processes are simulated and what processes are neglected. For example, a failure in the concept will very likely lead to inaccurate predictions with the numerical model. Bear in mind that a wrong concept may well produce a reasonable solution. This may lead to the following situation:

> "*A hydrological misconception becomes a virtually insurmountable obstacle to progress in hydrology, when the models take the shape of easy-to-use software packages.*" [Klemeš, 1986].

It is therefore essential to know what is relevant to the hydrologic system you want to model.

In this step of the modelling protocol, the following topics can be identified:

1. the relevant hydrologic phenomena which are taken into account

   Conversion from all observed phenomena in a hydrologic system to mathematical descriptions of some selected phenomena obviously requires professional skill. Inspiration can be found from the already present scientific knowledge and through observation of relevant quantities. It may always be possible that you have skipped a relevant hydrologic process which was not described with the mathematical de-

scription you formulated. Be therefore always critical on the results of the modelling simulation phase.

In addition, the water, the solute and/or the sediment budget in the hydrologic system is prepared. The order of magnitude of sources (e.g. precipitation, deepwell infiltration, contamination sources, groundwater extraction) as well as the flow direction of water, solute or sediment should be known quantitatively in order to summarize the magnitudes of the flows and the changes in storage. During the calibration of the model (see section 3.5), the measured budget is compared with computations by the model.

2. the system boundaries
   The area of interest or the size of the system is defined by identifying the boundaries of the model (a Dirichlet, Neumann or Cauchy condition, see section 3.4). When possible, the natural hydrological boundaries of the system should be used. In groundwater problems, the impermeable base is a logical no-flow boundary at the lower part of the model. Obviously, in many cases, a natural boundary is not available: then an artificial boundary is simulated (see also section 3.4).

3. the physiographic characteristics of the hydrologic system, both variables and parameters
   Detailed information of the hydrologic system involved is gathered. Field data are assembled to assign values for the parameters of the described hydrologic system. They should be obtained by observing, studying and measuring. For example, the following information could be relevant for a groundwater problem:

   - Subsoil parameters: geometry, position of layers, hydraulic conductivity, transmissivity, hydraulic resistance, porosity, specific storativity, anisotropy,
   - In- and outflows: precipitation, evaporation, evapotranspiration, surface runoff (overland flow), natural groundwater recharge, infiltration, percolation, recharge form surface water bodies, baseflow,
   - Initial conditions: piezometric head and solute concentration,
   - Geochemical data: cations (e.g. Ca^{+2}, Mg^{+2}, Na^{+}) and anions (e.g. SO_4^{-2}, HCO_3^{-}, Cl^{-}), temperature, pH, trace metals, isotopes and organic compounds.

   In addition, hydrological units with similar hydrologic properties are defined, based on the information of the area of interest. In groundwater problems, a geologic formation is subdivided into aquifers and aquitards: the concept is frequently represented in the form of a block diagram or a cross-section. For example, the so-called *Holland profile* is a hydrogeological schematisation of the subsoil which consists of a Pleistocene sandy aquifer overlain by a Holocene (clayey) aquitard. It is representative for large (low-lying) parts of the western part of the Netherlands. The division into hydrologic units can be supplied by hydrogeologic survey (e.g. geo-electric prospecting: see the lecture notes Geohydrologisch Onderzoek f15C of the Delft University of Technology [van Dam & Boekelman, 1996]).

4. the mathematical model which describes the relevant processes
   Based on the concept of a hydrologic system, the governing mathematical equations

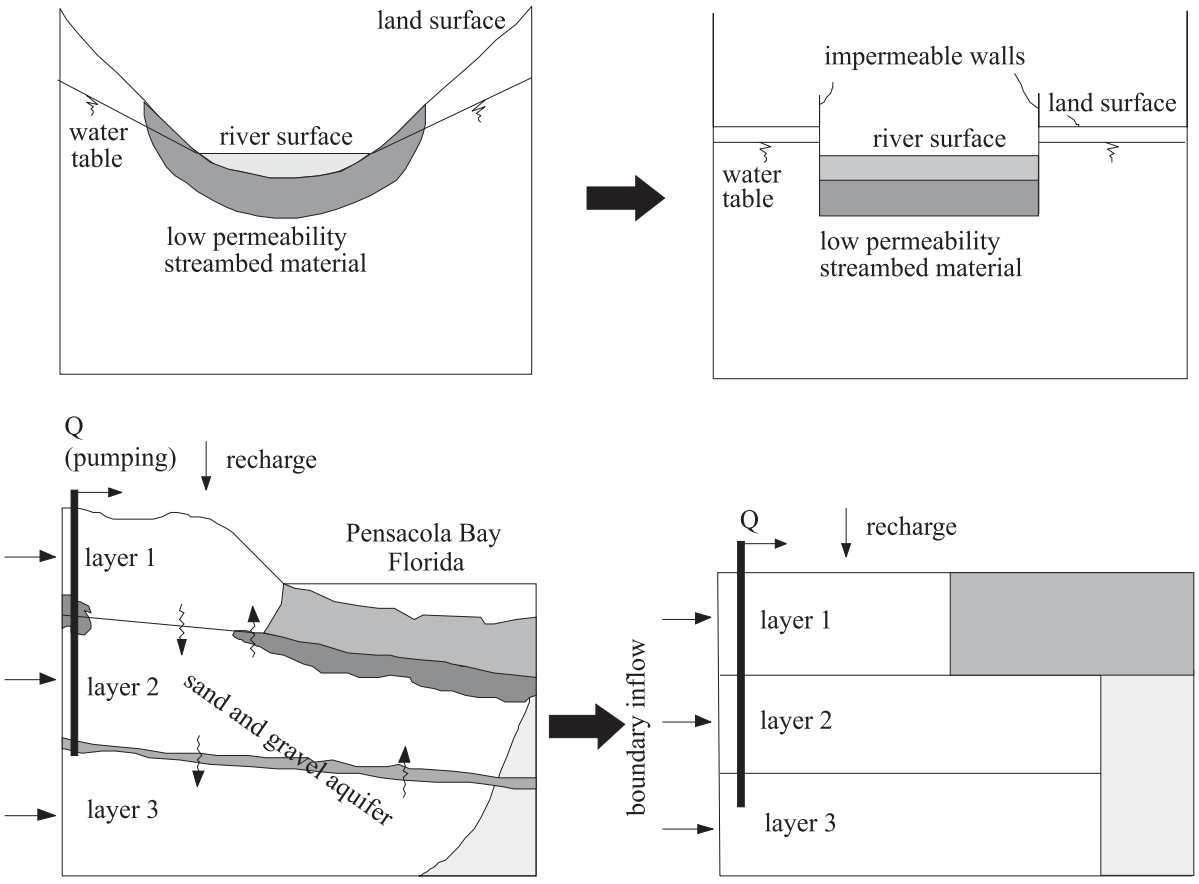

Figure 3.4: *Translation of the hydrogeologic information of a schematised groundwater flow system to a concept suitable for numerical modelling [adapted from Anderson & Woessner, 1992].*

are formulated. This implies that only the equations are defined of the considered processes. See section 6.1 for some mathematical equations of groundwater problems. Verification of the mathematical model will be done in a later step (see section 3.3).

During this step of the modelling protocol, it is recommended to visit the field site in order to keep you tied to reality and to provide you the necessary background information during the subjective modelling phase.

Figure 3.4 shows two examples of how a concept can be constructed from a schematised groundwater flow system.

3.3 Selection of the computer code

A very wide range of computer codes exists for application of different problems. In order to select the best code, you have to formulate a list of demands. When choosing a code from the selection available, the following points should be considered:

- What code is best in solving your particular problem ?
- What are the data requirements for both code and problem ?
- What computer hardware and supporting staff are required ?
- How much will the computer code cost ?
- How accurate will the code be in representing the real world ?

Based on these questions, you should select your code. There are two choices: you choose one of the many codes available or you will develop your own code. Points can be stated in favour of and against each choice.

The use of an existing computer code has advantages in saving both time and money since programme code development is avoided. Large institutes, such as the U.S. Geological Survey, employ tens of scientists who develop and update computer codes for public domain purposes (see page 187, for the addresses and internet-sites of some large institutes). Moreover, you can benefit from experience gained from previous applications (verification cases, test-cases, etc.). On the other hand, it is possible that you will not fully understand the theory and especially the assumptions that are applied in the existing code. This could lead to the situation that the code may be a kind of black box under specific circumstances. This problem is often exaggerated by the lack of basic documentation.

When an own code is developed, you must obviously understand the problem in more details. Nowadays, however, you are advised against developing your own computer code for several reasons: (1) it is a very time-consuming activity, (2) your model, obtained from your code, still has to prove its robustness, reliability and accuracy, (3) your code may not be applicable for other (nearly similar) hydrological problems, and (4) the code may still contain so-called 'childhood diseases'.

Anyway, it is important that the code you use has been verified by comparisons between numerical solutions generated by the code and analytical solutions. Newly developed codes also require to be *debugged* to remove errors on programming and logic prior to their use in hydrological analysis. Even with rigorous checking you should be on the look-out for programming errors. In general, newly released codes are not free of programming errors. This can be deduced from the existence of code versions (e.g. 3.6 or 5.3)[1]. Testing of the computer code or *code verification* comprises verification of problems for which analytical solutions exist. Often the testing of the computer code for problems with known solutions is erroneously called *validation* [Konikow & Bredehoeft, 1992]. A mathematical model is said to be validated, if sufficient testing has been performed to show an acceptable degree of correlation [Huyakorn *et al.*, 1984]. However, as a matter of fact, the models can only be invalidated, since the testing or code verification is only a limited demonstration of the reliability of the model (figure 3.5). Though analytical solutions can be complex, mostly straightforward hypothetical cases are considered.

During the past decades, so many computer codes have been developed that it is very likely that there already exists a code for your hydrologic problem with the appropriate

[1]The integer number mostly indicates that a new (major) procedure or feature is implemented in the computer code, whereas the decimal number mostly indicates that the computer code is debugged, adapted, improved and updated, viz. made free of programming errors.

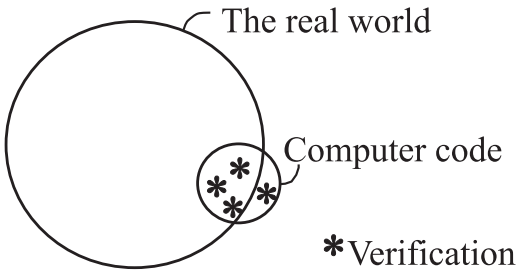

Figure 3.5: *Verification of a computer code: the application of the computer code is limited and may not represent parts of the reality you want to model [after Heikens, 1995].*

characteristics and with documentation on test-cases e.g. in articles and journals. Therefore, it is advisable to be lazy and let other people do the job. Although it is tempting to fix on the first computer code that is brought to your attention, open your mind to other computer codes. Assure yourself of selecting the most suitable computer code available, within the demands you have listed.

Numerous sources can provide you suitable computer codes. First of all, check the database at your own organisation. Second, for the Netherlands, the STOWA[2] database (formerly called SAMWAT) for computer codes in water management [Volp & Lambrechts, 1988; Heikens *et al.*, 1991] contains codes on fluid, solute (sediment) and heat transport, chemical and biological processes in surface water and groundwater. Numerous computer codes for hydrological problems have been developed in the United States of America. The US Geological Survey is one of the leading institutes in developing two and three dimensional groundwater computer codes: http://water.usgs.gov/software/ground_water.html[3]. Important distributors of affordable codes of groundwater problems are the International Ground Water Modeling Center [IGWMC: Golden, USA, 1995], http://www.mines.edu/igwmc/, and the Scientific Software Group, Washington D.C., USA [1996], http://www.scisoftware.com/. The Hydrological Operational Multipurpose System (HOMS) of the World Meteorological Organization (WMO) includes a number of computer codes for hydrologic analysis.

3.4 Model design

The concept of the mathematical model is transformed to a form suitable for numerical modelling. In other words, you have to convert the concept of the your specific hydrologic problem to a model which can be implemented in the chosen computer code. This step in the modelling protocol includes the design of the domain partition, the selection of the length of the time steps (when transient), the setting of the boundary and initial conditions, and the selection of the initial values for system parameters and hydrologic stresses.

[2]STOWA=Stichting Toegepast Onderzoek Waterbeheer, see http://www.waterland.net/stowa.
[3]Hydrology web: http://terrassa.pnl.gov:2080/EESC/resourcelist/hydrology.html

3.4.1 Grid design

In a numerical model, the continuous space domain of your hydrological problem is replaced by a discretised domain, the so-called *grid*. The concept, the selected code and the model scale determine the overall dimensions of the *elements* (also called *blocks* or *grid cells*) in the grid. There are numerous types of elements, see figure 3.6. The two most commonly used grids, applied in mathematical models, are based on the finite difference method and the finite element method (see section 7.5 and 7.6). As can be seen, the finite element concept tolerates more shapes of the elements due to the nature of the interpolation (basis) function (see section 7.6). As a result, elements by the finite element concept allows more flexibility in designing the domain. However, the block-centered approach in the finite difference concept is often applied in a large number of computer codes, because this approach can treat the boundaries more easily.

The number of layers which are considered in the discretised domain, depend on the diversity of the hydrogeologic units of the system, and thus, on the concept. If the gradient in the piezometric head in one aquifer differs significantly, more layers are necessary. In most cases, the slope of aquifers is insignificant. However, if the aquifers slope at some significant angle (e.g. larger than 1 or 2 degrees), two-dimensional models in vertical cross-sections or fully three-dimensional models should be used. Once in a while, models can also be constructed with an adapted orientating of the grid. In those cases, the coordinate system is aligned with the principal direction of the hydraulic conductivity tensor (see figure 3.7).

The spatial discretisation of the grid and the temporal discretisation are determined by: (a.) the scale of the natural variation, (b.) the scale of the concept of the model and the model domain, and (c.) the sampling scale:

ad a. this is the smallest scale on which the natural processes are taking place (as far as we know). As such, the heterogeneity of the hydrologic system has a major effect on the grid design. For example, Darcy's law for the flow of fluid through a porous medium is defined for a specific spatial scale which corresponds with the so-called *Representative Elementary Volume (REV)* [Bear, 1972]. The size of the REV is selected such that the averaged values of all geometrical characteristics of the microstructure of the void space is a single valued function. At a scale smaller than the REV, groundwater also flows, viz. flow through pores and channels, but at that scale of Darcy's law is not valid any more. Note that the laws of continuity of mass, momentum and energy are applicable on each scale. Upscaling from the base equations at REV scale to regional flow of groundwater requires a lot of knowledge about the processes involved: which processes may be neglected and which processes should be taken into account.

ad b. this is the scale on which the parameters and variables are implemented in the model. The dimensions of the elements as well as the length of the time step influence the design of the grid.

ad c. this is the scale on which the measurements of system parameters and variables are taking place. For example, in groundwater problems, the location of wells influences the grid design. In addition, if only one observation well is recording the piezometric head in an area of e.g. 25 km^2, the spatial discretisation of the grid should match

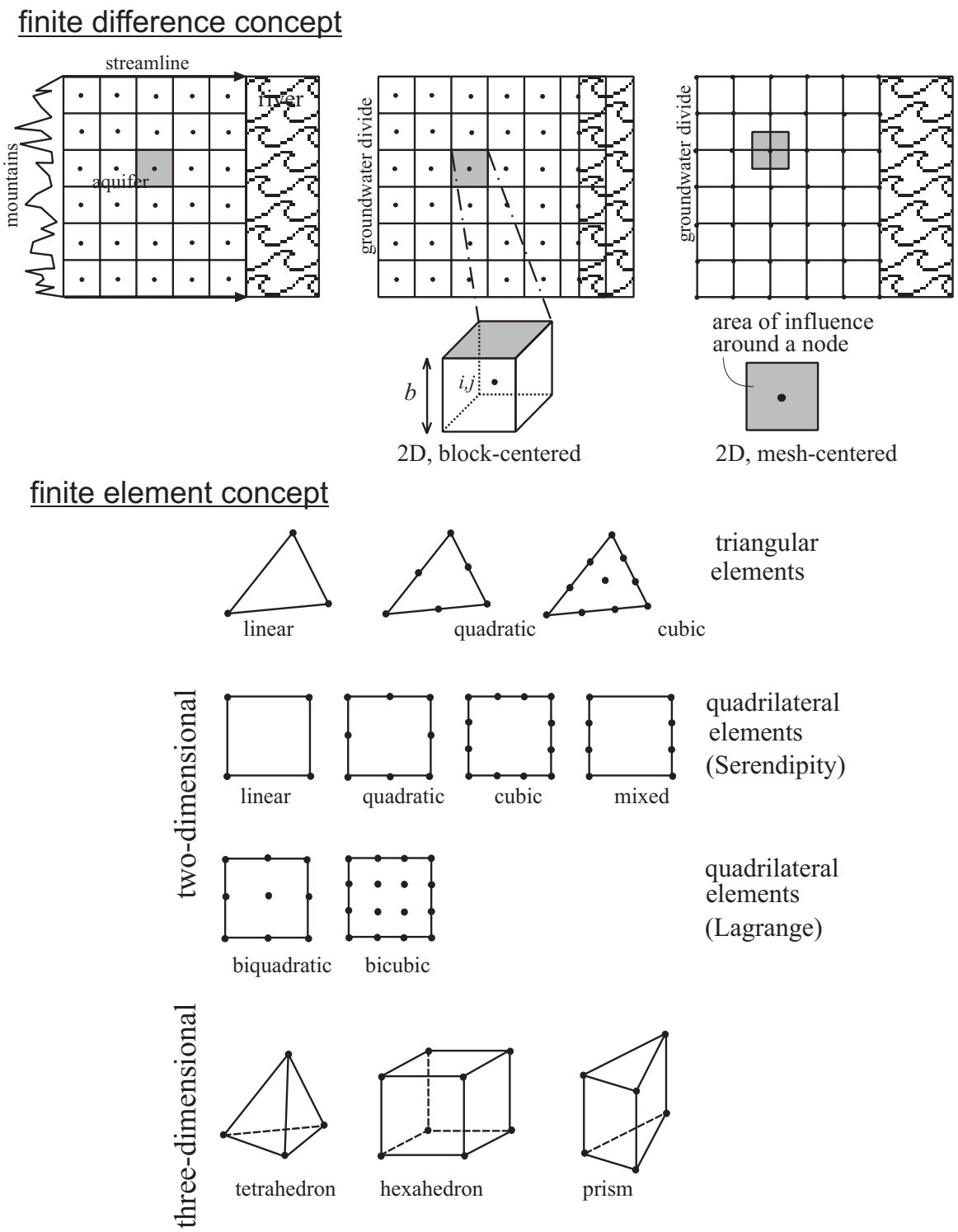

Figure 3.6: *Some types of elements, based on the finite difference concept and the finite element concept.*

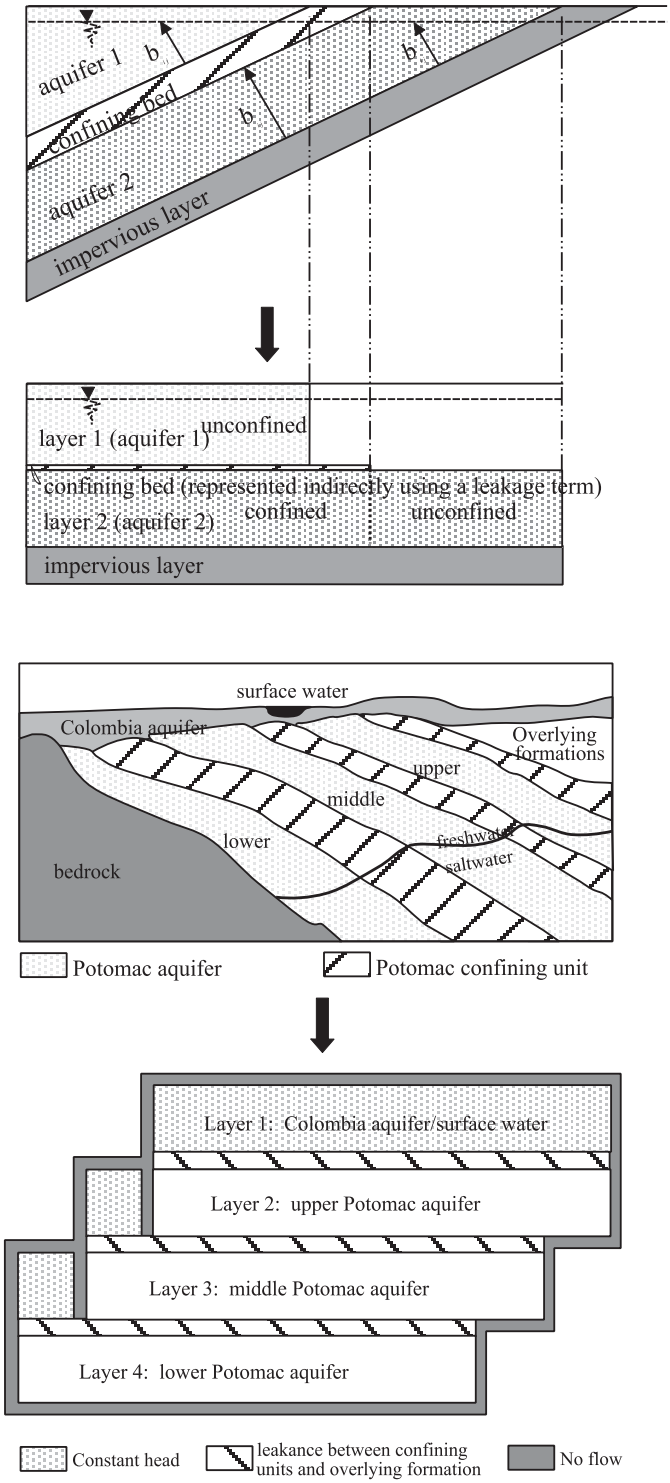

Figure 3.7: *Two representations of dipping hydrogeologic units in a numerical model by adaption of the grid orientation [after Anderson & Woessner, 1992].*

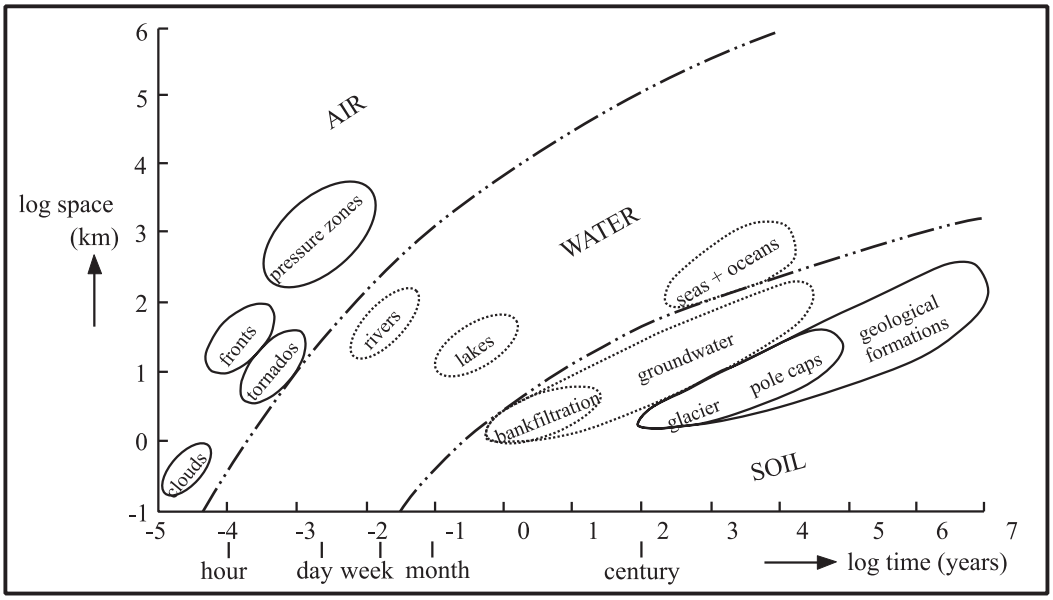

Figure 3.8: *Time-space dimensions of some natural phenomena in air, water and soil [Zoeteman, 1987].*

Table 3.1: *Length of time steps for various hydrologic processes.*

Hydrologic process to be modelled	Order of magnitude of time step
(dynamic) flood wave in open channels (short term forecasting & control)	hours
salt water intrusion into aquifers	years/decades/centuries‡
solute transport in groundwater	years
river basin management (water shortage and pollution)	days/week
large-scale planning of water resource use (control strategies)	week/month
changes in the length of glaciers due to climate change	years/decades
river and flood plain management (flood control)	hours
drawdown in an aquifer due to groundwater extraction	hours/days/weeks
‡: salinisation of the subsoil can be a very slow process.	

with the availability of the data. If data is scarce, it make no sense to apply a three-dimensional model which demands a vast quantity of input data that cannot be supplied.

Note that a universal methodology cannot be given here, as the exact form of your grid depends primarily on the hydrologic system and the hydrological problem to be solved.

3.4.2 Temporal discretisation

The length of the time step depends on the dynamic character of the hydrologic process you want to model. Figure 3.8 shows the spatial and temporal scales of some (hydrologic) processes. Various examples of different time steps are shown in table 3.1.
The following considerations determine the selection of the temporal discretisation:

- what is the purpose of the model application (transient or steady state),
- which (external) hydrologic stresses must be modelled (e.g. transient or steady state well extraction; changes in polder levels),
- what is the availability of input data (daily or weekly data; storage data; initial conditions),
- which storage processes must be modelled (system dependence: slow, rapid groundwater flow; areal dependency: topography),
- which computer code is available.

The length of the time step should be determined accurately for transient simulations. In principle, the specific storativity S_s should not be equal to zero. When the interest is focused on the development to a new state of dynamic equilibrium for the piezometric head, the length of the time step should not be too large, because the new state of dynamic equilibrium may be approached within some (tens of) days, e.g. due to changes in pumping rates.

Most computer codes for groundwater problems allow the time step to increase as the simulation progresses (e.g. a geometric progression of ratio 1.2 to $\sqrt{2}$) [de Marsily, 1986]. It is, however, recommended to decrease the time step once again when new stresses are imposed on the hydrologic system. See page 100 for the determination of a critical time step in a non-steady aquifer system.

3.4.3 Boundary conditions

Besides a governing equation and initial conditions, mathematical models consist of boundary conditions. These boundary conditions are mathematical statements at the boundary of the problem domain. A correct selection of boundary conditions is a critical step in the model design, as a wrong boundary may lead to serious errors in the results. Mathematically, the boundaries are divided in three types:

I. Dirichlet condition (specific head boundary),

describing specified head boundaries for which a head is given. Examples of specified head boundaries are: the water level at a lake or at the sea. A specified head boundaries represent an inexhaustible supply of water. For example, water is pulled from or discharged in the boundary without changing the head at the boundary. In some situations, this is probably an unrealistic approximation of the response of the system.

A specified head boundary ($\phi_{(x,y,z,t)}=\phi_{constant,t}$) difficult to model is the water table, because the location of the water table is usually unknown, whereas it often the feature we want the model to calculate. This is a feature of the so-called *moving-boundary-problem*. For example, in transient simulations, the purpose is to predict the effect on the location of the water table of pumping or changes in recharge. The problem can be avoided by using an unsaturated/saturated flow model (though it may lead to

other complications) or use the *Dupuit assumption*[4] to model flow in the top layer of the model.

II. Neumann condition (specific flow boundary),
describing specified flow boundaries ($q_{(x,y,z,t)} = \alpha\frac{\partial\phi}{\partial x}$=$q_{constant,t}$) for which a flow (the derivative of head) is given across the boundary. Examples of specified flow boundaries are: natural groundwater recharge in an aquifer (areal recharge); groundwater injection or extraction wells; groundwater springflow or underflow; seepage to a hydrologic system. A special Neumann condition is the *no-flow boundary condition*. A no-flow boundary condition is set by specifying the flux to be zero. Examples of no-flow boundaries are: the groundwater divide in a catchment area; a streamline (a cross-section perpendicular to the contour lines of the piezometric head may also be considered as a no-flow boundary for groundwater problems); a fresh-saline interface in a coastal aquifer (interface is a streamline boundary); and an impermeable fault zone. The no-flow boundary condition is simulated in a (block-centered) finite difference grid by assigning zeros to the transmissivities or the hydraulic conductivities in the inactive elements just outside the boundary. In a finite element grid, the no-flow boundary condition is simulated by simply setting the flux in the node equal to zero.

III. Cauchy condition (head-dependent flow boundary),
describing head-dependent flow boundaries for which flux across a boundary is calculated, given a value of the boundary head. This condition ($\alpha\frac{\partial\phi}{\partial x} + \beta\phi$ =constant) is also called the *mixed boundary condition*, as it relates boundary heads to boundary flows. It is dependent on the difference between a specified head, supplied by the user, on one side of the boundary and the model calculated head at the other side. Examples of head-dependent flow boundaries are: leakage to or from a river, lake or reservoir[5]; evapotranspiration (flux across the boundary is proportional to the depth of the water table below the land surface).

Physical boundaries are formed by the *physical* presence of an impermeable body of rock[6] or a large body of water (e.g. river, lake or ocean), whereas hydraulic boundaries are the result of invisible hydrologic conditions, such as groundwater divides and dividing streamlines. An important characteristic of a hydraulic boundary is that it is not a stable feature: it may be shifted or even disappear if hydrologic conditions change. This situation may obviously occur for transient processes when heads along hydraulic conditions might change due to stresses on the system. If a constant head condition is applied, a serious error may occur because the model will retain the head at the boundaries. As a first estimate whether or not the error is serious, the head boundary should be changed to a flux boundary: if the effect of the head or flux boundary is small, the error is probably small as well.

[4] Dupuit indicated that for flow towards a well in the center of a circular island in a unconfined aquifer the following assumptions hold: (1) the flow is horizontal, (2) the velocity over the depth of flow is uniform, and (3) the velocity at the free surface is a derivative of the radius towards the well instead of the flow path towards the well.

[5] L=$k_z/b\,(\phi_{source} - \phi)$, where L=the leakage; k_z=the vertical hydraulic conductivity; b=the thickness of the riverbed sediments; ϕ_{source}=the head of the source reservoir; and ϕ=the head in the aquifer itself.

[6] In many groundwater problems, a two order of magnitude contrast in hydraulic conductivity may be sufficient to justify the placement of an impermeable boundary [Anderson & Woessner, 1992].

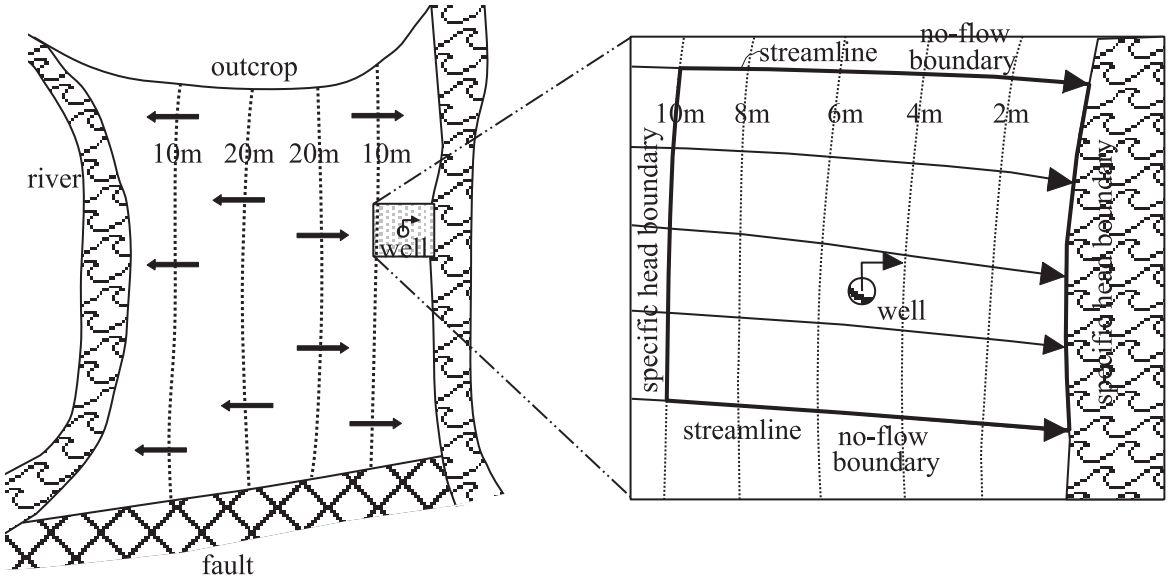

Figure 3.9: *Determination of boundary conditions: zooming in the system is possible as long as the pumping from the well will not affect heads or fluxes in the vicinity of the (hydraulic) boundaries.*

It is not necessary to design a grid with physical boundaries which are located far away from the area of interest, as long as the zone of influence of hydrologic stresses do not reach the boundaries during the simulation. Then, *hydraulic boundaries* closer to your specific hydrological problem are more convenient (see figure 3.9). When the boundary conditions, located far away from your problem, still influence the solution of your hydrological model, you should consider *grid refinement*. In this technique, the solution of a large regional grid is applied to set the boundary conditions (e.g. heads conditions) for the small local grid of the hydrological problem in which you are interested. This technique is often applied in groundwater models which simulate solute transport. A large grid is used for groundwater flow whereas a smaller subgrid is applied for the movement of solutes.

You should avoid using only specified flow conditions for a mathematical reason: a non-unique solution may occur, because then both the boundary conditions (flux is equal to derivatives) and the governing equation are written in terms of derivatives. For example, in steady state groundwater problems, at least one boundary node is necessary to give the model a reference elevation from which the heads can be calculated. Note that it is usually easier to measure heads than fluxes.

After calculations have been carried out, one should be sure whether or not the effects of certain hydrologic stresses in the system (measures such as groundwater extractions) appear at the boundaries of the model: if so, this could lead to wrong results. One of the possibilities is to check the water balance and see if it remains the same. Another possibility is to enlarge the model area and to check whether or not the heads at the location of the (fixed head) boundaries of the original model area are still the same. If so, then the original model area was probably large enough; if not, then the area has to be enlarged, e.g. by expanding the grid and moving the boundaries farther from the area of interest which is

normally situated in the center of the grid.

3.4.4 Initial conditions

When the problem is transient, an initial condition is necessary at the beginning of the simulation everywhere in the hydrologic system.

It appears to be a standard practice to apply the steady state initial condition which is generated with the calibrated model (by setting the storage equal to zero or by setting the time step to a very large value) instead of the initial condition which is obtained with field-measured head values. The reason is that the parameters and hydrologic stresses inserted in the model are consistent with the generated heads and not with the field-measured heads during the early time steps of the simulation. Note that the initial condition generated by the calibrated model is simulated prior to the transient simulation itself. In groundwater models which simulate solute transport, not only the head distribution, but also the solute concentration should be specified at the beginning of the simulation.

Another alternative in selecting a starting variable distribution is to use an arbitrarily defined variable distribution and then run the transient model until it matches field-measured variables. Then, these new calibrated variables are used as starting conditions in predictive simulations. In this selection, the influence of errors in the initial condition diminishes as the simulation progresses. Note that in groundwater models which simulate solute transport, this alternative should not be used, as during the run before the new calibrated heads are found, the solute is transported also. In density dependent groundwater flow, solute influences the groundwater flow, and as such, this alternative cannot be applied either.

In a (normal) groundwater flow problem, the initial condition can be given in three features (see figure 3.10): (1) the static steady state condition in which the head is constant throughout the problem domain and in which there is no flow is the system (e.g. used for drawdown simulations in response to pumping); (2) the dynamic average steady state condition in which the head varies spatially and flow into the system equals flow out the system (this condition is used most frequently); and (3) the dynamic cyclic steady state condition in which the head varies in both space and time (a set of heads represent cyclic water level fluctuations, e.g. monthly head fluctuations or monthly average recharge rates).

In transient situations, it is important to monitor the way in which transient effects propagate at the boundaries. The effects on the boundaries should be evaluated by checking whether the change in flow rate at specified head boundaries and the change in head at specified flow boundaries remain zero between the initial situation and the final time step of the transient simulation.

3.4.5 Preliminary selection of parameters and hydrologic stresses

In this phase, the physiographic characteristics of the hydrologic system (e.g. subsoil parameters as porosity and hydraulic conductivity) and hydrologic stresses (e.g. sources and sinks as injection and pumping well rates; flux across a water table as natural groundwater recharge and leakage through a resistance layer) have to be discretised for the input data

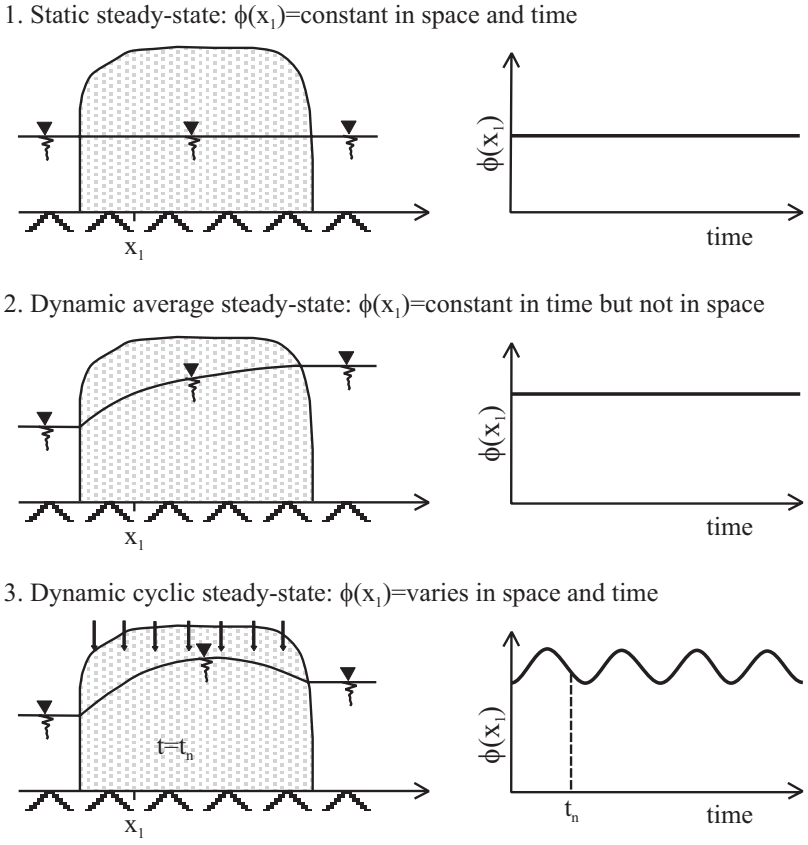

Figure 3.10: *Three types of initial conditions for one-dimensional groundwater flow.*

file of the model. Moreover, mostly numerous other model parameters, such as dummy parameters which set the printing options, must also be inserted in the input data file.

3.5 Calibration

A numerical model, which is applied to simulate hydrologic processes, must be validated with available data in order to prove its predictive capability, accuracy and reliability. Note that in fact, *"a valid model is an unattainable goal of model validation"*. Most hydrological models require adjustments to the system parameters in order to tune the model to match model output with measured data. This procedure of adjusting parameters is called *calibration*[7]. Calibration of a model is one of the most important steps in the application of models. Note that some types of models do not use a calibration procedure, where parameters are assessed from tables and measurements and then used in the model without further adjustment.

The parameters are adjusted within a predetermined range of uncertainty until the model produces results that approximate the set of field measurements selected as *calibration targets*. A calibration target is defined as a calibration value and its associated

[7]Calibration is essentially synonymous to parameter estimation.

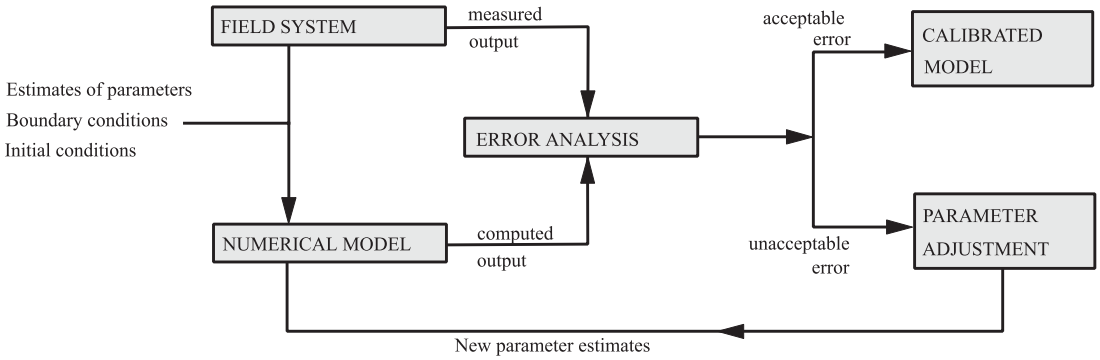

Figure 3.11: *Procedure of the trial-and-error calibration.*

error. The effects of uncertainty in hydrologic parameters, hydrologic stresses, and possibly boundary and initial conditions are tested. Furthermore, both spatial and temporal discretisations are considered. They are varied in the early stages of the calibration and possible adjusted. Most of the time the transmissivities are the least known parameters and thus, they are often modified during the calibration procedure. In addition, when a hydrologic system is in a steady state situation, the calibration is more easily then when the hydrologic system is in a transient situation, because one of the unknown parameters, viz. the storativity, drops out. The accuracy of the whole study will depend on the level of calibration achieved. Though calibration procedures vary from model to model, general alternatives can be listed:

I. Trial-and-error calibration

In this alternative, the user inputs all the parameters that can be based on physical observation, and provides estimates of the unknown parameters as a first trial. As such, the adjustment of parameters is manual. The model is run and the computed output is compared to the measured output from the prototype (figure 3.11). The comparison is done by means of visual pattern recognition of the measured and computed flow hydrographs or solute distributions, or it is based on some mathematical criterion. Based on this comparison, adjustments are made to one or more of the trial parameters to improve the fit between measured and computed output. The trial runs of the model are repeated until some kind of required accuracy or calibration target is achieved. Tens to hundreds of runs are typically needed to achieve calibration. Parameters which are known with a high degree of certainty should only be modified sightly or not at all during the calibration procedure. The modeller can influence the trail-and-error process twofold: by applying expertise on the responses of the hydrologic process to changes in parameters and conditions, and by applying subjective unquantifiable information.

II. Automated parameter estimation codes

In this alternative, also called *the inverse problem*[8], the model itself contains internal programming which will adjust the trial parameters in a systematic step by step

[8]Invers modelling means that point measurements of piezometric heads and solute concentrations are used to obtain a better estimate of subsoil parameters.

manner until the goodness of fit criterion (viz. the calibration target) is satisfied (note that it is a subjective choice to what is a close enough fit). In this way, the model will automatically calibrate itself and carry out the necessary number of trial runs until the best set of parameters is achieved. The purpose is to minimise an objective function such as to minimise the sum of the square residuals (which are the difference between measured and computed heads), whereas the likelihood or plausibility of the applied parameters should be maximised. For this goal, a statistical framework is formulated to quantify the errors in parameters. For example, in a so-called *weighted least square statistical framework* prior information is weighted to place emphasis on measurements that are thought to be of higher reliability, whereas in a so-called *Fisherian statistical framework* the subjective procedure of assigning reliability weights to piezometric heads and parameter measurements is avoided. Note that unstable and unreasonable solutions can also be possible (e.g. by giving negative parameters). Only now in the 1990's, computer codes, that perform automated calibration, are actually introduced to the modellers, though it may take still some time before the use of automated calibration codes becomes standard practice due to the complexity of most hydrological problems. In contrast with the trial-and-error calibration, this alternative gives information on the degree of uncertainty in the final parameter selection and it gives the statistically best solution.

III. Combination of I and II

In this alternative, first a trail-and-error manual adjustment of parameters is carried out until the model is almost calibrated, then to introduce the automatic search technique to refine the goodness of fit.

A model calibrated with the automated technique is not necessarily superior to a model calibrated with the trial-and-error method. Points in favour of the automated calibration codes is that they are objective compared to the trial-and-error method, they provide information on uncertainty in the calibrated parameters and they may speed the modeller in the time-consuming (thus expensive) and frustrating part of the modelling protocol. On the other hand, they are criticized because of problems of non-uniqueness (e.g. due to the absence of prior information on transmissivities in groundwater problems) and instability.

To decrease the uncertainty of the calibration, the errors in the sample information or calibration values should be minimised. Examples of such errors are:

- interpolation errors, as the calibration values do not coincide with nodes.
- measurement errors, which are associated with the measuring device, the operator, and the location of the observation point.
- errors due to transient effects, which may be present in the field-measured values but are not included in the model.
- errors due to scaling effects, which may be caused by small-scale heterogeneities but are not captured in the model. Moreover, scaling effects are also caused by the conversion from field-measured values to point values required in the model (e.g. the head in an observation well represents the head over the entire length of the screen, whereas

in two-dimensional models in vertical cross-sections or three-dimensional models the head is required as point values).

Some presentation techniques to show the calibration results are: (1) to present the results in a tabular listing of calibration targets versus simulation values in combination with the *residual error* (viz. the difference between field-measurement values and computed values); (2) to display the residual errors on a contour map (they should be randomly distributed over the model grid); (3) to display the residual errors on a *scatterplot* which is a linear plot of field-measured values on the horizontal axis versus computed values on the vertical axis; (4) to calculate the average measure of the residual, such as the *mean absolute error* (viz. average of the absolute values of the residuals) or the *root mean squared error* (viz. average of the squares of the residuals), see page 39.

Model calibration can be performed to steady state or transient data sets. It is common practice to begin the calibration of a transient hydrologic process with a steady state data set and then to continue the calibration under the transient conditions. The selection of a proper steady state data set can be difficult, especially when the hydrologic process to be modelled is really a transient one. For example, it is complicated to define a steady state water level when seasonal fluctuations in water level are large.

Models can be calibrated to time series (e.g. changes in water level in response to a drought, discharge in a channel, solute concentration in an observation well, pumping test data in response to long-term pumping or to a particular moment in time (e.g. contour map of water levels, solute concentrations, rainfall).

Note that, in general, calibration does not have a unique solution: different acceptable sets of parameters may give reliable results. Moreover, the possibility to a non-unique solution is enhanced if there is no or little prior information on parameters, if the calibration targets are large, and/or if the calibration targets are few and poorly distributed. It is advisable to use both heads and fluxes to increase the likelihood of a unique calibration. It should be the hydrologist's experience to tell which set of parameters is the most likelihood.

3.5.1 Evaluating the calibration

The results of the calibration should be evaluated both qualitatively and quantitatively. Whether or not the fit between model and reality is good is a subjective judgment. For example, statements such as

> *"The measured and computed contours compared favourable, and therefore, the transient state model is considered calibrated."*

cannot easily be evaluated.

Traditionally, two methods are used to evaluate the calibration: (a) qualitatively, by comparison of contour maps of measured[9] and computed parameters, which provides only a *qualitative* measure of the similarity between the patterns; and (b) quantitatively, by a scatterplot of measured and computed parameters, where the deviation of points from the straight line should be randomly distributed. The objective is to minimise the error in the calibration. Three ways of expressing the average difference between measured and computed parameters are normally used to quantify the *average* error in the calibration:

[9] Note that interpolation techniques also introduce errors in the contour map of the measured parameters.

1. The mean error (ME)
   which is the mean difference between measured ($p_{measured}$) and computed ($p_{computed}$) parameters, such as piezometric heads:

$$\mathrm{ME} = \frac{1}{n}\sum_{i=1}^{n}(p_{measured} - p_{computed})_i \tag{3.1}$$

   where

   - n = number of calibration values,

   As both negative and positive differences are incorporated in the calculation, they may cancel out the error. As such, a small error may not indicate a good calibration, and this way of quantifying the error should be used with care.

2. The mean absolute error (MAE)
   which is the mean of the absolute value of the difference between measured and computed parameters:

$$\mathrm{MAE} = \frac{1}{n}\sum_{i=1}^{n}|(p_{measured} - p_{computed})_i| \tag{3.2}$$

   This error clears away the difficulty in item 1.

3. The root mean squared error (RMS), standard deviation or standard error of estimate (SE)
   which is the average of the squared differences between measured and computed parameters:

$$\mathrm{RMS} = \left[\frac{1}{n}\sum_{i=1}^{n}(p_{measured} - p_{computed})_i^2\right]^{0.5} \tag{3.3}$$

   This error is usually thought to be the best measure of error if errors are normally distributed.

Ideally, the maximum acceptable value of the calibration criterion should be established prior to the calibration, though normally, it is set during the calibration itself.

The evaluation of the model calibration can be quantified by using so-called *levels of calibration*, viz. level ξ means that the computed value falls within ξ times the associated error of the calibration target. For example, level 1 represents the highest level of calibration as the computed value lies within the calibration target. For each calibrated parameter one map is required, e.g. for head or solute concentration (at each time step when transient). The results can also be presented in tabular form, in box plots (see figure 3.12) or in a time series plot.

3.5.2 Error criterion

When iteration is involved to solve the mathematical equations, an *error criterion* or *convergence criterion* can be used to judge whether or not the solution converges. Iteration stops when the change in e.g. fluxes, water balance, heads or solutes (the latter two in all

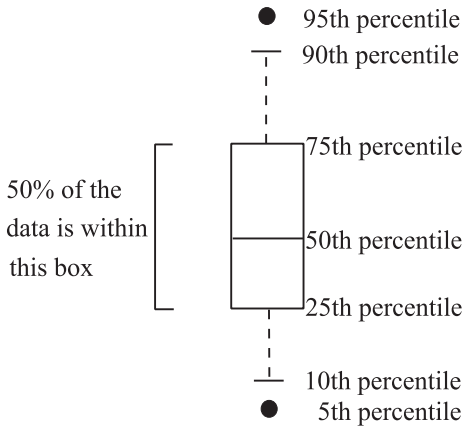

Figure 3.12: *Box plot of data which graphically represents the experimental distribution: continuous lines show the quartiles and the median (thus the box contains 50 % of the data) and the discontinuous lines contain 80 % of the data.*

elements) between two successive iterations is less than the error criterion. As a rule of thumb, the error criterion should be one or two orders of magnitude smaller than the level of accuracy desired in the results. The residual error of the iteration should progressively decrease during the solution of the mathematical equations.

For example, the accuracy of the solution of the groundwater flow equation in the MOC[10] code of Konikow & Bredehoeft [1978] can easily be enlarged by decreasing the value of the convergence criterion TOL. Numerous causes are possible if the solution fails to converge. Examples of such causes are: the initial guesses of variables and parameters may be inappropriate (e.g. transmissivity is so large that within one time step all groundwater is pumped out of the aquifer, the contrast in transmissivity between an aquifer and an aquitard is too large); the grid design may be incorrect (e.g. modelling a sloping groundwater flow system by means of a grid with rectangular elements may induce difficulties); errors can be made in typing input into computer files (print and check the output file); the error criterion is set below the precision of numerical solution (no convergence can be reached due to machine truncation); and the concept of the model may be poor (e.g. a model for simulating steady state groundwater flow in an aquifer with natural groundwater recharge and no-flow boundaries).

The check on the water balance can be very useful in designing the model. For example, when the fluxes to or from the model are unreasonable high or low, then the inserted transmissivity file may be wrong, whereas unreasonable high or low volumes of water entering or leaving the storage may indicate a wrong storage parameter. As a rule of thumb, the ideal error in the water balance for numerical modelling should be less than 0.1 %, whereas an error around 1 % is usually considered acceptable.

In the following example, the water balance of a groundwater flow system is considered. The incoming and outgoing water masses over a boundary are determined from the velocities perpendicular to that boundary and the lengths of the boundary segments. In

[10]Nowadays, MOC is also called USGS 2-D TRANSPORT.

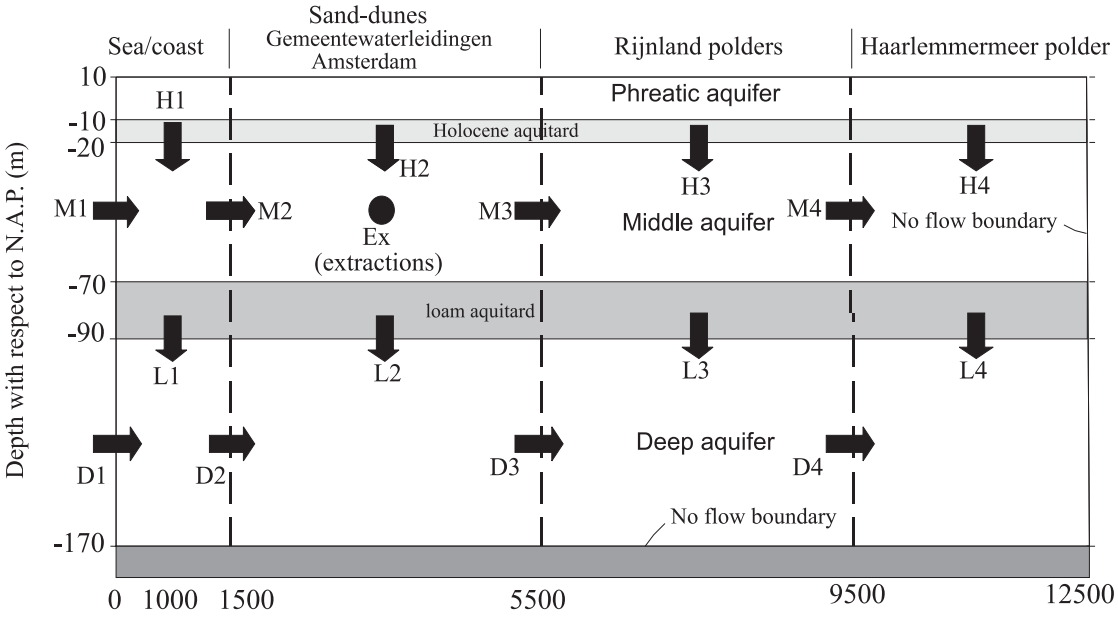

Figure 3.13: *Symbols of water masses in the hydrogeologic system of the sand-dune area of Gemeentewaterleidingen Amsterdam.*

Table 3.2: *Flow of water masses in million m^3/yr during some specific years. See figure 3.13 for the meaning of the symbols.*

Holocene aquitard				Middle aquifer				Loam aquitard				Deep aquifer				Extr.
H1	H2	H3	H4	M1	M2	M3	M4	L1	L2	L3	L4	D1	D2	D3	D4	Ex
1853: before the reclamation of the Haarlemmermeer polder																
0.0	6.3	-4.1	-0.8	-1.2	-2.2	2.2	0.2	1.0	1.9	-2.1	-0.6	-0.2	0.8	2.7	0.6	-
1956: high rates of groundwater extractions																
0.5	7.5	3.6	-4.5	2.8	3.1	-0.4	2.5	0.2	-6.9	0.7	-2.0	8.0	8.2	1.3	2.0	17.9
1987: low rates of groundwater extractions																
-0.2	5.2	0.3	-5.9	0.3	-0.3	1.8	2.9	0.4	1.4	-0.8	-3.0	2.0	2.4	3.8	3.0	1.7

figure 3.13, the symbols and positive directions of the water masses are given flowing over specific boundary segments of the hydrogeologic system. Table 3.2 shows the flow of water masses at the sand-dune area of Gemeentewaterleidingen Amsterdam during specific years in million m^3/yr. In the year 1854 AD the lake Haarlemmermeer was completely reclaimed. Before 1854, groundwater has flowed from the deep and middle aquifers towards the sea (the symbols M1 and D1), while since 1854 salinisation of the hydrogeologic system occurs. Moreover, high groundwater extraction rates from the middle aquifer (symbolised by Ex) at the sand-dune area of Gemeentewaterleidingen Amsterdam seriously affect the groundwater flow in the hydrogeologic system. For example, the salt water intrusion from the sea in both the deep and middle aquifer is more severe in 1956 than in 1987, when the groundwater extraction rates from the middle aquifer are again low. Based on these simulations, the effects of different groundwater extraction rates can be assessed.

In addition, errors in the computed output variables may also arise due to wrong discretisations of both time and space. Some solution techniques have a limit on the time

step as otherwise the solution does not converge. For example, the size of the grid Δx may be restricted when the finite element method solves solute transport (by means of the advection-dispersion equation) in combination with groundwater flow (e.g. the Peclet number should be small, up to maximum 10, see section 8.3).

3.5.3 First model execution

In general, the making of the first error-free output will probably require many additional hours, at least, more than you expected. The whole phase of the *first model execution* includes the preparation of the input data file, the entry of input data file into computer lines, the execution of the model (the so-called *run*), and the interpretation of the results.

Preparing the input data file can be time-consuming if the problem is complex and/or if you, as a modeller, are unfamiliar with the code. Many computer codes are written in FORTRAN (viz. FORmula TRANslator), probably because the creators are raised with this symbolic algorithm computer language. If not written properly, this language can be very chaotic and difficult to understand. In a badly written FORTRAN programme the statement GO TO causes switches between different parts of the programme, and the programme can rapidly be a fuzzy and indistinct one. In addition, old versions of FORTRAN requires that data in the input data file have specific formats.

Some entry errors during the first runs due to a wrong input data file is normal, and usually, after a few runs these errors are removed. Preprocessors may help you in assembling the input data file by means of user-friendly screen menus. However, if not all options are included in these preprocessors, they may limit the flexibility of the model. As such, a familiar user would probably prefer to compose the input data file directly, e.g. by means of a simple editor. Note that, at present, many preprocessors are available, so this step will rapidly be passed by.

To execute the model, an executable file of the computer code must be produced by an appropriate *compiler*. A compiler reads the source code and generates machine language statements for the computer hardware. A computer system with sufficient *random access memory* (RAM) is required to store data and arrays during the execution of the model. Until a few years ago, most FORTRAN compilers on the Personal computer accessed only 640 Kb of RAM, which is the standard memory limit of DOS. As such, the possibility to store large amounts of data was limited. So, the arrays which represent the parameters and the number of elements should not be dimensioned too large. The problem of insufficient memory, the so-called *memory problem* has recently been solved. Since the late 1980's, much more memory is available on the personal computer: the so-called *Extended Memory RAM* (EM RAM). Executables of computer codes can address this EM RAM beyond the usual 640 Kb RAM-limit of DOS through sophisticated compilers (e.g. the Lahey Fortran compiler F77L-EM/32 in combination with the Lahey/Ergo/Phar-Lab 386 Operating System). As such, even stand-alone personal computers can accommodate a much larger number of elements than under 640 Kb of conventional RAM. Meanwhile, as three-dimensional models appear more and more on the scene, much more data must be stored, and consequently, the EM RAM must increase simultaneously. Now, in 1999, the true application on a broad scale of three-dimensional models for (regional) complex geometries is still in a primary stage, even though the computer systems rapidly increase their abilities in terms of processors

Table 3.3: *Execution time of different computer systems (processors) with different MHz on a benchmark problem [Anderson & Woessner, 1992].*

Computer system	Speed (relative to PC)
PC	1
XT	1.9
286 (AT)	7.0
386 16 MHz	9.7
386 25 MHz	9.9
486 25 MHz	29.8
486 33 MHz	39.3
486 50 MHz†	49.7
Pentium 120 MHz†	186.4
SUN OS 5.7 UNIX †*	293.2
Pentium Pro 200 MHz†	382.7
SUN OS 5.5.1 UNIX †‡	1186.4
Pentium III 733 MHz†	1461.3

†: based on Oude Essink's experience.
*: UNIX workstation at Geophysics with 495 Mb EM RAM.
‡: UNIX workstation at Geophysics with 1500 Mb EM RAM.

(disk-speed) and RAM (standard computer systems contain several (tens of) Mb of EM RAM, see also figure 1.1).

The length of time necessary to execute the computations with the computer programme for a given set of input data of a hydrological problem is the so-called *execution time*. This execution time depends on four factors:

a. the speed of the computer

Table 3.3 illustrates how some types of computer systems perform. Note that the difference in MHz does not matter much. As can be seen, the new computer systems with faster processors (disk-speed) open the application of three-dimensional modelling.

b. the size of the model

The number of nodes and type of the governing equations being solved determines the size of the model. The larger the number of elements, the longer the execution time will be. The arrays which represent the parameters and the number of elements should not be dimensioned too large, as otherwise, insufficient memory is available. Table 3.4 shows how much memory is required for the groundwater computer code MOC as a function of the number of elements and the initial number of particles. In addition, table 3.5 gives the number of elements or grid blocks of some other computer codes.

c. the efficiency of the compiler

Some compilers go through commands and information more efficiently than others. For example, the Lahey Fortran compiler (e.g. F77L-EM/32) can very rapidly compile

Table 3.4: *Total memory required in* Mb *as a function of elements and the initial number of particles per element for the groundwater code MOC [Konikow & Bredehoeft, 1978; Oude Essink, 1996].*

Number of elements	Number of particles per element	Total initial number of particles per grid	Total memory requirement (Mb)
†400	8	3200	0.302
900	4	3600	0.418
900	9	8100	0.490
900	16	14,400	0.591
3200	9	28,800	1.249
7200	9	64,800	2.551
10,000	9	90,000	3.454
20,000	9	180,000	6.693
50,000	9	450,000	16.410
†: these are the characteristics of the original MOC code in 1978.			

Table 3.5: *The number of elements or grid blocks of executable computer codes depends on the free Extended Memory RAM (EM RAM) of the computer [source: Scientific Software Group, 1996]. Note that, e.g., in an 8 Mb EM RAM personal computer, only some 7 Mb is free for memory allocation.*

Computer code	Extended Memory RAM (Mb)	Number of 2D or 3D elements
MOCDENSE (2D)†	2.5	2500
SUTRA (2D)‡	4	1300
	8	2175
	16	6525
HST3D (3D)	4	2500
	8	7000
	16	14,000
MODFLOW (3D)	◇4	60,000
MOCDENS3D⋆	74 (8 particles/element)	125,000
	43 (27 particles/element)	40,000

†: MOCDENSE [Sanford & Konikow, 1985] is an adapted version of MOC, developed for vertical cross-sections (it is based on pressures).

‡: the main reason for this small number of elements relative to MOC is that SUTRA [Voss, 1984] has to allocate arrays for additional subsoil characteristics.

◇: it is also possible to apply a virtual memory system, which uses disk storage to supplement the computer's memory. Note, however, that then the computer speed will drop significantly.

⋆: MOCDENS3D [Oude Essink, 1998] is an adapted version of MOC3D [Konikow *et al.*, 1996], which can simulate density dependent groundwater flow (see also the lectures notes of Hydrological Transport Processes/Groundwater) Modelling II [Oude Essink, 2000].

FORTRAN-codes. This compiler for personal computers could already address the EM RAM at least since the end of the 1980's.

d. the type of the output device

Some models ask for keyboard input during the execution or frequently write to the screen printer or even an output file. These actions increase the execution time (massive output files of several Mb's may increase the execution time substantially). Examine whether or not you can reduce the output devices after the first model execution is finished, e.g. by setting the printing options to minimal output.

3.5.4 Sensitivity analysis

Given that the calibration may be non-unique, you have no guarantee that the predictive model will produce accurate results when the model is stressed differently from the calibrated conditions. Moreover, calibration is difficult as values for hydrologic parameters, stresses and boundary conditions are typically known at only a few nodes and are associated with uncertainty. In addition, there is even uncertainty about the geometry of the hydrologic system (e.g. lithology and stratigraphy) you are trying to analyse. In order to reduce the uncertainty, it is essential to subject the (already) calibrated model to a so-called *sensitivity analysis*. The purpose of a sensitivity analysis is to quantify the uncertainty in the calibrated model. A sensitivity analysis is typically performed by changing the value of one parameter at a time. The widest range of plausible solutions can also be examined by changing two or more parameters. The procedure of calculating sensitivities can also be automated or can be done by stochastic modelling.

During the sensitivity analysis, calibrated values of the most important hydrological parameters, such as transmissivities, are systematically changed within a (previous established) plausible range, e.g. by means of a coefficient of variation (standard deviation divided by the expected value). The sensitivity analysis of a parameter has its effect on relevant variables of the hydrologic process, such as head, solute concentration, sources of water to a pumping well, etc.

3.5.5 Kriging

Kriging is a method for optimizing the estimation of the spatial distribution of parameters in a network of already measured points (figure 3.14). It is a statistical interpolation method that chooses the best linear unbiased estimate (the so-called *BLUE*) for the variable in question. Kriging differs from other interpolation methods because it considers the spatial structure of the parameter and provides an estimate of the interpolation error in the form of a standard deviation of the kriged values. Moreover, kriging preserves the field value at measurement points. In hydrology, kriging has a wide variety of applications, such as:

- calculation of rainfall, temperatures, sunshine, etc., based on measurements from climatological stations.
- interpolation of thickness or elevation of geological formations based on logging of wells[11].

[11] The record of any phase of well drilling can be called a log [Davis & DeWiest, 1966].

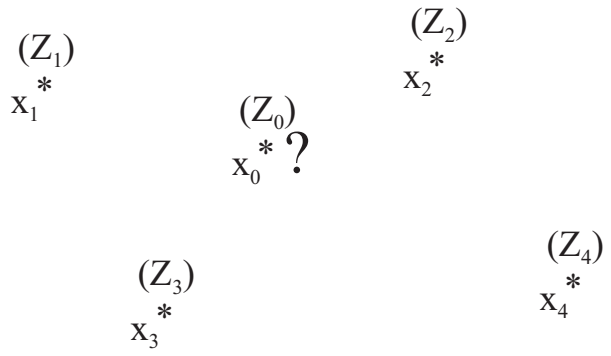

Figure 3.14: *Kriging: the so-called point estimation is based on the determination of the quantity Z_0 for any x_0 that has not been measured. By modifying the position of x_0, the whole field of Z can be estimated.*

- estimation of hydrogeological parameters (transmissivities, piezometric heads, solute concentrations) based on measurements in wells.

Kriging can also be used: (1) to estimate the confidence interval of an estimation, (2) to estimate the mean value on a given block (e.g. on the mesh of a grid of subdomain), and (3) to locate the best situation for a new measurement point through minimising the overall uncertainty in the field. Based on item (1) and (2), kriging can help to estimate parameters. Better estimates of parameters can be obtained when prior information is used in the analysis. The error estimates are applied in assigning plausible, reasonable ranges of parameters in the hydrologic setting.

3.6 Model verification

Due to a number of uncertainties, the set of parameters used in the calibrated model may not accurately represent the real hydrologic system. As such, it may occur that under a different set of hydrologic stresses, the hydrologic system is not accurately represented by the calibrated parameters. In order to improve the confidence in the calibration of the model, the model has to be tested by using a second independent set of data. This is called the *model verification* or *model validation* (see figure 3.15). The normal procedure is to split a record in half: one half for calibration and one half for verification.

A so-called *verification target* is satisfied when the accuracy and predictive capability of the model have been proven to lie within acceptable limits of error. A model is verified when the verification targets are matched without changing the calibrated parameters. If it is necessary to adjust parameters during the model verification because the verification targets are not matched, the verification becomes a second calibration and other independent data sets should be needed until the verification of the model is performed. Unfortunately, it is often impossible to verify a model because usually only one (reliable) set of data is available, which is already needed for the calibration. This is the so-called *verification-problem*.

"Once the available record has been used for calibration, there is nothing left

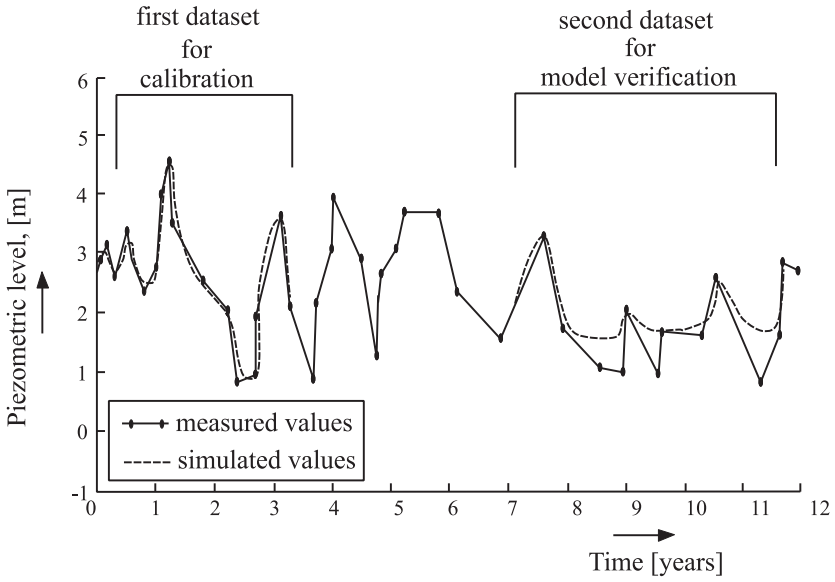

Figure 3.15: *Verification of a model: a new set of independent data is used to check whether or not the calibrated model is capable of accurately simulating a transient response.*

> *for model verification, and consequently, the adequacy of the model cannot be challenged by 'comparison with the actuality'...*" [Klemeš, 1986].

As such, the results simulated with an unverified model are generally more uncertain than with a verified model. Nevertheless, a calibrated but unverified model can still be applied to make predictions as long as the sensitivity analysis of the calibrated model is performed accurately.

3.7 Simulation

Whereas the objective of calibration was to demonstrate that the calibrated model can reproduce measured hydrologic processes, the ultimate modelling objective is to produce a model that can accurately simulate or predict (future) conditions for which no data is available. Once a model is calibrated as well as verified, it can be used for predicting the response of the hydrologic system to events either in the past, present or future. The confidence which is placed in model predictions largely depends on the results of the calibration, the verification and the sensitivity analysis.

An important problem is to determine the length of time for which the model accurately predict the response of the hydrologic process in the future. Klemeš [1986] subdivided the extrapolation of the calibrated and verified model is three categories, ranked in order of diminishing possibility of checking the results by observations:

1. short-term forecasting and prediction

   In this category, we can often rely on the laws of fluid mechanics and hydraulics. At

the most, interpolation and short extrapolation occurs. The availability of test data provide a relatively good safeguard against misconceptions.

2. hydrologic simulation
   In this category, at least an indirect testing on analogous empirical data is often possible. It is mentioned that a predictive simulation should not be extended into the future more than *twice* the period for which the calibration data are available.

3. long-term forecasting and prediction
   In this third category, the possibility of testing is nonexistent. Some environmental problems require a length of time of many years, perhaps as many as 10,000 years (see figure 3.8: long-term processes are taking place in the glaciers, regional groundwater; obviously, geological processes are also long-term processes). For example, as groundwater flow and solute transport are slow processes, a long simulation time of several centuries for large-scale coastal groundwater flow systems is not rare.

The results of predictive modelling are uncertain because of two reasons: (1) uncertainty in the calibrated model (the same parameters are used which are determined during the calibration and verification steps), and (2) uncertainty about the future hydrologic stresses. The likelihood of future hydrologic and human-regulated events such as future pumping rates introduce errors in the simulations. A sensitivity analysis is necessary to assess the effect of both calibrated parameters and hydrologic stresses on the results of the simulations.

Then, scenarios are formulated to assess future hydrologic stresses, such as human activities. If the number of scenarios is very large, a number of representative scenarios should be selected. Subsequently, the scenarios should be executed and the results should be presented.

3.8 Presentation of results

In this (final) phase, a report has to be completed. A good report is essential to the effective completion of the modelling study. A modelling report should contain the following elements[12]:

- purpose of the model
  An informative title of the report should reflect the goal or objective of your (modelling) effort. The long-term goal of the hydrological study should be recognised in this element. The success of the study will be judged by the degree to which the objectives are met. The overall approach or strategy to accomplish the goal of this study must be pointed out. A location map of the studied area should be presented.

- formulation of the concept of the model
  Field data (e.g. geologic and topographic setting, hydrologic parameters) and assumptions should not only be supplied to formulate the concept of the model, but also for

[12]Note that the standard elements of a report, such as a summary, conclusions, recommendations for further research, list of references and appendices with additional or supplemental information, are not considered in this listing of a modelling report.

several other reasons: to set the reasonable ranges of parameters, to calculate initial conditions, to calibrate the model and to estimate water balances. A definition of hydrostratigraphic units and water and/or solute budget information should be provided. The governing equations of the hydrologic process you want to model should be formulated.

- information about the computer code
  Especially information about the code should be added, if the computer code is a new one. Details of the governing equations, how boundary conditions are handled, data input requirements, the numerical method used to solve the equations, modifications in the code (if applicable), code verification results, a listing of the code and a user's manual (in appendices).

- model design
  The relation between the concept of the model and the numerical model should be described. The boundary conditions and initial conditions are selected. The parameters of the hydrologic system used in the model are set. The applied temporal as well as the spatial discretisations of the numerical model are defined, in combination with locations of the boundaries and types of the hydrologic stresses. The uncertainty of parameters and stresses must be discussed.

- calibration and model verification
  The calibration targets are defined. The sources and magnitudes of each calibration value are described. The changes in calibration values which led to the model calibration are described. The matches between measured and computed parameters are recorded by means of contours and/or box plots of residuals, location and value of calibration targets and plots of mean error, mean absolute error or root mean squared error as a function of calibration run number. A list of parameters, boundaries and stresses of the final calibrated model should be implemented. A second dataset which is used for model verification should be applied.

- sensitivity analysis
  The sensitivity of the results to variations in parameters, grid size, boundary conditions, and calibration criterion should be documented.

- results of the predictive simulations
  The scenarios of stresses (both natural and human-induced future alterations) to the hydrologic system are defined. The consequences of changes in stresses (e.g. water management practices) through graphical presentation are described. Information should be collected on the assumptions, uncertainties and limitations of the predictions, e.g. by means of a sensitivity analysis to quantify the effect of uncertainties in future changes in the hydrologic system. The limitations of the modelling effort itself should be discussed, such as the reliability of the calibration and sensitivity analyses, in order to state that the modelling results can be applied by decision makers, e.g. for water management practices.

In conclusion, sufficient data should be included in the report to allow a reader to reproduce your modelling effort.

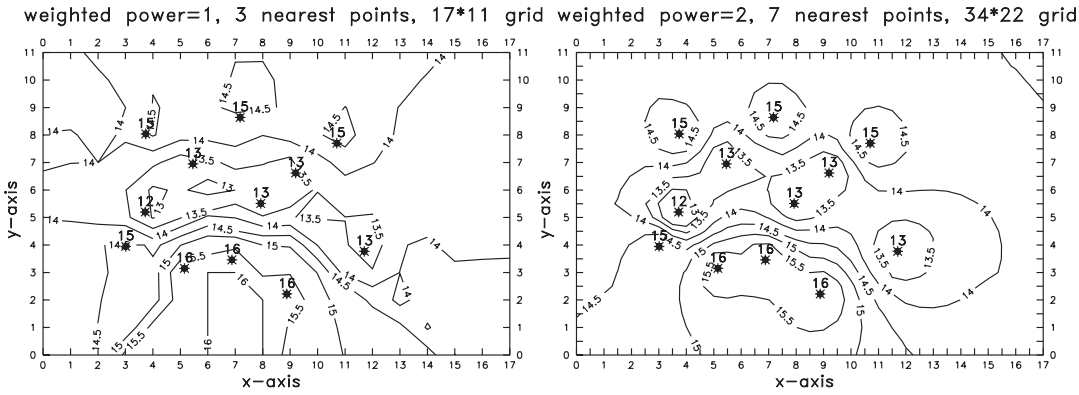

Figure 3.16: *Differences in contour lines in the* Inverse Distance *interpolation technique of SURFER due to different options: the weight is raised to a power to increase the influence of other nodes close to the node considered; the number of nearest points around the current grid node is increased which are applied in the calculation of the current grid node; and the grid size is increased from 1.0 versus 0.5.*

During a typical modelling study, parameters, boundary and initial conditions, and even (lines in) the computer code are changed. Therefore, it is advisable to keep a journal. Anyway, normally, you will start modelling with good intentions of recording each change in the original design and its effects on the modelling process, but when modelling is getting under way and the deadline is approaching, it may occur that the inclination to recording changes is diminishing. Moreover, the journal can help you in preparing the report. By documenting your modelling effort, the model can be regenerated after a time, e.g. by another investigator (see section 3.9). The journal should archive the purpose of each model run, the modifications of the computer code (if applicable), the changes in input files, and the effects of the changes on the results.

Nowadays, the graphical presentation of data output has really become professional. A large number of sophisticated graphical modules makes simulations understandable, (more) reliable, and more easy to interpret. However, remain critical, as impressive pictures could distract you from the real purpose of the modelling process. Several software packages are capable of generating smooth contour maps by applying interpolation techniques. In those software packages, an option is applied to eliminate irregularities in the output data. For example, in the SURFER software package, three interpolation techniques can be used: viz. *Inverse distance*, *Kriging* and *Minimum curvature*. The gridding interpolation method Inverse Distance, which is the most commonly used (default) technique SURFER applies, assumes a so-called *weighted average technique* to interpolate grid node from the XYZ data file. The weights are inversely proportional with the distance to the grid nodes. Data points further away from a given grid node will have less influence. Figure 3.16 shows that the contour maps can be significantly different due to different options in the method applied. Be aware that such techniques may manipulate the modelling results.

Mostly, results from model simulations are used by decision makers to plan the future changes in hydrologic processes. Therefore, the results of your simulations should (somewhat) be adapted to the imaginative powers of the decision maker.

3.9 Postaudit

Postaudits[13] or verifications of the complete modelling result examine the accuracy of a prediction by a model which was executed a considerable number of years ago (e.g. at least 10 years to allow adequate time for the hydrologic system to move far from the calibrated solution). As such, these postaudits can help us in answering the question: *"How good can models predict the future ?"*.

As there are large-scale (regional) hydrologic systems which have been simulated to predict long-term response to some applied stress since the 1960's, a number of postaudits can be possible. Now, in the 1990's, it is possible to evaluate the modelling effort in those years, for example by applying another computer code, another concept of the model, different boundary conditions or parameters. This method to increase the confidence in modelling is more reliable than methods which apply automated calibration techniques or stochastic simulations. There exists also the iterative way of improving a model to achieve a better calibration to measured conditions. When new data become available over the years, the concept of the model should be evaluated. If the concept of the model should be changed, then changes should also be incorporated into the numerical model.

For example, Anderson & Woessner [1992] discussed four postaudits, which were the four groundwater flow problems reported in literature up to that moment (in 1992). Though numerous predictive modelling studies have been executed since the 1960's, it can be stated, based on the small number of postaudits, that models are (traditionally) used rather in a crisis mode, to answer some pressing question and to be forgotten after served this purpose, than in a management mode on a day-to-day, month-to-month, or year-to-year basis. Two problems evaluated the response of pumping by means of electric analogue models, and the other two problems described solute transport in combination with groundwater flow by means of digital models. Anderson & Woessner [1992] concluded that all four models did not accurately predict the future, mainly due to:

1. errors in the concept of the model of the hydrologic system

   The modeller did not define a proper concept of the model. They defined an inadequate description of the state of the hydrologic system, and as a result, errors were introduced. Based in the four postaudits, errors did not occur due to the numerical or theoretical deficiencies in the model itself. For example, in one postaudit, to predict more reliable water level changes due to pumping, the concept of the model would be improved significantly if changes in aquifer storage and transmissivity could be represented in three-dimensions instead of in the two-dimensions of the electric analogue model.

2. errors in the estimations of future hydrologic stresses

   The errors in future stresses, such as recharge, pumping and contaminant loading rates, are easy to be understood, as we tend to extrapolate current trends into the future, though the current trends may not apply to future events. To overcome this problem, scenarios of future (hydrologic) stresses with different trends were applied in order to define a range in the predicted values.

[13] Dutch: 'na-controle'.

Table 3.6: *Comparison of prognoses of future sea level rise in cm relative to 1980, except for the prognosis of Oerlemans which is relative to 1985 and the estimates of the Intergovernmental Panel of Climate Change (IPCC).*

Author	2000	2025	2050	2075	2100
Extrapolation of historic data[a]	2-3	4.5-6.8	7-10.5	9.5-14.3	12-18
Revelle [1983][b]	70 in 2085 relative to 1980				
Hoffman *et al.* [1984]:[c]					
- Conservative Scenario	4.8	13.0	23.8	38.0	56.2
- Mid-range Moderate Scenario	8.8	26.2	52.3	91.2	144.4
- Mid-range High Scenario	13.2	39.3	78.6	136.8	216.6
- High Scenario	17.1	54.9	116.7	212.7	345.0
Polar Research Board [1985][d]	50-200 in 2100 relative to 1980				
Villach II Conference [1985][e]	20-140 when global warming is 1.5^oC to 4.5^oC.				
Robin [1986][f]		25.1	52.6	70.8	89.1
Oerlemans [1989]		20.5	33.0	50.5	65.6
IPCC [1990]	31-110 in 1990-2090, 66 *cm* as the best estimate				
IPCC [1995][g]	20-86 in 1990-2090, 49 *cm* as the best estimate				

[a] The historical sea level rises have been estimated by Barnett [1983] and Gornitz *et al.* [1982]: 10 à 15 cm per century in the period 1880-1980. The data are based on measurements of sea level variations with tidal gauges at particular locations over the past century.

[b] Revelle [Titus, 1987] ignored (and not added) the impact of global warming on Antarctica, though he noted that the latter contribution is likely to be 1 to 2 m/c after 2050.

[c] Hoffman *et al.* [1984] made projections of sea level rises for the next century at intermediate years, based on special case scenarios for changes in greenhouse gases. They assumed that the glacial contribution would be one to two times the contribution of thermal expansion.

[d] The USA National Academy of Science Polar Research Board [Titus, 1987].

[e] The predictions are based on observed changes since the beginning of this century [Bolin, 1986].

[f] These prognoses were calculated by Robin from the sea level-time regression (linear rela-) tionship to estimate sea level rise for a 3.5 K warming [Oerlemans, 1989].

[g] This lower figure is largely due to the downward revision of the rate of global warming.

For example, in the beginning of the 1980's, the predictions of rates of sea level rise were not very consistent (table 3.6). Within some ten years, it became clear that the early predictions were exaggerated. Nowadays, the predictions are more consistent. though several mechanisms, such as the feedbacks of clouds and oceans, are still not completely understood.

In conclusion, the predictions have been inaccurate due to the failures of the modeller, not of the model, though these failures are understandable and unavoidable. In order to overcome uncertainties in future stresses, you need to apply several different possible scenarios of future stresses.

3.10 Why can things go wrong ?

> "*Thus at the present stage of hydrologic science, hydrologic modelling is most credible when it does not pretend to be too sophisticated and all inclusive, and remains confined to those simple situations whose physics is relatively well understood and for which the modeller has developed a good 'common sense' within his primary discipline.*" [Klemeš, 1986].

Remain independent and critical towards the modelling results you have obtained. Never trust the results at first sight. Due to an increase in the complexity of modelling, sophisticated graphical techniques are applied to show comprehensible (simplified) pictures. As such, users and decision makers could get a poor understanding in the underlying idea of the hydrologic process you want to model. If you suspect that the results are not conform to your expectations, you should go back to the source, backwards in the modelling process and ask yourself what may be the cause of this discrepancy in expectation and outcome. Some causes could be:

- the conceptualisation of your problem is wrong. For example, a relevant component of the hydrologic process is not considered, as it was expected to be negligible.
- the governing (partial differential) equations do not comprise all relevant processes in your hydrological problem. Terms are averaged or even neglected which is not allowable in your specific situation, e.g. the dispersive term has been deleted in the solute transport equation. Through evaluating these terms and checking their order of magnitude with respect to the other terms, errors can be located and possibly solved.
- variables and parameters are not assessed properly, e.g. due to a lack in data. Moreover, initial and boundary conditions are not properly assigned or inserted in the input data file, e.g. due to a wrong discretisation of the hydrologic process.
- the computer code you apply may contain errors. In fact, as long as there are new releases (viz. version 3.2), computer codes are not completely finished to perfectly model the hydrologic process involved. You could bring out your findings to the developer of the code who will, (only) in the long run, be grateful of your investigations (provide the developer of sufficient output of the problem that goes wrong).
- numerical problems on wrong discretisations occur regular, such as oscillation and truncation errors (see chapter 8). Check whether different spatial as well as temporal discretisations significantly effect the modelling results. If so, smaller discretisations, smaller time-steps or even more stable numerical schemes should be considered.

Note however, that, in general, good thinking helps, most other things not !

Chapter 4

Data gathering

Obviously, a numerical model, which is applied to simulate a hydrologic process, must be calibrated and verified with available data in order to prove its predictive capability, accuracy and reliability. Regrettably, in many cases reliable and sufficient data are scarce. As such, the data problem, also known as the *parameter crisis*, is one of the most important problems in hydrological modelling, because the accuracy of the modelling results does not only depend on the degree to which the model structure 'correctly' represents the hydrologic process but mostly on the accuracy of the input data. It has no sense to develop a complex model when the input data requirements cannot be satisfied.

It is clear that the field data can be extracted from various sources, obtained from maps, cross-sections, well-logs, borings, data on precipitation, etc. Developments in remote sensing, geographical information systems (GIS) and data processing are with great potentials in the process of data gathering. Regrettably, in many cases sufficiently reliable data are still scarce, because data collection is expensive and labour-intensive. The availability of enough reliable data is obviously even more pinching for three-dimensional models than for two-dimensional models. As such, the application of three-dimensional computer codes is restricted seriously.

The availability of data is important for the conceptual construction of the model as well as the calibration of the numerical model (e.g. see figure 4.1). Examples of data are rainfall data, subsoil parameters (e.g. the hydraulic conductivity, the exact position of aquitards, the effective porosity, the anisotropy, and the hydrodynamic dispersion), groundwater extraction rates, and salinity and piezometric head distributions as a function of space and time. Data are necessary to calibrate the applied model as accurately as possible. When the existing network of recording instruments should be augmented, the records will probably be too short to allow adequate calibration of the mathematical model. Consequently, poor estimates will be given. Unfortunately, long time series are available only occasionally.

For example, calibration of groundwater models with salinities changing over time and space is still rather laborious. As the flow of groundwater and subsequently the transport of hydrochemical constituents are slow processes, it takes quite some years before (a change in) salinisation can be detected. As such, relative long time series of monitored salinities (of some tens of years or even more) are necessary in order to accurately calibrate 3D salt water intrusion in large-scale coastal aquifers. Unfortunately, these time series are available only occasionally and reliable measurements are scarce in many cases. As a consequence, the calibration will be less reliable. One has to collect many data during many years before a good calibration can be achieved.

The type and amount of parameters that should be measured depends on the purpose of the modelling exercise and on the physiographic characteristics of the hydrologic process

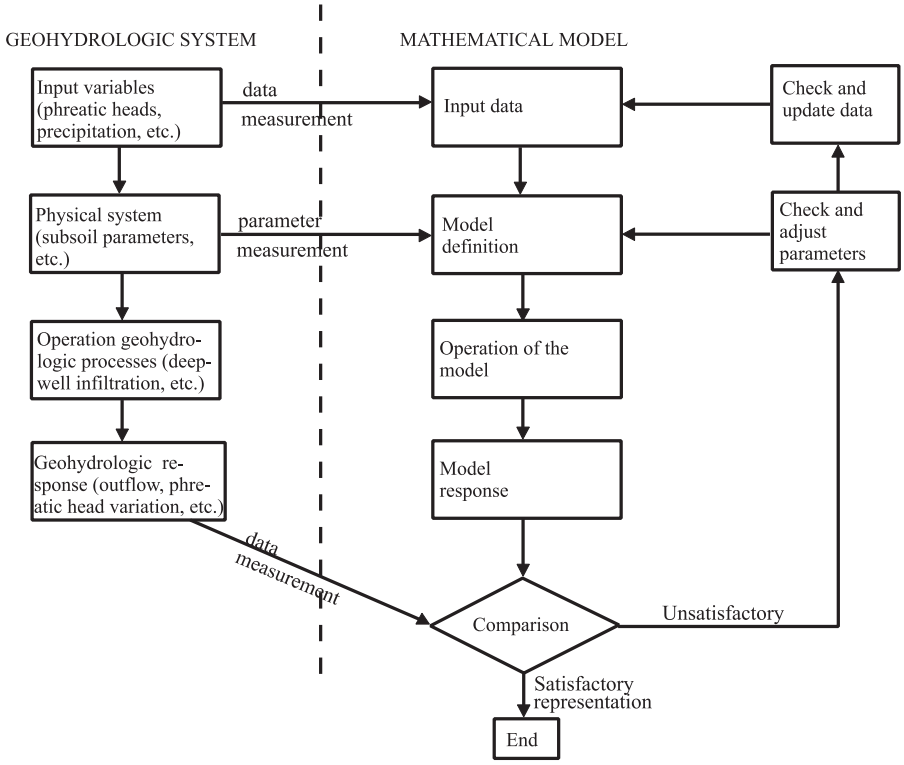

Figure 4.1: *Example of data requirements in a catchment model [modified from Fleming, 1979].*

and, as such, on the structure of the model. Some 'simple' models require only a few parameters, whereas 'complex' (distributed physically-based) models requires large data series.

Moreover, the density of data also depends on the scale of the representative elementary volume (REV, introduced by Bear [1972]) of the modelled hydrologic process. For example, for large-scale (regional) models only data in national data banks may be sufficient, whereas for local, detailed models data can probably be collected in the field.

In addition, for three-dimensional models, the upscaling of data from one-dimension and two-dimensions to three-dimensions may face some difficulties. In fact, the collection of data is one- or two-dimensional. For example, hydrogeologic information is mostly obtained from a point source (e.g. groundwater level from an observation well) or from a line source (hydrogeologic information from a hydrogeologic column). This information must be extrapolated or interpolated to a three-dimensional distribution of subsoil parameters.

Before data can be used in the calibration or application of the mathematical model, they must be checked for errors and deficiencies. For example, long-term errors in precipitation gauges, e.g. due to vegetation growth around a gauge, can be identified by plotting cumulative annual total of the gauge in question against the sum of the cumulative annual totals of the surrounding base gauges. Any long-term inconsistencies will be evident by a change in the slope of the plotted line.

When data series are inaccurate, the gaps in the model data input should be corrected

by correlation with nearby gauges (or weighted average of some more distant gauges) to obtain a homogeneous reliable data series with no gaps.

When data series are absent, the model data input should be filled by stochastic techniques to create data series with statistical characteristics identical to the original data series. Note that stochastic techniques do not account for changes in the hydrologic system, such as climate changes over long periods of time (for generating precipitation data).

Geographical Information System

To solve the data availability problem to a certain extent, so-called *Geographical Information Systems (GIS)* can be very useful. In these systems, all relevant hydrologic data can be stored. By analysing these systems, areas with a lack of data can be detected immediately.

In fact, a GIS only utilises a databank of spatial information. It is able to carry out all kinds of operations with the data, such as subtracting, averaging and interpolating. As such, a GIS provides a functional framework for coupling hydrological models with spatial units. As a user of geographical data, hydrology was in the foreground of the development of GIS at the end of the 1980's. Moreover, remote sensing data, e.g. obtained from satellites, makes it possible to consider large-scale hydrologic systems. For example, research on environmental changes on planetary scale (e.g. climate change and greenhouse effect) employs large-scale hydrologic systems. Distributed models make the greatest use of a GIS, because such models require spatially distributed model parameters. A GIS can obtain model parameters for each grid element from maps or points.

A GIS can be applied to process model input and model output. Basic GIS applications are: (1) digitalize analog data such as maps or time series to provide the geographic reference of variables; (2) accomplish relations between variables by overlaying maps; (3) assess outlines, lengths (e.g. pipes), surfaces (e.g. surface per land use), volumes (e.g. excavations of dumping ground to calculate the costs in guilders per m^3); (4) present maps and figures; (5) analyse spatial information; (6) interpolate discontinuous data of contour maps; and (7) convert input data file to a standardized format and visualise output data on maps.

Up till now, GISs are applied for input preparation of model parameters (*pre-processing*) and for output presentation of model results (*post-processing*). The possibility of a GIS to support hydrological models is limited by its ability to store, retrieve and perform operations with temporal data[1], such as time series on water quality variables and changes in water levels due to different pumping rates. The leading GIS is ARC/INFO, whereas PCRaster (http://www.geog.uu.nl/pcraster.html) at this Utrecht University, Faculty of Geographical Sciences, ILWIS (the Integrated Land and Water Information System) [ITC, 1996], IDRISI and GRASS (USGS) are also capable systems.

Future developments in hydrological modelling and GIS will probably focus on data collection, expanding databases, and advances in the integration of models in a GIS. The integration of a GIS and models, using a Structured Query Language (SQL), shortens the time on the exchange of data between the systems, but it may decrease the quality of modelling results when the GIS is treated as a *black box* without understanding the fundamental data manipulations that it carries out.

[1]As data storage in GIS has originally been concentrated on spatial data, a GIS is not specialized in temporal data.

For groundwater flow problems in the Netherlands, research institutes, governmental organisations and drinking water companies started in 1990 the development of a so-called *REgional Geohydrologic Information System (REGIS)*. The central system is administered by Netherlands Institute of Applied Geoscience TNO - National Geological Survey (NITG TNO)[2]. In REGIS, a database is available to supply all types of relevant hydrogeologic information, such as geo-electric data, groundwater levels (observation well data[3]), chemical data, hydrogeologic columns, topographic information, pumping and borehole test data, locations of contaminants, etc. Now, the system is operational and has already proven to be profitable. Note that, in addition, often applied sources in the Netherlands are borrowed from drinking water companies, waterboards, NITG TNO, Rijkswaterstaat, ILRI (International Institute for Land Reclamation and Improvement) and grey literature (articles and reports of site-specific problems descriptions). æ

[2]Dutch: Nederlands Instituut voor Toegepaste Geowetenschappen (formerly: TNO Grondwater Geo-Energie) and Rijks Geologische Dienst (RGD).

[3]Information can be retrieved from the so-called Grondwaterkaarten and the *On Line Grondwater Archief (OLGA)*.

Part II

Groundwater Modelling

Chapter 5

Introduction

The application of groundwater models can be described in terms of modelling *quantity problems* or *quality problems*.

For a quantity problem, only the flow of groundwater itself is modelled through mathematical description and interconnection of two equations: the equation of motion (Darcy's law) and the equation of continuity (equations 6.14 and 6.25), resulting in the *groundwater flow equation* (equation 6.30). For a quality problem, a new equation is added to the two equations of the quantity problem: the so-called *advection-dispersion equation* (equation 6.68). This equation is applied to simulate solute transport, including chemical and physical reactions. Note that the quality problem also concerns heat transport in groundwater, using in fact the same advection-dispersion equation, although now it is called the *convection-diffusion equation*.

5.1 Classification based on the design of the model

In the past, the behaviour of groundwater flow has been investigated by means of physical (scale) models, analogue models as well as by means of analytical methods. With the advent of high-speed computational capabilities (digital computer), the use of physical (scale) models and analogue models for simulating groundwater problems has decreased. The application of physical (scale) models is also limited by space, time as well as cost. They are still scarcely applied in laboratory studies on transport of groundwater contaminants.

Since computers appeared on the scene, *mathematical models* gained ground. They are subdivided into *analytical models* and *numerical models*. These analytical models, based on numerical techniques, apply infinite series of definite integrals to solve the solution (e.g. see section 7.7). For this application, computers are needed to solve the complicated (partial differential) equations involved. Numerical models, however, are directly based on computer codes. At present, a large number of mathematical models is available, which are capable of handling many types of groundwater flow. Figure 5.1 shows a classification of groundwater models based on the design of the model.

Computations with groundwater models result in data concerning piezometric heads, drawdowns, upconing, groundwater flow velocities, flow paths, travel times, solute concentration patterns, heat patterns, etc. In practice, based on these computational results, hydrogeologists have to make decisions based on the optimal positive effect of a solution and the minimal costs. The main applications of groundwater models are in the field of:

- prediction and simulation of certain measures or activities.

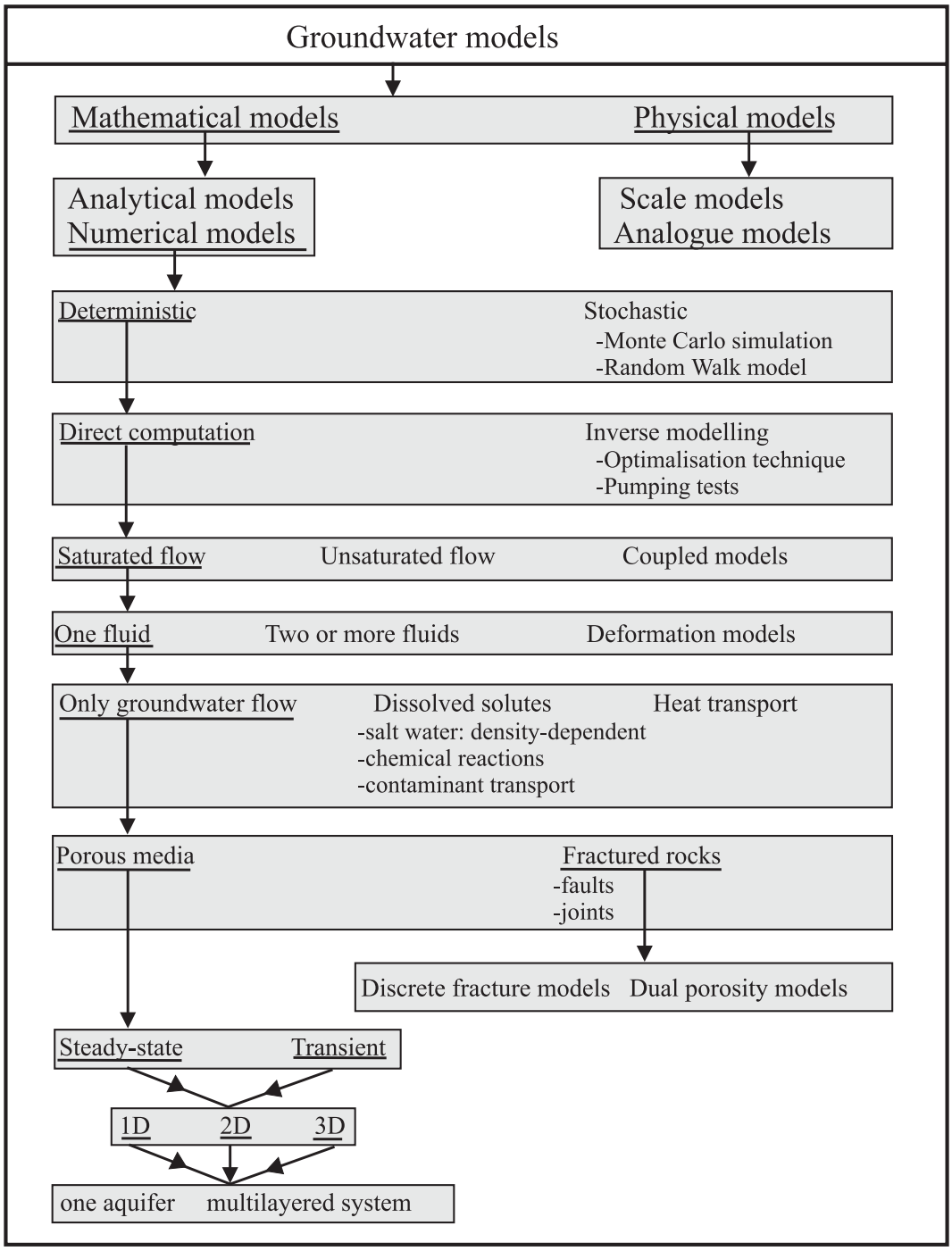

Figure 5.1: *A classification of groundwater models [Hemker, 1994].*

Table 5.1: *Analogies to groundwater flow: electricity and heat [Canter et al., 1987].*

Variable	Groundwater	Electricity	Heat
Potential	head, ϕ $[m]$	voltage, V $[Volt]$	temperature, T $[^oCelsius]$
Quantity transported	volume discharge rate $[m^3/s]$	electric charge $[Coulomb]$	heat $[calorie, Joule]$
Physical property of medium	hydraulic conductivity k $[m/s]$	electrical conductivity σ $[mhos/m]$	thermal conductivity λ $[Joule/(m\,s\,^oC)]$
Relation between potential and flow field	Darcy's law specific discharge $[m/s]$: q=-k grad ϕ	Ohm's law electric current $[Ampere/m^2]$: i=-σ grad V	Fourier's law heat flow $[Joule/(m^2\,s)]$: q=-λ grad T
Storage quantity	specific storage S_s $[1/m]$	capacitance C $[microfarad]$	heat capacity c_v $[Joule/(m^3\,^oC)]$

- planning and evaluation of different scenarios and strategies.
- optimization of the use of water resources.

5.1.1 Physical models

Physical model (also called scale models) are actual physical replicas of a groundwater flow system (mostly a simple aquifer) that have been scaled down for study in the laboratory. For example, the soil column (one-dimensional) and the sand tank (three-dimensional) are physical models. The behaviour of the prototype to hydrologic stresses can be simulated by subjecting the scale model to certain stresses such as water removal or injection or contaminated recharge. Scale relationships are used to interconnect the prototype with the physical model, for example U_ξ=ξ_m/ξ, where U is the ratio of the model parameter ξ_m divided by the actual aquifer parameter ξ.

5.1.2 Analogue models

Analogue models are based on the fact that several physical processes are governed by equations that are similar to the equations of groundwater flow (see table 5.1). As such, these processes are analogous with groundwater flow. If such a process can easily be realized and measured, it can be applied to study groundwater flow in a specific situation through interpretation and translation of the physical constants towards groundwater flow constants. Unfortunately, in most cases analogue models cannot be applied for simulating the movement of contaminants in groundwater.

Examples of analogue models are [Bear, 1972; Canter *et al.* 1987; Strack, 1989]:

1. the Hele Shaw model
   Sometimes, this model is also subdivided under the type of physical models. This analogue simulates slow flow of a viscous fluid in the narrow space between two parallel plates. It can be used to model problems with a free boundary, transient flow or multiple fluid flow (e.g. a model to study wastewater injection into a fresh-saline groundwater system).

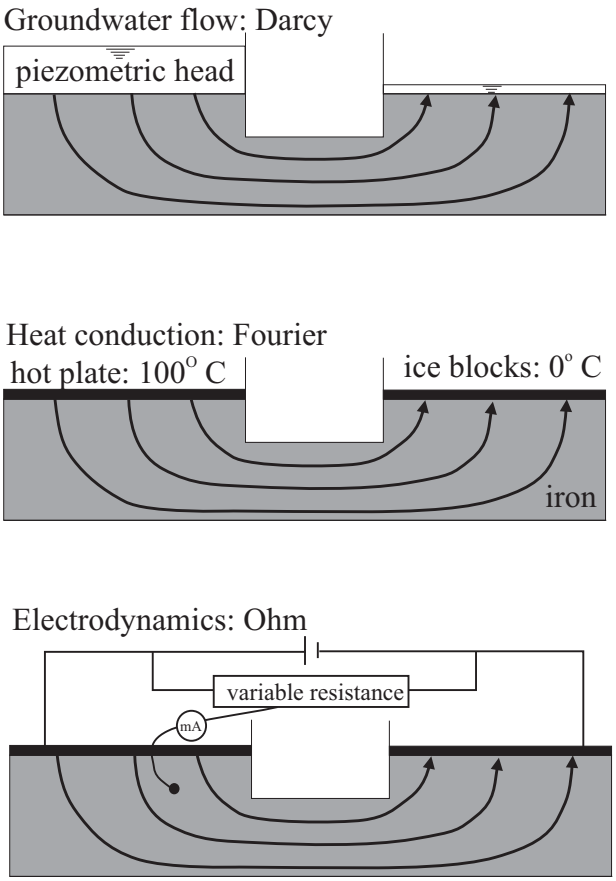

Figure 5.2: *Analogue of groundwater flow: electrodynamics and heat transfer.*

2. the electric model
   This model is based on the similarity between Ohm's law for the movement of electrons through a conducting material and Darcy's law for the movement of fluid through a porous media (see figure 5.2):

$$\Delta V = IR \tag{5.1}$$

$$R \propto \Delta l \quad R \propto \frac{1}{A} \Rightarrow R = \rho \frac{\Delta l}{A} \tag{5.2}$$

$$i = \frac{I}{A} = -\frac{1}{\rho}\frac{\Delta V}{\Delta l} \tag{5.3}$$

   where

   - V =electric potential ($Volt$),
   - i =electric current ($Ampere\ m^{-2}$),
   - R =electric resistance (Ω),
   - A =considered surface of the object (m^2),

- Δl =length of the considered object (m),
- ρ =specific electric resistance $(Ohm\ m,\ \Omega m)$.

$$\text{Ohm's law (2D):} \quad i_x = -\frac{1}{\rho}\frac{\partial V}{\partial x} \qquad i_y = -\frac{1}{\rho}\frac{\partial V}{\partial y} \tag{5.4}$$

$$\text{Continuity electrodynamics:} \quad \frac{\partial i_x}{\partial x} + \frac{\partial i_y}{\partial y} = 0 \tag{5.5}$$

The properties of an aquifer (e.g. permeability, storage coefficient) is simulated by electronic components (e.g. resistors, capacitors). For example, it can be used to measure pumping response in an aquifer through measuring appropriate voltages (similar to piezometric head) and currents (similar to groundwater flow).

3. the thermal model
   This model is based on the similarity between the flow of heat in a uniform body and groundwater flow in an aquifer (note that the same symbol q is usually used for groundwater flow and heat transfer):

$$\text{Fourier's law (2D):} \quad q_x = -\kappa\frac{\partial T}{\partial x} \qquad q_y = -\kappa\frac{\partial T}{\partial y} \tag{5.6}$$

   where

   - q = heat flow $(Joule\ m^{-2}\ s^{-1})$,
   - κ = thermal conductivity $(Joule\ m^{-1}\ s^{-1}\ {}^{o}Celcius)$.

$$\text{Continuity heat transfer:} \quad \frac{\partial q_x}{\partial x} + \frac{\partial q_y}{\partial y} = 0 \tag{5.7}$$

   Moreover, in case of a steady state isotropic homogeneous system with no sources or sinks, both processes obey the Laplace equation:

$$\frac{\partial^2 \tau}{\partial x^2} + \frac{\partial^2 \tau}{\partial y^2} + \frac{\partial^2 \tau}{\partial z^2} = 0 \tag{5.8}$$

   where τ = piezometric head (ϕ) (m) or temperature (T) $({}^{o}Celsius)$. The flow of heat is simulated through adding a heat source or sink to a given material and measuring the temperatures.

4. the membrane model
   This model is based on the similarity between the small slope of the surface of a stretched thin rubber membrane and (axial-symmetric) steady state groundwater flow in polar coordinates. Drawdowns due to a well is simulated through measurements of the deflections of the membrane caused by a protrusion[1].

[1] Dutch: 'uitsteeksel'.

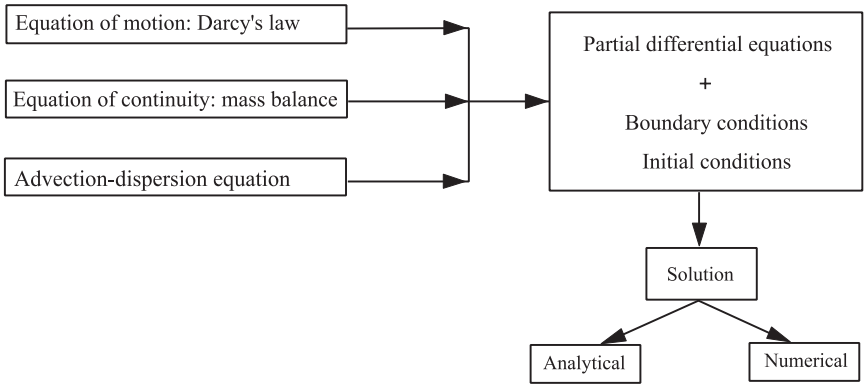

Figure 5.3: *The schematisation of the calculation scheme, applied for mathematical modelling of groundwater.*

5.1.3 Mathematical models

In general, a mathematical model for groundwater problems is formed by (partial) differential equations (e.g. including density dependent groundwater flow as well as solute and heat transport), together with specification of system geometry, boundary conditions[2] and initial conditions for transient processes (see figure 5.3). In combination with data of your specific groundwater flow problem, the (partial) differential equations of the mathematical model are solved by using: (a.) analytical methods and (b.) numerical methods.

ad a. Analytical methods

In the past, analytical methods[3] were commonly used for the analysis of groundwater problems. An analytical solution of the partial differential equation was brought up for a particular problem with its corresponding initial and boundary conditions. For example, the piezometric head ϕ and the groundwater flow Q were computed by solving the equations *directly* and *continuously* in time and space. For example, analytical solutions of groundwater flow and solute transport are given for the one-dimensional form of the advection-dispersion equation by Ogata & Banks [1961], Shamir & Harleman [1966] and Kinzelbach [1986, 1987a]. Bear [1972, 1979] has summarized examples of analytical solutions of the hydrodynamic dispersion with specific boundary and initial value problems. See also the TUDelft lecture notes Geohydrologie f15B [Boekelman & van Dijk, 1996] (chapters 5 to 9).

The trick is to find an analytical solution suitable for your specific problem. Various mathematical techniques are applied to find appropriate solutions. In addition, an effective approach is to obtain analytical equations from analogous physical processes. The similarity between groundwater flow and conduction of heat in solids appears to be very convenient. In this physical process, several analytical solutions are similar to those for groundwater

[2]Specification of appropriate boundary conditions on the flow domain is often the most difficult task in formulating the model, and one of the primary sources of uncertainty in model analysis.

[3]These methods are also referred to as exact solutions.

flow in aquifers. For example, Carslaw and Jaeger [1959] obtained equivalent problems in the theory of 'Conduction of Heat in Solids'.

The advantage of analytical methods is that they can give a quick insight in the sensitivity of the solution for various physical parameters (such as transmissivity, storativity). Moreover, they can serve as verification of solutions of more complex systems obtained by numerical methods. However, the application of analytical methods is limited as analytical solutions are only available for relatively simple and strongly schematised problems[4] (e.g. homogeneous aquifers, 1D or 2D, steady state, interface between fresh and saline groundwater).

For example, for problems of steady flow in two dimensions, the method of complex variables is commonly used (remember the equation $z = x + iy$). This method contains concepts such as the hodograph method and conformal transformations (also called conformal mapping). For problems of transient flow other transformation techniques are applied, such as Laplace and Fourier transformations. For more information about complex variable techniques, various transformations, the Cauchy-Riemann relations ($\frac{\partial u}{\partial x} = \frac{\partial v}{\partial y}$ and $\frac{\partial u}{\partial y} = -\frac{\partial v}{\partial x}$), the potential Φ and the stream function Ψ, etc.: see Verruijt [1970] and [Strack, 1989].

With the introduction of powerful computers the application of analytical methods is becoming less.

ad b. Numerical methods

If groundwater problems become more complex (e.g. inhomogeneous, anisotropic, transient, regional groundwater flow with changes of the properties of aquifers and semi-pervious layers, with wells, rivers, etc.), the system becomes too complicated for solutions obtained with analytical methods. In these cases, numerical methods have to be used. The introduction of micro-computers increased the application of numerical methods and these methods replaced almost completely the use of analytical methods.

A main characteristic of numerical methods is that the computations result in values at discrete points. For example, the piezometric head ϕ and the groundwater flow Q are computed by solving the equations at nodal points in time and space.

One of the basic principles of numerical methods is that for each discrete point one difference equation (or, if solute or heat transport problems are considered, two difference equations) are generated, which can be solved in two ways (see also [Stelling & Booij, 1996] and [Spaans, 1992]):

- explicit: one after another in a certain sequence, or
- implicit: as a set of equations by means of a matrix approach: (1) direct solution as a complete matrix (e.g. Gauss-Jordan Elimination (section 7.4), Decomposition and Matrix Inversion) or (2) indirect or iterative solution, where equation after equation is solved, using trial start values (e.g. Gauss-Seidel Substitution (subsection 7.2.3), Successive Overrelaxation (subsection 9.2.5) and Conjugate Gradient Methods).

Numerical methods and their solution techniques are discussed in chapter 7.

[4] Unfortunately, analytical solutions are very rarely available for problems with density dependent groundwater flow in combination with solute transport, governed by means of the advection-dispersion equation.

5.2 Outline

In this part II, the characteristics of groundwater models are discussed. In chapter 6, a classification of groundwater models is enumerated and mathematical descriptions of the relevant processes are given. In chapter 7, some numerical techniques are demonstrated and six methods which solve the partial differential equations of groundwater flow and/or solute transport are briefly described. In chapter 8, numerical aspects of groundwater models are considered intensively. Finally, in chapter 9, some computer codes which handle salt water intrusion are briefly mentioned[5]. In addition, four groundwater computer codes are discussed more intensively: MODFLOW, Micro-Fem, MOC3D and an adapted version of MOC (2D).

[5]See the lectures notes of Hydrological Transport Processes/Groundwater Modelling II: Density Dependent Groundwater Flow: Salt Water Intrusion and Heat Transport for more information.

Chapter 6

Mathematical description of hydrogeologic processes

In this chapter, the mathematical description of the some hydrogeologic processes is given.

6.1 Fluid flow: equation of motion and continuity

In so-called quantity problems, the interest is focussed on groundwater and related aspects, such as piezometric heads, streamlines and water balances. Examples of quantity problems are: modelling drawdowns due to groundwater extractions (for domestic, industrial and/or agricultural purposes), the pumping of groundwater out of an excavation by means of a system of shallow wells or the lowering of (polder) water levels through drainage and pumping.

The tools available for the mathematical modelling of quantity problems are the equation of motion (Darcy's law) and the equation of continuity (mass balance equation). Well-known groundwater computer codes for quantity problems are MODFLOW (section 9.2) and Micro-Fem (section 9.3).

6.1.1 Equation of motion: Darcy's law

Darcy (1856) did experiments on flow through a cylinder of saturated sand (homogeneous and isotropic porous medium) (see figure 6.1). He found relations between different parameters which influence the flow of water. The rate of flow appears to be proportional directly to head loss and inversely to the length of the flow path, with a constant proportionally factor, see the equations 6.1 to 6.5:

$$\text{Darcy's law (1856):} \qquad Q \propto \phi_1 - \phi_2 \tag{6.1}$$

$$Q \propto \frac{1}{L} \tag{6.2}$$

$$Q \propto A \tag{6.3}$$

$$Q \propto A\frac{\phi_1 - \phi_2}{L} \tag{6.4}$$

$$Q = kA\frac{\phi_1 - \phi_2}{L} \Rightarrow q = -k\frac{\partial \phi}{\partial x} \tag{6.5}$$

where

- Q = rate of flow ($L^3\,T^{-1}$),

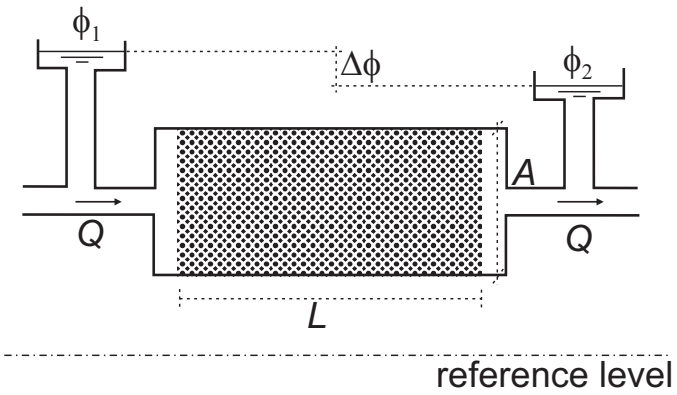

Figure 6.1: *Darcy's experiment.*

- q = Darcian specific discharge ($L\,T^{-1}$),
- A = cross-sectional area of diameter of the cylinder (L^2),
- ϕ = head (L),
- L = length of the flow path (L),
- k = proportionally factor or hydraulic conductivity or permeability[1] ($L\,T^{-1}$).

Darcy's law is only valid in case of laminar flow: viz. at relative low velocities when water particles move more or less parallel to each other. In quantified terms, Darcy's law is valid as long as the so-called Reynolds number Re ($-$) does not exceed some value between 1 and 10:

$$\text{Reynolds number:} \qquad Re = \frac{\rho q R}{\mu} < 1 - 10 \tag{6.6}$$

where

- q = Darcian specific discharge ($L\,T^{-1}$),
- μ = dynamic viscosity ($M\,L^{-1}\,T^{-1}$),
- R = hydraulic radius of the pore (L).

Darcy's law can also be obtained from a mathematical point of view. Three forces are working on a water particle, see figure 6.2:

1. Pressure differences: $p_{z1}\Delta y\Delta z - p_{z2}\Delta y\Delta z$ (6.7)

2. Gravity forces: $-\rho_i g\Delta x\Delta y\Delta z$ (6.8)

3. Friction forces: $-\frac{\mu}{\kappa}q_z\Delta x\Delta y\Delta z$ (6.9)

where

[1] Dutch: 'doorlatendheid' or 'doorlatendheidscoëfficient'.

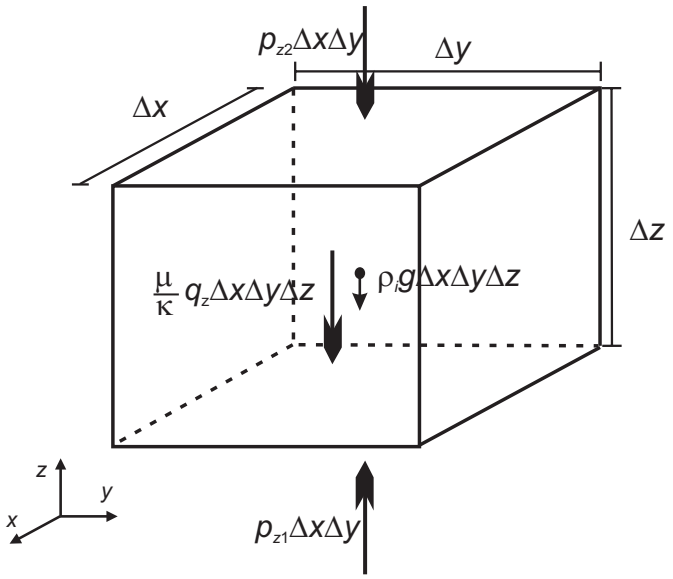

Figure 6.2: *Forces on a water particle.*

- κ = intrinsic permeability (L^2).

Combination of these three terms gives:

$$p_{z1}\Delta x\Delta y - p_{z2}\Delta x\Delta y - \rho_i g\Delta x\Delta y\Delta z - \frac{\mu}{\kappa} q_z \Delta x\Delta y\Delta z = 0 \tag{6.10}$$

$$\frac{p_{z2}-p_{z1}}{\Delta z} + \frac{\mu}{\kappa} q_z + \rho_i g = 0 \tag{6.11}$$

$$q_z = -\frac{\kappa}{\mu}\left(\frac{\partial p}{\partial z} + \rho_i g\right) \tag{6.12}$$

Similar for the x - and y-direction:

$$q_x = -\frac{\kappa}{\mu}\frac{\partial p}{\partial x} \qquad q_y = -\frac{\kappa}{\mu}\frac{\partial p}{\partial y} \qquad q_z = -\frac{\kappa}{\mu}(\frac{\partial p}{\partial z} + \rho_i g) \tag{6.13}$$

In conclusion, the equation of motion for three-dimensional (laminar) groundwater flow in an anisotropic non-homogeneous porous medium in the principal directions is described by Darcy's law [e.g. Bear, 1972]:

$$q_x = -\frac{\kappa_x}{\mu_i}\frac{\partial p}{\partial x} \qquad q_y = -\frac{\kappa_y}{\mu_i}\frac{\partial p}{\partial y} \qquad q_z = -\frac{\kappa_z}{\mu_i}(\frac{\partial p}{\partial z} + \gamma) \tag{6.14}$$

where

- q_x, q_y, q_z = Darcian specific discharges in the principal directions ($L\,T^{-1}$),
- $\kappa_x, \kappa_y, \kappa_z$ = principal intrinsic permeabilities (L^2),

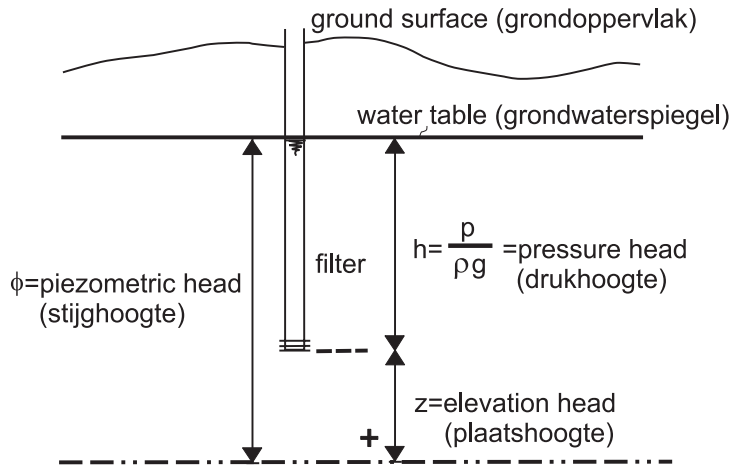

Figure 6.3: *Definition of the piezometric head (terms in Dutch between brackets).*

- μ_i = dynamic viscosity of water at point $[x, y, z]$ $(M\,L^{-1}\,T^{-1})$,
- p = pressure $(M\,L^{-1}\,T^{-2})$,
- $\gamma = \rho_i g$ = specific weight $(M\,L^{-2}\,T^{-2})$,
- ρ_i = density of groundwater at point $[x, y, z]$ $(M\,L^{-3})$,
- g = gravity acceleration $(L\,T^{-2})$.

6.1.2 Piezometric head

The relation between the pressure and the so-called piezometric head is as follows (if the atmospheric pressure equals zero), see figure 6.3:

$$\phi = \frac{p}{\rho_i g} + z \tag{6.15}$$

where

- ϕ = piezometric head (L). Also called hydraulic head or piezometric level,
- $\frac{p}{\rho_i g}$ = pressure head (L),
- z = elevation with respect to the reference level, e.g. $N.A.P.$ (L).

or

$$p = \rho_i g\,(\phi - z) \tag{6.16}$$

6.1.3 Hydraulic conductivity and permeability

If $\rho_i g$ is constant, then the hydraulic conductivities of groundwater k_i in the principal directions can be defined as follows:

$$k_x = \frac{\kappa_x \rho_i g}{\mu_i} \qquad k_y = \frac{\kappa_y \rho_i g}{\mu_i} \qquad k_z = \frac{\kappa_z \rho_i g}{\mu_i} \qquad (L\,T^{-1}) \tag{6.17}$$

Combination of the equations 6.14, 6.16 and 6.17 gives[2]:

$$q_x = -k_x \frac{\partial \phi}{\partial x} \qquad q_y = -k_y \frac{\partial \phi}{\partial y} \qquad q_z = -k_z \frac{\partial \phi}{\partial z} \tag{6.18}$$

The intrinsic permeability κ largely depends on the size of the pores through the effective porosity n_e. A commonly-used equation is the one of Kozeny-Carmen to clearly demonstrate the relation between κ and n_e:

$$\text{Kozeny-Carmen:} \qquad \kappa = c\, d^2 \frac{n_e^3}{(1-n_e)^2} \qquad (m^2) \tag{6.19}$$

where

- c = depending on the structure of the pores, e.g. c=1/180 $(-)$,
- d = main grain size (diameter of the pore) (L),
- n_e = effective porosity $(-)$.

Some values for k and κ are given in table 6.1.3. In addition, it can be deduced that the permeability varies with depth due to increasing pressure or effective stress. Though exact relations are difficult to obtain as in situ data are scarce and upscaling of data from laboratory-scale experiments is somewhat unreliable, a correlation between permeability κ and depth z becomes widely accepted. For instance, the following equation is given for the permeability as a function of depth in the continental crust (Manning & Ingebritsen, 1999):

$$\log \kappa = -14 - 3.2 \log z \tag{6.20}$$

where z is the depth in kilometres (L). An empirical porosity-depth relation is given by Athy (1930):

$$n_e = n_{e,0} \exp(-B_s(z_0 - z)) \tag{6.21}$$

where B_s and $n_{e,0}$ are fit coefficients. For instance, $n_{e,0}$=0.5, B_s=-0.5 $\times$ 10^{-5} and z_0=0 for sands (z in cm) and $n_{e,0}$=0.6, B_s=-0.6 $times$ 10^{-5} and z_0=0 for shales (Bethke, 1985).

[2]Here it is assumed that the variation of the density with the pressure can be neglected. This is very often possible in hydrogeologic practice.

Soil	k **(m/s)**	κ **(m^2)**
Unconsolidated deposits		
Clay	$<10^{-9}$	$<10^{-17}$
Sandy clay	10^{-9}-10^{-8}	10^{-16}-10^{-15}
Silt	10^{-8}-10^{-7}	10^{-15}-10^{-14}
Peat	10^{-9}-10^{-7}	10^{-16}-10^{-14}
Very fine sand	10^{-6}-10^{-5}	10^{-13}-10^{-12}
Fine sand	10^{-5}-10^{-4}	10^{-12}-10^{-11}
Coarse sand	10^{-4}-10^{-3}	10^{-11}-10^{-10}
Sand with gravel	10^{-3}-10^{-2}	10^{-10}-10^{-9}
Gravel	$>10^{-2}$	$>10^{-9}$
Rocks		
Unfractured rocks	$<10^{-9}$	$<10^{-17}$
Sandstone	10^{-10}-10^{-6}	10^{-17}-10^{-13}
Limestone & dolomite	10^{-9}-10^{-6}	10^{-16}-10^{-13}
Fractured rocks	10^{-8}-10^{-4}	10^{-15}-10^{-11}
Permeable basalt	10^{-7}-10^{-2}	10^{-14}-10^{-9}
Karst limestone	10^{-6}-10^{-2}	10^{-13}-10^{-9}

Table 6.1: *Values for the hydraulic conductivity k and the intrinsic permeability κ. In conclusion: fine sand 1 à 10 m/day and clay 10^{-5}-10^{-4} m/day.*

Fractures

A fractured medium is a special case of voids in solid rocks [de Marsily, 1986]. Almost all rocks in the earth's crust are fractured because of tectonic movements, e.g. faults, fissures, joints, cracks. If the fractures are not sealed by some kind of deposit such as clay, calcite or quartz, a network of (interconnected) fracture is created: a fractured medium with a so-called fracture porosity. It is possible that a fractured medium consists of two types of porosities: the regular ('porous medium') porosity and this fracture porosity. Examples are (some types of) sandstones and limestomes. In these media, a so-called double porosity model can be applied to simulate groundwater flow.

Modelling flow in the fractured medium can be considered in two different concepts: (a) considering the fractures one by one, or (b) considering the fractured medium as an equivalent continuous medium. Flow in a fracture can be laminar or turbulent[3].

For an equivalent continuous fractured medium where the flow is laminar, the effective permeability κ_{eff} can also be estimated as follows:

$$\kappa_{eff} = \frac{\delta^3}{12f} \tag{6.22}$$

where

- δ = width (aperture) of the fracture (L),

[3]The Reynolds number (equation 6.6) classifies whether the flow regime is laminar ($Re < 2000$) or turbulent ($Re > 2000$).

- f = distance between the fractures (L).

See for more information on fractures de Marsily [1986].

6.1.4 Density of groundwater

Density should be considered to be a function of pressure, temperature of the fluid and concentration of dissolved solids:

$$\rho = f(p, T, S) \tag{6.23}$$

where:

- ρ = density (kg/m^3),
- p=pressure ($kg\, m^{-1}\, s^{-2}$),
- T = temperature (^oC).
- S = salinity[4] or total dissolved solids (TDS) (g/l).

However, the influence of pressure can be neglected under the given circumstances of most considered hydrogeologic systems. Furthermore, the influence of temperature on the density is of minor importance with respect to the influence of dissolved solids concentration within many hydrogeologic systems, see figure 6.4. Therefore, the density of groundwater is often only related to the concentration of dissolved solids in the groundwater, whereas the temperature is considered to be equal to a constant value (in the Netherlands $\approx 10\ ^oC$). In general, when the quality of groundwater is in question, the salinity or total dissolved solids TDS is considered. An advantage of using TDS is that a rapid determination of TDS is possible by measuring the electrical conductivity of a groundwater sample.

The concentration of dissolved solids is subdivided into negative (anions) and positive ions (cations). For instance, ocean water consists of 11 main components: Since in coastal groundwater chloride (Cl^-) is the predominant negative ion, which is moreover investigated intensively, the interest is often focused on the chloride distribution. When, in fact, only changes in the chloride distribution are simulated, the distribution of all dissolved solids is meant. In other words, the distribution of chloride ions is considered to represent the distribution of all dissolved solids. As such, a proportional distribution of all dissolved solids, which is present in ocean water, is also assumed to be present in groundwater under consideration.

The applied classification of fresh, brackish and saline groundwater based on chloride concentrations according to Stuyfzand [1986b] is presented in table 6.3. Obviously, there are various other classification systems possible, e.g. because the definition for fresh groundwater depends on the application of the groundwater. For instance, the drinking water standard in the European Community equals 150 $mg\ Cl^-/l$ [Stuyfzand, 1986b], while according to the World Health Organization, a convenient chloride concentration limit is 200 $mg\ Cl^-/l$ [Custodio *et al.*, 1987]. A chloride concentration equal to 300 $mg\ Cl^-/l$ indicates the taste limit of human beings according to ICW [1976], while Todd [1980] gives 100 mg

[4]The salinity is the concentration of dissolved solids in water, expressed in ($M\, L^{-3}$) (g/l), *p.p.t.* (*parts per thousand*) or *p.p.m.* (*parts per million*).

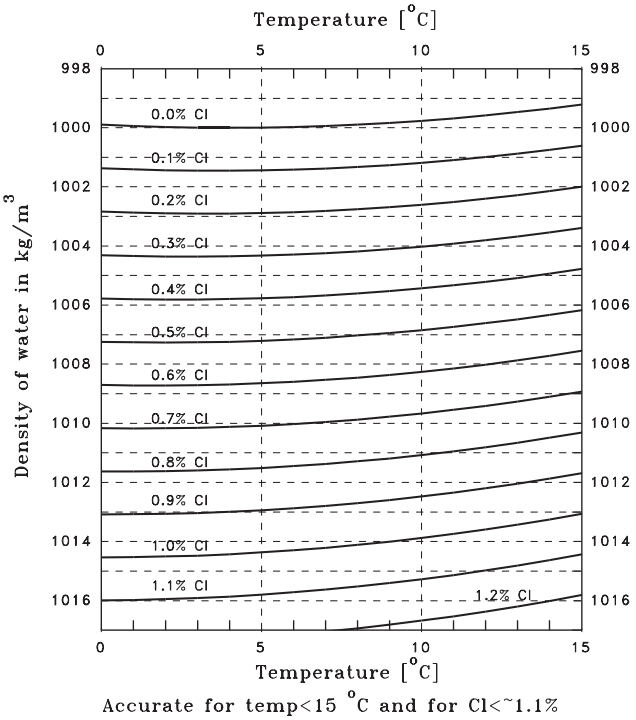

Figure 6.4: *Density of water as a function of the salinity and temperature (ILRI, 1972).*

Ions		mg/l
negative ions	Cl^-	19,000
	SO_4^{-2}	2700
	HCO_3^-	140
	Br^-	65
total negative ions		21905
positive ions	Na^+	10,600
	Mg^{+2}	1270
	Ca^{+2}	400
	K^+	380
total positive ions		12650
Total Dissolved Solids		34555

Table 6.2: *Composition of ocean water. The three components with low concentrations are Strontium (± 8 mg/l), Borium (± 5 mg/l) and Fluoride (± 1 mg/l).*

Cl^-/l as the limit when salt can be tasted. The chloride concentration of sprinkler water for horticulture should be less than 200 $mg\ Cl^-/l$, while livestock can endure higher concentrations: up to 1500 $mg\ Cl^-/l$ may be accepted, provided that the chloride concentration stays constant.

Table 6.3: *Classification into six main types of fresh, brackish or saline groundwater depending on the basis of chloride concentration, after Stuyfzand [1986b].*

Main type of groundwater	Chloride concentration $[mg\ Cl^-/l]$
fresh	$Cl^- \leq 150$
fresh-brackish	$150 < Cl^- < 300$
brackish	$300 < Cl^- < 1000$
brackish-saline	$1000 < Cl^- < 10{,}000$
saline	$10{,}000 < Cl^- < 20{,}000$
hyperhaline or brine	$Cl^- \geq 20{,}000$

Table 6.4: *Variation of the dynamic viscosity μ with temperature T at a pressure of 100 kPa (1 bar) [Verruijt, 1970; Bear, 1972; Voss, 1984; CRC, 1994].*

Temperature T	Dynamic viscosity μ $(kg/m\,s)$	
(^oC)	Verruijt, Bear, CRC	Voss, equation 6.24
0	$1.79 \cdot 10^{-3}$	$1.76 \cdot 10^{-3}$
5	$1.52 \cdot 10^{-3}$	$1.50 \cdot 10^{-3}$
10	$1.31 \cdot 10^{-3}$	$1.30 \cdot 10^{-3}$
15	$1.14 \cdot 10^{-3}$	$1.14 \cdot 10^{-3}$
20	$1.00 \cdot 10^{-3}$	$1.00 \cdot 10^{-3}$
40	$0.65 \cdot 10^{-3}$	$0.65 \cdot 10^{-3}$
70	$0.41 \cdot 10^{-3}$	$0.40 \cdot 10^{-3}$
100	$0.28 \cdot 10^{-3}$	$0.28 \cdot 10^{-3}$

6.1.5 Dynamic viscosity

The dynamic viscosity μ highly depends on the temperature [Huyakorn & Pinder, 1977], see table 6.4. Voss [1984] uses in SUTRA the following expression:

$$\mu = f(T) \cong (239.4 \cdot 10^{-7}) \cdot 10^{\frac{248.37}{T+133.15}}\ kg/ms \tag{6.24}$$

Note that this equation should only be applicable for $T < 100\ ^oC$. The dynamic viscosity μ is relatively insensitive to pressure within the range of groundwater systems that are considered in these lecture notes. Furthermore, the dynamic viscosity also depends on the solute concentration, though only for very high solute concentrations. In general, the range in temperature in the deep aquifers of Dutch groundwater flow systems is small. Temperature in the top layers in the Netherlands is about 9 à 10 ^oC, whereas the gradient is about 3 ^oC per 100 m. For instance, data from Stuyfzand [1986, 1988] in sand-dune areas along the Dutch coast show that the temperature of groundwater in the aquifers directly under the Holocene aquitard (at roughly -20 m $N.A.P.$[5]) is normally between 10.0 and 11.0 ^oC, while the annual mean air temperature near the coast is roughly 9.5 ^oC. In deeper layers, the mean temperature of the groundwater varies between 11.0 and 12.5 ^oC. In the United

[5] $N.A.P.$ stands for Normaal Amsterdams Peil and is the reference level in the Netherlands. $N.A.P.$ roughly equals Mean Sea Level.

States, most measured geothermal gradients for groundwater temperatures fall within the range from +1.8 to +3.6^oC *per* 100 m below the zone of surface influence [Todd, 1980]. The geothermal gradient in strongly anisotropic karstic aquifers in the Salentine Peninsula, Italy, is some 2.5 ^oC to 3.0 ^oC *per* 100 m [Cotecchia *et al.*, 1997]. In case groundwater flows, smoother gradients could occur [Domenico & Schwartz, 1998]. This phenomenon was pointed out by analysing temperature logs in a large number of boreholes. For instance, several boreholes in the Murgia aquifer show an increase in temperature of less than 1.5 ^oC over the top 200 m. On the other hand, changes in temperature near the groundlevel due to geothermal flow could sometimes be significant.

6.1.6 Equation of continuity

Equation (6.25) describes the non-steady three-dimensional mass flow in a small element of a saturated anisotropic, porous medium [e.g. Bear, 1972; van der Heide & Boswinkel, 1982]:

$$-\left[\frac{\partial(\rho_i q_x)}{\partial x}+\frac{\partial(\rho_i q_y)}{\partial y}+\frac{\partial(\rho_i q_z)}{\partial z}\right]=\frac{\partial(n_e\rho_i)}{\partial t}+W'(x,y,z,t) \tag{6.25}$$

where

- t = time (T),
- n_e = effective porosity of the medium ($-$),
- $W'(x,y,z,t)$ = source function, which describes the mass flux of the fluid into (negative sign) or out of (positive sign) the system ($M\,L^{-3}\,T^{-1}$).

The effective porosity is a function of pressure, $n_e = n_e(p)$. Due to the fact that a slightly compressible fluid is present, it is necessary to introduce the *specific storativity* S_s (L^{-1}) [Bear, 1972]:

$$S_s = g\frac{\partial(n_e\rho_i)}{\partial p} = g(\rho_i\frac{\partial n_e}{\partial p}+n_e\frac{\partial \rho_i}{\partial p}) \tag{6.26}$$

with

$$S_s = \frac{S}{b} \tag{6.27}$$

where

- S = storage coefficient ($-$),
- b = saturated thickness of the aquifer (L).

The non-stationary equation of continuity is also obtained in another way by Verruijt, see page 177 for a short review (in Dutch).

In many situations, the density is assumed to be constant: ρ_i=ρ. Taking the partial derivative of equation 6.16, that is $\frac{\partial p}{\partial t} = \rho_i g\frac{\partial \phi}{\partial t}$, and the pressure gradient can be replaced by a term containing the gradient of the piezometric head ϕ, equation 6.25 becomes:

$$-\left[\frac{\partial q_x}{\partial x}+\frac{\partial q_y}{\partial y}+\frac{\partial q_z}{\partial z}\right]=S_s\frac{\partial \phi}{\partial t}+\frac{W'(x,y,z,t)}{\rho} \tag{6.28}$$

where

- ρ = density of fresh groundwater at point $[x, y, z]$ $(M\,L^{-3})$.

In fact, however, the density of groundwater is a function of pressure, concentration of dissolved solids and temperature of the fluid: $\rho_i = \rho_i(p, C, T)$. First, the influence of pressure p can be neglected in the hydrogeologic systems considered in these lecture notes. Second, in many groundwater flow problems, the concentration of dissolved solids C in the groundwater is fortunately so low that the density of groundwater ρ_i can be taken equal to a constant value, e.g. of fresh groundwater ρ=1000 kg/m^3. Third, the influence of temperature T on the density is of minor importance with respect to the influence of dissolved solids concentration within the range of many hydrogeologic systems. For the Dutch situation, the temperature is often considered to be equal to 10 ^oC.

As such, equation 6.28 is a stripped version of the complete continuity equation 6.25, as the density is assumed to be constant. This condition significantly simplifies the equation of continuity. Assure yourself whether or not this condition is the case in your specific groundwater flow problem.

6.1.7 Groundwater flow equation

The two equations 6.18 and 6.28 result in the so-called *groundwater flow equation*:

$$\frac{\partial(k_x \frac{\partial \phi}{\partial x})}{\partial x} + \frac{\partial(k_y \frac{\partial \phi}{\partial y})}{\partial y} + \frac{\partial(k_z \frac{\partial \phi}{\partial z})}{\partial z} = S_s \frac{\partial \phi}{\partial t} + \frac{W'(x, y, z, t)}{\rho} \tag{6.29}$$

When the aquifer has a constant thickness b and a constant hydraulic conductivity k_i, the equation becomes:

$$T_{xx} \frac{\partial^2 \phi}{\partial x^2} + T_{yy} \frac{\partial^2 \phi}{\partial y^2} + T_{zz} \frac{\partial^2 \phi}{\partial z^2} = S \frac{\partial \phi}{\partial t} + W(x, y, z, t) \tag{6.30}$$

where

- T_{xx}, T_{yy}, T_{zz} = transmissivity in the principal directions $(L^2\,T^{-1})$,
- $W(x, y, z, t) = (W'(x, y, z, t)b)/\rho_i$ = volume flux per unit area (positive sign for outflow, e.g. well pumpage; negative for inflow, e.g. well injection and natural groundwater recharge) $(L\,T^{-1})$,

Steady state groundwater flow equation

The determination of the steady state groundwater flow equation is mathematically described below, see figure 6.5. Assumptions are:

- ground not deformable,
- ground completely saturated,
- no changes in the piezometric head as a function of time.

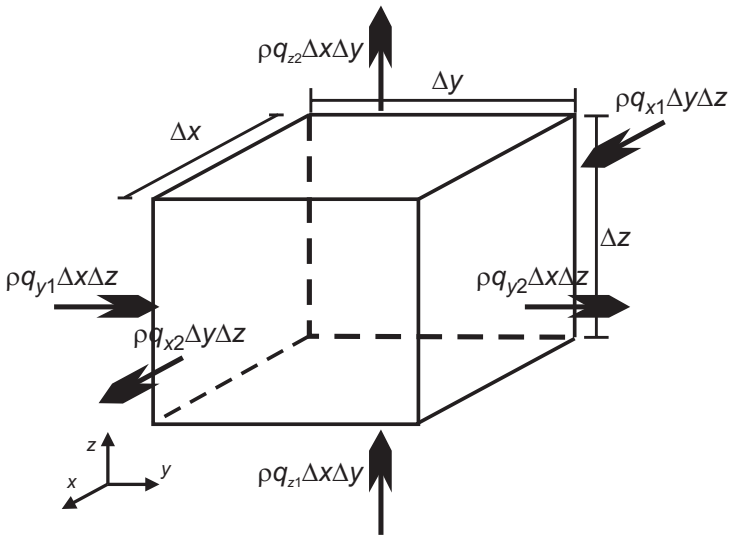

Figure 6.5: *Determination of the steady state groundwater flow equation.*

Conservation of mass per unit of time gives (no change in storage of groundwater: S=0):

$$\text{Balance in horizontal } x\text{-direction:} \quad \rho q_{x2}\Delta y\Delta z - \rho q_{x1}\Delta y\Delta z \tag{6.31}$$

$$\text{Balance in horizontal } y\text{-direction:} \quad \rho q_{y2}\Delta x\Delta z - \rho q_{y1}\Delta x\Delta z \tag{6.32}$$

$$\text{Balance in vertical direction:} \quad \rho q_{z2}\Delta x\Delta y - \rho q_{z1}\Delta x\Delta y \tag{6.33}$$

Combination gives:

$$\begin{aligned}\left(\tfrac{\rho q_{x2}-\rho q_{x1}}{\Delta x}\right)\Delta x\Delta y\Delta z + \left(\tfrac{\rho q_{y2}-\rho q_{y1}}{\Delta y}\right)\Delta x\Delta y\Delta z \\ + \left(\tfrac{\rho q_{z2}-\rho q_{z1}}{\Delta z}\right)\Delta x\Delta y\Delta z = 0\end{aligned} \tag{6.34}$$

or

$$\frac{\partial \rho q_x}{\partial x} + \frac{\partial \rho q_y}{\partial y} + \frac{\partial \rho q_z}{\partial z} = 0 \tag{6.35}$$

Combination with Darcy gives:

$$\frac{\partial \rho\left(-k_x\frac{\partial \phi}{\partial x}\right)}{\partial x} + \frac{\partial \rho\left(-k_y\frac{\partial \phi}{\partial y}\right)}{\partial y} + \frac{\partial \rho\left(-k_z\frac{\partial \phi}{\partial z}\right)}{\partial z} = 0 \tag{6.36}$$

When ρ and k_i are constant in time and in space (this means that $\frac{\partial \rho k_i}{\partial x_i} = 0$) than the Laplace equation is created:

$$\frac{\partial^2 \phi}{\partial x^2} + \frac{\partial^2 \phi}{\partial y^2} + \frac{\partial^2 \phi}{\partial z^2} = 0 \qquad \text{(Laplace equation)} \tag{6.37}$$

or

$$\nabla^2 \phi = 0 \tag{6.38}$$

6.1.8 Equation of state

Numerous conversion formulas relating density to chloride concentration, salinity, temperature and pressure, can be found in literature, see e.g. Sorey (1978), Weast (1982), Voss (1984), Holzbecher (1998). For example, eqn. 6.39 gives an equation of state with a linear relation between chlorinity and density.

$$\rho(C) = \rho_f \left(1 + \alpha \frac{C}{C_s}\right) \tag{6.39}$$

where

- $\rho(C)$ = density of groundwater ($M\,L^{-3}$),
- ρ_f = reference density, usually the density of fresh groundwater (without dissolved solids) at mean subsoil temperature ($M\,L^{-3}$),
- ρ_s = density of saline groundwater at mean subsoil temperature ($M\,L^{-3}$),
- $\alpha = (\rho_s - \rho_f)/\rho_f$ = relative density difference ($-$),
- $C_{(i,j)}$ = chloride concentration or the so-called *chlorinity* ($mg\ Cl^-/l$). The salinity S is related to the chlorinity C by the formula: $C = 0.554\ S$,
- C_s = reference chloride concentration ($mg\ Cl^-/l$). In eqn. 6.39, a linear relation exists between ρ_s and C_s.

The following data can be applied for sea (ocean) water: $\rho_f = 1000\ kg/m^3$; $\rho_s = 1025\ kg/m^3$; thus $(\rho_s - \rho_f)/\rho_f = 0.025$; $C_s = 19{,}300\ mg\ Cl^-/l$; and TDS = 34,500 mg/l. The TDS in oceans can be higher, due to, among others, a high degree of evaporation and oceanic currents, and consequently, the density is higher than $\rho_s = 1025\ kg/m^3$. For instance, the chloride concentration in the Mediterranean Sea can be as high as 22,000 $mg\ Cl^-/l$ (ρ=1028 kg/m^3), and the TDS of the Red Sea and some areas of the Mediterranean can reach some 45,000 mg/l (the Dead Sea even reaches ρ=1200 kg/m^3).

Knudsen developed in 1902 the following formula:

$$\rho_{(S,T)} = 1000 + 0.8054S - 0.0065(T - 4 + 0.2214S)^2 \tag{6.40}$$

Expression 6.40 (see fig. 6.4) gives a rather good approximation for the density as a function of salinity and temperature, at a (constant) pressure of 1 atmosphere and for temperatures $< 15\ ^oC$ and salinity values $< 20{,}000\ mg/l$ or $< 20\ ppt$. Sorey (1978) gives a temperature-dependent formula:

$$\rho_{(T)} = \rho_0 \left[1 - \beta(T - T_0) - \gamma(T - T_0)^2\right] \tag{6.41}$$

or

$$\rho_{(T)} = 1000 \left[1 - 3.17 \times 10^{-4}(T - 4) - 2.56 \times 10^{-6}(T - 4)^2\right] \tag{6.42}$$

Hassanizadeh (1997) gives a formula which depends on temperature T, pressure p and salt mass fraction ω:

$$\rho_{(T,p,\omega)} = \rho_0 e^{-\alpha(T-T_0)+\beta(p-p_0)+\gamma\omega} \tag{6.43}$$

where

- α=2 $\times$ 10^{-4} per $^{o}Kelvin$,
- β=4.45 $\times$ 10^{-10} $(m\,s^2\,kg^{-1})$,
- γ=0.7 $(-)$.

Note that at high pressures, this equation is not applicable.

6.2 Solute transport: advection-dispersion equation

In so-called quality problems, the interest is focussed on the transport of dissolved solids[6]. A further division of qualitative groundwater models is into:

I. solute transport[7] which does not affect the flow of groundwater through density differences. Examples of this type of quality problems are eutrophication, the transport of contaminations caused by industry (e.g. oil pollution at dumps or petrol stations) or agriculture (nitrogen and phosphorus contamination due to atmospheric deposition and the application of fertilizers). Examples of computer codes of this type of problem are: the original MOC code [Konikow & Bredehoeft, 1978], a random walk code by Uffink [1990], MT3D [Zheng, 1990], MOC3D [Konikow *et al.*, 1996].

II. solute transport which affects the flow of groundwater as the density of the groundwater is not constant: the so-called *density dependent groundwater flow*. This type of solute transport is applied to model salt water intrusion in coastal aquifers where mostly non-uniform density distributions occur. In many coastal hydrogeologic systems, a relatively thick transition zone[8] between fresh, brackish and saline groundwater is present because of various processes during geological history (regressions, transgressions). In addition, the transition zone is also increasing as a result of the circulation of brackish water due to inflow of saline groundwater (mixing with fresh groundwater due to hydrodynamic dispersion), the tidal regime and human activities, such as (artificial) recharge and groundwater extraction at high and variable rates [Cooper, 1964]. For example, this situation occurs in Dutch hydrogeologic cross-sections with Holocene and Pleistocene deposits of marine and fluviatile origin [Meinardi, 1973; Maas, 1989], see figure 3.2. Under such conditions, sophisticated models are required which take into account variable densities. These models are referred to as *solute transport models* or *salt water intrusion models*. They apply the advection-dispersion equation to convert solute concentration (or total dissolved solids) to density. As such, the solute transport equation and the groundwater flow equation are coupled with each other. They are able to simulate, among others, changes in solute concentration (e.g. near pumping wells due to upconing), changes in volumes of freshwater in sand-dune areas and changes in the salinity of seepage in polder areas.

[6] Note again that simulating the transport of heat in groundwater is mathematically practically similar to simulating the transport of dissolved solids, see subsection 6.3.

[7] Note that modelling the contamination of porous media by complex dissolved substances, such as the so-called nonaqueous phase liquids (NAPL), goes beyond the scope of these lecture notes.

[8] Other terms are mixing zone, zone of dispersion or brackish zone.

Examples of computer codes of this type of problem are: SUTRA [Voss, 1984], HST3D [Kipp, 1986], SWICHA [Huyakorn *et al.*, 1987; Lester, 1991], METROPOL [Sauter *et al.*, 1993] and the adapted MOC code (2D [Oude Essink, 1996], see section 9.5 and 3D, MOCDENS3D [Oude Essink, 1998], see the lectures notes of Hydrological Transport Processes/Groundwater Modelling II: Density Dependent Groundwater Flow: Salt Water Intrusion and Heat Transport).

III. a special type of a qualitative groundwater model is the interface model. Though the transport of dissolved solids is not directly considered, an interface model can simulate density dependent groundwater flow. They are based on the assumption that a interface between fresh and saline groundwater represents the actual situation. This is the well-known *Badon Ghyben-Herzberg principle*. These straightforward interface models can be applied as an educational means to gain a clear insight in the behaviour of fresh and saline groundwater in coastal aquifer systems. As such, interface models are still widely applied. Two important restrictions on the applicability of the principle should be considered:

- First, the principle only approximates the actual occurrence of fresh, brackish and saline groundwater in the subsoil. In fact, the brackish zone between fresh and saline groundwater should only be schematised by a interface when the maximum thickness of the brackish zone is in the order of several metres only. This condition applies only in rare situations where the freshwater lens is evolved by natural recharge, as occurs in undisturbed (viz. a system at rest) sand-dune areas or (coral) islands.
- Second, the principle assumes a hydrostatic equilibrium, whereas in reality the hydrogeologic system might considerably deviate from this equilibrium situation. In those cases, e.g. in freshwater bodies near the shoreline, the Badon Ghyben-Herzberg principle should not be applied, because the computed position of the interface significantly deviates from the actual position.

Examples of computer codes of this type of problem are: van Dam [1976]; SALINA [IWACO, 1987]; Beaversoft [Bear & Verruijt, 1987].

6.2.1 Equation of solute transport

Solute transport is caused by (see figure 6.6):

1. Advection:
   process where groundwater flow is caused by gravity,

2. Diffusion:
   molecular process where constituents are spread due to differences in concentrations,

3. Dispersion:
   mixing process caused by differences in velocity (in magnitude and in direction) of water particles, see figure 6.6

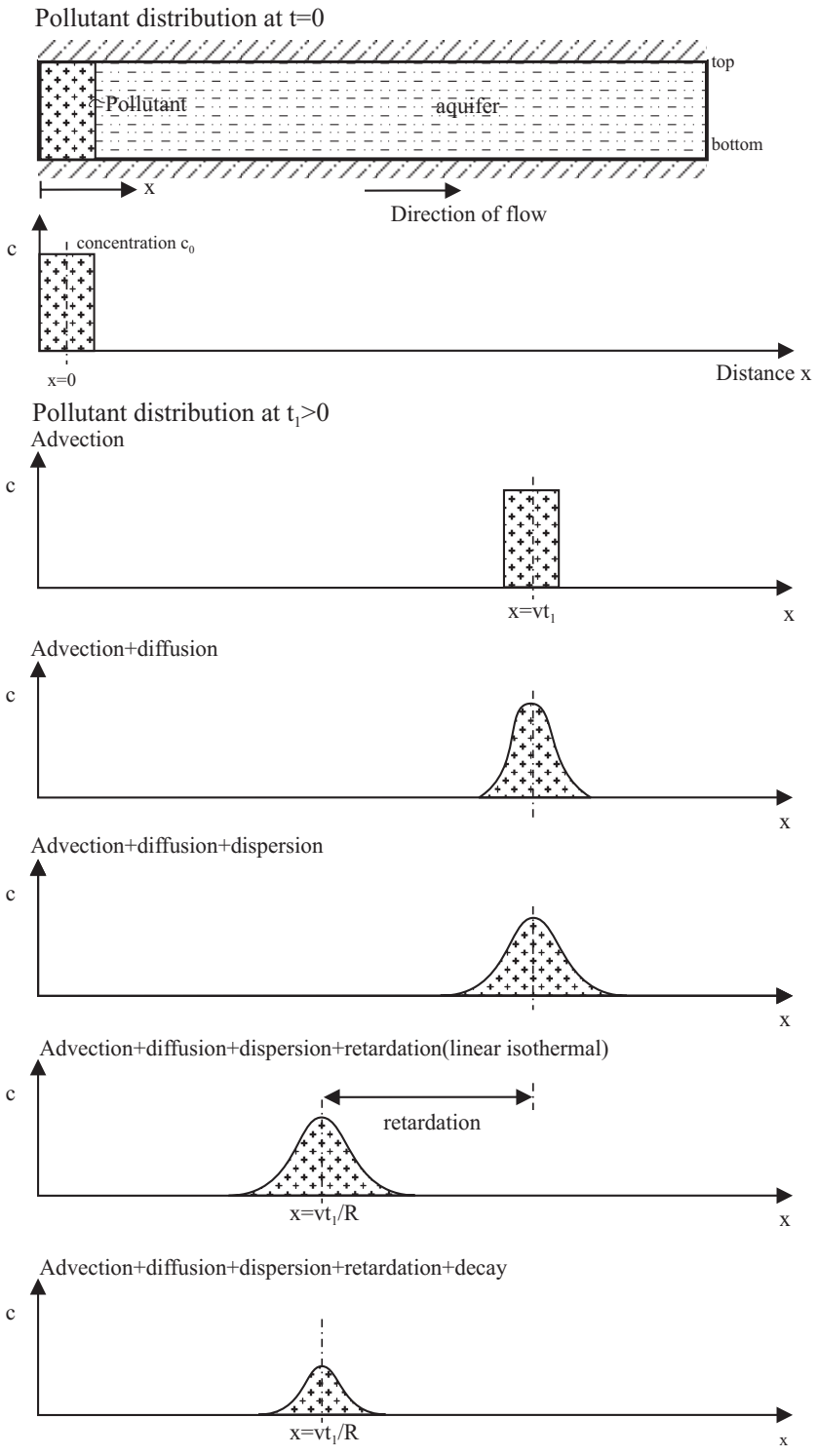

Figure 6.6: *Various processes involving solute transport in porous media.*

4. Adsorption:
   process where certain constituents are attached to grain material

5. Decay:
   change in concentration by biologic or radioactive decline

From an educational point of view, the solute transport equation is obtained in only the x-direction (1D). Mass fluxes ($M\,L^{-2}\,T^{-1}$) of each process of the solute transport equation per unit of time per unit of cross-sectional area are:

ad 1. Advection

Mass flux:

$$f_{adv} = V_x C + V_y C + V_z C \tag{6.44}$$

ad 2. Molecular diffusion (Fick's law)

$$f_{diff} = -D_m \left(\frac{\partial C}{\partial x} + \frac{\partial C}{\partial y} + \frac{\partial C}{\partial z} \right) = -D_m \nabla C \tag{6.45}$$

ad 3. Dispersion

$$f_{disp} = -D \nabla C \tag{6.46}$$

$$D_h = D + D_m \qquad \text{(where } D_h\text{=hydrodynamic dispersion coefficient)} \tag{6.47}$$

Balance in x-direction:

$$-n_e \frac{\partial f_{adv.}}{\partial x} \Delta x \Delta y \Delta z \Delta t - n_e \frac{\partial f_{hydr.disp}}{\partial x} \Delta x \Delta y \Delta z \Delta t = n_e \Delta x \Delta y \Delta z \frac{\partial C}{\partial t} \Delta t \tag{6.48}$$

$$-n_e \frac{\partial V_x C}{\partial x} \Delta x \Delta y \Delta z \Delta t - n_e \frac{\partial (-D_h \frac{\partial C}{\partial x})}{\partial x} \Delta x \Delta y \Delta z \Delta t = n_e \Delta x \Delta y \Delta z \frac{\partial C}{\partial t} \Delta t \tag{6.49}$$

$$D_x \frac{\partial^2 C}{\partial x^2} - V_x \frac{\partial C}{\partial x} = \frac{\partial C}{\partial t} \tag{6.50}$$

ad 4. Adsorption

Mathematical description of adsorption in x-direction (1D):

$$\frac{\partial (\rho_b S)}{\partial t} \tag{6.51}$$

where

- ρ_b = bulk density of the porous material ($M\,L^{-3}$),
- S = fraction of the solute sorbed (or exchanged) on the porous material ($M\,M^{-1}$).

$$\frac{\partial C_{ads.}}{\partial t} = -\frac{\rho_b}{n_e}\frac{\partial S}{\partial t} \tag{6.52}$$

The linear sorption exchange reaction considers that the concentration of solute sorbed to the porous medium S is directly proportional to the concentration of the solute in the pore fluid C, according to the relation:

$$S = K_d C \tag{6.53}$$

where

- K_d = distribution coefficient ($M^{-1}\,L^3$).

The slope (derivative) of the sorbed concentration versus dissolved concentration curve, $\frac{dS}{dC}$, is equal to distribution coefficient K_d. Examples of two nonlinear sorption isotherms are the Freundlich and Langmuir sorption isotherms [Goode & Konikow, 1989]:

$$\text{Freundlich sorption} \qquad S = K_f C^n \qquad \text{slope: } \frac{dS}{dC} = nK_f C^{n-1} \tag{6.54}$$

where

- K_f = Freundlich sorption equilibrium constant (units are a function of n),
- n = Freundlich exponent ($-$).

$$\text{Langmuir sorption} \qquad S = \frac{K_l Q C}{1 + K_l C} \qquad \text{slope: } \frac{dS}{dC} = \frac{K_l Q C}{1 + K_l C}^{\,2} nK_f C^{n-1} \tag{6.55}$$

where

- K_l = Langmuir sorption equilibrium constant ($M^{-1}\,L^3$),
- Q = maximum sorption capacity ($M\,M^{-1}$).

These two nonlinear sorption isotherms, as well as ion-exchange [Goode & Konikow, 1989] are not considered further. So, by including the linear sorption isotherm, equation 6.51 becomes:

$$\frac{\partial S}{\partial t} = \frac{dS}{dC}\frac{\partial C}{\partial t} = K_d \frac{\partial C}{\partial t} \tag{6.56}$$

$$\frac{\partial C_{ads.}}{\partial t} = -\frac{\rho_b}{n_e} K_d \frac{\partial C}{\partial t} \tag{6.57}$$

$$D_x \frac{\partial^2 C}{\partial x^2} - V_x \frac{\partial C}{\partial x} - \frac{\rho_b}{n_e} K_d \frac{\partial C}{\partial t} = \frac{\partial C}{\partial t} \tag{6.58}$$

$$D_x \frac{\partial^2 C}{\partial x^2} - V_x \frac{\partial C}{\partial x} = R_d \frac{\partial C}{\partial t} \tag{6.59}$$

$$R_d = (1 + \frac{\rho_b}{n_e} K_d) \tag{6.60}$$

where

- $R_d = 1 + (\rho_b / n_e) K_d$ = retardation factor governing adsorption ($-$).

ad 5. Decay

Mathematical description of decay in x-direction (1D):

$$C = C_0 \; e^{-\lambda t} \tag{6.61}$$

- C_0 = original concentration of the dissolved solids ($M\,L^{-3}$),
- λ = first-order rate constant, governing hydrolysis and decay (T^{-1}). Radioactive decay rates are often expressed as halflives ($t_{1/2}$), where the half-life is the time required for the concentration to decrease to one-half of the original value: $t_{1/2} = (\ln 2)/\lambda$.

$$\frac{\partial C_{dec.}}{\partial t} = -\lambda \; C_0 \; e^{-\lambda t} = -\lambda \; C \tag{6.62}$$

$$\frac{\partial S_{dec.}}{\partial t} = -\lambda S \tag{6.63}$$

$$\frac{\partial C_{ads.dec.}}{\partial t} = -\frac{\rho_b}{n_e}\left(\frac{\partial S}{\partial t} + \lambda S\right) \tag{6.64}$$

$$D_x \frac{\partial^2 C}{\partial x^2} - V_x \frac{\partial C}{\partial x} - \frac{\rho_b}{n_e}\left(K_d \frac{\partial C}{\partial t} + \lambda K_d C\right) - \lambda C = \frac{\partial C}{\partial t} \tag{6.65}$$

$$D_x \frac{\partial^2 C}{\partial x^2} - V_x \frac{\partial C}{\partial x} - (1 + \frac{\rho_b}{n_e} K_d)\lambda C = (1 + \frac{\rho_b}{n_e} K_d)\frac{\partial C}{\partial t} \tag{6.66}$$

$$\frac{D_x}{R_d}\frac{\partial^2 C}{\partial x^2} - \frac{V_x}{R_d}\frac{\partial C}{\partial x} - \lambda C = \frac{\partial C}{\partial t} \tag{6.67}$$

Three-dimensional equation of solute transport

Extending to three dimensions, the three-dimensional equation for solute transport in homogeneous isotropic porous media can be written as follows:

$$\frac{\partial C}{\partial t} = \frac{\partial}{\partial x_i}(D_{ij}\frac{\partial C}{\partial x_j}) - \frac{\partial}{\partial x_i}(C\,V_i) + \frac{(C - C')\,W}{n_e b} + \frac{\Psi}{n_e} \tag{6.68}$$

where

- C = concentration of the dissolved solids ($M\,L^{-3}$),
- D_{ij} = coefficient of hydrodynamic dispersion ($L^2\,T^{-1}$),
- $V_i = q_i/n_e$ = effective velocity of the groundwater in the direction of x_i ($L\,T^{-1}$),
- C' = concentration of the dissolved solids in a source or sink ($M\,L^{-3}$),
- $W(x, y, z, t)$ = general term for sources and sinks ($L\,T^{-1}$),
- n_e = effective porosity of the medium ($-$),

- Ψ = chemical reaction source or sink per unit volume ($M\,L^{-3}\,T^{-1}$), where Ψ is based on the equations 6.53, 6.62 and 6.64 when linear adsorption and decay are included.

Equation 6.68 is called the *advection-dispersion equation*, the *solute transport equation* or the *transport-dispersion equation*. The first term on the right hand side represents the change in concentration of solutes due to hydrodynamic dispersion. The second term represents the effect of advective transport which is the movement of solutes attributed to transport by flowing groundwater. The third term represents the contribution and removal of solutes due to fluid sources and sinks, whereas the fourth term represents chemical reactions.

If the velocity V_i is equal to zero, no sources and sinks are considered ($W = 0$) and no chemical reaction (adsorption nor decay) are taken into account, then the advection-dispersion equation is reduced to the so-called *diffusion equation* (see page 101 for a numerical example).

6.2.2 Hydrodynamic dispersion

Hydrodynamic dispersion D_h is defined as the combined effect of two processes:

$$D_h = D + D_m \tag{6.69}$$

where

- D ($L^2\,T^{-1}$) = mechanical (or convective) dispersion coefficient. This process is caused by velocity variations at the microscopic scale, see fig. 6.7. The spreading depends on both fluid flow and the characteristics of the pore system through which the flow takes place,

- D_m ($L^2\,T^{-1}$) = molecular diffusion coefficient. This process is caused by the random movement of molecules in a fluid and depends on concentration gradients, the properties of the fluid and the soil. For a conservative solute as chloride, the molecular diffusion D_m for porous media is approximately 10^{-9} m^2/s at a temperature of 25 ^oC.

Under normal groundwater flow conditions, molecular diffusion is of marginal importance with respect to mechanical dispersion. In fact, the subdivision of the hydrodynamic dispersion into mechanical dispersion and molecular diffusion is artificial. The mechanical dispersion coefficient, which is a second-rank symmetrical tensor, is given by Scheidegger [1961]:

$$D_{ij} = \alpha_{ijmn} \frac{V_m V_n}{|V|} \tag{6.70}$$

or

$$D_{ij} = \alpha_T\,|V|\,\delta_{ij} + (\alpha_L - \alpha_T)\,\frac{V_i V_j}{|V|} \tag{6.71}$$

where

- D_{ij} = coefficient of mechanical dispersion ($L^2\,T^{-1}$),

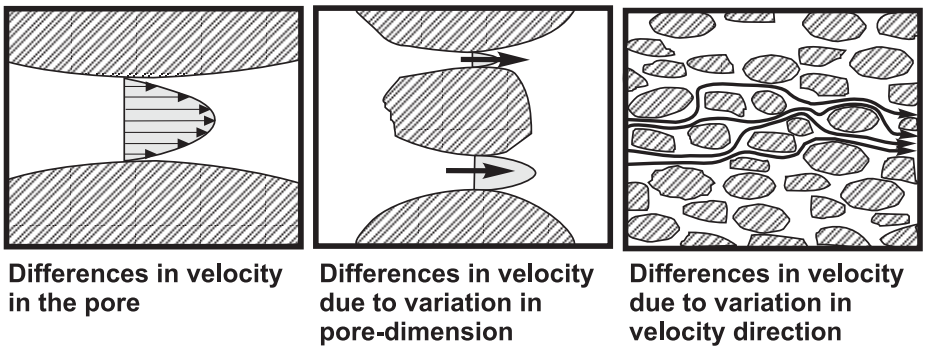

Figure 6.7: Causes of dispersion on microscale.

- α_{ijmn} = *geometrical dispersivity tensor* of the aquifer (L),
- V_m, V_n = components of the real velocity in m and n direction ($L\,T^{-1}$),
- $|V|$ = magnitude of the real velocity ($L\,T^{-1}$),
- $\delta_{ij} = 1$ if $i = j$ and $\delta_{ij} = 0$ if $i \neq j$.

Scheidegger defines the dispersivity tensor for an isotropic aquifer in terms of two constants:

$$\begin{aligned} D_L &= \alpha_L\,|V| \\ D_T &= \alpha_T\,|V| \end{aligned} \tag{6.72}$$

where

- α_L = longitudinal dispersivity of the aquifer (L),
- α_T = transversal dispersivity of the aquifer (L).

For example, the components of hydrodynamic dispersion (in the principal directions) for two-dimensional and three-dimensional flow in an isotropic aquifer, considering mechanical dispersion as well as molecular diffusion D_m, are as follows:

$$\begin{aligned} D_{xx} &= \alpha_L \frac{(V_x)^2}{|V|} + \alpha_T \frac{(V_z)^2}{|V|} + D_m \\ D_{zz} &= \alpha_T \frac{(V_x)^2}{|V|} + \alpha_L \frac{(V_z)^2}{|V|} + D_m \\ D_{xz} &= D_{zx} = (\alpha_L - \alpha_T)\frac{V_x\,V_z}{|V|} \end{aligned} \tag{6.73}$$

$$\begin{aligned} D_{xx} &= \alpha_L \frac{(V_x)^2}{|V|} + \alpha_T \frac{(V_y)^2}{|V|} + \alpha_T \frac{(V_z)^2}{|V|} + D_m \\ D_{yy} &= \alpha_T \frac{(V_x)^2}{|V|} + \alpha_L \frac{(V_y)^2}{|V|} + \alpha_T \frac{(V_z)^2}{|V|} + D_m \end{aligned}$$

$$
\begin{aligned}
D_{zz} &= \alpha_T \frac{(V_x)^2}{|V|} + \alpha_T \frac{(V_y)^2}{|V|} + \alpha_L \frac{(V_z)^2}{|V|} + D_m \\
D_{xy} &= D_{yx} = (\alpha_L - \alpha_T) \frac{V_x V_y}{|V|} \\
D_{xz} &= D_{zx} = (\alpha_L - \alpha_T) \frac{V_x V_z}{|V|} \\
D_{yz} &= D_{zy} = (\alpha_L - \alpha_T) \frac{V_y V_z}{|V|}
\end{aligned} \tag{6.74}
$$

The exact determination of the hydrodynamic dispersion is very difficult, if not impossible, as it depends on many features (e.g. scale effect, fingering, transient effects [Anderson & Woessner, 1992]). In fact, the more one knows about the hydraulic conductivity and porosity distribution, and subsequently, the exact velocity distribution, the more the hydrodynamic dispersion value will converge to the value of molecular diffusion. As such, one should model the heterogeneous and anisotropic medium as accurately as possible. However, as it is not possible to determine the exact hydraulic conductivity distribution as well as the exact velocity distribution, the exact value of the dispersion coefficient can not be given. For this reason, the value of mechanical dispersion, which is inserted in the model, may (somewhat) be increased to take into account these uncertainties in the subsoil parameters. The less one knows, the higher the model dispersivities will often be.

Gelhar *et al.* [1992] reviewed 59 different field sites in order to classify the dispersivity data into three reliability classes (see figure 6.8). The representative scale of the cases ranges from 10^{-1} to 10^5 m. They found that for these cases, the longitudinal dispersivity ranges from 10^{-2} to 10^4 m. In conclusion, the variation in dispersivity reflects the influence of different degrees of aquifer heterogeneity at different field sites. They concluded that in general, longitudinal dispersivities in the lower part of the indicated range are more likely to be realistic for field applications. Therefore, the so-called *scale-dependency* of dispersivities ($\alpha_L = 0.1\,L$, where L is the traveled distance of the contaminant), determined from field data, should be reviewed critically. For instance, Schulze-Makuch & Cherkauer [1997] show that for carbonate aquifers the relationship of longitudinal dispersivity to scale is exponential according to $\alpha_L = 0.2\,L^{1.07}$, until an upper bound of traveled flow distance L=100 metre (α_L=27.6 metre) is reached, after which the longitudinal dispersivity remains constant with scale.

Furthermore, Gelhar *et al.* indicated that there is a need for long-term, very large-scale experiments extending to several kilometres.

In contrast with some field sites in especially the USA (see, e.g., the cases in Gelhar *et al.*, 1992), the best estimates of the longitudinal dispersivities in Dutch and Belgian large-scale hydrogeologic systems with Holocene and Pleistocene deposits of marine and fluviatile origin appear to yield rather small values. This manifests itself in sand-dune areas along the Dutch coast, where freshwater lenses with (relatively sharp) fresh-salt interfaces have been formed. This observation is based on various case studies, such as Lebbe [1983], Kooiman *et al.* [1986], Stuyfzand [1991]; Walraevens *et al.* [1993]; and Oude Essink [1993]. For example, computations have indicated that if a great hydrodynamic dispersion (that means a great longitudinal dispersivity) is simulated during long simulation times, unrealistic solutions are generated [Oude Essink, 1996]. In this example, the cross-section is situated in the sand-

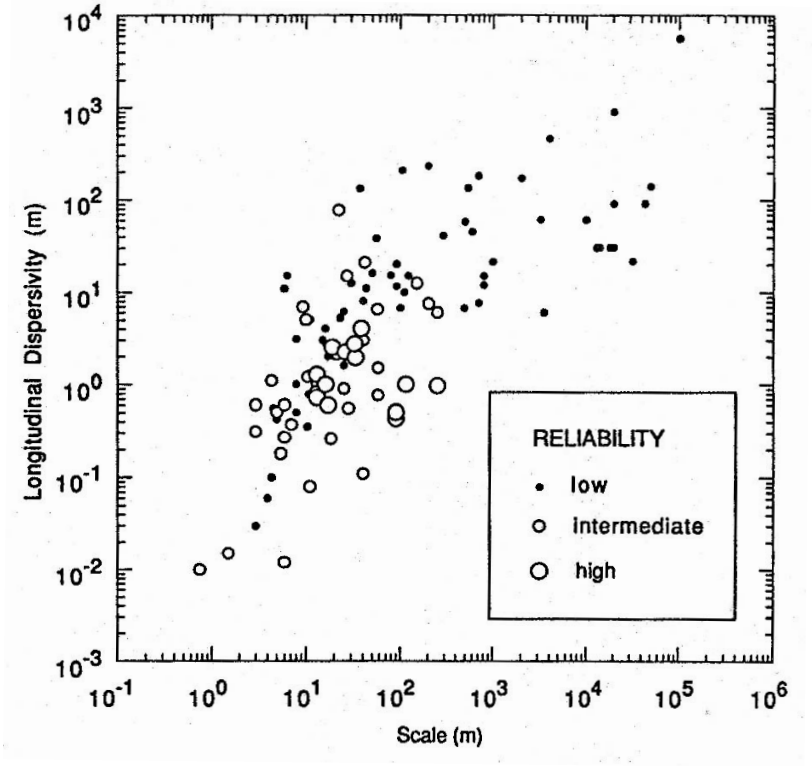

Figure 6.8: *Longitudinal dispersivity versus scale with data classified by reliability [Gelhar et al., 1992].*

dune area of Gemeentewaterleidingen Amsterdam along the Dutch coast where a freshwater lens has been formed. In figure 6.9, the effect of the longitudinal dispersivity α_L is evaluated by comparing the results of simulations with four different values of α_L: 0.02 m, 0.2 m, 2.0 m and 20.0 m. The chloride distributions of the cross-section are given after a simulation time of 134 years: from 1854 (the reclamation of the Haarlemmermeer polder) till the end of 1987. The computed chloride distribution matches the measured distribution best if small longitudinal dispersivities are applied, namely α_L=0.02 m and α_L=0.2 m. By contrast, the case with α_L=2.0 m shows a freshwater lens that is too thin compared to reality, whereas the case with α_L=20.0 m does not simulate a freshwater lens any more: the hydrogeologic system only consists of a large brackish zone. Obviously, this situation does not occur in reality.

6.2.3 Chemical reactions

The term Ψ for chemical reactions in equation 6.68 includes equilibrium-controlled sorption or exchange and first-order irreversible rate (radioactive decay) reactions. Here follows a summary of processes associated with dissolved solids transport [Maidment, 1993]:

- Sorption is the reaction between solute and the surfaces of solids causing the solute to bond (to varying degrees) to the surface.

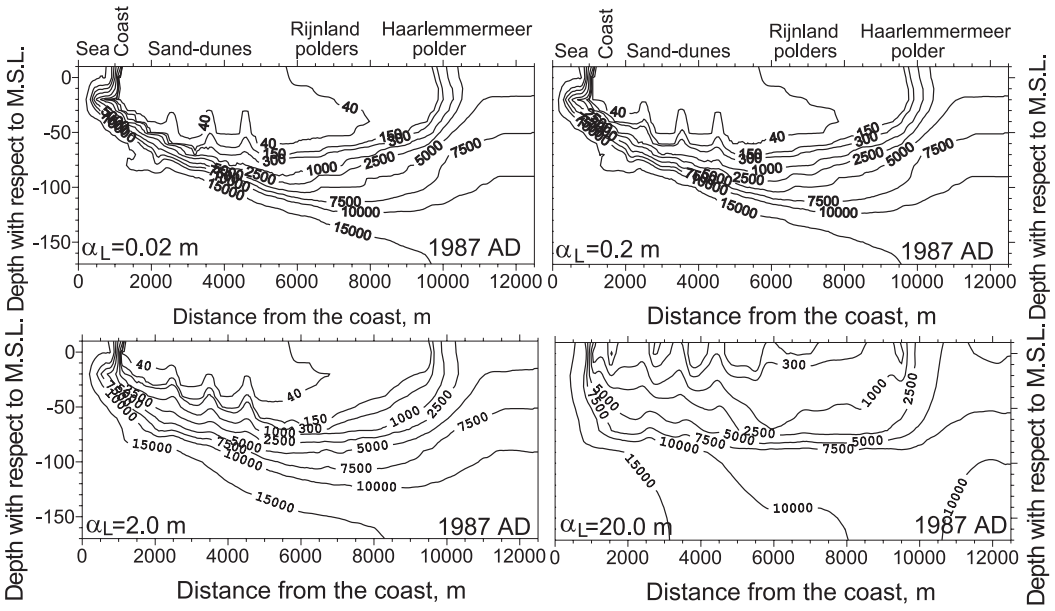

Figure 6.9: *Chloride distributions (in mg Cl^-/l) in 1987 in a cross-section through the sand-dune area of Gemeentewaterleidingen Amsterdam and the Haarlemmermeer polder, computed for 4500 elements with MOC [Konikow & Bredehoeft, 1978] (adapted for density differences to model vertical cross-sections [Oude Essink, 1996]) for four different longitudinal dispersivities: α_L=0.02 m, α_L=0.2 m, α_L=2.0 m and α_L=20.0 m. A thick freshwater lens is only simulated for small dispersivities.*

- Radioactive decay is the irreversible decline in the activity of a radionuclide through a nuclear reaction.
- Biodegradation or biologic transformation is the reaction involving the degradation of organic compounds and whose rate is controlled by the abundance of the microorganisms and redox conditions.
- Hydrolysis is the reaction on an organic compound with water or a component ion of water. Substitution is the reaction with another anion. Often, hydrolysis and substitution reactions make an organic compound more susceptible to biodegradation and more soluble.

For example, if decay and linear sorption is included, equation 6.68 becomes [Goode & Konikow, 1989]:

$$R_d \frac{\partial C}{\partial t} = \frac{\partial}{\partial x_i}(D_{ij} \frac{\partial C}{\partial x_j}) - \frac{\partial}{\partial x_i}(C\, V_i) + \frac{(C - C')\, W}{n_e b} - R_d\, \lambda\, C \qquad (6.75)$$

where

- $R_d = 1 + (\rho_b / n_e) K_d$ = retardation factor governing adsorption $(-)$. K_d is the distribution coefficient $(M^{-1}\, L^3)$ and ρ_b is the bulk density of the porous material $(M\, L^{-3})$,

Material	**Thermal conductivity**
	κ $(cal\ m^{-1}\ s^{-1}\ ^oCelcius^{-1})$
Quartz	2
Sandstone	0.9
Limestone	0.5
Dolomite	0.4-1
Clay	0.2-0.3
Water	0.11
Air	0.006

Table 6.5: *Thermal conductivity of rocks, water and air. To convert Calorie to Joule, multiply by 4.187.*

- λ = first-order rate constant, governing hydrolysis and decay (T^{-1}). Radioactive decay rates are often expressed as halflives ($t_{1/2}$), where the half-life is the time required for the concentration to decrease to one-half of the original value: $t_{1/2} = (\ln 2)/\lambda$.

With regard to the transport of a conservative solute, viz. salt, Ψ is assumed to be equal to zero: this means that R_d=1 and λ=0.

6.3 Heat transport: conduction-convection equation

Mathematical description of heat transport in x-direction 1D (Fourier and convection):

$$\text{Fourier's law:} \quad q = -\lambda_e \frac{\partial T}{\partial x} + n_e\, \rho_f\, c_f\, T\, V \quad \text{with} \quad \lambda_e = n_e \lambda_f + (1 - n_e)\lambda_s \tag{6.76}$$

where

- q=heat flux ($Joule\ m^{-2}\ s^{-1}$) or ($Watt\ m^{-2}$),
- λ_e=thermal conductivity ($Joule\ m^{-1}\ s^{-1}\ ^oCelcius^{-1}$). λ_f, λ_s are thermal conductivities of fluid and solid material, respectively.
- T=temperature ($^oCelcius$),
- c_f=specific heat capacity ($Joule\ kg^{-1}\ ^oCelcius^{-1}$),
- ρ_f, ρ_s= density of fluid and solid material, respectively ($kg\ m^{-3}$).

$$\text{Equation of continuity:} \quad -\frac{\partial q}{\partial x} = \rho' c' \frac{\partial T}{\partial t} \tag{6.77}$$

with $\rho' c' = n_e \rho_f c_f + (1 - n_e)\rho_s c_s$.

$$\lambda_e \frac{\partial^2 T}{\partial x^2} - n_e \rho_f c_f \frac{\partial T\ V}{\partial x} = \rho' c' \frac{\partial T}{\partial t} \tag{6.78}$$

$$\text{Steady state:} \quad \frac{\partial V}{\partial x} = 0 \Longrightarrow \lambda_e \frac{\partial^2 T}{\partial x^2} - n_e \rho_f c_f V \frac{\partial T}{\partial x} = \rho' c' \frac{\partial T}{\partial t} \tag{6.79}$$

$$\text{Heat transport:} \quad \frac{\lambda_e}{\rho' c'} \frac{\partial^2 T}{\partial x^2} - \frac{n_n \rho_f c_f}{\rho' c'} V \frac{\partial T}{\partial x} = \frac{\partial T}{\partial t} \tag{6.80}$$

$$\text{Analogy with solute transport:} \quad \frac{D_x}{R_d} \frac{\partial^2 C}{\partial x^2} - \frac{1}{R_d} V \frac{\partial C}{\partial x} = \frac{\partial C}{\partial t} \tag{6.81}$$

See the lecture notes of Hydrological Transport Processes/Groundwater Modelling II: Density Dependent Groundwater Flow: Salt Water Intrusion and Heat Transport).

Chapter 7

Solution techniques

7.1 Introduction

Many solution techniques have been developed to solve the groundwater flow equation and the advection-dispersion equation. Computer codes with suitable solution techniques are already available since at least three decades.

In quantity problems, only the groundwater flow equation have to be solved. It appears that most groundwater computer codes are based on the *finite element method* or the *finite different method*. In quality problems, this means when the groundwater flow equation and the advection-dispersion equation have to be solved simultaneously, e.g. for salt water intrusion or contaminant transport, also the *method of characteristics* and the *random walk method* come to the front. These methods can more easily simulate the flow of groundwater in combination with the transport of solutes without (numerical) dispersion problems.

The problem to be solved and the preference of the user determine the choice of the solution technique (a combination of solution techniques is also possible). In this chapter, first some basic numerical techniques are summarised: some iterative methods in section 7.2, the Thomas algorithm in section 7.3 and the Gauss-Jordan elimination in section 7.4. Subsequently, six solution techniques used by computer codes are discussed in the sections 7.5 to 7.10.

7.2 Iterative methods

7.2.1 Taylor series development

$$\phi_{i+1,j} = \phi_{i,j} + \Delta x \frac{\partial \phi}{\partial x} + \frac{1}{2}\Delta x^2 \frac{\partial^2 \phi}{\partial x^2} + \frac{1}{6}\Delta x^3 \frac{\partial^3 \phi}{\partial x^3} + \frac{1}{24}\Delta x^4 \frac{\partial^4 \phi}{\partial x^4} + ... \tag{7.1}$$

$$\phi_{i-1,j} = \phi_{i,j} - \Delta x \frac{\partial \phi}{\partial x} + \frac{1}{2}\Delta x^2 \frac{\partial^2 \phi}{\partial x^2} - \frac{1}{6}\Delta x^3 \frac{\partial^3 \phi}{\partial x^3} + \frac{1}{24}\Delta x^4 \frac{\partial^4 \phi}{\partial x^4} + ... \tag{7.2}$$

Adding equation 7.1 and equation 7.2 gives:

$$\phi_{i+1,j} + \phi_{i-1,j} = 2\phi_{i,j} + \Delta x^2 \frac{\partial^2 \phi}{\partial x^2} + \frac{1}{12}\Delta x^4 \frac{\partial^4 \phi}{\partial x^4} + ... \tag{7.3}$$

$$\frac{\partial^2 \phi}{\partial x^2} = \frac{\phi_{i+1,j} - 2\phi_{i,j} + \phi_{i-1,j}}{\Delta x^2} + O(-\frac{1}{12}\Delta x^2 \frac{\partial^4 \phi}{\partial x^4} + ...) \tag{7.4}$$

$$\frac{\partial^2\phi}{\partial x^2} \approx \frac{\phi_{i+1,j} - 2\phi_{i,j} + \phi_{i-1,j}}{\Delta x^2} \tag{7.5}$$

Subtracting equation 7.1 from equation 7.2 gives:

$$\phi_{i+1,j} - \phi_{i-1,j} = 2\Delta x\frac{\partial\phi}{\partial x} + \frac{1}{3}\Delta x^3\frac{\partial^3\phi}{\partial x^3} + ... \tag{7.6}$$

$$\frac{\partial\phi}{\partial x} = \frac{\phi_{i+1,j} - \phi_{i-1,j}}{2\Delta x} + O(-\frac{1}{6}\Delta x^2\frac{\partial^3\phi}{\partial x^3} + ...) \tag{7.7}$$

$$\frac{\partial\phi}{\partial x} \approx \frac{\phi_{i+1,j} - \phi_{i-1,j}}{2\Delta x} \tag{7.8}$$

7.2.2 Laplace equation

Discretisation of the Laplace equation (2D) gives:

$$\frac{\partial^2\phi}{\partial x^2} + \frac{\partial^2\phi}{\partial y^2} = 0 \tag{7.9}$$

$$\nabla^2\phi = 0 \tag{7.10}$$

Note that when a source or sink term is included, viz. $\nabla^2\phi = N$, the equation is called to be a Poisson equation. Using the Taylor series expansions gives:

$$\frac{\partial^2\phi}{\partial x^2} \approx \frac{\phi_{i+1,j} - 2\phi_{i,j} + \phi_{i-1,j}}{\Delta x^2} \tag{7.11}$$

$$\frac{\partial^2\phi}{\partial y^2} \approx \frac{\phi_{i,j+1} - 2\phi_{i,j} + \phi_{i,j-1}}{\Delta y^2} \tag{7.12}$$

$$\nabla^2\phi = \frac{\phi_{i+1,j} - 2\phi_{i,j} + \phi_{i-1,j}}{\Delta x^2} + \frac{\phi_{i,j+1} - 2\phi_{i,j} + \phi_{i,j-1}}{\Delta y^2} = 0 \tag{7.13}$$

If $\Delta x = \Delta y$ than:

$$\phi_{i+1,j} + \phi_{i-1,j} - 4\phi_{i,j} + \phi_{i,j+1} + \phi_{i,j-1} = 0 \tag{7.14}$$

$$\phi_{i,j} = \frac{1}{4}\left(\phi_{i+1,j} + \phi_{i-1,j} + \phi_{i,j+1} + \phi_{i,j-1}\right) \qquad \text{(five-point operator)} \tag{7.15}$$

Example 7.1: Matrix of the Laplace equation

A solution for a grid of 25 points is given (figure 7.1). The assumptions are:

- Dirichlet boundary for the entire grid,
- Piezometric heads for the nine points 7, 8, 9 12, 13, 14, 17, 18 en 19.

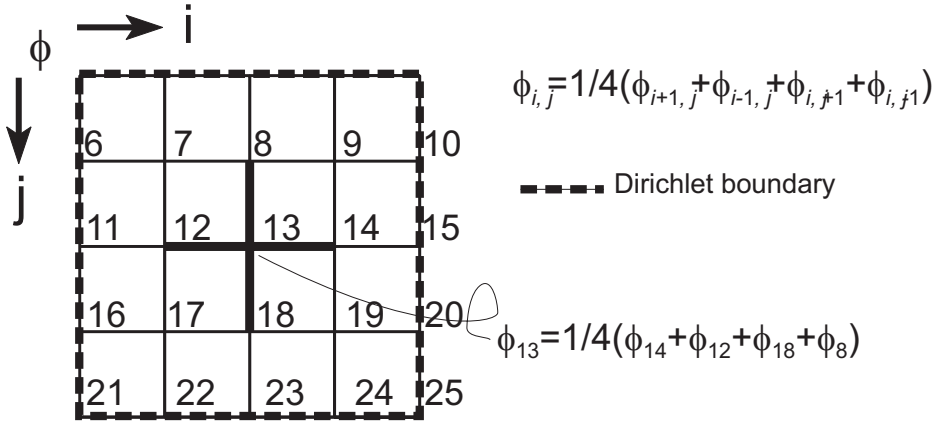

Figure 7.1: *Discretisation of the Laplace equation for a grid with 25 points. The boundaries are of the Dirichlet type (constant head).*

$$\begin{gathered}\phi_2+\phi_6-4\phi_7+\phi_8+\phi_{12}=0\\ \phi_3+\phi_7-4\phi_8+\phi_9+\phi_{13}=0\\ \phi_4+\phi_8-4\phi_9+\phi_{10}+\phi_{14}=0\\ \text{etc.}\end{gathered} \tag{7.16}$$

Combining the equations together in one matrix gives:

$$\begin{bmatrix} -4 & 1 & 0 & 1 & 0 & 0 & 0 & 0 & 0\\ 1 & -4 & 1 & 0 & 1 & 0 & 0 & 0 & 0\\ 0 & 1 & -4 & 0 & 0 & 1 & 0 & 0 & 0\\ 1 & 0 & 0 & -4 & 1 & 0 & 1 & 0 & 0\\ 0 & 1 & 0 & 1 & -4 & 1 & 0 & 1 & 0\\ 0 & 0 & 1 & 0 & 1 & -4 & 0 & 0 & 1\\ 0 & 0 & 0 & 1 & 0 & 0 & -4 & 1 & 0\\ 0 & 0 & 0 & 0 & 1 & 0 & 1 & -4 & 1\\ 0 & 0 & 0 & 0 & 0 & 1 & 0 & 1 & -4 \end{bmatrix} \times \begin{Bmatrix} \phi_7\\ \phi_8\\ \phi_9\\ \phi_{12}\\ \phi_{13}\\ \phi_{14}\\ \phi_{17}\\ \phi_{18}\\ \phi_{19} \end{Bmatrix} = \begin{Bmatrix} -\phi_2-\phi_6\\ -\phi_3\\ -\phi_4-\phi_{10}\\ -\phi_{11}\\ 0\\ -\phi_{15}\\ -\phi_{16}-\phi_{22}\\ -\phi_{23}\\ -\phi_{20}-\phi_{24} \end{Bmatrix} \tag{7.17}$$

or

$$[A]\,\{\phi\}=\{R\} \tag{7.18}$$

7.2.3 Steady state methods

Iterative methods are used to determine the piezometric head $\phi_{i,j}$. The iterations stop when the error tolerance or convergence criterium is reached. Here follow three well-known iterative methods:

1. Jacobi iteration: uses only old values:

$$\phi_{i,j}^{n+1}=\frac{1}{4}\left(\phi_{i+1,j}^{n}+\phi_{i-1,j}^{n}+\phi_{i,j+1}^{n}+\phi_{i,j-1}^{n}\right) \qquad \text{(n=iteration-step)} \tag{7.19}$$

2. Gauss-Seidel iteration: uses also two new values (this method is somewhat more efficient):

$$\phi_{i,j}^{n+1}=\frac{1}{4}\left(\phi_{i+1,j}^{n}+\phi_{i-1,j}^{n+1}+\phi_{i,j+1}^{n}+\phi_{i,j-1}^{n+1}\right) \tag{7.20}$$

3. Overrelaxation: uses the Gauss-Seidel iteration method:

$$\Delta r = (\phi_{i,j}^{n+1} - \phi_{i,j}^{n}) \qquad \text{(Gauss-Seidel residue)} \tag{7.21}$$

$$\phi_{i,j}^{n+1} = \phi_{i,j}^{n} + \xi \Delta r \qquad (\xi\text{=relaxation factor}) \tag{7.22}$$

$$\phi_{i,j}^{n+1} = (1-\xi)\phi_{i,j}^{n} + \frac{\xi}{4}\left(\phi_{i+1,j}^{n} + \phi_{i-1,j}^{n+1} + \phi_{i,j+1}^{n} + \phi_{i,j-1}^{n+1}\right) \tag{7.23}$$

Optimal value for ξ is between 1 and 2 ($\approx$ 1.5 à 1.6).

7.2.4 Non-steady state methods

The basic equation for non-steady state groundwater flow is:

$$S\frac{\partial \phi}{\partial t} = T\frac{\partial^2 \phi}{\partial x^2} \tag{7.24}$$

Note that this type of the equation, which is called the diffusion equation, can also be applied for many other geophysic processes, such as the diffusion processes, shoreline movements, consolidation of soil, heat transport in solids and transport of solutes in a river.

- Explicit (forwards difference approach), see figure 7.2:

$$\frac{\partial^2 \phi}{\partial x^2} \approx \frac{\phi_{i+1}^{t} - 2\phi_{i}^{t} + \phi_{i-1}^{t}}{\Delta x^2} \tag{7.25}$$

$$\frac{\partial \phi}{\partial t} \approx \frac{\phi_{i}^{t+\Delta t} - \phi_{i}^{t}}{\Delta t} \tag{7.26}$$

$$\phi_{i}^{t+\Delta t} = \phi_{i}^{t} + \frac{T\Delta t}{S\Delta x^2}\left(\phi_{i+1}^{t} - 2\phi_{i}^{t} + \phi_{i-1}^{t}\right) \tag{7.27}$$

- Implicit (backwards difference approach):

$$\frac{\partial^2 \phi}{\partial x^2} \approx \frac{\phi_{i+1}^{t+\Delta t} - 2\phi_{i}^{t+\Delta t} + \phi_{i-1}^{t+\Delta t}}{\Delta x^2} \tag{7.28}$$

$$\frac{\partial \phi}{\partial t} \approx \frac{\phi_{i}^{t+\Delta t} - \phi_{i}^{t}}{\Delta t} \tag{7.29}$$

$$\phi_{i+1}^{t+\Delta t} - \left(2 + \frac{S\Delta x^2}{T\Delta t}\right)\phi_{i}^{t+\Delta t} + \phi_{i-1}^{t+\Delta t} = -\frac{S\Delta x^2}{T\Delta t}\phi_{i}^{t} \tag{7.30}$$

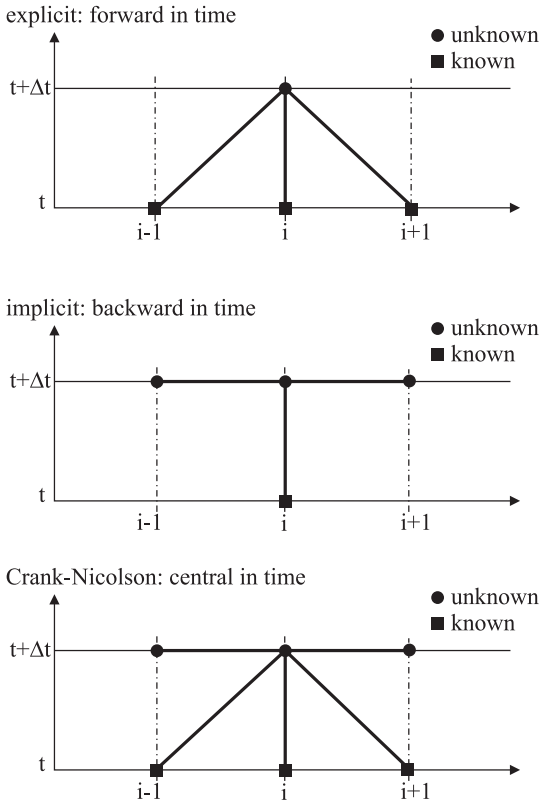

Figure 7.2: *Numerical schemes: explicit, implicit and Crank-Nicolson.*

- no direct solution possible,
- making use of the (three diagonal coefficients) matrix: $[A]\{\phi\} = \{R\}$,
- always stable,
- more memory necessary when explicit solution

- Crank-Nicolson (central difference approach):

$$\frac{\partial^2 \phi}{\partial x^2} \approx \alpha \left(\frac{\phi_{i+1}^{t+\Delta t} - 2\phi_i^{t+\Delta t} + \phi_{i-1}^{t+\Delta t}}{\Delta x^2} \right) + (1-\alpha) \left(\frac{\phi_{i+1}^{t} - 2\phi_i^{t} + \phi_{i-1}^{t}}{\Delta x^2} \right) \tag{7.31}$$

$$\text{Crank-Nicolson:} \quad \alpha = 0.5 \tag{7.32}$$

$$\frac{\partial \phi}{\partial t} \approx \frac{\phi_i^{t+\Delta t} - \phi_i^t}{\Delta t} \tag{7.33}$$

$$\begin{aligned} &\phi_{i+1}^{t+\Delta t} - \left(2 + 2\tfrac{S\Delta x^2}{T\Delta t}\right) \phi_i^{t+\Delta t} + \phi_{i-1}^{t+\Delta t} = \\ &-\tfrac{S\Delta x^2}{T\Delta t}\phi_i^t - \left(\phi_{i+1}^t - \left(2 - \tfrac{S\Delta x^2}{T\Delta t}\right)\phi_i^t + \phi_{i-1}^t\right) \end{aligned} \tag{7.34}$$

– solving equal to implicit,
– stable though sometimes (temporary) oscillations occur.

Numerical solution of 1D non-steady state situation

The basic equation for an one dimensional non-steady state situation for a phreatic aquifer is:

$$\mu \frac{\partial \phi}{\partial t} = T \frac{\partial^2 \phi}{\partial x^2} + N \tag{7.35}$$

where

- μ = phreatic storage coefficient $(-)$,
- N = recharge during a time step $(L\,T^{-1})$,
- Δt = time step (T),
- Δx = length step (L),
- T = transmissivity $(L^2\,T^{-1})$.

Discretisation of the system gives:

$$\frac{\partial^2 \phi}{\partial x^2} \approx \frac{\phi_{i+1} - 2\phi_i + \phi_{i-1}}{\Delta x^2} \tag{7.36}$$

$$\frac{\partial \phi}{\partial t} \approx \frac{\phi_i^{t+\Delta t} - \phi_i^t}{\Delta t} \tag{7.37}$$

Combination gives:

$$\mu \frac{\phi_i^{t+\Delta t} - \phi_i^t}{\Delta t} = T \frac{\phi_{i+1}^t - 2\phi_i^t + \phi_{i-1}^t}{\Delta x^2} + N \tag{7.38}$$

or

$$\phi_i^{t+\Delta t} = \phi_i^t + \frac{N \Delta t}{\mu} + \frac{T \Delta t}{\mu \Delta x^2} \left(\phi_{i+1}^t - 2\phi_i^t + \phi_{i-1}^t \right) \tag{7.39}$$

Stability analysis: (N=0)

$$\phi_i^t = 10 + \varepsilon \tag{7.40}$$

$$\phi_{i+1}^t = \phi_{i-1}^t = 10 - \varepsilon \tag{7.41}$$

$$\phi_i^{t+\Delta t} = 10 + \varepsilon + \frac{T \Delta t}{\mu \Delta x^2} (-4\varepsilon) = 10 + \varepsilon \left(1 - 4 \frac{T \Delta t}{\mu \Delta x^2} \right) \tag{7.42}$$

$$\left| 1 - 4 \frac{T \Delta t}{\mu \Delta x^2} \right| < 1 \tag{7.43}$$

$$1 - 4 \frac{T \Delta t}{\mu \Delta x^2} < 1 \qquad \cup \qquad 1 - 4 \frac{T \Delta t}{\mu \Delta x^2} > -1 \tag{7.44}$$

$$\Delta t > 0 \qquad \cup \qquad \frac{T \Delta t}{\mu \Delta x^2} < 0.5 \tag{7.45}$$

Example 7.2: Non-steady situation of the diffusion equation

Diffusion in a saline environment is described by the diffusion equation. The time aspect of smoothing a contrast in chloride concentration between three layers with different chloride concentration is analysed. Molecular diffusion causes constituents to be spread due to differences in concentrations. Here, the diffusion equation is applicable (only in x-direction):

$$\frac{\partial C}{\partial t} = D_m \frac{\partial^2 C}{\partial x^2} \tag{7.46}$$

where D_m=the molecular diffusion coefficient ($L^2\,T^{-1}$). Consider the following composition: between 0 m and 100 m: initial concentration C_0 is 16000 $mg\ Cl^-/l$ and D_m= 0.69 $\times$ 10^{-4} m^2/d; between 100 m and 160 m: C_0 is 6000 $mg\ Cl^-/l$ and D_m= 0.44 $\times$ 10^{-4} m^2/d; and between 160 m and 200 m: C_0 is 12000 $mg\ Cl^-/l$ and D_m= 0.69 $\times$ 10^{-4} m^2/d. The equation is numerically modelled with an explicit discretisation (see the equations 7.25 and 7.26):

$$C_i^{t+\Delta t} = C_i^t + D_m \frac{\Delta t}{\Delta x^2}\left(C_{i+1}^t - 2C_i^t + C_{i-1}^t\right) \tag{7.47}$$

At t >0, the concentration at x=0 becomes equal to 0 $mg\ Cl^-/l$. At x=200 m, no flux of solute is assumed. Based on the stability criterion $D_m \frac{\Delta t}{\Delta x^2} < 0.5$, the following model parameters are chosen: Δx=5 m, Δt=250 $year$. Fig. 7.3 shows the change in chloride content as a function of time. As can be seen, molecular diffusion smoothens the contrast in concentration, though it is a slow process.

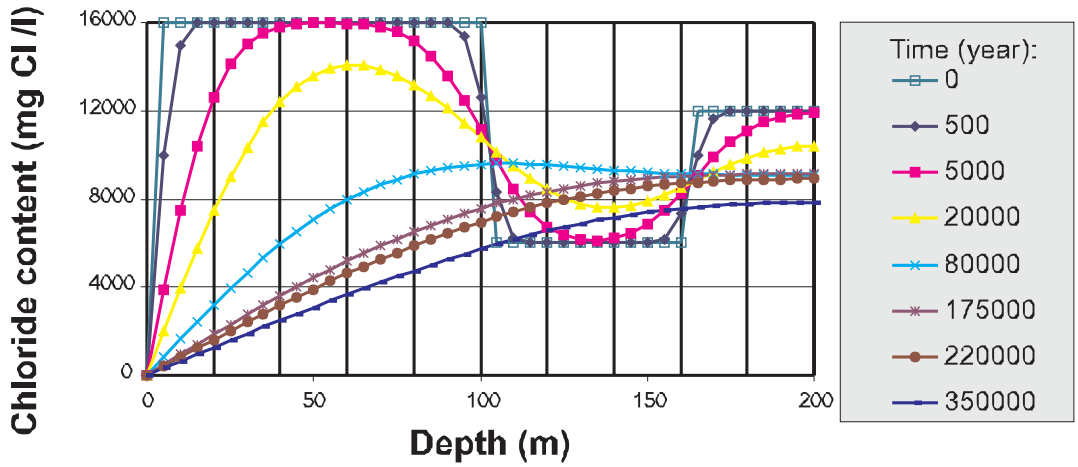

Figure 7.3: Change in chloride concentration in $mg\ Cl^-/l$ as a function of time in a layered aquifer due to molecular diffusion.

Example 7.3: Non-steady situation

The following parameters are given:

- $\mu = 1/3$,

- $N = 0.001$ m/day,
- $\Delta t = 1$ day and 10 days,
- $\Delta x = 10$ m,
- $T = 10$ m^2/day,
- $\frac{N\Delta t}{\mu}$ =0.003 and 0.03,
- $\frac{T\Delta t}{\mu \Delta x^2}$ =0.3 and 3.

7.3 Thomas algorithm

The Thomas algorithm can be used to solve matrices with coefficients in only three diagonals.

$$\begin{bmatrix} B_1 & C_1 & 0 & 0 & 0 & 0 & 0 & 0 & 0 \\ A_2 & B_2 & C_2 & 0 & 0 & 0 & 0 & 0 & 0 \\ 0 & A_3 & B_3 & C_3 & 0 & 0 & 0 & 0 & 0 \\ 0 & 0 & A_4 & B_4 & C_4 & 0 & 0 & 0 & 0 \\ 0 & 0 & 0 & A_5 & B_5 & C_5 & 0 & 0 & 0 \\ 0 & 0 & 0 & 0 & A_6 & B_6 & C_6 & 0 & 0 \\ 0 & 0 & 0 & 0 & 0 & A_7 & B_7 & C_7 & 0 \\ 0 & 0 & 0 & 0 & 0 & 0 & A_8 & B_8 & C_8 \\ 0 & 0 & 0 & 0 & 0 & 0 & 0 & A_9 & B_9 \end{bmatrix} \times \begin{Bmatrix} \phi_1 \\ \phi_2 \\ \phi_3 \\ \phi_4 \\ \phi_5 \\ \phi_6 \\ \phi_7 \\ \phi_8 \\ \phi_9 \end{Bmatrix} = \begin{Bmatrix} D_1 \\ D_2 \\ D_3 \\ D_4 \\ D_5 \\ D_6 \\ D_7 \\ D_8 \\ D_9 \end{Bmatrix} \tag{7.48}$$

or

$$[A]\{\phi\} = \{D\} \tag{7.49}$$

Introduction of dummy variables:

$$w_j = B_j - \frac{A_j C_{j-1}}{w_{j-1}} \tag{7.50}$$

$$g_j = \frac{D_j - A_j g_{j-1}}{w_j} \tag{7.51}$$

The solution of ϕ_j equals:

$$\phi_j = g_j - \frac{C_j \phi_{j+1}}{w_j} \tag{7.52}$$

Prove

$$A_j \phi_{j-1} + B_j \phi_j + C_j \phi_{j+1} = D_j \tag{7.53}$$

Suppose:

$$\phi_j = g_j - \frac{C_j \phi_{j+1}}{w_j} \tag{7.54}$$

and

$$\phi_{j-1} = g_{j-1} - \frac{C_{j-1}\phi_j}{w_{j-1}} \tag{7.55}$$

Substitution of equation 7.54 and 7.55 in equation 7.53 gives:

$$A_j\left(g_{j-1} - \frac{C_{j-1}\phi_j}{w_{j-1}}\right) + B_j\phi_j + C_j\phi_{j+1} = D_j \tag{7.56}$$

$$\phi_j = \frac{D_j - A_j g_{j-1} - C_j\phi_{j+1}}{B_j - A_j\frac{C_{j-1}}{w_{j-1}}} \tag{7.57}$$

$$\phi_j = \frac{D_j - A_j g_{j-1}}{B_j - A_j\frac{C_{j-1}}{w_{j-1}}} - \frac{C_j\phi_{j+1}}{B_j - A_j\frac{C_{j-1}}{w_{j-1}}} \tag{7.58}$$

Suppose:

$$w_j = B_j - \frac{A_j C_{j-1}}{w_{j-1}} \tag{7.59}$$

and

$$g_j = \frac{D_j - A_j g_{j-1}}{w_j} \tag{7.60}$$

then:

$$\phi_j = g_j - \frac{C_j\phi_{j+1}}{w_j} \tag{7.61}$$

Example 7.4: Thomas algorithm

Find the piezometric heads ϕ of the the following matrix equation by means of the Thomas algorithm. Take care what the coefficients A_1, B_1, C_1, A_2, B_2, etc. are exactly.

$$\begin{bmatrix} 2 & -1 & 0 \\ 1 & -3 & 1 \\ 0 & 1 & 2 \end{bmatrix} \begin{Bmatrix} \phi_1 \\ \phi_2 \\ \phi_3 \end{Bmatrix} = \begin{Bmatrix} 1 \\ -6 \\ 5 \end{Bmatrix}$$

Answer: ϕ_1=2, ϕ_2=3 and ϕ_3=1.

7.4 Gauss-Jordan elimination

The Gauss-Jordan elimination is a straightforward method to solve a matrix. From:

$$\begin{bmatrix} \text{eq. (a)} \\ \text{eq. (b)} \\ \text{eq. (c)} \end{bmatrix} \qquad \begin{pmatrix} a_{11} & a_{21} & a_{31} \\ a_{12} & a_{22} & a_{32} \\ a_{13} & a_{23} & a_{33} \end{pmatrix} \times \begin{Bmatrix} \phi_1 \\ \phi_2 \\ \phi_3 \end{Bmatrix} = \begin{Bmatrix} r_1 \\ r_2 \\ r_3 \end{Bmatrix} \tag{7.62}$$

to eventually a matrix with the form:

$$\begin{pmatrix} 1 & b_{21} & b_{31} \\ 0 & 1 & b_{32} \\ 0 & 0 & 1 \end{pmatrix} \times \begin{Bmatrix} \phi_1 \\ \phi_2 \\ \phi_3 \end{Bmatrix} = \begin{Bmatrix} s_1 \\ s_2 \\ s_3 \end{Bmatrix} \tag{7.63}$$

gives a rapid solution:

$$\begin{aligned} \phi_3 &= s_3 \\ \phi_2 &= s_2 - b_{32}\phi_3 \\ \phi_1 &= s_1 - b_{21}\phi_2 - b_{31}\phi_3 \end{aligned} \tag{7.64}$$

Equation (a) of equation 7.63 divided by a_{11} gives equation (d):

$$\text{[eq. (d)]} \qquad \phi_1 + \frac{a_{21}}{a_{11}}\phi_2 + \frac{a_{31}}{a_{11}}\phi_3 = \frac{r_1}{a_{11}} \tag{7.65}$$

$$\begin{bmatrix} \text{eq. (d)} \\ \text{eq. (b)} \\ \text{eq. (c)} \end{bmatrix} \qquad \begin{pmatrix} 1 & \frac{a_{21}}{a_{11}} & \frac{a_{31}}{a_{11}} \\ a_{12} & a_{22} & a_{32} \\ a_{13} & a_{23} & a_{33} \end{pmatrix} \times \begin{Bmatrix} \phi_1 \\ \phi_2 \\ \phi_3 \end{Bmatrix} = \begin{Bmatrix} \frac{r_1}{a_{11}} \\ r_2 \\ r_3 \end{Bmatrix} \tag{7.66}$$

Equation (d) of equation 7.66 times a_{12} gives equation (e):

$$\text{[eq. (e)]} \qquad a_{12}\phi_1 + a_{12}\frac{a_{21}}{a_{11}}\phi_2 + a_{12}\frac{a_{31}}{a_{11}}\phi_3 = a_{12}\frac{r_1}{a_{11}} \tag{7.67}$$

Equation (b) minus equation (e) gives equation (f):

$$\text{[eq. (f)]} \qquad \left(a_{22} - a_{12}\frac{a_{21}}{a_{11}}\right)\phi_2 + \left(a_{32} - a_{12}\frac{a_{31}}{a_{11}}\right)\phi_3 = r_{2-}a_{12}\frac{r_1}{a_{11}} \tag{7.68}$$

Equation (f) divided by $\left(a_{22} - a_{12}\frac{a_{21}}{a_{11}}\right)$ gives equation (g):

$$\text{[eq. (g)]} \qquad \phi_2 + \frac{\left(a_{32} - a_{12}\frac{a_{31}}{a_{11}}\right)}{\left(a_{22} - a_{12}\frac{a_{21}}{a_{11}}\right)}\phi_3 = \frac{\left(r_{2-}a_{12}\frac{r_1}{a_{11}}\right)}{\left(a_{22} - a_{12}\frac{a_{21}}{a_{11}}\right)} \tag{7.69}$$

$$\begin{bmatrix} \text{eq. (d)} \\ \text{eq. (g)} \\ \text{eq. (c)} \end{bmatrix} \qquad \begin{pmatrix} 1 & \frac{a_{21}}{a_{11}} & \frac{a_{31}}{a_{11}} \\ 0 & 1 & \frac{\left(a_{32}-a_{12}\frac{a_{31}}{a_{11}}\right)}{\left(a_{22}-a_{12}\frac{a_{21}}{a_{11}}\right)} \\ a_{13} & a_{23} & a_{33} \end{pmatrix} \times \begin{Bmatrix} \phi_1 \\ \phi_2 \\ \phi_3 \end{Bmatrix} = \begin{Bmatrix} \frac{r_1}{a_{11}} \\ \frac{\left(r_{2-}a_{12}\frac{r_1}{a_{11}}\right)}{\left(a_{22}-a_{12}\frac{a_{21}}{a_{11}}\right)} \\ r_3 \end{Bmatrix} \tag{7.70}$$

Etc., etc. !

Example 7.5: Gauss-Jordan elimination

$$\begin{bmatrix} \text{eq. (1)} \\ \text{eq. (2)} \\ \text{eq. (3)} \\ \text{eq. (4)} \end{bmatrix} \qquad \begin{pmatrix} 1 & 0 & 2 & 4 \\ -2 & 2 & 6 & 2 \\ 1 & 1 & 2 & 4 \\ 0 & -1 & 2 & 0 \end{pmatrix} \begin{Bmatrix} \phi_1 \\ \phi_2 \\ \phi_3 \\ \phi_4 \end{Bmatrix} = \begin{Bmatrix} 7 \\ 8 \\ 8 \\ 1 \end{Bmatrix}$$

Equation [2]/2 and move equation [4] to second position:

$$\begin{bmatrix} \text{eq. (1)} \\ \text{eq. (4)} \\ \text{eq. (5)} \\ \text{eq. (3)} \end{bmatrix} \qquad \begin{pmatrix} 1 & 0 & 2 & 4 \\ 0 & -1 & 2 & 0 \\ -1 & 1 & 3 & 1 \\ 1 & 1 & 2 & 4 \end{pmatrix} \begin{Bmatrix} \phi_1 \\ \phi_2 \\ \phi_3 \\ \phi_4 \end{Bmatrix} = \begin{Bmatrix} 7 \\ 1 \\ 4 \\ 8 \end{Bmatrix}$$

Equation [5]+equation [1], equation [3]+equation [5] and equation [4]*-1:

$$\begin{bmatrix} \text{eq. (1)} \\ \text{eq. (6)} \\ \text{eq. (7)} \\ \text{eq. (8)} \end{bmatrix} \qquad \begin{pmatrix} 1 & 0 & 2 & 4 \\ 0 & 1 & -2 & 0 \\ 0 & 1 & 5 & 5 \\ 0 & 2 & 5 & 5 \end{pmatrix} \begin{Bmatrix} \phi_1 \\ \phi_2 \\ \phi_3 \\ \phi_4 \end{Bmatrix} = \begin{Bmatrix} 7 \\ -1 \\ 11 \\ 12 \end{Bmatrix}$$

Equation [7]-equation [6] and equation [8]-equation [6]*2:

$$\begin{bmatrix} \text{eq. (1)} \\ \text{eq. (6)} \\ \text{eq. (9)} \\ \text{eq. (10)} \end{bmatrix} \qquad \begin{pmatrix} 1 & 0 & 2 & 4 \\ 0 & 1 & -2 & 0 \\ 0 & 0 & 7 & 5 \\ 0 & 0 & 9 & 5 \end{pmatrix} \begin{Bmatrix} \phi_1 \\ \phi_2 \\ \phi_3 \\ \phi_4 \end{Bmatrix} = \begin{Bmatrix} 7 \\ -1 \\ 12 \\ 14 \end{Bmatrix}$$

Equation [9]/7 and equation [10]*7-equation [9]*9:

$$\begin{bmatrix} \text{eq. (1)} \\ \text{eq. (6)} \\ \text{eq. (11)} \\ \text{eq. (12)} \end{bmatrix} \qquad \begin{pmatrix} 1 & 0 & 2 & 4 \\ 0 & 1 & -2 & 0 \\ 0 & 0 & 1 & 5/7 \\ 0 & 0 & 0 & -10 \end{pmatrix} \begin{Bmatrix} \phi_1 \\ \phi_2 \\ \phi_3 \\ \phi_4 \end{Bmatrix} = \begin{Bmatrix} 7 \\ -1 \\ 12/7 \\ -10 \end{Bmatrix}$$

$\phi_4 = \frac{-10}{-10} = 1$, $\phi_3 = \frac{12}{7} - \frac{5}{7} * 1 = 1$, $\phi_2 = 2 * 1 - 1 = 1$, $\phi_1 = -2 * 1 - 4 * 1 + 7 = 1$.

$$\begin{bmatrix} \text{eq. (1)} \\ \text{eq. (2)} \\ \text{eq. (3)} \\ \text{eq. (4)} \end{bmatrix} \qquad \begin{pmatrix} 1 & 0 & 2 & 4 \\ -2 & 2 & 6 & 2 \\ 1 & 1 & 2 & 4 \\ 0 & -1 & 2 & 0 \end{pmatrix} \begin{Bmatrix} 1 \\ 1 \\ 1 \\ 1 \end{Bmatrix} = \begin{Bmatrix} 7 \\ 8 \\ 8 \\ 1 \end{Bmatrix}$$

7.5 Finite difference method

The finite difference method (fdm) is probably the oldest, most popular, and conceptually simplest of the numerical procedures governing groundwater behaviour. The finite difference method consists of discretising the problem area into rectangular elements which are identified with discrete points or nodes. It is based on the Taylor series expansions in order to determine approximations of the first-order and the second-order derivatives of the variable in question.

The first-order derivatives of the piezometric head ϕ are obtained as follows:

$$\phi(x + \Delta x) = \phi(x) + \frac{\partial \phi}{\partial x}\Delta x + \frac{\partial^2 \phi}{\partial x^2}\frac{(\Delta x)^2}{2!} + \frac{\partial^3 \phi}{\partial x^3}\frac{(\Delta x)^3}{3!} + \frac{\partial^4 \phi}{\partial x^4}\frac{(\Delta x)^4}{4!} + \dots \tag{7.71}$$

$$\phi(x - \Delta x) = \phi(x) - \frac{\partial \phi}{\partial x}\Delta x + \frac{\partial^2 \phi}{\partial x^2}\frac{(\Delta x)^2}{2!} - \frac{\partial^3 \phi}{\partial x^3}\frac{(\Delta x)^3}{3!} + \frac{\partial^4 \phi}{\partial x^4}\frac{(\Delta x)^4}{4!} - \dots \tag{7.72}$$

where

- x = centre of an element located at x (L),
- Δx = distance between this centre and the centre of the bounding element: the stepsize (L).

After rewriting:

forward in space

$$\frac{\partial \phi}{\partial x} = \frac{\phi(x + \Delta x) - \phi(x)}{\Delta x} - \frac{\partial^2 \phi}{\partial x^2}\frac{\Delta x}{2} - \frac{\partial^3 \phi}{\partial x^3}\frac{(\Delta x)^2}{6} - \frac{\partial^4 \phi}{\partial x^4}\frac{(\Delta x)^3}{24} - \dots \tag{7.73}$$

backward in space

$$\frac{\partial \phi}{\partial x} = \frac{\phi(x) - \phi(x - \Delta x)}{\Delta x} + \frac{\partial^2 \phi}{\partial x^2}\frac{\Delta x}{2} - \frac{\partial^3 \phi}{\partial x^3}\frac{(\Delta x)^2}{6} + \frac{\partial^4 \phi}{\partial x^4}\frac{(\Delta x)^3}{24} - \dots \tag{7.74}$$

In addition, subtracting equation 7.72 from equation 7.71 gives:

central in space

$$\frac{\partial \phi}{\partial x} = \frac{\phi(x + \Delta x) - \phi(x - \Delta x)}{2\Delta x} - \frac{\partial^3 \phi}{\partial x^3} \frac{(\Delta x)^2}{6} - \dots \tag{7.75}$$

As can be seen, the central in space approximation (equation 7.75) is one order of magnitude more accurate: $O(\Delta x)^2$ instead of $O(\Delta x)$. By adding equation 7.71 to equation 7.72, the second-order derivatives are obtained after rewriting:

$$\frac{\partial^2 \phi}{\partial x^2} = \frac{\phi(x + \Delta x) - 2\phi(x) + \phi(x - \Delta x)}{(\Delta x)^2} - \frac{\partial^4 \phi}{\partial x^4} \frac{(\Delta x)^2}{12} - \dots \tag{7.76}$$

A similar approach leads to an approximation for the time derivative of ϕ:

$$\frac{\partial \phi}{\partial t} = \frac{\phi(t) - \phi(t - \Delta t)}{\Delta t} + O(\frac{\partial^2 \phi}{\partial t^2} \frac{\Delta t}{2} - \dots) \tag{7.77}$$

where Δt is the so-called *time step* (T). In summary, a set of approximating algebraic equations thereby replaces the original continuous partial differential equation, such as equation 6.30.

The general principle is that the piezometric head ϕ, which is a function of space $[x, y, z]$, is represented for every value of the time t. The values of the piezometric head in each point is related to the values in the surrounding points at the beginning and at the end of a time step. Combined with boundary conditions, the solution of the groundwater problem can be found, by simultaneously solving the sets of equations of the aquifers. The transformation of differential to differences can be done using various numerical schemes (e.g. explicit, implicit, Crank-Nicolson), each having their advantages (accuracy, speed) and disadvantages (complexity, stability of the numerical solution), see subsection 7.2.4, page 98.

Note that the finite difference method is not often used for solving the advection-dispersion equation because numerical dispersion can easily develop in the finite difference scheme (see chapter 8).

For more information, see Konikow & Bredehoeft [1978]; de Marsily [1986]; and Kinzelbach [1987a].

7.6 Finite element method

The finite element method (fem) is a very well-known method to solve the governing partial differential equations. It was already applied in the early 1950's to problems of solid mechanics, whereas by the mid of the late 1960's it was being used to solve the groundwater flow equation with some success. When groundwater modellers began to look at transport problems in the early 1970's, they noticed that solving the advection-dispersion equation by the finite difference method encountered numerical dispersion to a certain extent. As such, they turned to the finite element approach, as the occurrence of numerical dispersion was less dominant (though still possible).

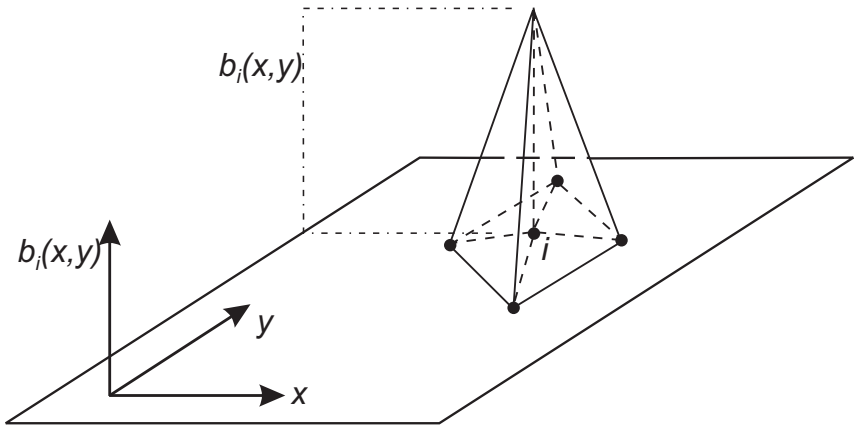

Figure 7.4: *Basis-function in the finite element method.*

For the finite element method an integral approach (instead of a differential approach for the finite difference method) is applied. The domain is decomposed into a set of sub-regions, the so-called *elements*. The corners of the elements are called nodes. In groundwater problems, the polygonal shape of the element is almost always triangular (in two-dimensions triangles), whereas occasionally more complex quadrilaterals are used. An irregular polygonal mesh allows the modeller to follow the natural shapes more accurately.

Two main solution principles of the finite element method can be distinguished [Connor & Brebbia, 1976]: (1) the *variational principle* (using so-called *functionals* U) and (2) the *weighted residual technique*. One of the most popular weighted residual technique for groundwater problems is the Galerkin method.

In the Galerkin method, on each element the approximative value for the piezometric head $\phi_a(x, y)$ is given as a combination of the real value of the level in node i (ϕ_i) and a so-called *basis-function* or *shape function* $b_i(x, y)$, see figure 7.4. The basis-function is defined as follows:

$$\phi_a(x, y) = \sum_{i=1}^{N} \phi_i b_i(x, y) \tag{7.78}$$

where N = number of nodes $(-)$. This function varies between 0 and 1 along the sides of the elements and has a value of 1 for node i and 0 for all other nodes. The basis-function is linear in case of triangular elements, for rectangular elements a second-order function is applied. For each node this equation can be developed. It should satisfy the general groundwater differential equation, however, $\phi_a(x, y)$ is only an approximative value, a so-called *on the average* value. As such, it will not exactly satisfy the partial differential equation and there will be a residue. The method now is to minimise the residues, resulting in a piezometric head which gives the best approximation for the whole model domain.

The finite element method treats each element separately and then assembles the equations for all elements into a global matrix equation. Systematic numbering across the shortest dimension of the grid reduces the bandwidth of the coefficient matrix. As such, the computer storage requirements and execution time reduce significantly.

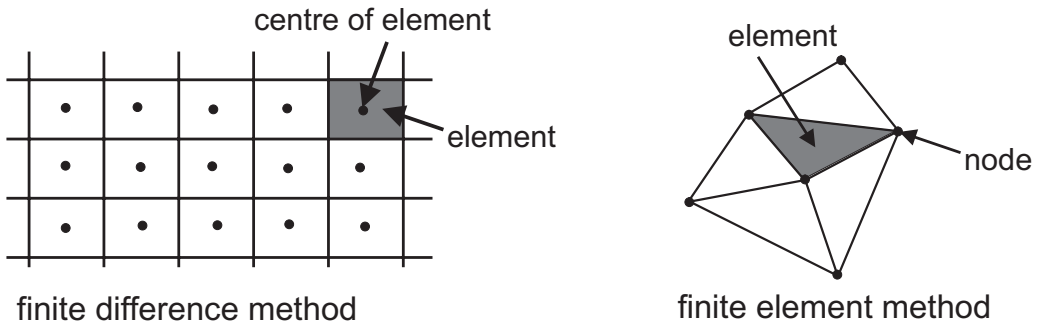

Figure 7.5: *The finite difference method and the finite element method.*

A disadvantage of the finite element method is the rather complicated computational framework which makes the accompanying computer code rather inaccessible to non-mathematics. Relevant information about this method can be found in Verruijt [1970]; Zienkiewicz [1971]; Pinder & Gray [1977]; Kinzelbach [1987a] and Bear & Verruijt [1987].

Finite difference method versus the finite element method

Both the finite difference method and the finite element method are most widely used numerical techniques for solving mathematical models. These two groups have the division of the domain into elements in common and the generation of one difference equation for each element node.

In the case of finite difference models, the elements have to be rectangular[1], whereas in case of finite element models, not only rectangular but also triangular elements may be used, see figure 7.5. In conclusion, the need for a rectangular grid is a major disadvantage of the finite difference method, as irregular shaped boundaries cannot be covered too exact and efficient. On the other hand, with the advance of fast computer systems, you can easily increase the number of elements and, as such, irregular shaped geometries can be followed more accurately.

It is easier to change a finite element grid because nodes can be added very easily without redesigning the entire grid. This is in contrast with a finite difference grid, although sophisticated preprocessors can relieve the effort to redesign the grid (e.g. Visual MODFLOW). In addition, when the exact representation of the boundaries is important, a finite element method is preferred above a finite difference method. In a model based on the finite difference method, the number of nodes that fall outside the boundaries of the model domain, the so-called *inactive nodes*, should be minimised. Inactive nodes are not part of the solution but still use up storage space in the arrays needed by the code. Still, the finite difference method is used in many computer codes, such as MODFLOW, and they serve very well.

You should realize that the computations result in values at nodal points. This means

[1]Note that the so-called *integrated finite difference method*, a variant on the classical finite difference methods, discretises the domain into irregular polygons of any shape or number of side rather than rectangular elements [de Marsily, 1986].

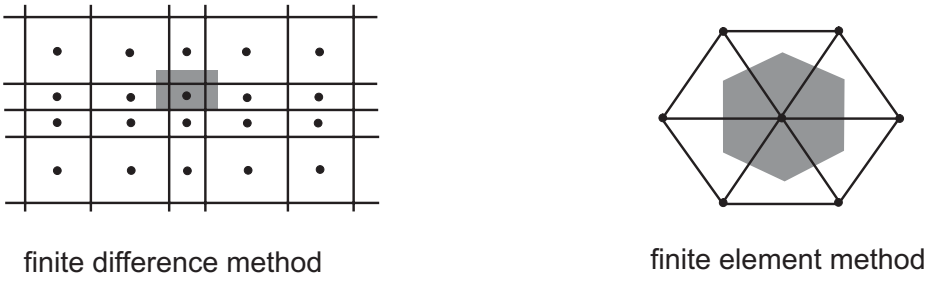

Figure 7.6: *The influence area.*

that the piezometric head is determined for a certain area around these points. So the piezometric head is an average for the so-called *influence area*. Figure 7.6 shows influence areas for triangular and rectangular elements. In areas of interest a more dense grid may be required. In the finite difference method, fluxes through a boundary are inserted over the area of the elements, whereas in the finite element method, boundary fluxes are inserted in the node.

The finite difference method can cope with anisotropy provided that the anisotropy is described to directions parallel to the sides of the elements. In addition, for solute transport, the finite element method is superior to the finite difference method, as they can handle the anisotropy of the dispersion tensor. As such, it is possible to seek a compromise between stability and numerical dispersion.

Unfortunately, the finite element method is less easy to explain and far less easy to program than the finite element method. For defining a grid for the finite element method, it consumes much time to set up an input data file, though rapid preprocessors are available to relieve the effort.

7.7 Analytic element method

The main difference between using the analytic element method and using other solution techniques originates from the application of so-called analytic elements. Each analytic element is used to describe a feature in groundwater flow in an infinite aquifer, such as an extraction well, a river, a polder, an infiltration area, a domain with different transmissivity, a sheet pile wall, etc. Each element can be used independently of other elements. Each single element generates a piezometric head distribution and a flow in the entire infinite aquifer. The analytic elements are combined through the *principle of superposition*: they may cross, overlap and link together.

Hydrogeologic features have to be recognised and the appropriate type of analytic element has to be chosen, instead of giving each element in a finite element or finite difference grid the same standard properties such as hydraulic conductivity and thickness of the layer. Reality is discretised using elements that are *exact solutions* of the differential equation, instead of applying a discretised equation such as by the finite element method and finite difference method.

Analytical solutions are determined for head and discharge that satisfy the governing

flow equations and specified boundary conditions within the aquifer. The boundary of a model of analytic elements is a zone of elements that globally simulate the behaviour of the hydrogeologic features in that zone. As such, the most important advantage over conventional numerical methods is its lack of a fixed grid. In addition, other advantages are its simple input, accuracy, speed and direct graphical output. Due to its lack of a fixed grid, it is possible to extend the model any distance to incorporate regional features without sacrificing accuracy in the area of interest. Moreover, refinement of the discretisation and zooming into a local problem can easily be accomplished.

The analytic element method is based on the theory of Strack [1989]. Some typical analytic elements are [de Lange, 1996]:

- the *point-sink*, representing a *fully-penetrating well*.

$$\Omega(z) = Q_w \ln(z - z_0)/2\pi + \Phi_{ref} \tag{7.79}$$

  where

  - $\Omega(z)$ = function of the complex potential $\Phi + i\Psi$, describing both the potential Φ and the stream function Ψ ($L^3\,T^{-1}$),
  - Q_w = discharge or strength of the well ($L^3\,T^{-1}$),
  - $z - z_0$ = distance between well and observation point (L),
  - Φ_{ref} = potential at the reference point ($L^3\,T^{-1}$).

- the *line-sink*, representing a *river*. Actually, a line-sink is an infinite number of point-sinks (wells) along a straight line with the length L.

$$\Omega(z) = \int_L \sigma_{lin} \ln(z - \delta)/2\pi \; \mathrm{d}\delta + \Phi_{ref} \tag{7.80}$$

  where

  - σ_{lin} = line-sink strength per unit length, function of δ ($L^2\,T^{-1}$),
  - $z - \delta$ = distance between observation point z and point of integration δ (L).

- the *dipole*, defining a sink and a source with equal but opposite strength, nearly at the same place. It expresses no useful element in hydrogeologic practice, though it appears to be an essential step in the theory of analytic elements.

$$\Omega(z) = \Gamma_{dip} \exp(i\beta^o - \Theta)/2\pi r + \Phi_{ref} \tag{7.81}$$

  where

  - Γ_{dip} = strength of the dipole ($L^4\,T^{-1}$),
  - β^o = orientation of the dipole ($-$),
  - Θ = orientation of the dipole with respect to the observation point ($-$),
  - r = distance between dipole and observation point (L).

- the *line-dipole*, representing an infinite number of dipoles along a line. The orientation of each dipole is equal to the orientation of the line. It represents a thin zone of very high hydraulic conductivity, such as a *crack*, a *drain* or a *canal*.

$$\Omega(z) = \int_L -\sigma_{dip} \exp(i\beta^o)/2\pi(z-\delta)\ \mathrm{d}\delta + \Phi_{ref} \tag{7.82}$$

  where

  - σ_{dip} = strength per unit length, function of δ $(L^2\,T^{-1})$,
  - β^o = orientation of the line-dipole (equal to orientation of dipole) $(-)$.

- the *non-connectable line-doublet*, representing a *leaky wall* or *impermeable wall*. The orientation of the dipole is perpendicular to the orientation of the line.

$$\Omega(z) = i/2\pi \int_L \sigma_{dou} \exp(i\alpha^o)/(z-\delta)\ \mathrm{d}\delta + \Phi_{ref} \tag{7.83}$$

  where

  - σ_{dou} = strength per unit length, function of δ $(L^2\,T^{-1})$,
  - α^o = orientation of the line-doublet $(\beta^o + \pi/2)$ $(-)$.

- the *surface area-sink* for surface conditions, generating a constant vertical in- or outflow,

- the *leakage area-sink* for the connection of two aquifers.

An example of a computer code, based on the analytic element method, is MVAEM [Strack, 1995]. It is the analytic element computer code MLAEM (Multi-Layer Analytic Element Model) which has recently been extended with a variable density module. MVAEM is now able to compute the three-dimensional water pressure distribution, on condition that the three-dimensional density distribution within an aquifer is given. De Lange [1996] has applied the analytic element method to develop the NAtional GROundwater Model (NAGROM) for density dependent aquifer systems in the Netherlands. Note that, at present, MVAEM has some drawbacks. First, it is not (yet) possible to simulate hydrodynamic dispersion and anisotropy. Second, it is still a steady state code for the simulation of density-dependent groundwater flow. The displacement of the points with densities through the known velocity distributions is not solved yet. As such, salt water intrusion as a function of time can not be simulated. Third, it appears that the so-called multiquadric-biharmonic interpolator, which is used to provide the initial three-dimensional density distribution within an aquifer and to control the smoothness and the spatial behaviour of the distribution, may not be robust enough to produce reliable three-dimensional density distribution under all circumstances [van Gerven & de Lange, 1994].

For more information on this method, see Strack [1989] and de Lange [1996].

7.8 Method of characteristics

The solution of the advection-dispersion equation is faced with difficulties, since models based on the standard finite element method and the finite difference method may yield unreliable results if spatial discretisation conditions are not met. Both widely used methods have in common that they produce poor results at great Peclet numbers[2].

Which of the terms of the advection-dispersion equation (see equation 6.68) is more dominant depends on the advective and dispersive fluxes at the level of the discretisation element [Kinzelbach, 1987a]. The so-called *grid-Peclet-numbers* Pe_{grid} can be applied to assess the most dominant process:

$$Pe_{grid,i} = \left| \frac{V_i \Delta x_i}{D_{ii}} \right| \tag{7.84}$$

where

- $Pe_{grid,i}$ = grid-Peclet-numbers in i-direction $(-)$,
- Δx_i = size of the element in i-direction (L),
- V_i = real velocity of the groundwater in i-direction $(L\,T^{-1})$.

For small grid-Peclet-numbers ($Pe_{grid} < 1$) the *parabolic nature* of the advection-dispersion equation prevails, whereas for great grid-Peclet-numbers ($Pe_{grid} > 2$) the *hyperbolic nature* dominates. As it appears that advective transport of solute dominates over dispersive transport in most field problems, the hyperbolic nature prevails. Unfortunately, numerical solving of an equation with a hyperbolic nature is more difficult than solving an equation with a parabolic nature. Fortunately, however, the method of characteristics can easily handle hyperbolic equations, and as a consequence, numerical dispersion can be suppressed to a large extent.

Originally, the method of characteristics was developed to solve hyperbolic partial differential equations during the end of the 1950's. A very well-known solute transport code is MOC (Method Of Characteristics) of Konikow & Bredehoeft [1978] (see also section 9.5). In the USA, MOC is even accepted in judicial matters on environmental pollution (contaminant transport) and cleaning costs ('who is the polluter ?').

Anyway, the rate of change of concentration $\frac{\partial C}{\partial t}$, as measured from a fixed point (e.g. the node of an element), can be redefined by:

$$\frac{dC}{dt} = \frac{\partial C}{\partial t} + \frac{\partial C}{\partial x}\frac{dx}{dt} + \frac{\partial C}{\partial y}\frac{dy}{dt} + \frac{\partial C}{\partial z}\frac{dz}{dt} \tag{7.85}$$

where

- $\frac{dC}{dt}$ = the so-called *material derivative* of concentration: the rate of change of concentration as measured when moving with the fluid particle,
- $\frac{\partial C}{\partial t}$ = rate of change of concentration as measured from a fixed point.

[2] It is peculiar that this well-known fact does not have a broader attention in numerical modelling practices of groundwater contaminant transport [Uffink, 1990].

The material derivatives of position $\frac{dx}{dt}$, $\frac{dy}{dt}$ and $\frac{dz}{dt}$ in equation 7.85, which correspond with the movement of fluid particles through the flow field, are defined by the real velocity:

$$\frac{dx}{dt} = V_x \qquad \frac{dy}{dt} = V_y \qquad \frac{dz}{dt} = V_z \tag{7.86}$$

Thus, combination of the equations 6.68, 7.85 and 7.86 yields:

$$\frac{dC}{dt} = \frac{\partial}{\partial x_i}\left(D_{ij}\frac{\partial C}{\partial x_j}\right) + \frac{(C - C')W}{n_e b} + \frac{\Psi}{n_e} \tag{7.87}$$

The solutions of the system of equations 7.86 and 7.87 are:

$$x = x(t); \quad y = y(t); \quad z = z(t); \quad C = C(t) \tag{7.88}$$

which are called the *characteristic curves*. Garder, Peaceman & Pozzi [1964] were the first to introduce the so-called *method of characteristics* into the solution of multidimensional miscible displacement (flow trough porous media). They stated that:

> *"Each point corresponds to one characteristic curve, and the values of x, y and C are obtained as functions of t for each characteristic."*

The basis concept underlying the application of the method of characteristics is to decouple the advective and the dispersive component of the equation, and to solve them separately [Konikow & Bredehoeft, 1978]:

a. the advection term (equation 7.86) is solved through a so-called *particle tracking* procedure. In fact, the method of characteristics is developed for solving the advective term. The solution of equation 7.86 can be obtained by following the characteristic curves. This following of curves is numerically achieved by introducing *moving points*, namely particles that can be traced through the flow field within the stationary coordinates of the (e.g. finite difference) grid.

   Each particle has a specific position and a concentration associated with it[3]. The initial concentration assigned to each particle is the initial concentration associated with the node of the element containing that particle. As a result, a number of particles are placed in each element of the (finite difference) grid to form a set of particles that is distributed in a geometrically uniform pattern. For each time level k, every particle is moved over a distance through the flow field in proportion to the length of the time step, the so-called *solute time step* Δt_s, and the flow velocity at the location of that particle:

$$\begin{aligned} x_p^k &= x_p^{k-1} + \delta x_p = x_p^{k-1} + \Delta t_s \, V_{x\,[x_p^k, y_p^k, z_p^k]} \\ y_p^k &= y_p^{k-1} + \delta y_p = y_p^{k-1} + \Delta t_s \, V_{y\,[x_p^k, y_p^k, z_p^k]} \\ z_p^k &= z_p^{k-1} + \delta z_p = z_p^{k-1} + \Delta t_s \, V_{z\,[x_p^k, y_p^k, z_p^k]} \end{aligned} \tag{7.89}$$

   where

[3] As such, the method requires a consecutive switching from element to particle concentrations.

- p = index number for particle identification,
- $\delta x_p, \delta y_p, \delta z_p$ = distances moved in the x, y and z-direction (L),
- Δt_s = solute time step at time level k (T),
- $V_{i\,[x_p^k, y_p^k, z_p^k]}$ = real velocity at the position of any particular particle p in the i-direction ($L\,T^{-1}$).

b. the dispersion term as well as the term for sources and sinks and chemical reactions (equation 7.87) are solved through finite difference approximations, using a coordinate system at rest relative to the advective movement.

For more information on this method, see Garder, Peaceman & Pozzi [1964]; Konikow & Bredehoeft [1978]; Kinzelbach [1987a, 1987b]; and subsection 9.5.2 (page 164).

7.9 Random walk method

The random walk method also uses the particle tracking method. Each particle represents a fixed mass of pollutant. Both the advective and the dispersive transport are represented by particle movements. The first step in the procedure is to follow particles along the direction of the flow field while the second step consists of adding a random movement by means of statistical properties in order to take into account the dispersive transport. This random walk can be seen intuitively as a Brownian motion, which is known to be responsible for molecular diffusion. If the number of particles is large enough, these random walks will indeed correctly represent dispersion. Only the superposition of the particle paths and the counting of mass gives the concentrations in each element of the overlain grid. The random walk method can be used to simulate groundwater contaminant transport at great Peclet numbers (see e.g. equation 7.84 and section 8.3). An advantage of this method is that particles are only introduced where contaminants are present.

The method can easily accommodate chemistry if linear terms are involved: a first-order reaction can be modelled by destroying particles with a constant probability or by assigning to each particle a mass which diminishes with time according to an exponential decay law [Kinzelbach, 1988]. If nonlinear reaction terms are required, the random walk method becomes less efficient as the adjustment of the particle mass due to the reaction requires the computation of concentrations after every time step. The advantage of this method is that no numerical dispersion is introduced, because there is no switching from element to particle concentrations as in the method of characteristics.

For more information on this method, see Kinzelbach [1987a, 1988] and Uffink [1990].

One-dimensional case of the random walk method

Now, for the sake of simplicity, the random walk method is illustrated for an one-dimensional case (see figure 7.7). Assume at the start (t=0) all particles are located at x=0. After one time step $t = \tau$ the average position of the particles is at x=$V\tau$, where V is the velocity. The interval in which they are located is $[V\tau - J, V\tau + J]$, where J is the maximum jump.

The probability distribution is constant in this interval[4]. The variance[5] is equal to $J^2/3$. After the second time step the average position is at $x{=}V2\tau$. The interval now is $[V2\tau -$

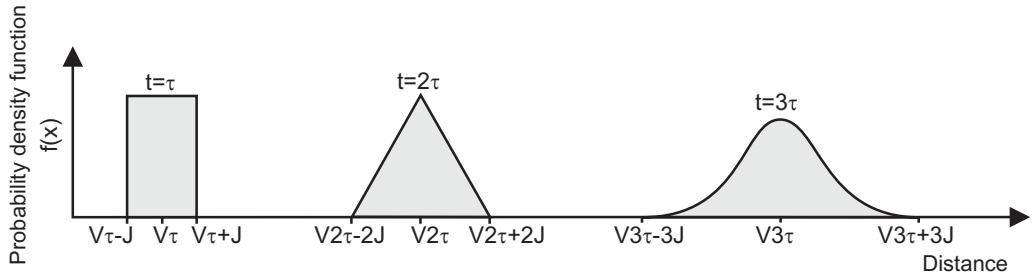

Figure 7.7: *Probability density distribution of x-coordinate of a particle in a random walk after 1, 2 and 3 steps.*

$2J$, $V2\tau + 2J]$ and the variance of the second time step[6] is $2J^2/3$. Now, the probability distribution is a triangle. After a few more time steps n the probability distribution will approximate a Gaussian distribution with average position $x{=}Vn\tau$ and variance $nJ^2/3$. As n increases, the density distribution becomes Gaussian, which is represented by the next probability distribution $f_n(x)$:

$$f_n(x) \cong \frac{1}{\sqrt{2\pi\sigma^2}} \exp\left(-\frac{(x-n\mu)^2}{2\sigma^2}\right) \tag{7.90}$$

where

- μ= average (L),
- $\sigma^2 = nJ^2/3$ = variance (L^2),
- n = number of time step.

This method can very easily be demonstrated by using a dice to determine the position of a water particle. Starting at zero, the position after one throw can be 1, 2, 3, 4, 5, 6. Each position having the same probability. The location of the average will be (1+2+3+4+5+6)/6 = 3.5. After the second throw, the location of the average will be at $2 \cdot 3.5 = 7$. The probabilities of the positions 2, 3, 4, 5, 6, 7, 8, 9, 10, 11, 12 are 1/36; 2/36; 3/36; 4/36; 5/36; 6/36; 5/36 ... 1/36 respectively, which is a triangular probability distribution. The third throw will already give a good approximation of a Gaussian distribution.

[4]The density distribution of the first time step is $f(x){=}\frac{1}{2J}$, $V\tau - J \leq x \leq V\tau + J$ (because $\int_{-\infty}^{\infty} f(x)dx{=}\int_{V\tau-J}^{V\tau+J} \frac{1}{2J}dx{=}1$). The mean value or expectation of X with density function $f(x)$ is $\mathbf{E}(X){=}\int_{-\infty}^{\infty} f(x)xdx{=}\int_{V\tau-J}^{V\tau+J} \frac{1}{2J}xdx{=}V\tau$.

[5]The variance $Var(X){=}\mathbf{E}((X{-}\mathbf{E}(X))^2){=}\mathbf{E}(X^2)$-$(\mathbf{E}(X))^2$. As $\mathbf{E}(X){=}V\tau$ and $\mathbf{E}(X^2){=}\int_{V\tau-J}^{V\tau+J} \frac{1}{2J}x^2dx = (V\tau)^2 + J^2/3$, the variance $Var(X){=}J^2/3$.

[6]$Var(X+Y) = Var(X) + Var(Y)$.

In addition, the solution of the one-dimensional dispersion equation, viz. the concentration $C(x, t_n)$ of a tracer injection of 1 kg/m^2 in a uniform flow with velocity V, is as follows:

$$C(x, t_n) = \frac{1}{2\sqrt{\pi D t_n}} \exp\left(-\frac{(x - V t_n)^2}{4 D t_n}\right) \tag{7.91}$$

The analogy between the probability density in a random walk and this equation, the concentration for a tracer injection, is evident. As a consequence, the process of dispersion can be simulated by moving the particles with the average velocity and giving each of them a random jump after each time step.

If t_n=$n\tau$, when the next relations can be found by comparing the two equations:

$$\sqrt{2\pi\sigma^2} = 2\sqrt{\pi D t_n} \quad \Longleftrightarrow \quad D = \frac{\sigma^2}{2t_n} = \frac{J^2}{6\tau} \tag{7.92}$$

and

$$\mu = V\tau \tag{7.93}$$

Solutions are possible for steady state and two-dimensional problems. Also horizontal layering can be taken into account, via an approximative method.

7.10 Vortices method

The vortices method can be applied for the analysis of problems in the field of fresh and saline groundwater, separated by an interface (see for more information on density dependent groundwater flow the lecture notes of Hydrological Transport Processes/Groundwater Modelling II). The principle is based on the fact that an interface at an inclination create rotations in the groundwater flow due to density differences. As a result, the direction of the rotation is such that the interface will eventually be situated in a horizontal direction, as the density of saline groundwater is larger than that of fresh groundwater. This rotation can be modelled with so-called *vortex distributions*, which cause that the interface will be horizontal again. The equation of the rotation per length is as follows:

$$q = \frac{\kappa}{\mu}(\gamma_s - \gamma_f) \sin\beta \tag{7.94}$$

where

- q= vortex strength ($L\,T^{-1}$),
- κ = intrinsic permeability (L^2),
- μ = dynamic viscosity of both fluids ($M\,L^{-1}\,T^{-1}$),
- $\gamma_s, \gamma_f = \rho_s g, \rho_f g$ = specific weight ($M\,L^{-2}\,T^{-2}$),
- ρ_s, ρ_f = density of respectively saline and fresh groundwater ($M\,L^{-3}$),
- g = gravity acceleration ($L\,T^{-2}$),

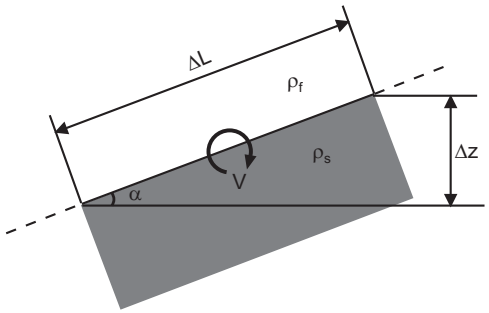

Figure 7.8: *The vortex at the fresh-saline interface is caused by the difference in density.*

- β = inclinatie van de interface $(-)$.

Over a line ΔL, the vortex V is (see figure 7.8):

$$\begin{aligned} V &= \frac{\kappa}{\mu}(\gamma_s - \gamma_f)\Delta L \sin\beta \qquad \text{or} \\ V &= k\frac{\Delta\rho}{\rho_f}\Delta z \end{aligned} \tag{7.95}$$

where

- $k = \frac{\kappa\rho g}{\mu}$ = hydraulic conductivity of fresh water $(L\,T^{-1})$.

The principle of superposition makes sure that the resulting flow can be computed by means of two steps: (1) account for the effect of density differences, and (2) account for the flow of the hypothetical fluid. The concept is to replace all fluids with different densities by one hypothetical fluid and then to introduce singularities at those places where the densities of the actual fluids change [Peters, 1983]. As such, the vortices generate the effect of varying density. If the fresh-saline interface has an inclination in a steady state situation, this means that other hydrogeologic factors such as groundwater extractions affect the system.

Note that the vortices method has an analytic character and that transient problems can be considered. Obviously, this method is rather limited in its applications, for example: the separation of groundwater with different densities by means of an interface is necessary and mixing of the fluids is not possible.

For more information on this method, see de Josselin de Jong [1977]; Haitjema [1977]; and Peters [1983]. æ

Chapter 8

Numerical aspects of groundwater models

Whatever numerical approach is chosen, always inaccuracies or errors are induced. They can be subdivided into [Spaans, 1992]:

- *physical system errors*, due to an wrong concept, an inadequate simplification or an incorrect schematisation of the hydrologic system, variables, parameters and boundary conditions,
- *mathematical errors*, due to wrong or incomplete expressions of the differential equations,
- *numerical errors*, due to an incorrect transformation of differential into difference equations (e.g. order of approximation is too low, faults in the computer code, numerical dispersion),
- *computational errors*, due to convergence and computer inaccuracies (e.g. machine truncation).

In this chapter, the interest is focussed on the numerical errors. The numerical approximations, that define the derivatives of the groundwater flow and solute transport equations, may introduce errors in the numerical solution. These errors limit the techniques that solve partial equations.

Artificial *numerical dispersion* occurs in the solution as a result of numerical approximation of the nonlinear solute transport equation (see figure 8.1). It depends on the applied discretisation scheme of the advective term in the solute transport equation whether or not a *truncation error* arises. This truncation error has the appearance of an additional dispersion-like term. It may dominate the numerical accuracy of the solution (see section 8.1).

In addition, over and undershooting of the solute concentration values, which is called *oscillation* (see figure 8.1), may lead to *oscillation errors* in the solution of the solute concentration. If the oscillation reaches unacceptable values, the solution may even become unstable.

There exists a close relation between numerical accuracy (numerical dispersion) and stability (oscillation) [Peaceman, 1977; Pinder & Gray, 1977]. In fact, numerical dispersion acts to stabilize the solution of the equation. Numerical dispersion spreads the sharp front by generating a solution which applies a greater dispersion than the hydrodynamic dispersion. In order to suppress the numerical dispersion, the numerical scheme (spatial as well as temporal) can be adapted. Meanwhile, this scheme may lead to over and undershooting,

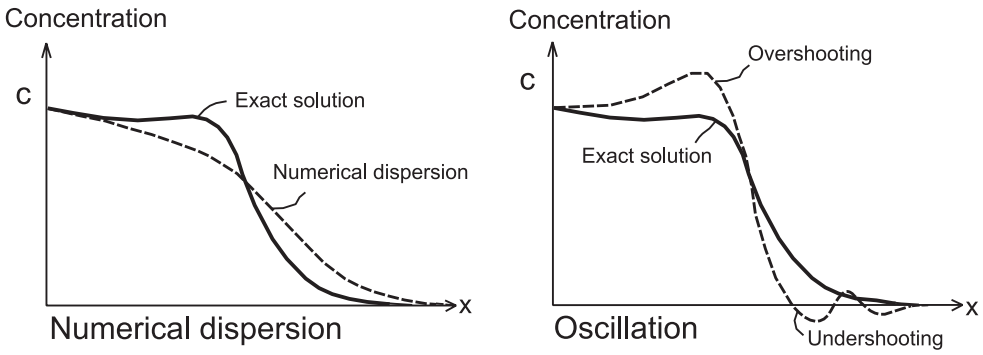

Figure 8.1: *Schematisation of numerical dispersion and oscillation (after Kinzelbach, 1987a).*

and subsequently, oscillation can be amplified. For these reasons, the discretisation scheme should be chosen carefully in order to control both numerical accuracy and stability.

8.1 Numerical dispersion

Standard finite difference methods may generate significant truncation errors. In this section, an one-dimensional schematisation is applied to demonstrate in a simple way the principle of assessing truncation errors. The standard (one-dimensional) advection-dispersion equation is defined as follows:

$$D\frac{\partial^2 C}{\partial x^2} - V\frac{\partial C}{\partial x} = \frac{\partial C}{\partial t} \tag{8.1}$$

where

- V = real velocity of groundwater $[L\,T^{-1}]$,
- D = hydrodynamic dispersion $[L^2\,T^{-1}]$.

In most examples, this equation is discretised as (backwards in space and time: implicit):

$$D\frac{C_{i+1}^k - 2C_i^k + C_{i-1}^k}{\Delta x^2} - V\frac{C_i^k - C_{i-1}^k}{\Delta x} = \frac{C_i^k - C_i^{k-1}}{\Delta t} \tag{8.2}$$

Here, the interest is focussed on the truncation errors, made in the Taylor series development of the partials (see the equations 7.71 to 7.76 for the Taylor series expansions), in order to detect the numerical errors caused by the discretisation:

Backwards in space (implicit):

$$\frac{\partial C}{\partial x} = \frac{C_i - C_{i-1}}{\Delta x} + \frac{\Delta x}{2}\frac{\partial^2 C}{\partial x^2} - \frac{\Delta x^2}{6}\frac{\partial^3 C}{\partial x^3} + O(\Delta x^3) \tag{8.3}$$

Central in space (Crank-Nicolson):

$$\frac{\partial C}{\partial x} = \frac{C_{i+1} - C_{i-1}}{2\Delta x} - \frac{\Delta x^2}{6}\frac{\partial^3 C}{\partial x^3} + O(\Delta x^4) \tag{8.4}$$

$$\frac{\partial^2 C}{\partial x^2} = \frac{C_{i+1} - 2C_i + C_{i-1}}{\Delta x^2} - \frac{\Delta x^2}{12}\frac{\partial^4 C}{\partial x^4} + O(\Delta x^4) \tag{8.5}$$

Forwards in time (explicit):

$$\frac{\partial C}{\partial t} = \frac{C_i^{k+1} - C_i^k}{\Delta t} - \frac{\Delta t}{2}\frac{\partial^2 C}{\partial t^2} - \frac{\Delta t^2}{6}\frac{\partial^3 C}{\partial t^3} + O(\Delta t^3) \tag{8.6}$$

Backwards in time (implicit):

$$\frac{\partial C}{\partial t} = \frac{C_i^{k} - C_i^{k-1}}{\Delta t} + \frac{\Delta t}{2}\frac{\partial^2 C}{\partial t^2} - \frac{\Delta t^2}{6}\frac{\partial^3 C}{\partial t^3} + O(\Delta t^3) \tag{8.7}$$

Central in time (Crank-Nicolson):

$$\frac{\partial C}{\partial t} = \frac{C_i^{k+1} - C_i^{k}}{\Delta t} - \frac{\Delta t^2}{24}\frac{\partial^3 C}{\partial t^3} + O(\Delta t^4) \tag{8.8}$$

Inserting the three upper above-mentioned expressions in the discretised advection-dispersion equation 8.2 gives:

$$D\left(\frac{\partial^2 C}{\partial x^2} + \frac{\Delta x^2}{12}\frac{\partial^4 C}{\partial x^4}\right) - V\left(\frac{\partial C}{\partial x} - \frac{\Delta x}{2}\frac{\partial^2 C}{\partial x^2} + \frac{\Delta x^2}{6}\frac{\partial^3 C}{\partial x^3}\right) = \frac{\partial C}{\partial t} - \frac{\Delta t}{2}\frac{\partial^3 C}{\partial t^3} \tag{8.9}$$

Neglecting third and fourth order terms gives:

$$D\frac{\partial^2 C}{\partial x^2} - V\left(\frac{\partial C}{\partial x} - \frac{\Delta x}{2}\frac{\partial^2 C}{\partial x^2}\right) = \frac{\partial C}{\partial t} - \frac{\Delta t}{2}\frac{\partial^2 C}{\partial t^2} \tag{8.10}$$

Rewriting the term $\frac{\partial^2 C}{\partial t^2}$ gives:

$$\frac{\partial^2 C}{\partial t^2} = \frac{\partial}{\partial t}\left(\frac{\partial C}{\partial t}\right) = \frac{\partial}{\partial t}\left(D\frac{\partial^2 C}{\partial x^2} - V\frac{\partial C}{\partial x}\right) = D\frac{\partial^2}{\partial x^2}\left(\frac{\partial C}{\partial t}\right) - V\frac{\partial}{\partial x}\left(\frac{\partial C}{\partial t}\right) \tag{8.11}$$

$$\frac{\partial^2 C}{\partial t^2} = D\frac{\partial^2}{\partial x^2}\left(D\frac{\partial^2 C}{\partial x^2} - V\frac{\partial C}{\partial x}\right) - V\frac{\partial}{\partial x}\left(D\frac{\partial^2 C}{\partial x^2} - V\frac{\partial C}{\partial x}\right) \tag{8.12}$$

$$\frac{\partial^2 C}{\partial t^2} = D^2\frac{\partial^4 C}{\partial x^4} - VD\frac{\partial^3 C}{\partial x^3} - VD\frac{\partial^3 C}{\partial x^3} + V^2\frac{\partial^2 C}{\partial x^2} \tag{8.13}$$

$$\frac{\partial^2 C}{\partial t^2} \approx V^2\frac{\partial^2 C}{\partial x^2} \tag{8.14}$$

Combining this result with equation 8.10 gives:

$$D\frac{\partial^2 C}{\partial x^2} - V\left(\frac{\partial C}{\partial x} - \frac{\Delta x}{2}\frac{\partial^2 C}{\partial x^2}\right) = \frac{\partial C}{\partial t} - V^2\frac{\Delta t}{2}\frac{\partial^2 C}{\partial x^2} \tag{8.15}$$

$$\left(D + V\frac{\Delta x}{2} + V^2\frac{\Delta t}{2}\right)\frac{\partial^2 C}{\partial x^2} - V\frac{\partial C}{\partial x} = \frac{\partial C}{\partial t} \tag{8.16}$$

Here an interesting appearance occurs: approximations of the first-order derivatives generates errors in the order of second-order derivatives. Two extra terms have been added to

the real hydrodynamic dispersion coefficient D: $V\frac{\Delta x}{2} + V^2\frac{\Delta t}{2}$. These terms are called the numerical dispersion terms:

backwards in space and time (implicit):

$$D_{apparent} = D + D_{num} = D + V\frac{\Delta x}{2} + V^2\frac{\Delta t}{2} \tag{8.17}$$

Similar equations can be found for:

central in space (Crank-Nicolson) and backwards in time (implicit):

$$D_{num} = V^2\frac{\Delta t}{2} \tag{8.18}$$

backwards in space (implicit) and forwards in time (explicit):

$$D_{num} = V\frac{\Delta x}{2} - V^2\frac{\Delta t}{2} \tag{8.19}$$

Suppose your discretised model has the following parameters: D=1.2 m^2/d V=1 m/d, Δt=0.4 d and Δx=1 m. In this situation, the value of the dispersion coefficient (for the backwards in space and time discretisation) used in the model is equal to:

$$D_{apparent} = D + D_{num} = 1.2 + 1\frac{1}{2} + 1^2\frac{0.4}{2} = 1.9\,m^2/d \tag{8.20}$$

Thus, the dispersion coefficient is larger and your computational results for the solute transport will deviate significantly for what you would expect with a smaller dispersion coefficient. Remedy to reduce the effect of numerical dispersion:

- make Δt and Δx smaller,
- use central in space and time discretisations: however, these solutions can easily create oscillations of the solution,
- use another hydrodynamic dispersion coefficient D: e.g.: use D=0.7 m^2/d instead of D=1.2 m^2/d in order to account for the numerical dispersion: now $D_{apparent}$=1.2 m^2/d.

In summary, the truncation errors depends on the chosen numerical approximation [Bear & Verruijt, 1987]:

- Backward difference in space (upstream weighting)
  The finite difference approximations in space also introduce truncation errors. It is well-known that a backward difference in space approximation gives the following equation for the term $\frac{\partial C}{\partial x}$:

  $$\frac{\partial C}{\partial x} = \frac{C_i - C_{i-1}}{\Delta x} + \frac{\Delta x}{2}\frac{\partial^2 C}{\partial x^2} + \ldots \tag{8.21}$$

  The term $\frac{\partial C}{\partial x}$ should be multiplied with $-V$ to be inserted properly in equation 8.1. Thus, the approximation results in an additional truncation error term of the dispersion-term: $-\frac{1}{2}V\Delta x$. Focusing on only the backward spatial approximation, the numerical dispersion D_{num} due to the truncation error in space will be:

  $$D_{num} = +\frac{\Delta x}{2}V \tag{8.22}$$

Approximation scheme		Numerical dispersion
Time	Spatial	Truncation error
FIT: forward in time (explicit)	BIS (upstream)	$\frac{1}{2}V\Delta x - \frac{1}{2}V^2\Delta t$
	CIS (centered)	$-\frac{1}{2}V^2\Delta t$
BIT: backward in time (implicit)	BIS (upstream)	$\frac{1}{2}V\Delta x + \frac{1}{2}V^2\Delta t$
	CIS (centered)	$\frac{1}{2}V^2\Delta t$
CIT: centered in time (Crank-Nicolson)	BIS (upstream)	$\frac{1}{2}V\Delta x$
	CIS (centered)	none

Table 8.1: *Summary of numerical dispersion for the one-dimensional equation [modified from Lantz, 1971; INTERCOMP, 1976; Bear & Verruijt, 1987].*

Table 8.1 summarizes the truncation error forms for the one-dimensional equation.

- Central difference in space
  As the central finite difference in space does not generate a space truncation error of the second-order derivative, no numerical dispersion due to this approximation occurs.
$$\frac{\partial C}{\partial x} = \frac{C_{i+1} - C_{i-1}}{2\Delta x} + \mathrm{O}\left((\Delta x)^2, \frac{\partial^3 C}{\partial x^3}\right) \tag{8.23}$$

- Forward difference in space
  Forward difference in space also results in a truncation error term, as the derivation for the term $\frac{\partial C}{\partial x}$ gives:
$$\frac{\partial C}{\partial x} = \frac{C_{i+1} - C_i}{\Delta x} - \frac{\Delta x}{2}\frac{\partial^2 C}{\partial x^2} + \ldots \tag{8.24}$$
  As this spatial difference approximation is not commonly used for the advective term, this truncation error is not be displayed in table 8.1.

- Forward difference in time (explicit)
  A truncation error in the time derivative may cause numerical dispersion for the finite difference approximation in time:
$$\frac{\partial C}{\partial t} = \frac{C^{k+1} - C^k}{\Delta t} - \frac{\Delta t}{2}\frac{\partial^2 C}{\partial t^2} + \ldots \tag{8.25}$$
  By applying the original equation 8.1, this expression can be rewritten as [Lantz, 1971]:
$$\frac{\partial C}{\partial t} = \frac{C^{k+1} - C^k}{\Delta t} - \frac{\Delta t}{2}V^2\frac{\partial^2 C}{\partial x^2} + \ldots \tag{8.26}$$
  Accordingly, the term which contributes to the numerical dispersion is $-\frac{1}{2}V^2\Delta t$ (see also table 8.1).

- Backward difference in time (implicit)
  Analogous to the forward difference in time, the backward difference in time induces an equivalent error in numerical dispersion, though now the sign is opposite: $+\frac{1}{2}V^2\Delta t$ (see table 8.1).

- Central difference in time (Crank-Nicolson)

  This scheme is the most often used second-order time approximation, as the time truncation error contribution to numerical dispersion is removed. Nonetheless, oscillations in time can still occur [INTERCOMP, 1976].

8.1.1 Stability analysis of the advection-dispersion equation

The so-called von Neumann stability analysis is often applied to analyse the stability of a solution[1]. The question is asked whether or not the errors in the equation can grow uncontrolled during subsequent time steps Δt.

Backwards in space (implicit) and forwards in time (explicit)

Here follows the analysis of the advection-dispersion equation which is discretised backwards in space (implicit) and forwards in time (explicit):

$$D\frac{C_{i+1}^k - 2C_i^k + C_{i-1}^k}{\Delta x^2} - V\frac{C_i^k - C_{i-1}^k}{\Delta x} = \frac{C_i^{k+1} - C_i^k}{\Delta t} \tag{8.27}$$

It is assumed that the solution of the equation is defined as:

$$C^k = \tilde{C}^k + \varepsilon \Longleftrightarrow C^k = \tilde{C}^k + r_t \mathrm{e}^{i\beta x} \tag{8.28}$$

where:

- $\tilde{C}$=the correct solution on time k,
- ε=$r_t\mathrm{e}^{i\beta x}$=the error written as a Fourier component, where i indicates that a complex imaginary number is used.

The new solution is of the equation is:

$$C^{k+1} = \tilde{C}^{k+1} + r_{t+\Delta t}\mathrm{e}^{i\beta x} \tag{8.29}$$

Substituting these two equations in the discretised equation gives:

$$\begin{aligned} D\frac{\tilde{C}_{i+1}^k - 2\tilde{C}_i^k + \tilde{C}_{i-1}^k}{\Delta x^2} + D\frac{r_t\mathrm{e}^{i\beta(x+\Delta x)} - 2r_t\mathrm{e}^{i\beta x} + r_t\mathrm{e}^{i\beta(x-\Delta x)}}{\Delta x^2} \\ -V\frac{\tilde{C}_i^k - \tilde{C}_{i-1}^k}{\Delta x} - V\frac{r_t\mathrm{e}^{i\beta x} - r_t\mathrm{e}^{i\beta(x-\Delta x)}}{\Delta x} \\ = \frac{\tilde{C}_i^{k+1} - \tilde{C}_i^k}{\Delta t} + \frac{r_{t+\Delta t}\mathrm{e}^{i\beta x} - r_t\mathrm{e}^{i\beta x}}{\Delta t} \end{aligned} \tag{8.30}$$

[1] This section is based on lecture notes of A. Leijnse (LUW, RIVM).

As the following equation is valid:

$$D\frac{\tilde{C}_{i+1}^k - 2\tilde{C}_i^k + \tilde{C}_{i-1}^k}{\Delta x^2} - V\frac{\tilde{C}_i^k - \tilde{C}_{i-1}^k}{\Delta x} = \frac{\tilde{C}_i^{k+1} - \tilde{C}_i^k}{\Delta t} \tag{8.31}$$

and dividing the equation by $e^{i\beta x}$, equation 8.30 becomes:

$$D\frac{r_t e^{i\beta\Delta x} - 2r_t + r_t e^{-i\beta\Delta x}}{\Delta x^2} - V\frac{r_t - r_t e^{-i\beta\Delta x}}{\Delta x} = \frac{r_{t+\Delta t} - r_t}{\Delta t} \tag{8.32}$$

$$r_{t+\Delta t} = r_t\left[1 + \frac{D\Delta t}{\Delta x^2}\left(e^{i\beta\Delta x} - 2 + e^{-i\beta\Delta x}\right) - \frac{V\Delta t}{\Delta x}\left(1 - e^{-i\beta\Delta x}\right)\right] \tag{8.33}$$

$$\rho = \frac{r_{t+\Delta t}}{r_t} = 1 - \frac{2D\Delta t}{\Delta x^2}\left(1 - \frac{e^{i\beta\Delta x} + e^{-i\beta\Delta x}}{2}\right) - \frac{V\Delta t}{\Delta x}\left(1 - e^{-i\beta\Delta x}\right) \tag{8.34}$$

$$\rho = 1 - \frac{2D\Delta t}{\Delta x^2}\gamma_1 - \frac{V\Delta t}{\Delta x}\gamma_2 \tag{8.35}$$

where:

- ρ=$\frac{r_{t+\Delta t}}{r_t}$= the amplification factor
- γ_1=$1 - \frac{e^{i\beta\Delta x}+e^{-i\beta\Delta x}}{2}$
- γ_2=$1-e^{-i\beta\Delta x}$

The equation is stable when the absolute value of the amplification factor ρ is smaller than or equal to one:

$$|\rho| \leq 1 \tag{8.36}$$

$$-1 \leq 1 - \frac{2D\Delta t}{\Delta x^2}\gamma_1 - \frac{V\Delta t}{\Delta x}\gamma_2 \leq 1 \qquad \Longleftrightarrow \qquad -2 \leq -\frac{2D\Delta t}{\Delta x^2}\gamma_1 - \frac{V\Delta t}{\Delta x}\gamma_2 \leq 0 \tag{8.37}$$

$$0 \leq \frac{2D\Delta t}{\Delta x^2}\gamma_1 + \frac{V\Delta t}{\Delta x}\gamma_2 \leq 2 \tag{8.38}$$

Analysing γ_1 and γ_2 gives the following equations (making use of the theory of complex functions !):

$$\gamma_1 = 1 - \frac{e^{i\beta\Delta x} + e^{-i\beta\Delta x}}{2} = 1 - \cos\beta\Delta x \tag{8.39}$$

Knowing that a cosine is always between -1 en 1 gives:

$$0 \leq \gamma_1 \leq 2 \tag{8.40}$$

The term γ_2 is somewhat more complex:

$$\gamma_2 = 1 - e^{-i\beta\Delta x} = 1 - \cos\beta\Delta x + i\sin\beta\Delta x \tag{8.41}$$

To determine the length of this complex term γ_2, the absolute value must be calculated:

$$|\gamma_2| = |1 - \cos\beta\Delta x + i\sin\beta\Delta x| = \sqrt{(1 - \cos\beta\Delta x)^2 + (\sin\beta\Delta x)^2} \tag{8.42}$$

$$|\gamma_2| = \sqrt{1 - 2\cos\beta\Delta x + \cos\beta\Delta x^2 + \sin\beta\Delta x^2} = \sqrt{2 - 2\cos\beta\Delta x} \tag{8.43}$$

Knowing, once again, that a cosine is always between -1 en 1 gives:

$$0 \leq \gamma_2 \leq 2 \tag{8.44}$$

Based on the equations 8.38, 8.40 and 8.44, it can be obtained that:

$$V\frac{\Delta t}{\Delta x} + \frac{2D\Delta t}{\Delta x^2} \leq 1 \tag{8.45}$$

If this equation is valid then $V\frac{\Delta t}{\Delta x} \leq 1$ (V is positive) and $\frac{2D\Delta t}{\Delta x^2} \leq 1$. Suppose that $V\frac{\Delta t}{\Delta x} > \frac{2D\Delta t}{\Delta x^2}$, then equation 8.38 becomes:

$$0 \leq \frac{2D\Delta t}{\Delta x^2}\gamma_1 + \frac{V\Delta t}{\Delta x}\gamma_2 \leq 2 \Longrightarrow 0 \leq \frac{V\Delta t}{\Delta x}(\gamma_1 + \gamma_2) \leq 2 \tag{8.46}$$

As $V\frac{\Delta t}{\Delta x} \leq 1$, then:

$$0 \leq \gamma_1 + \gamma_2 \leq 2 \tag{8.47}$$

Knowing the equations 8.40 and 8.44, this equation is valid if the terms $V\frac{\Delta t}{\Delta x}$ plus $\frac{2D\Delta t}{\Delta x^2}$ is smaller/equal than 1 (check it). A similar analysis can be obtained if $\frac{2D\Delta t}{\Delta x^2} > V\frac{\Delta t}{\Delta x}$. In conclusion, based on the von Neumann stability analysis, the following criterion can be obtained for the backwards in space (implicit) and forwards in time (explicit):

$$V\frac{\Delta t}{\Delta x} + \frac{2D\Delta t}{\Delta x^2} \leq 1 \tag{8.48}$$

In fact: this criterion is also used in the stability criteria of the MOC code (but then in 2D):

$$V\frac{\Delta t}{\Delta x} \leq 1, \text{where } V\frac{\Delta t}{\Delta x} \text{is the so-called Courant number} \tag{8.49}$$

$$\frac{2D\Delta t}{\Delta x^2} \leq 1 \qquad \text{or} \qquad \frac{D\Delta t}{\Delta x^2} \leq 0.5, \text{ which is the so-called Neumann-criterion} \tag{8.50}$$

Backwards in space (implicit) and backwards in time (implicit)

When applying a backwards in time (implicit) discretisation, the discretised equation becomes:

$$D\frac{C_{i+1}^k - 2C_i^k + C_{i-1}^k}{\Delta x^2} - V\frac{C_i^k - C_{i-1}^k}{\Delta x} = \frac{C_i^k - C_i^{k-1}}{\Delta t} \tag{8.51}$$

or, if $k = k + 1$:

$$D\frac{C_{i+1}^{k+1} - 2C_i^{k+1} + C_{i-1}^{k+1}}{\Delta x^2} - V\frac{C_i^{k+1} - C_{i-1}^{k+1}}{\Delta x} = \frac{C_i^{k+1} - C_i^k}{\Delta t} \tag{8.52}$$

The von Neumann analysis gives the following equation:

$$\rho = \frac{r_{t+\Delta t}}{r_t} = \frac{1}{1 + \frac{2D\Delta t}{\Delta x^2}\gamma_1 + \frac{V\Delta t}{\Delta x}\gamma_2} \tag{8.53}$$

$$|\rho| \leq 1 \quad \text{for each } \Delta x,\ \Delta t \ \text{ unless } D_{apparent} = D - V\tfrac{\Delta x}{2} - V^2\tfrac{\Delta t}{2} \tag{8.54}$$

For this situation, ρ is stable if:

$$\frac{2D_{apparant}\Delta t}{\Delta x^2}\gamma_1 + \frac{V\Delta t}{\Delta x}\gamma_2 \geq 0 \qquad \text{or} \qquad \frac{2D_{apparant}\Delta t}{\Delta x^2} + \frac{V\Delta t}{\Delta x} \geq 0 \tag{8.55}$$

$$\frac{2\left(D - V\frac{\Delta x}{2} - V^2\frac{\Delta t}{2}\right)\Delta t}{\Delta x^2} + \frac{V\Delta t}{\Delta x} \geq 0 \qquad \text{or} \qquad \frac{2D\Delta t - V^2\Delta t^2}{\Delta x^2} \geq 0 \tag{8.56}$$

$$\Delta t \leq \frac{2D}{V^2} \tag{8.57}$$

How to obtain the following central in time (Crank-Nicolson) approximation:

$$\text{Central in time (Crank-Nicolson):} \qquad \frac{\partial C}{\partial t} = \frac{C_i^{k+1} - C_i^k}{\Delta t} - \frac{\Delta t^2}{24}\frac{\partial^3 C}{\partial t^3} + O(\Delta t^4) \tag{8.58}$$

$$C_i^{k+1} = C_i^{k+1/2} + \frac{\Delta t}{2}\frac{\partial C}{\partial t} + \frac{1}{2}\left(\frac{\Delta t}{2}\right)^2\frac{\partial^2 C}{\partial t^2} + \frac{1}{6}\left(\frac{\Delta t}{2}\right)^3\frac{\partial^3 C}{\partial t^3} + \frac{1}{24}\left(\frac{\Delta t}{2}\right)^4\frac{\partial^4 C}{\partial t^4} + \frac{1}{120}\left(\frac{\Delta t}{2}\right)^5\frac{\partial^5 C}{\partial t^5}\ldots \tag{8.59}$$

$$C_i^{k} = C_i^{k+1/2} - \frac{\Delta t}{2}\frac{\partial C}{\partial t} + \frac{1}{2}\left(\frac{\Delta t}{2}\right)^2\frac{\partial^2 C}{\partial t^2} - \frac{1}{6}\left(\frac{\Delta t}{2}\right)^3\frac{\partial^3 C}{\partial t^3} + \frac{1}{24}\left(\frac{\Delta t}{2}\right)^4\frac{\partial^4 C}{\partial t^4} - \frac{1}{120}\left(\frac{\Delta t}{2}\right)^5\frac{\partial^5 C}{\partial t^5}\ldots \tag{8.60}$$

Equations 8.59-8.60 give:

$$C_i^{k+1} - C_i^k = 2\frac{\Delta t}{2}\frac{\partial C}{\partial t} + 2\frac{1}{6}\left(\frac{\Delta t}{2}\right)^3\frac{\partial^3 C}{\partial t^3} + 2\frac{1}{120}\left(\frac{\Delta t}{2}\right)^5\frac{\partial^5 C}{\partial t^5} + \ldots \tag{8.61}$$

$$\frac{\partial C}{\partial t} = \frac{C_i^{k+1} - C_i^k}{\Delta t} - \frac{\Delta t^2}{24}\frac{\partial^3 C}{\partial t^3} + O(\Delta t^4) \tag{8.62}$$

8.2 Oscillation

Oscillations may occur in case the total dispersion (that is the sum of hydrodynamic dispersion D and numerical dispersion D_{num}) is negative. Thus, the following expression should be obeyed:

$$D + D_{num} \geq 0 \tag{8.63}$$

A stability analysis indicates whether or not the approximation scheme for the solute transport equation causes an instable solution [e.g. INTERCOMP, 1976; Peaceman, 1977]. Various analyses can be applied to determine the stability criteria for each approximation scheme. Two examples of this scheme are briefly discussed in this section:

- Central difference in time (Crank Nicolson)
  No numerical dispersion occurs if a central difference in time scheme is applied in combination with central difference in space (see table 8.1). Hence, this approximation scheme seems to be ideal. There is, however, a tendency of central difference approximations to over and undershoot the maximum and minimum limits, and subsequently, oscillations in time are caused. These oscillation errors could be reduced

by limiting the time step. This criterion appears to be related to the criterion of the explicit scheme: in fact, it equals about one-half of the forward in time first-order stability criterion [INTERCOMP, 1976]:

$$\frac{V\Delta t}{\Delta x} \leq 2 \tag{8.64}$$

- Backward difference in time (implicit)
  No stability criteria exist for implicit schemes. Still, however, a so-called *spatial oscillation* may occur in the central in space approximation [Price *et al.*, 1966; INTERCOMP, 1976]. In order to limit this oscillation, the following equation should be fulfilled:

$$\frac{V\Delta x}{2} \leq D \quad \text{or} \quad Pe_{grid} = \frac{V\Delta x}{D} \leq 2 \tag{8.65}$$

  where Pe_{grid} = grid-Peclet-number $(-)$, which determines the relative size of the advective and dispersive fluxes on the level of a discretisation element.

8.3 Analysis of truncation and oscillation errors

The solution of the solute transport equation may be faced with difficulties, since standard finite difference and finite element models may yield unreliable results if the discretisation conditions are not met. Although, in general, representation of the dispersion by the finite element method[2] is accurate if numerical dispersion is small with respect to the hydrodynamic dispersion [Bear & Verruijt, 1987], it is recommended to analyse the solute transport equation anyway.

In order to quantify numerical accuracy, an *eigenvalue analysis* of the advection-dispersion equation should be performed. Such an analysis will demonstrate the importance of mesh spacing [e.g. Frind & Pinder, 1983]. In addition, a stability analysis should determine the stability condition. For example, the von Neumann criterion for stability defines that the modulus of the amplification factor must be less than or equal to one for all the components [Peaceman, 1977; Stelling & Booij, 1996]. In order to obtain real and distinct eigenvalues, the spatial discretisation in the finite element formulations should meet the condition [Daus *et al.*, 1985]:

$$Pe_{grid} = \frac{V\Delta x}{D} \leq 2 \tag{8.66}$$

In advective-dominant solute transport, the hydrodynamic dispersion D approximates $D{=}\alpha_L\, V$, and thus, equation 8.66 becomes:

$$Pe_{grid} = \frac{\Delta x}{\alpha_L} \leq 2 \tag{8.67}$$

[2]The analysis of (truncation and oscillation) errors due to numerical dispersion and oscillation for the finite difference method by means of central finite difference approximations is similar for the finite element method [Pinder & Gray, 1977, Kinzelbach, 1987a].

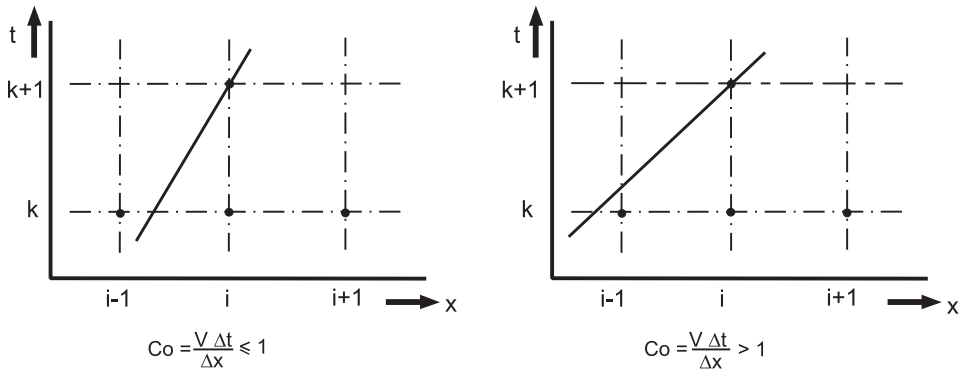

Figure 8.2: *Schematisation of the Courant condition.*

Daus *et al.* [1985] obtains for the temporal discretisation:

$$Co = \frac{V\Delta t}{\Delta x} \leq \frac{Pe_{grid}}{2} \tag{8.68}$$

where Co = the Courant number [−]. The Courant condition Co is physically interpreted as the ratio of the advective distance during one time step to the spatial discretisation. Figure 8.2 illustrates the Courant condition in a numerical scheme. If the grid-Peclet-number Pe_{grid} is assumed to be maximum (viz. $Pe_{grid} = 2$), the Courant constraint becomes:

$$Co = \frac{V\Delta t}{\Delta x} \leq 1 \tag{8.69}$$

Grid-Peclet-numbers and Courant numbers have been mentioned in various quantitative descriptions. Whether or not the numerical dispersion is suppressed, depends on the discretisation technique applied [e.g. Jensen & Finlayson, 1978; Campbell *et al.*, 1981; Voss & Souza, 1987]. In summary, the criteria for the grid-Peclet-number are:

$Pe_{grid} \leq 2$	Finite difference algorithm, central-in-space	
$Pe_{grid} \leq 2$	Finite element algorithm, linear basic functions	
$Pe_{grid} \leq 4$	Finite element algorithm, quadratic basic functions	(8.70)

If mechanical dispersion dominates over molecular diffusion, the hydrodynamic dispersion D in equation 8.65 can be expressed as $D{=}\alpha_L\,|V|$, and thus, equation 8.70 becomes:

$\Delta x \leq 2\ \alpha_L$	Finite difference algorithm, central-in-space	
$\Delta x \leq 2\ \alpha_L$	Finite element algorithm, linear basic functions	
$\Delta x \leq 4\ \alpha_L$	Finite element algorithm, quadratic basic functions	(8.71)

Note that there are acceptable solutions obtained with values up to $\Delta x < 10\,\alpha_L$[3]. As such, this restriction is not very compulsory. Under those circumstances, the solution can still be satisfactory though in some places over and undershooting (viz. oscillation) may occur.

[3]Sudicky [1989] even obtained highly accurate solutions for grid-Peclet-numbers in excess of 30 for the finite element method, based on a Laplace transformation of the temporal derivatives.

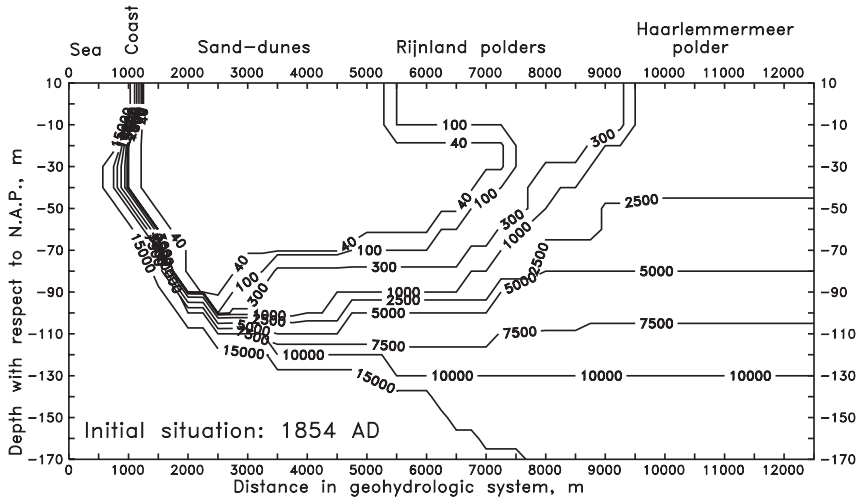

Figure 8.3: *Initial chloride distribution (values in mg Cl^-/l) at the beginning of 1854 AD, computed for 900 elements [Kooiman, 1989].*

Effect of the magnitude of α_L on the numerical solution: a case-study

The influence of longitudinal dispersivities α_L on the solution is analysed through simulation of a specific cross-section in Noord-Holland with two groundwater flow computer codes: SUTRA [Voss, 1984] (see the lecture notes of Hydrological Transport Processes/Groundwater Modelling II) based on the finite element method and the adapted MOC code [Konikow & Bredehoeft, 1978; Oude Essink, 1996] (see section 9.5) based on the method of characteristics. The cross-section through the sand-dune area of Gemeentewaterleidingen Amsterdam up to halfway the Haarlemmermeer polder is taken as the reference case.

The simulations start with an initial chloride distribution at the beginning of 1854 AD (see figure 8.3), as it is proposed by Kooiman [1989] through 'trial and error'. Each of the models computes the chloride distribution after a simulation time of 134 years, from the reclamation of the Haarlemmermeer polder till the end of 1987. The following two longitudinal dispersivities are applied: α_L=0.02 m and α_L=20.0 m. In order to compare the two models with each other, the dimension of the elements should be equal. The dimension is set to Δx=250 m and Δz=10 m. This implies for a cross-section with the dimensions 12,500 m by 180 m = 50 columns by 18 rows = 900 elements.

Figure 8.4 shows four chloride distributions in the cross-section at the end of 1987, after a simulation time of 134 years. The computed chloride distribution matches measured chloride distribution (not shown here) best if the longitudinal dispersivity α_L is small. The case with a small longitudinal dispersivity, that is α_L=0.02 m, has a freshwater lens that corresponds with measurements. For both models, the case with α_L=20.0 m does not simulate a freshwater lens any more. The aquifer system consists of only a large zone with brackish groundwater. Obviously, this situation does not match reality.

Moreover, as can be seen in the figure 8.4, the chloride distributions by the adapted MOC code are smooth. This is in contrast with the distributions by SUTRA. When lon-

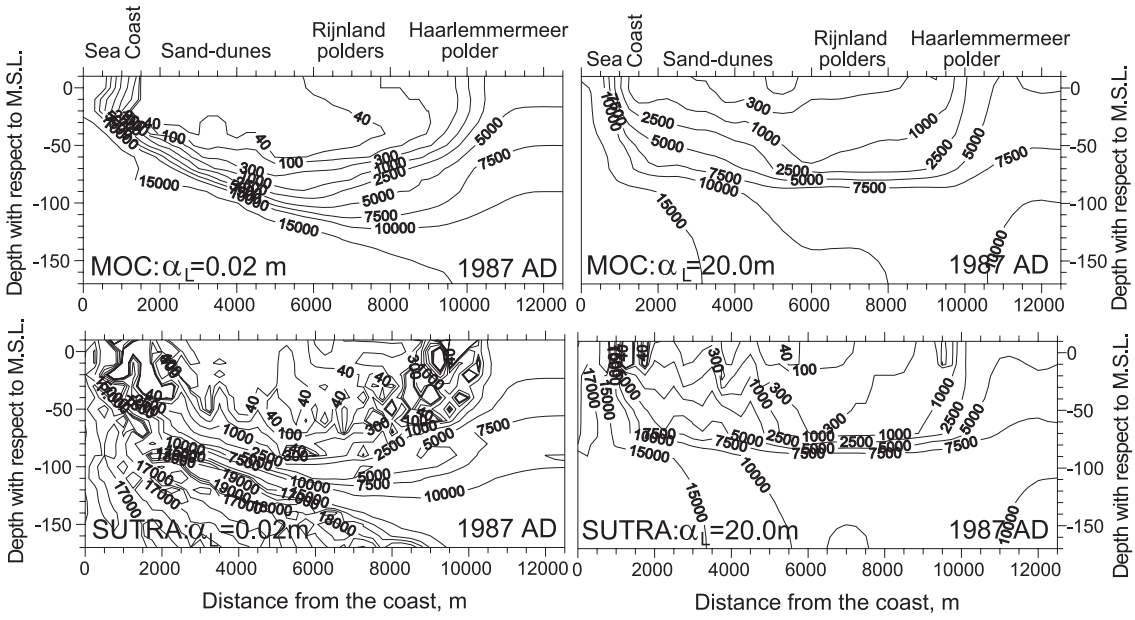

Figure 8.4: *Chloride distributions (in mg Cl^-/l) in 1987, computed for 900 elements with MOC and SUTRA for α_L=0.02 m and α_L=20.0 m. Note that here 900 elements are applied, whereas in figure 6.9 4500 elements are applied.*

Table 8.2: *Influence of the longitudinal dispersivity on the accuracy of the solution: the minimum and maximum chloride concentrations; and the number of elements undershooting a chloride concentration of 0 mg Cl^-/l and overshooting 17,000 mg Cl^-/l (the maximum chloride concentration which is inserted in the cross-section).*

SUTRA				
α_L	Minimum	Maximum	Undershoot	Overshoot
(m)	$(mg\ Cl^-/l)$	$(mg\ Cl^-/l)$	(elements)	(elements)
0.02	-8707	37,580	66	133
0.2	-7506	25,436	50	130
2.0	-7063	27,089	21	70
20.0	-1958	22,970	6	14

gitudinal dispersivities are small, SUTRA computes inaccurate chloride distributions, and over and undershooting of the maximum and minimum chloride concentrations frequently occur. Table 8.2 shows that in SUTRA over and undershooting occur in several elements. The smaller the longitudinal dispersivity, the more elements are subject to over and undershooting. The main reason for this phenomenon is that SUTRA applies the finite element method, whereas the adapted MOC code applies the method of characteristics to simulate solute transport. æ

Chapter 9

Some selected groundwater codes

9.1 Introduction

The number of computer codes available on the market is enormous, and as such, a complete overview is not possible. Therefore, only a selection[1] is given.

For purposes of illustration, four groundwater codes are discussed more intensively:

1. MODFLOW[2] [McDonald & Harbaugh, 1984; 1988] is a three-dimensional code, which considers groundwater flow through discretisation of the domain into grid blocks. It is based on the finite difference method.

2. Micro-Fem [Hemker & Elburg, 1988] is based on the finite element method. The computer code subdivides the hydrogeologic system into aquifers and aquitards, and as such, a three-dimensional situation is schematised.

3. MOC3D[3] [Konikow *et al.*, 1996] is a three-dimensional computer code. It combines MODFLOW (simulation of groundwater flow) with the three-dimensional version of MOC (simulation of solute transport). These two processes are coupled with each other.

4. the adapted MOC code[4] [Konikow & Bredehoeft, 1978; Oude Essink, 1996] is a two-dimensional groundwater code, which also considers solute transport. Through the conversion from solute (salt) to density, also density dependent groundwater flow is taken into account. The code is based on the finite difference method for groundwater flow and the method of characteristics for solute transport.

The codes MODFLOW, MOC3D and MOC are treated intensively during the computer workshop. Additional information on these two codes will follow.

[1] Note that computer codes, which can handle non-uniform density distributions (e.g. in coastal aquifers), are mentioned in the lecture notes of Hydrological Transport Processes/Groundwater Modelling II: Density Dependent Groundwater Flow: Salt Water Intrusion and Heat Transport).

[2] This computer code is present at the ICHU (Interfaculty Centre of Hydrology Utrecht) as a part of the package Visual MODFLOW, together with the three-dimensional solute transport computer code MT3D [Zheng, 1990].

[3] This computer code is present at the ICHU (Interfaculty Centre of Hydrology Utrecht) as well as available on the web: 'http://water.usgs.gov/software/moc3d.html'.

[4] This computer code is present at the ICHU (Interfaculty Centre of Hydrology Utrecht), Institute of Earth Sciences, Geophysics.

9.2 MODFLOW

Introduction

MODFLOW is currently (one of) the most widely used groundwater flow code in the field of hydrogeology. Within MODFLOW the groundwater system is modelled by a set of mathematical equations representing the flow phenomenon and physiographic characteristics of the groundwater system. A finite difference scheme is utilised where the applied equations incorporate the (groundwater) flow equation of Darcy and a continuity equation. MODFLOW is able to simulate steady state and transient flow conditions in one, two, or three dimensions. The overall structure of the MODFLOW programme consists of a preprocessing, a processing and a postprocessing part. It has a modular structure that allows it to be easily modified to adapt the code for a particular application. MODFLOW consists of a core module, the 'main', and a series of independent subroutines called 'modules' which simulate a specific feature of the hydrogeologic system. MODFLOW version 1401 of December 1996 [McDonald & Harbaugh, 1984; 1988; Harbaugh & McDonald, 1996], which is fully integrated with MOC3D, is applied for the computer workshop.

Concept of the code

In concept of the mathematical model underlying the MODFLOW package, a number of simplifications and assumptions are made in schematising and conceptualising to convert the "real world" groundwater system into the mathematical (computerised) groundwater system. For example, some concepts of the model are:

- the groundwater system can be simulated for steady state and for transient flow conditions,
- the mathematical groundwater system utilises a block-centered finite-difference approach,
- there is no flow of water over the model boundary,
- the medium to be modelled can be heterogeneous,
- the medium to be modelled can be anisotropic,
- the flow system can be shaped irregularly in which aquifer layers can be confined, unconfined, or a combination of confined and unconfined.
- flow can be fully three-dimensional.

Some model assumptions of MODFLOW are:

- in the original code, the density of the fluid is a constant, whereas in the one which is used in the computer workshop (as a part of MOC3D [Konikow *et al.*, 1996]) can take into account density differences.
- water movement can be in three (orthogonal) directions (X,Y,Z),
- properties within a block are assumed to be distributed homogeneous.

Discretisation of the model domain

In MODFLOW, the model domain is discretised in space by subdividing the area into blocks. The sizes of the blocks in x and y-direction are uniform over a row and over a column and are defined by the modeller in the preprocessing stage. In this way it is possible to obtain a varying spatial resolution for a region of interest. Note that when you also simulating solute transport (with the solute module in MOC3D), the size of the blocks should not vary too much. The elements may be of different sizes with different volumes, but in each individual element hydraulic parameters are assumed to be uniformly distributed. As MODFLOW uses since 1988 a dynamic memory allocation, you only have to increase the so-called LENX number in the code (and to compile the FORTRAN-code) to increase the number of elements of the computer code. For the order of magnitude: the computer code of 1984 could cope with the 60,000 elements of the model domain, with a maximum of 120 elements in x-direction, 120 elements in y-direction, and 80 elements in z-direction.

In the z-direction is the spatial distribution achieved by dividing the system in a number of layers. Each defined layer is characterised by a "flag" indicating that the layer is modelled under confined, unconfined or confined/unconfined flow conditions. Within a layer it is possible to model varying layer thickness by entering the top and bottom elevation for each element.

Modelling the time factor

In steady state simulations the values of the model input expressed in input and output flow sources are constant as well as the values of the model output. In transient flow situations the model input and output sources can be time variant and the model output is time dependent. Examples of time variant input are the change of the natural recharge rate over a certain period or the in time fluctuating discharge of a well.

The finite difference equation of groundwater flow

Equation 6.29 describes groundwater flow simulated by MODFLOW. If the fluid density is constant, the water balance of a block, expressed by the sum of all flows into or out of a block and its change in storage, represents the equation:

$$\sum Q_i = S_s \frac{\Delta\phi}{\Delta t} \Delta V \tag{9.1}$$

where

- S_s = specific storage of the porous material (L^{-1}),
- Q_i = total flow rate into the block ($L^3\,T^{-1}$),
- ΔV = volume of the block (L^3),
- $\Delta\phi$ = change in head over a time interval of length Δt (L).

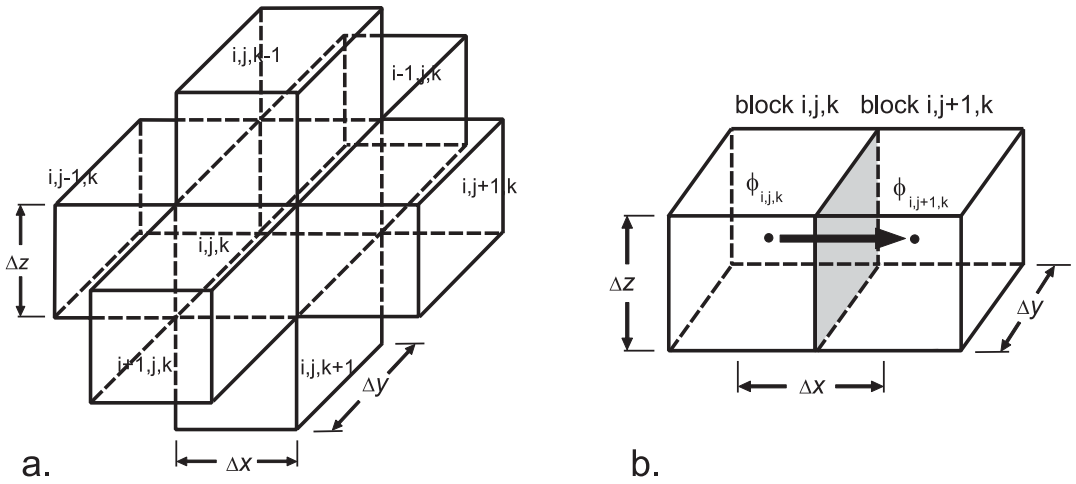

Figure 9.1: a: *block $[i, j, k]$ with the surrounding blocks.* b: *flow between block $[i, j, k]$ and block $[i, j + 1, k]$.*

Calculation of the flow rates in block $[i, j, k]$ is achieved through the calculation of the head field of the (six) blocks surrounding block $[i, j, k]$, see figure 9.1a. The flow at the interface between two blocks in x-direction, $[i, j, k]$ and $[i, j + 1, k]$, can be calculated with Darcy, see figure 9.1b:

$$Q_{i,j+1/2,k} = k_{i,j+1/2,k} \cdot \Delta y \cdot \Delta z \cdot \frac{\phi_{i,j,k} - \phi_{i,j+1,k}}{\Delta x} \tag{9.2}$$

where

- $Q_{i,j+1/2,k}$ = flow discharge through the face between $[i, j, k]$ and $[i, j + 1, k]$ $(L^3\,T^{-1})$,
- $k_{i,j+1/2,k}$ = hydraulic conductivity between $[i, j, k]$ and $[i, j + 1, k]$ $(L\,T^{-1})$,

The orientation of the model is given in figure 9.2. Similar expressions can be written for the other five blocks surrounding block $[i, j, k]$. Applying equation 9.1 to block $[i, j, k]$ taking into account the flows from the six adjacent blocks, as well as an external flow rate Q_{ext} (e.g. a well, a drain, evapotranspiration or river seepage) yields:

$$Q_{i,j-1/2,k} + Q_{i,j+1/2,k} + Q_{i-1/2,j,k} + Q_{i+1/2,j,k} + Q_{i,j,k-1/2} + Q_{i,j,k+1/2} + Q_{ext_{i,j,k}} = SS_{i,j,k}\frac{\phi^t_{i,j,k} - \phi^{t-\Delta t}_{i,j,k}}{\Delta t}\Delta V \tag{9.3}$$

where $\phi^t_{i,j,k} - \phi^{t-\Delta t}_{i,j,k}$ is a *backward difference* approach, which means that $\frac{\Delta\phi}{\Delta t}$ is approximated over a time interval which extends backward in time from t. The backward difference approach is always numerically stable[5]. For reasons of stability, the backward difference approach is preferred even though it leads to large systems of equations which must be solved simultaneously for each time at which the piezometric heads are to be computed. In MODFLOW, discretization of time can be in seconds, minutes, hours, days or years.

[5]Numerically stable means that errors introduced at any time diminish progressively at succeeding times.

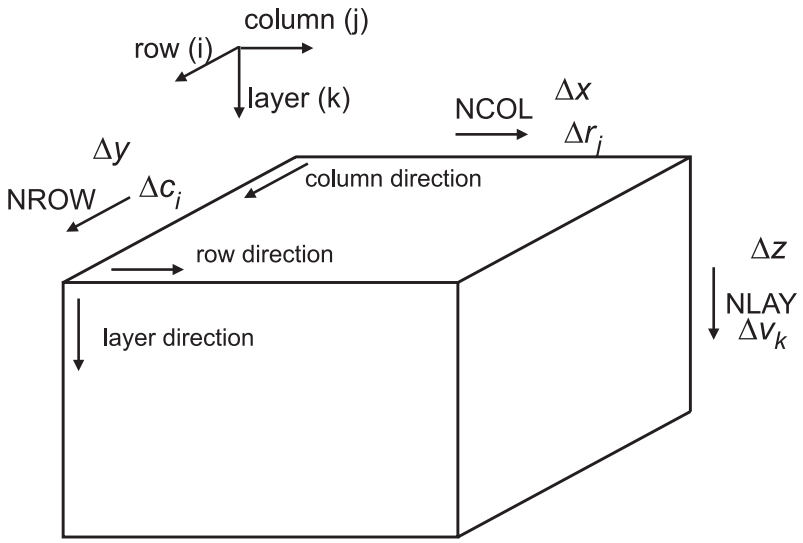

Figure 9.2: *Orientation of the three-dimensional groundwater code MODFLOW: NCOL=number of columns; NROW=number of rows and NLAY=number of layers.*

Hydraulic conductance

The groundwater flow equation 9.3 is simplified by introducing the so-called *hydraulic conductance* which is defined as:

$$CR_{i,j+1/2,k} = \frac{k_{i,j+1/2,k}\Delta y \Delta z}{\Delta x} \tag{9.4}$$

where $CR_{i,j+1/2,k}$ is the hydraulic conductance between nodes $[i, j, k]$ and $[i, j+1, k]$ in the row direction $(L^2\,T^{-1})$. As such, the hydraulic conductance is the product of hydraulic conductivity and cross-sectional area of flow divided by the length of the flow path. The same procedure can be followed for the hydraulic conductances in the respectively column and layer directions:

$$CC_{i+1/2,j,k} = \frac{k_{i+1/2,j,k}\Delta x \Delta z}{\Delta y} \tag{9.5}$$

and

$$CV_{i,j,k+1/2} = \frac{k_{i,j,k+1/2}\Delta x \Delta y}{\Delta z} \tag{9.6}$$

The value of the hydraulic conductance depends on the layer characteristics and the saturation rate. The exact determination of the hydraulic conductance can be found in McDonald & Harbaugh [1984; 1988].

Introducing these hydraulic conductances in equation 9.3 gives the backward finite difference equation 9.7:

$$\begin{aligned} &CR_{i,j-1/2,k}(\phi^m_{i,j-1,k} - \phi^m_{i,j,k}) + CR_{i,j+1/2,k}(\phi^m_{i,j+1,k} - \phi^m_{i,j,k}) + \\ &CC_{i-1/2,j,k}(\phi^m_{i-1,j,k} - \phi^m_{i,j,k}) + CC_{i+1/2,j,k}(\phi^m_{i+1,j,k} - \phi^m_{i,j,k}) + \end{aligned}$$

$$CV_{i,j,k-1/2}(\phi^m_{i,j,k-1} - \phi^m_{i,j,k}) + CV_{i,j,k+1/2}(\phi^m_{i,j,k+1} - \phi^m_{i,j,k}) + P_{i,j,k}\phi_{i,j,k} + Q_{i,j,k} = SS_{i,j,k}\frac{\phi^m_{i,j,k} - \phi^{m-1}_{i,j,k}}{t_m - t_{m-1}}\Delta r_j \Delta c_i \Delta v_k \quad (9.7)$$

where

- $P_{i,j,k}\phi_{i,j,k} + Q_{i,j,k} = Qext_{i,j,k}$ = combined flow of all external sources and stresses into block $[i, j, k]$,
- $SS_{i,j,k}$ = specific storage of block $[i, j, k]$ (L^{-1}),
- $\phi^m_{i,j,k}$ = piezometric head at block $[i, j, k]$ at moment of time m (L),
- $\Delta r_j \Delta c_i \Delta v_k$ = volume ΔV of block $[i, j, k]$ (L^3).

Rewriting this equation gives:

$$\begin{aligned} &CV_{i,j,k-1/2}\phi^m_{i,j,k-1} + CC_{i-1/2,j,k}\phi^m_{i-1,j,k} + CR_{i,j-1/2,k}\phi^m_{i,j-1,k} \\ &+(-CV_{i,j,k-1/2} - CC_{i-1/2,j,k} - CR_{i,j-1/2,k} \\ &-CR_{i,j+1/2,k} - CC_{i+1/2,j,k} - CV_{i,j,k+1/2} + HCOF_{i,j,k})\phi^m_{i,j,k} \\ &+CR_{i,j+1/2,k}\phi^m_{i,j+1,k} + CC_{i+1/2,j,k}\phi^m_{i+1,j,k} + CV_{i,j,k+1/2}\phi^m_{i,j,k+1} \\ &= RHS_{i,j,k} \end{aligned} \quad (9.8)$$

where

- $HCOF_{i,j,k} = P_{i,j,k} - SC1_{i,j,k}/(t_m - t_{m-1})$,
- $RHS_{i,j,k} = -Q_{i,j,k} - SC1_{i,j,k}\phi^{m-1}_{i,j,k}/(t_m - t_{m-1})$, and
- $SC1_{i,j,k} = SS_{i,j,k}\Delta r_j \Delta c_i \Delta v_k$.

or

$$[A] \times \{\phi\} = \{R\} \quad (9.9)$$

where

- A = matrix of the coefficients of piezometric head,
- ϕ = vector of piezometric head values at the end of time step m for all active elements in the mesh,
- R = vector of constant terms, RHS, for all elements in the mesh.

For each active block this equation can be written, deriving a system of n equations in n unknowns. Such a system can be solved simultaneously. MODFLOW utilizes iterative methods to obtain the solution to the system for each time step (e.g. strongly implicit procedure; slice-successive overrelaxation solution and preconditioned conjugate gradient solution).

Water budget

A water budget is a summary of all inflows and outflows to a region. MODFLOW calculates a water budget for the entire model domain as a measure to confirm the acceptability of the solution and in order to provide summarized information on the flow system. The budget module is activated for each time step in order to calculate the rate of flow into and out of the system for the processes simulated by the combined (external) flow packages.

Boundary condition

In MODFLOW it is in fact only possible to define a *constant piezometric head* boundary, the so-called *Dirichlet problem*, since due to the implementation of the block-centered discretisation scheme flow over the model boundary is not possible. However, groundwater system boundaries with a *constant flow* or *Neumann problem* into the model domain can be modelled by using external flow source terms just interior of the boundary.

Data requirements

The transmissivity and the hydraulic conductivity are required at each block in the grid. For both these subsoil parameters the layer thickness and the hydraulic conductivity are required. In case transient flow are simulated, every block must have a storage coefficient S and/or a specific yield μ $(-)$ (depending on the condition of the groundwater system: respectively confined and unconfined aquifers).

Mathematical description

The following features in MODFLOW are described mathematically:

- External sources into a block: packages,
- Layer types,
- Boundary conditions,
- Numerical solutions of the groundwater flow equation: SIP and SSOR).

9.2.1 External sources into a block: packages

External sources in MODFLOW are taken into account through the term $Q_{ext,i,j,k} = P_{i,j,k}\phi_{i,j,k} + Q_{i,j,k}$ (lectures notes equation 9.7) where $P_{i,j,k}$ (head dependent term) is part of $HCOF_{i,j,k}$ and $Q_{i,j,k}$ of $RHS_{i,j,k}$. In the original version of MODFLOW, six types of external sources or packages[6] due to external stresses are available to simulate the different (geo)hydrologic features (note that some types resemble each other):

1. River package
   Rivers, streams, canals, or ditches contribute water to the groundwater system or drain water from it depending on the piezometric head gradient between the stream

[6]These packages are discussed intensively in McDonald & Harbaugh [1984; 1988].

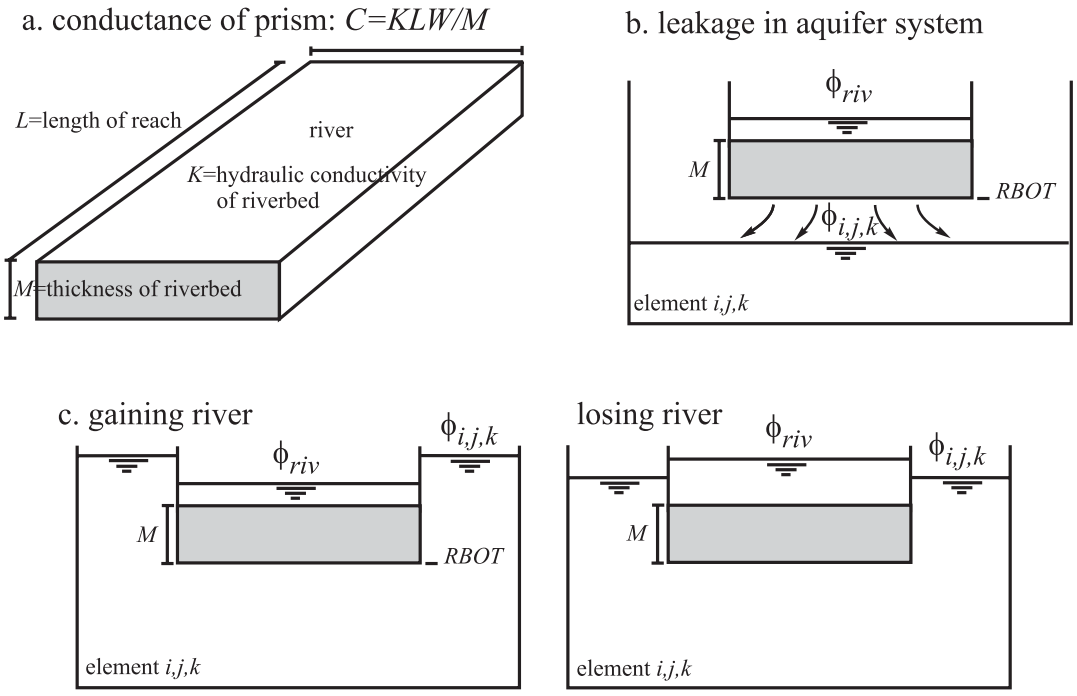

Figure 9.3: *Simulating a river: a. a riverbed viewed as a prism of porous material; b. leakage through the bottom of the riverbed if $\phi_{i,j,k} < RBOT$; c. cross-section showing the relation between head in the aquifer and in the river: rivers gaining and losing water.*

stage and the groundwater table. The purpose of the river package is to simulate the interaction of flow between surface water features and groundwater systems, using a so-called leakage. Figure 9.4 shows the river package as a function of the head ϕ in the aquifer. The purpose of the river package is to simulate the interaction of flow between surface water features and groundwater systems, using a so-called conductance. The following equation is valid (see figure 9.3):

$$Q_{riv} = \frac{KLW\left(\phi_{riv} - \phi_{aquifer}\right)}{M} \tag{9.10}$$

where:

- Q_{riv}=leakage through the reach of the riverbed (L^3T^{-1}),
- K=hydraulic conductivity of the riverbed (LT^{-1}),
- L=length of the reach (L),
- W=width of the river (L),
- M=thickness of the riverbed (L),
- ϕ_{riv}=head on the river side of the riverbed (L),
- $\phi_{aquifer}$=head on the aquifer side of the riverbed (L).

Rewriting the equation gives:

$$Q_{riv} = C_{riv} \left(\phi_{riv} - \phi_{aquifer} \right) \tag{9.11}$$

where:

- C_{riv}=KLW/M=conductance of the reach of the riverbed (L^2T^{-1}).

If the porous material at the side of the aquifer is fully saturated, the equation becomes:

$$Q_{riv} = C_{riv} \left(\phi_{riv} - \phi_{i,j,k} \right) \tag{9.12}$$

where:

- $\phi_{i,j,k}$=head in the aquifer (L).

Inserting the river contribution in the basic groundwater flow equation gives: add $-C_{riv}$ to $HCOF_{i,j,k}$ and add $-C_{riv}\phi_{riv}$ to $RHS_{i,j,k}$. However, if the porous material at the side of the aquifer is not saturated, the equation becomes:

$$Q_{riv} = C_{riv} \left(\phi_{riv} - RBOT \right) \tag{9.13}$$

where:

- $RBOT$=elevation of the bottom of the riverbed (L).

Inserting the not saturated river contribution in the basic groundwater flow equation gives: add 0 to $HCOF_{i,j,k}$ and add $-C_{riv} \left(\phi_{riv} - RBOT \right)$ to $RHS_{i,j,k}$.

2. Recharge package
The recharge package is designed to simulate areal distributed recharge to the groundwater system:

$$Q_{rch} = I_{i,j,k} \Delta r_j \Delta c_i \tag{9.14}$$

where:

- Q_{rch}=areal distributed recharge into the aquifer system (L^3T^{-1}),
- $\Delta r_j \Delta c_i$=horizontal area of the block (L^2),
- $I_{i,j,k}$=infiltration rate in block $[i, j, k]$ (LT^{-1}).

Inserting the recharge contribution in the basic groundwater flow equation gives: add 0 to $HCOF_{i,j,k}$ and add $-I_{i,j,k}\Delta r_j \Delta c_i$ to $RHS_{i,j,k}$. Most commonly, areal recharge occurs as a result of precipitation that percolates to the groundwater system. It is possible to insert recharge in other blocks than the blocks of the top layer (see McDonald & Harbaugh, 1984; 1988).

3. Well package
The well package is designed to simulate wells in order to withdraw water from or add water to the aquifer at a specified rate during a given stress period. Q_{well} is positive in case of infiltration and negative in case of extraction. Inserting the well contribution in the basic groundwater flow equation gives: add 0 to $HCOF_{i,j,k}$ and add $-Q_{well}$ to $RHS_{i,j,k}$.

4. Drain package
The drain package is designed to simulate water discharge from an aquifer by little ditches or agricultural drains. Figure 9.4 shows the drain package as a function of the head ϕ in the aquifer:

$$\text{if } \phi_{i,j,k} > d_{i,j,k} \text{ then} \qquad Q_{dr} = C_{dr}\left(\phi_{i,j,k} - d_{i,j,k}\right) \tag{9.15}$$

$$\text{if } \phi_{i,j,k} \leq d_{i,j,k} \text{ then} \qquad Q_{dr} = 0 \tag{9.16}$$

where:

- Q_{dr}=rate water flows into the drain and out the aquifer system (L^3T^{-1}),
- C_{dr}=conductance of the interface between the aquifer and the drain (L^2T^{-1}),
- $d_{i,j,k}$=head in the drain (L).

Inserting the drain contribution in the basic groundwater flow equation gives: if $\phi_{i,j,k} > d_{i,j,k}$ then: add $-C_{dr}$ to $HCOF_{i,j,k}$ and add $-C_{dr}d_{i,j,k}$ to $RHS_{i,j,k}$.

5. Evapotranspiration package
The evapotranspiration package simulates the effects of plant transpiration and direct evaporation in removing water from the saturated groundwater system. Figure 9.4 shows the evapotranspiration package as a function of the head ϕ in the aquifer:

$$Q_{eva} = 0 \qquad \text{when} \qquad \phi_{i,j,k} < EXEL \tag{9.17}$$

$$Q_{eva} = EVTR\frac{\phi_{i,j,k} - EXEL}{EXDP} \qquad \text{when} \qquad SURF \geq \phi_{i,j,k} \geq EXEL \tag{9.18}$$

$$Q_{eva} = EVTR \qquad \text{when} \qquad \phi_{i,j,k} > SURF \tag{9.19}$$

where:

- Q_{eva}=evapotranspiration rate (L^3T^{-1}),
- $EXEL$=extinction elevation; below this elevation, no evapotranspiration occurs (L),
- $EVTR$=maximum evapotranspiration rate (L^3T^{-1}),
- $SURF$=evapotranspiration surface elevation (L),
- $EXDP$=extinction depth ($SURF - EXEL$) (L).

Inserting the evapotranspiration contribution in the basic groundwater flow equation gives:

- for equation 9.17: add 0 to $HCOF_{i,j,k}$ and add 0 to $RHS_{i,j,k}$;
- for equation 9.18: add $-\frac{EVTR}{EXDP}$ to $HCOF_{i,j,k}$ and add $-EVTR\frac{EXEL}{(SURF-EXEL)}$ to $RHS_{i,j,k}$;
- for equation 9.19: add 0 to $HCOF_{i,j,k}$ and add $EVTR$ to $RHS_{i,j,k}$.

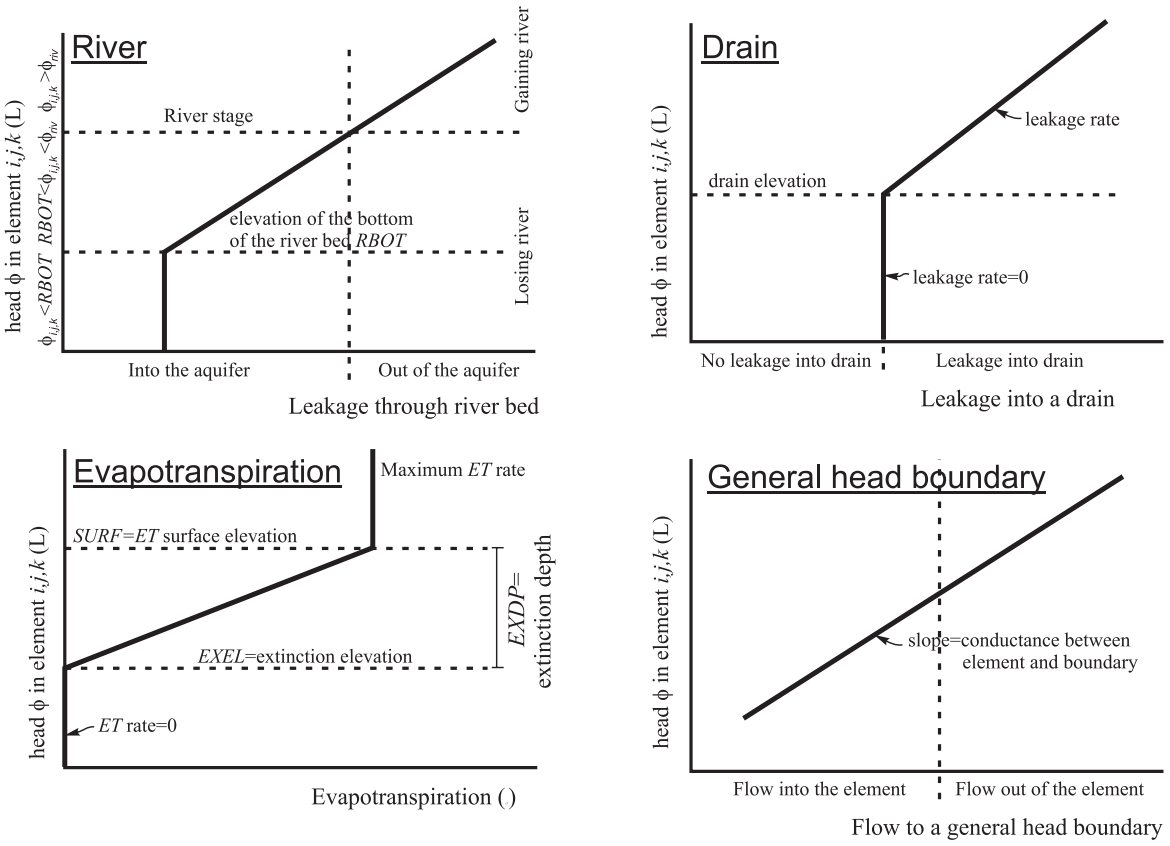

Figure 9.4: *Schematisations of four packages of MODFLOW as a function of the head $\phi_{i,j,k}$ in the aquifer: evapotranspiration, drain, river and general head boundary.*

6. General head boundary package
   The function of the general head boundary package is mathematically similar to that of the river or drain package. Flow into or out of a block $[i, j, k]$ due an external source, is provided in proportion to the difference between the piezometric head in the block $\phi_{i,j,k}$ and the head assigned to the external source $\phi^{ext}_{i,j,k}$. Figure 9.4 shows the general head boundary as a function of the head ϕ in the aquifer:

$$Q_{ghb} = C_{ghb}\left(\phi^{ext}_{i,j,k} - \phi_{i,j,k}\right) \tag{9.20}$$

   where:

   - Q_{ghb}=rate at which water is supplied to the block from a boundary (L^3T^{-1}),
   - C_{ghb}=conductance of proportionality for the external source (L^2T^{-1}),
   - $\phi^{ext}_{i,j,k}$=head at the external source (L).

   Inserting the general head boundary contribution in the basic groundwater flow equation gives: add $-C_{ghb}$ to $HCOF_{i,j,k}$ and add $-C_{ghb}\phi^{ext}_{i,j,k}$ to $RHS_{i,j,k}$.

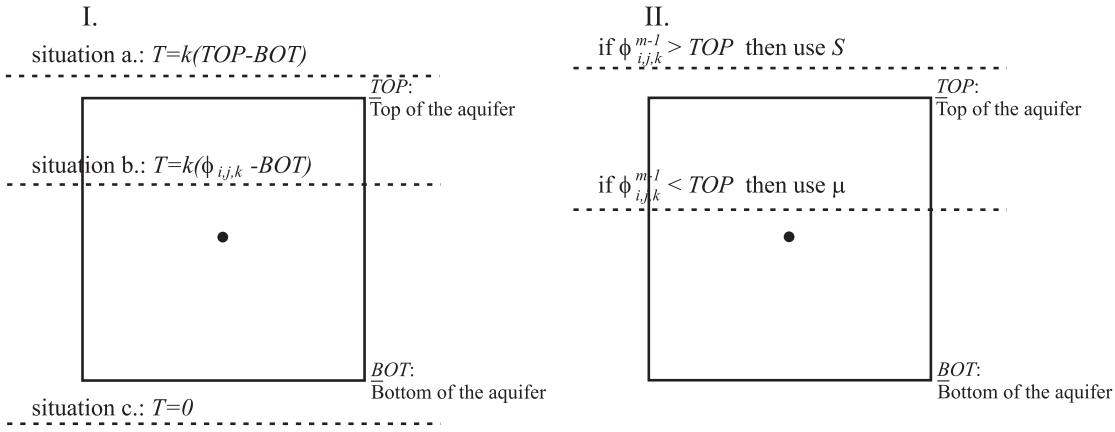

Figure 9.5: *Discretisation of: I. the transmissivity T and II. the storage of groundwater in the system.*

9.2.2 Layer types

There are four layer types:

a. LAYCON=0

Confined: T=kD=constant

Change in storage of groundwater in an element can be written as:

$$Q = SA\frac{\phi_{i,j,k}^{m-1} - \phi_{i,j,k}^{m}}{\Delta t} \tag{9.21}$$

where:

- S=storage coefficient $(-)$,
- A=$\Delta r_j \Delta c_i$=horizontal area of the element (L^2),
- $\phi_{i,j,k}^{m-1}$=head at the end of the previous time step $m-1$ (L),
- $\phi_{i,j,k}^{m}$=new head being calculated for the end of the current time step m (L),
- Δt=length of the time step (T).

b. LAYCON=1

Unconfined: T=variable (see figure 9.5.I):

$$1.\quad T = k(TOP - BOT) \qquad \text{when} \quad \phi_{i,j,k} \geq TOP \tag{9.22}$$

$$2.\quad T = k(\phi_{i,j,k} - BOT) \qquad \text{when} \quad BOT<\phi_{i,j,k} < TOP \tag{9.23}$$

$$3.\quad T = 0 \qquad \text{when} \quad \phi_{i,j,k} \leq BOT \tag{9.24}$$

where:

- k=hydraulic conductivity of element $[i,j,k]$ (L^2T^{-1}),
- TOP=the elevation of the top of the aquifer in element $[i,j,k]$ (L),
- BOT=the elevation of the bottom of the aquifer in element $[i,j,k]$ (L).

If LAYCON=1, also the values of k, TOP, and BOT must be given in the *.bas file.

Change in storage of groundwater in an element can be written as:

$$Q = \mu A \frac{\phi_{i,j,k}^{m-1} - \phi_{i,j,k}^{m}}{\Delta t} \tag{9.25}$$

where:

- μ=specific yield $(-)$.

c. LAYCON=2

Confined as well as unconfined, depending on the circumstances, yet T=kD=constant

Change in storage of groundwater in an element can be written as (see figure 9.5.II):

$$Q = S_1 A \frac{\phi_{i,j,k}^{m-1} - TOP}{\Delta t} + S_2 A \frac{TOP - \phi_{i,j,k}^{m}}{\Delta t} \tag{9.26}$$

$$\text{if } \phi_{i,j,k}^{m-1} > TOP \text{ then use } S \tag{9.27}$$

$$\text{if } \phi_{i,j,k}^{m-1} < TOP \text{ then use } \mu \tag{9.28}$$

where:

- S_1=storage coefficient in effect at the start of the time step $(-)$,
- S_2=storage coefficient in effect at the current time step $(-)$.

d. LAYCON=3

Confined as well as unconfined, depending on the circumstances, T=variable: see LAYCON=1.

Change in storage of groundwater in an element is written as in LAYCON=2.

9.2.3 Boundary conditions

The IBOUND array contains a code for each element, which is inserted in the *.bas-file (see figure 9.6):

- IBOUND<0: head is constant (constant-head element);
- IBOUND=0: no flow takes place within the element (no-flow or inactive element);
- IBOUND>0: head varies with time (variable-head element).

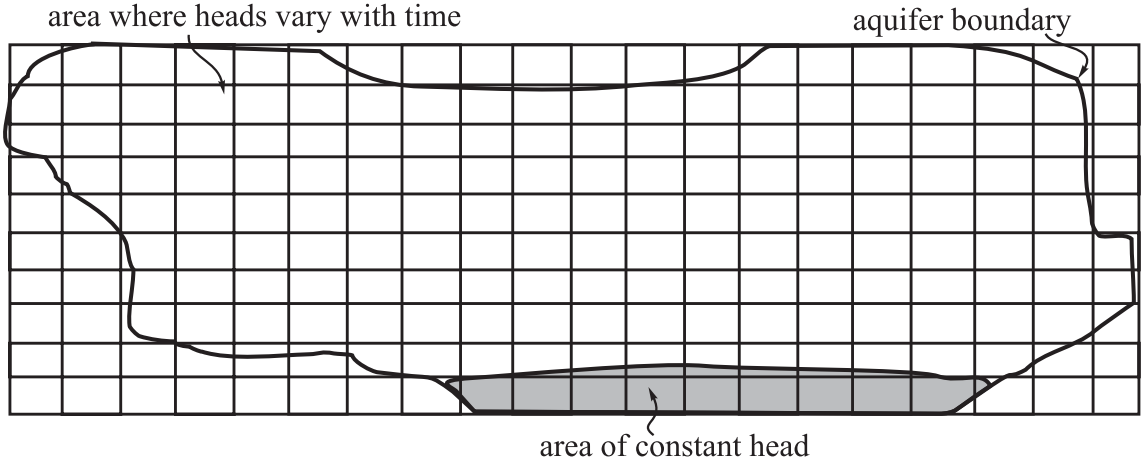

0	1	1	1	1	1	0	0	0	0	0	0	0	1	1	1	1	1	0	0
1	1	1	1	1	1	1	1	1	1	1	1	1	1	1	1	1	1	1	0
1	1	1	1	1	1	1	1	1	1	1	1	1	1	1	1	1	1	1	0
0	1	1	1	1	1	1	1	1	1	1	1	1	1	1	1	1	1	1	0
0	0	1	1	1	1	1	1	1	1	1	1	1	1	1	1	1	1	1	0
0	0	1	1	1	1	1	1	1	1	1	1	1	1	1	1	1	1	1	1
0	0	1	1	1	1	1	1	1	1	1	1	1	1	1	1	1	1	1	1
0	0	1	1	1	1	1	1	1	1	1	1	1	1	1	1	1	1	1	0
0	0	0	0	0	0	1	1	1	1	1	1	1	1	1	1	1	1	0	0
0	0	0	0	0	0	0	-1	-1	-1	-1	-1	-1	-1	-1	-1	-1	0	0	0

IBOUND codes: **<0 constant head**
=0 no flow
>0 variable head

Figure 9.6: *Example of the boundary array IBOUND for a single layer.*

9.2.4 Strongly Implicit Procedure package (SIP)

The basic groundwater flow equation is:

$$\begin{aligned} &CV_{i,j,k-1/2}\phi^m_{i,j,k-1} + CC_{i-1/2,j,k}\phi^m_{i-1,j,k} + CR_{i,j-1/2,k}\phi^m_{i,j-1,k} \\ &+(-CV_{i,j,k-1/2} - CC_{i-1/2,j,k} - CR_{i,j-1/2,k} \\ &-CR_{i,j+1/2,k} - CC_{i+1/2,j,k} - CV_{i,j,k+1/2} + HCOF_{i,j,k})\phi^m_{i,j,k} \\ &+CR_{i,j+1/2,k}\phi^m_{i,j+1,k} + CC_{i+1/2,j,k}\phi^m_{i+1,j,k} + CV_{i,j,k+1/2}\phi^m_{i,j,k+1} \\ &= RHS_{i,j,k} \end{aligned} \tag{9.29}$$

or, based on the notation of the developers of SIP (Weinstein, Stone and Kwan, 1969), this equation can be rewritten as:

$$Z_{i,j,k}\phi_{i,j,k-1} + B_{i,j,k}\phi_{i-1,j,k} + D_{i,j,k}\phi_{i,j-1,k} + E_{i,j,k}\phi_{i,j,k}$$

$$
\begin{bmatrix}
E_1 & F_1 & 0 & 0 & H_1 & 0 & 0 & 0 & 0 & 0 & 0 & 0 & S_1 & 0 & 0 & 0 & 0 & 0 & 0 & 0 & 0 & 0 & 0 & 0 \\
D_2 & E_2 & F_2 & 0 & 0 & H_2 & 0 & 0 & 0 & 0 & 0 & 0 & 0 & S_2 & 0 & 0 & 0 & 0 & 0 & 0 & 0 & 0 & 0 & 0 \\
0 & D_3 & E_3 & F_3 & 0 & 0 & H_3 & 0 & 0 & 0 & 0 & 0 & 0 & 0 & S_3 & 0 & 0 & 0 & 0 & 0 & 0 & 0 & 0 & 0 \\
0 & 0 & D_4 & E_4 & F_4 & 0 & 0 & H_4 & 0 & 0 & 0 & 0 & 0 & 0 & 0 & S_4 & 0 & 0 & 0 & 0 & 0 & 0 & 0 & 0 \\
B_5 & 0 & 0 & D_5 & E_5 & F_5 & 0 & 0 & H_5 & 0 & 0 & 0 & 0 & 0 & 0 & 0 & S_5 & 0 & 0 & 0 & 0 & 0 & 0 & 0 \\
0 & B_6 & 0 & 0 & D_6 & E_6 & F_6 & 0 & 0 & H_6 & 0 & 0 & 0 & 0 & 0 & 0 & 0 & S_6 & 0 & 0 & 0 & 0 & 0 & 0 \\
0 & 0 & B_7 & 0 & 0 & D_7 & E_7 & F_7 & 0 & 0 & H_7 & 0 & 0 & 0 & 0 & 0 & 0 & 0 & S_7 & 0 & 0 & 0 & 0 & 0 \\
0 & 0 & 0 & B_8 & 0 & 0 & D_8 & E_8 & F_8 & 0 & 0 & H_8 & 0 & 0 & 0 & 0 & 0 & 0 & 0 & S_8 & 0 & 0 & 0 & 0 \\
0 & 0 & 0 & 0 & B_9 & 0 & 0 & D_9 & E_9 & F_9 & 0 & 0 & H_9 & 0 & 0 & 0 & 0 & 0 & 0 & 0 & S_9 & 0 & 0 & 0 \\
0 & 0 & 0 & 0 & 0 & B_{10} & 0 & 0 & D_{10} & E_{10} & F_{10} & 0 & 0 & H_{10} & 0 & 0 & 0 & 0 & 0 & 0 & 0 & S_{10} & 0 & 0 \\
0 & 0 & 0 & 0 & 0 & 0 & B_{11} & 0 & 0 & D_{11} & E_{11} & F_{11} & 0 & 0 & H_{11} & 0 & 0 & 0 & 0 & 0 & 0 & 0 & S_{11} & 0 \\
0 & 0 & 0 & 0 & 0 & 0 & 0 & B_{12} & 0 & 0 & D_{12} & E_{12} & F_{12} & 0 & 0 & H_{12} & 0 & 0 & 0 & 0 & 0 & 0 & 0 & S_{12} \\
Z_{13} & 0 & 0 & 0 & 0 & 0 & 0 & 0 & 0 & 0 & 0 & 0 & E_{13} & F_{13} & 0 & 0 & H_{13} & 0 & 0 & 0 & 0 & 0 & 0 & 0 \\
0 & Z_{14} & 0 & 0 & 0 & 0 & 0 & 0 & 0 & 0 & 0 & 0 & D_{14} & E_{14} & F_{14} & 0 & 0 & H_{14} & 0 & 0 & 0 & 0 & 0 & 0 \\
0 & 0 & Z_{15} & 0 & 0 & 0 & 0 & 0 & 0 & 0 & 0 & 0 & 0 & D_{15} & E_{15} & F_{15} & 0 & 0 & H_{15} & 0 & 0 & 0 & 0 & 0 \\
0 & 0 & 0 & Z_{16} & 0 & 0 & 0 & 0 & 0 & 0 & 0 & 0 & 0 & 0 & D_{16} & E_{16} & F_{16} & 0 & 0 & H_{16} & 0 & 0 & 0 & 0 \\
0 & 0 & 0 & 0 & Z_{17} & 0 & 0 & 0 & 0 & 0 & 0 & 0 & B_{17} & 0 & 0 & 0 & E_{17} & F_{17} & 0 & 0 & H_{17} & 0 & 0 & 0 \\
0 & 0 & 0 & 0 & 0 & Z_{18} & 0 & 0 & 0 & 0 & 0 & 0 & 0 & B_{18} & 0 & 0 & D_{18} & E_{18} & F_{18} & 0 & 0 & H_{18} & 0 & 0 \\
0 & 0 & 0 & 0 & 0 & 0 & Z_{19} & 0 & 0 & 0 & 0 & 0 & 0 & 0 & B_{19} & 0 & 0 & D_{19} & E_{19} & F_{19} & 0 & 0 & H_{19} & 0 \\
0 & 0 & 0 & 0 & 0 & 0 & 0 & Z_{20} & 0 & 0 & 0 & 0 & 0 & 0 & 0 & B_{20} & 0 & 0 & D_{20} & E_{20} & 0 & 0 & 0 & H_{20} \\
0 & 0 & 0 & 0 & 0 & 0 & 0 & 0 & Z_{21} & 0 & 0 & 0 & 0 & 0 & 0 & 0 & B_{21} & 0 & 0 & 0 & E_{21} & F_{21} & 0 & 0 \\
0 & 0 & 0 & 0 & 0 & 0 & 0 & 0 & 0 & Z_{22} & 0 & 0 & 0 & 0 & 0 & 0 & 0 & B_{22} & 0 & 0 & D_{22} & E_{22} & F_{22} & 0 \\
0 & 0 & 0 & 0 & 0 & 0 & 0 & 0 & 0 & 0 & Z_{23} & 0 & 0 & 0 & 0 & 0 & 0 & 0 & B_{23} & 0 & 0 & D_{23} & E_{23} & F_{23} \\
0 & 0 & 0 & 0 & 0 & 0 & 0 & 0 & 0 & 0 & 0 & Z_{24} & 0 & 0 & 0 & 0 & 0 & 0 & 0 & B_{24} & 0 & 0 & D_{24} & E_{24}
\end{bmatrix}
\begin{bmatrix} \phi_1 \\ \phi_2 \\ \phi_3 \\ \phi_4 \\ \phi_5 \\ \phi_6 \\ \phi_7 \\ \phi_8 \\ \phi_9 \\ \phi_{10} \\ \phi_{11} \\ \phi_{12} \\ \phi_{13} \\ \phi_{14} \\ \phi_{15} \\ \phi_{16} \\ \phi_{17} \\ \phi_{18} \\ \phi_{19} \\ \phi_{20} \\ \phi_{21} \\ \phi_{22} \\ \phi_{23} \\ \phi_{24} \end{bmatrix}
=
\begin{bmatrix} R_1 \\ R_2 \\ R_3 \\ R_4 \\ R_5 \\ R_6 \\ R_7 \\ R_8 \\ R_9 \\ R_{10} \\ R_{11} \\ R_{12} \\ R_{13} \\ R_{14} \\ R_{15} \\ R_{16} \\ R_{17} \\ R_{18} \\ R_{19} \\ R_{20} \\ R_{21} \\ R_{22} \\ R_{23} \\ R_{24} \end{bmatrix}
$$

Figure 9.7: *Correspondence between finite-difference equations and the matrix equation for a grid with three rows, four columns and two layers.*

$$+F_{i,j,k}\phi_{i,j+1,k} + H_{i,j,k}\phi^m_{i+1,j,k} + S_{i,j,k}\phi^m_{i,j,k+1} = Q_{i,j,k} \tag{9.30}$$

Figure 9.7 shows an example of such a matrix, whereas figure 9.8 shows the structure of the matrix with the non-zero (seven) diagonals.

Symmetric matrix

As can be deduced, the $Z_{i,j,k}$-coefficient at element $[i, j, k]$ is equal to the $S_{i,j,k-1}$-coefficient at element $[i, j, k-1]$. As such, the following statements are true:

$$Z_{i,j,k} \quad = \quad S_{i,j,k-1}$$

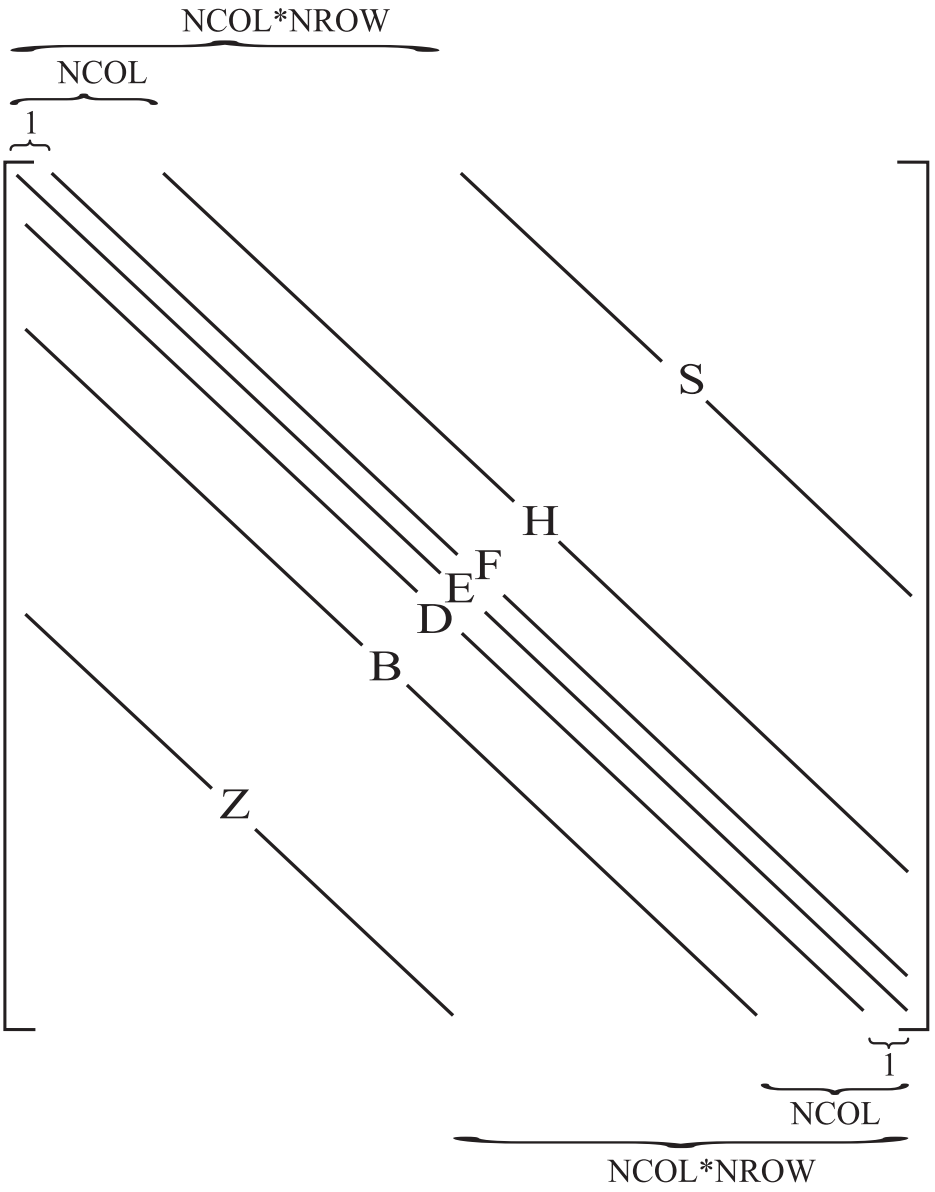

Figure 9.8: *Structure of the coefficient matrix showing seven non-zero diagonals.*

$$\begin{aligned} \text{similarly } Z_{i,j,k} &= H_{i-1,j,k} \\ \text{and } D_{i,j,k} &= F_{i,j-1,k} \end{aligned} \tag{9.31}$$

Based on this information, a symmetric coefficient matrix can be produced. For example, the following matrix is for a grid with two rows, three columns and two layers:

$$\begin{bmatrix}
E_{1,1,1} & F_{1,1,1} & 0 & H_{1,1,1} & 0 & 0 & S_{1,1,1} & 0 & 0 & 0 & 0 & 0 \\
F_{1,1,1} & E_{1,2,1} & F_{1,2,1} & 0 & H_{1,2,1} & 0 & 0 & S_{1,2,1} & 0 & 0 & 0 & 0 \\
0 & F_{1,2,1} & E_{1,3,1} & 0 & 0 & H_{1,3,1} & 0 & 0 & S_{1,3,1} & 0 & 0 & 0 \\
H_{1,1,1} & 0 & 0 & E_{2,1,1} & F_{2,1,1} & 0 & 0 & 0 & 0 & S_{2,1,1} & 0 & 0 \\
0 & H_{1,2,1} & 0 & F_{2,1,1} & E_{2,2,1} & F_{2,2,1} & 0 & 0 & 0 & 0 & S_{2,2,1} & 0 \\
0 & 0 & H_{1,3,1} & 0 & F_{2,2,1} & E_{2,3,1} & 0 & 0 & 0 & 0 & 0 & S_{2,3,1} \\
S_{1,1,1} & 0 & 0 & 0 & 0 & 0 & E_{1,1,2} & F_{1,1,2} & 0 & H_{1,1,2} & 0 & 0 \\
0 & S_{1,2,1} & 0 & 0 & 0 & 0 & F_{1,1,2} & E_{1,2,2} & F_{1,2,2} & 0 & H_{1,2,2} & 0 \\
0 & 0 & S_{1,3,1} & 0 & 0 & 0 & 0 & F_{1,2,2} & E_{1,3,2} & 0 & 0 & H_{1,3,2} \\
0 & 0 & 0 & S_{2,1,1} & 0 & 0 & H_{1,1,2} & 0 & 0 & E_{2,1,2} & F_{2,1,2} & 0 \\
0 & 0 & 0 & 0 & S_{2,2,1} & 0 & 0 & H_{1,2,2} & 0 & F_{2,1,2} & E_{2,2,2} & F_{2,2,2} \\
0 & 0 & 0 & 0 & 0 & S_{2,3,1} & 0 & 0 & H_{1,3,2} & 0 & F_{2,2,2} & E_{2,3,2}
\end{bmatrix} \tag{9.32}$$

or

$$[A] \times \{\phi\} = \{R\} \tag{9.33}$$

where

- A = matrix of the coefficients of piezometric head,
- ϕ = vector of piezometric head values at the end of time step m for all active elements in the mesh,
- R = vector of constant terms, RHS, for all elements in the mesh.

LU-decomposition

The SIP package uses the LU-decomposition to solve the matrix. For this purpose, the matrix A is divided into two triangular matrices, L and U, such that in L, all non-zero elements are below the main diagonal ('L of low'), and in U, all non-zero elements are above the main diagonal ('U of up'). Equation 9.33, $A\ \phi = q$, is solved by:

$$L\,U\ \phi = q \tag{9.34}$$

Equation 9.34 is divided into two equations:

$$L\ v = q \tag{9.35}$$

$$U\ \phi = v \tag{9.36}$$

First equation 9.35 will be solved. This gives values of the vector v. With this information, the vector ϕ can found through solving equation 9.36.

Example 9.1: LU-decomposition

For example, decomposition of the following matrix into a lower and a upper triangular matrices gives:

$$A \qquad \phi \quad = \quad q$$

$$\begin{bmatrix} 1 & 2 & 1 \\ -1 & 1 & 2 \\ 3 & 2 & -2 \end{bmatrix} \begin{Bmatrix} \phi_1 \\ \phi_2 \\ \phi_3 \end{Bmatrix} = \begin{Bmatrix} 1 \\ 2 \\ -3 \end{Bmatrix}$$

$$L \qquad\qquad U \qquad\quad \phi \quad = \quad q$$

$$\begin{bmatrix} 1 & 0 & 0 \\ -1 & 3 & 0 \\ 3 & -4 & -1 \end{bmatrix} \begin{bmatrix} 1 & 2 & 1 \\ 0 & 1 & 1 \\ 0 & 0 & 1 \end{bmatrix} \begin{Bmatrix} \phi_1 \\ \phi_2 \\ \phi_3 \end{Bmatrix} = \begin{Bmatrix} 1 \\ 2 \\ -3 \end{Bmatrix}$$

First solving $L\ v = q$:

$$\begin{bmatrix} 1 & 0 & 0 \\ -1 & 3 & 0 \\ 3 & -4 & -1 \end{bmatrix} \begin{Bmatrix} v_1 \\ v_2 \\ v_3 \end{Bmatrix} = \begin{Bmatrix} 1 \\ 2 \\ -3 \end{Bmatrix}$$

Starting at the top of the matrix gives:

$$\begin{Bmatrix} v_1 \\ v_2 \\ v_3 \end{Bmatrix} = \begin{Bmatrix} 1 \\ 1 \\ 2 \end{Bmatrix}$$

Then solving $U\ \phi = v$:

$$\begin{bmatrix} 1 & 2 & 1 \\ 0 & 1 & 1 \\ 0 & 0 & 1 \end{bmatrix} \begin{Bmatrix} \phi_1 \\ \phi_2 \\ \phi_3 \end{Bmatrix} = \begin{Bmatrix} 1 \\ 1 \\ 2 \end{Bmatrix}$$

Starting at the bottom of the matrix gives:

$$\begin{Bmatrix} \phi_1 \\ \phi_2 \\ \phi_3 \end{Bmatrix} = \begin{Bmatrix} 1 \\ -1 \\ 2 \end{Bmatrix}$$

Strongly Implicit Procedure: SIP

Now, the LU matrices must be found. As you can see in figure 9.7, many coefficients of the matrix A are equal to zero: matrix A is called 'sparse' ('dun bezaaid met getallen $\neq$ nul'). This will be used in finding the LU matrices. A matrix B is introduced such that $[A+B]$ is 'close' to A: $[A+B]\phi \approx A\phi$. Adding $B\phi$ to both sides of equation 9.33 gives:

$$[A+B]\{\phi\} = q + B\phi \tag{9.37}$$

Now, we introduce the iterative part of the SIP package. As the value $B\phi$ is not known, it can be approximated by using the best estimate of ϕ:

$$[A+B]\phi^m = q + B\phi^{m-1} \tag{9.38}$$

The vector ϕ^m is the m-th iteration estimate of the vector ϕ. On subsequent iterations, ϕ^{m-1} would be the head vector calculated at the previous iteration. In addition, by subtracting the term $[A+B]\phi^{m-1}$ from both sides of equation 9.38 gives:

$$[A+B]\left\{\phi^m - \phi^{m-1}\right\} = q - A\phi^{m-1} \tag{9.39}$$

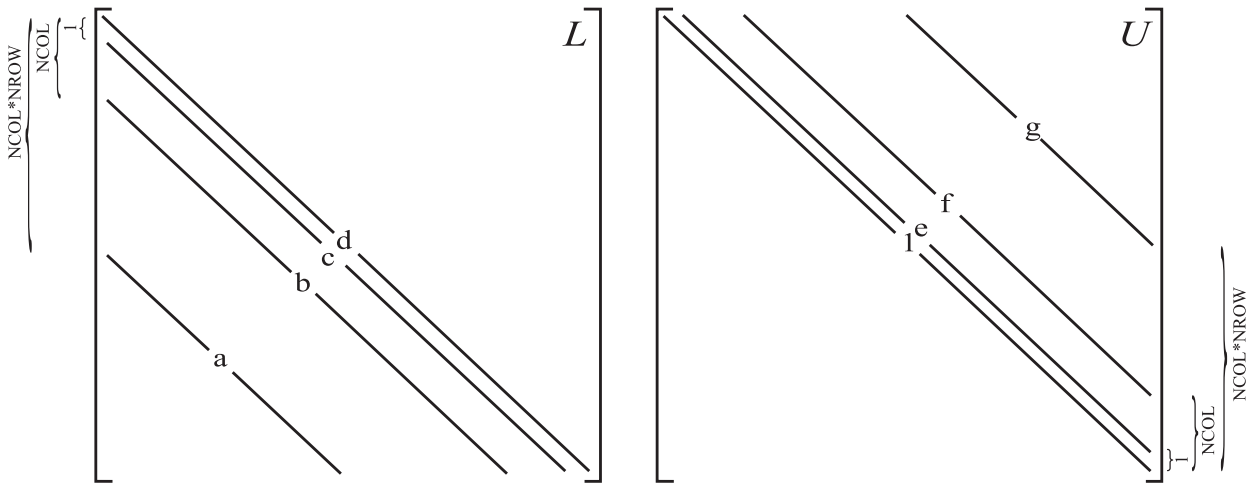

Figure 9.9: *Desired structure of L en U, showing nonzero diagonals of the lower triangular matrix L and the upper triangular matrix U.*

So, now, the problem in SIP is to find two matrices L and U, such that LU is equal to $[A + B]$. It appears that there do exists two matrices L and U: see figure 9.9. You can see that these matrices are also sparse. Multiplication of L and U gives $[A + B]$, see figure 9.10. The exact determination of these two matrices is not discussed here: see for more information McDonald and Harbaugh (1984). Introducing the LU matrices gives:

$$LU\left\{\phi^m - \phi^{m-1}\right\} = q - A\phi^{m-1} \tag{9.40}$$

$$LU\left\{\phi^m - \phi^{m-1}\right\} = RES^m \tag{9.41}$$

$$Lv = RES^m \quad \text{gives} \quad v \tag{9.42}$$

$$U\left\{\phi^m - \phi^{m-1}\right\} = v \quad \text{gives} \quad \phi^m - \phi^{m-1} = \Delta\phi \tag{9.43}$$

$$\phi^m = \phi^{m-1} + \Delta\phi \tag{9.44}$$

The moment that $\Delta\phi$ in all elements are smaller than a so-called closure criterion HCLOSE (head change criterion for convergence), the iteration stops.

9.2.5 Slice-Successive Overrelaxation package (SSOR)

This technique solves the system of linear equation iterative. The corresponding equation is:

$$\begin{aligned} &CV_{i,j,k-1/2}\phi^{t,m+1}_{i,j,k-1} + CC_{i-1/2,j,k}\phi^{t,m+1}_{i-1,j,k} + CR_{i,j-1/2,k}\phi^{t,m+1}_{i,j-1,k} \\ &\quad +(-CV_{i,j,k-1/2} - CC_{i-1/2,j,k} - CR_{i,j-1/2,k} \\ &-CR_{i,j+1/2,k} - CC_{i+1/2,j,k} - CV_{i,j,k+1/2} + HCOF_{i,j,k})\phi^{t,m+1}_{i,j,k} \\ &+CR_{i,j+1/2,k}\phi^{t,m+1}_{i,j+1,k} + CC_{i+1/2,j,k}\phi^{t,m+1}_{i+1,j,k} + CV_{i,j,k+1/2}\phi^{t,m+1}_{i,j,k+1} \\ &\quad = RHS_{i,j,k} \end{aligned} \tag{9.45}$$

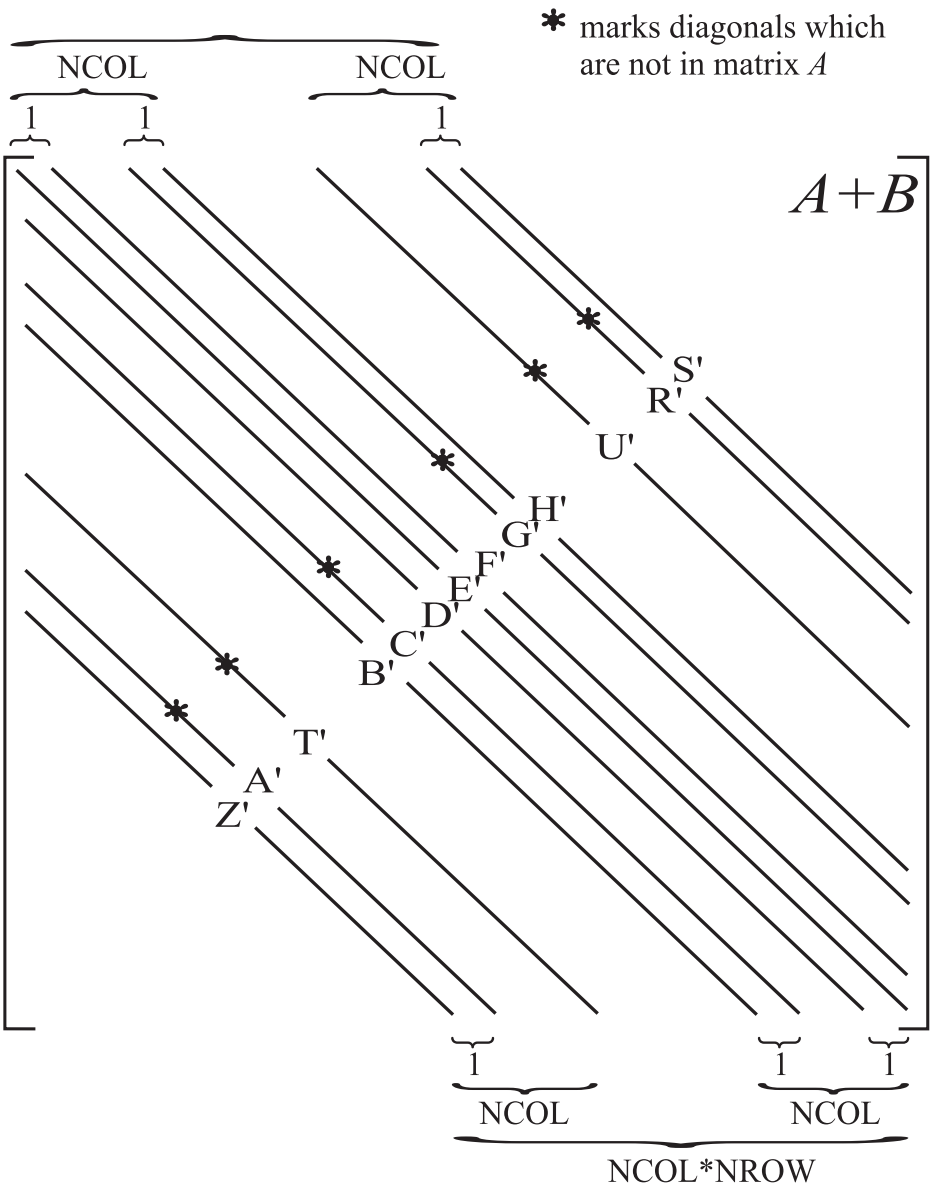

Figure 9.10: *Structure of the matrix $A + B$ showing nonzero diagonals.*

where:

- t=the time step counter $(-)$,
- m=the iteration counter $(-)$.

Rewriting equation 9.45 in residual form (by adding terms of $-\ \phi^{t,m}$ on both sides) gives:

$$CV_{i,j,k-1/2}(\phi^{t,m+1}_{i,j,k-1} - \phi^{t,m}_{i,j,k-1}) + CC_{i-1/2,j,k}(\phi^{t,m+1}_{i-1,j,k} - \phi^{t,m}_{i-1,j,k})$$

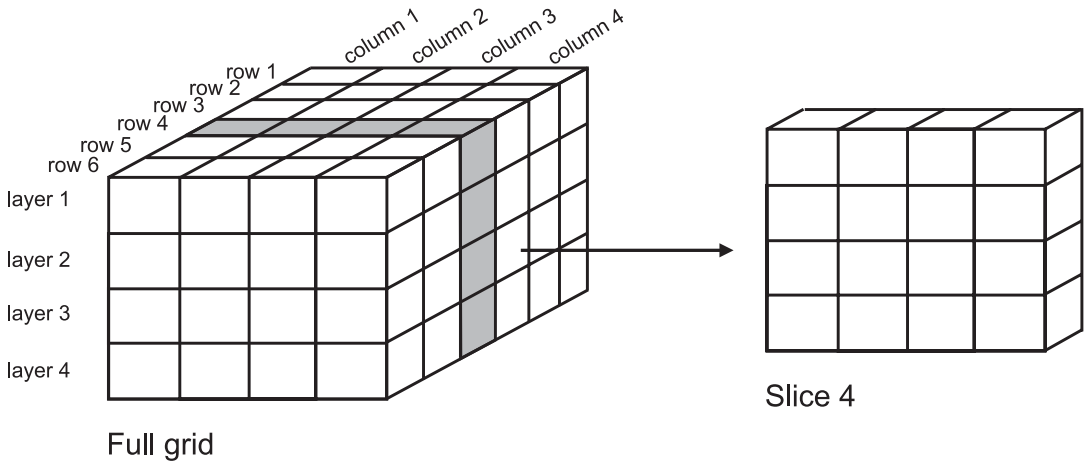

Figure 9.11: *SSOR reduces the number of equations that must be solved simultaneously by considering only a single vertical slice at a time.*

$$
\begin{aligned}
&+CR_{i,j-1/2,k}(\phi^{t,m+1}_{i,j-1,k}-\phi^{t,m}_{i,j-1,k})+(-CV_{i,j,k-1/2}-CC_{i-1/2,j,k}-CR_{i,j-1/2,k}\\
&-CR_{i,j+1/2,k}-CC_{i+1/2,j,k}-CV_{i,j,k+1/2}+HCOF_{i,j,k})(\phi^{t,m+1}_{i,j,k}-\phi^{t,m}_{i,j,k})\\
&+CR_{i,j+1/2,k}(\phi^{t,m+1}_{i,j+1,k}-\phi^{t,m}_{i,j+1,k})+CC_{i+1/2,j,k}(\phi^{t,m+1}_{i+1,j,k}-\phi^{t,m}_{i+1,j,k})\\
&+CV_{i,j,k+1/2}(\phi^{t,m+1}_{i,j,k+1}-\phi^{t,m}_{i,j,k+1})=RHS_{i,j,k}-CV_{i,j,k-1/2}\phi^{t,m}_{i,j,k-1}\\
&-CC_{i-1/2,j,k}\phi^{t,m}_{i-1,j,k}-CR_{i,j-1/2,k}\phi^{t,m}_{i,j-1,k}-(-CV_{i,j,k-1/2}-CC_{i-1/2,j,k}-CR_{i,j-1/2,k}\\
&-CR_{i,j+1/2,k}-CC_{i+1/2,j,k}-CV_{i,j,k+1/2}+HCOF_{i,j,k})\phi^{t,m}_{i,j,k}\\
&-CR_{i,j+1/2,k}\phi^{t,m}_{i,j+1,k}-CC_{i+1/2,j,k}\phi^{t,m}_{i+1,j,k}-CV_{i,j,k+1/2}\phi^{t,m}_{i,j,k+1}
\end{aligned}
\tag{9.46}
$$

The left hand side of equation 9.46 consists of terms involving the seven head changes, e.g. $\phi^{t,m+1}_{i,j,k}-\phi^{t,m}_{i,j,k}$, for iteration $m+1$. The SSOR package reduces the number of equations by simultaneously solving only those equations representing elements in a single slice (or row number), see figure 9.11. The two assumptions which come with this approach are:

1. consider the equation for elements in slice 1: $i=1$. In this slice, the heads at the positions $i-1$ are equal to zero: $CC_{i-1/2,j,k}\left(\phi^{t,m+1}_{i-1,j,k}-\phi^{t,m}_{i-1,j,k}\right)=0$,

2. furthermore, the head $\phi^{t,m+1}_{i+1,j,k}$, which is the head in row 2, is approximated by $\phi^{t,m}_{i+1,j,k}$, which is the head in row 2 calculated at the previous iteration: this means that $CC_{i+1/2,j,k}\left(\phi^{t,m+1}_{i+1,j,k}-\phi^{t,m}_{i+1,j,k}\right)=0$.

As such, equation 9.46 can be rewritten:

$$
\begin{aligned}
&CV_{i,j,k-1/2}(\tilde{\phi}^{t,m+1}_{i,j,k-1}-\phi^{t,m}_{i,j,k-1})+CR_{i,j-1/2,k}(\tilde{\phi}^{t,m+1}_{i,j-1,k}-\phi^{t,m}_{i,j-1,k})\\
&+(-CV_{i,j,k-1/2}-CC_{i-1/2,j,k}-CR_{i,j-1/2,k}-CR_{i,j+1/2,k}-CC_{i+1/2,j,k}-CV_{i,j,k+1/2}\\
&+HCOF_{i,j,k})(\tilde{\phi}^{t,m+1}_{i,j,k}-\phi^{t,m}_{i,j,k})+CR_{i,j+1/2,k}(\tilde{\phi}^{t,m+1}_{i,j+1,k}-\phi^{t,m}_{i,j+1,k})
\end{aligned}
$$

$$+CV_{i,j,k+1/2}(\tilde{\phi}^{t,m+1}_{i,j,k+1} - \phi^{t,m}_{i,j,k+1}) = RHS_{i,j,k} - CV_{i,j,k-1/2}\phi^{t,m}_{i,j,k-1}$$
$$-CC_{i-1/2,j,k}\phi^{t,m}_{i-1,j,k} - CR_{i,j-1/2,k}\phi^{t,m}_{i,j-1,k} - (-CV_{i,j,k-1/2} - CC_{i-1/2,j,k} - CR_{i,j-1/2,k}$$
$$-CR_{i,j+1/2,k} - CC_{i+1/2,j,k} - CV_{i,j,k+1/2} + HCOF_{i,j,k})\phi^{t,m}_{i,j,k}$$
$$-CR_{i,j+1/2,k}\phi^{t,m}_{i,j+1,k} - CC_{i+1/2,j,k}\phi^{t,m}_{i+1,j,k} - CV_{i,j,k+1/2}\phi^{t,m}_{i,j,k+1} \quad (9.47)$$

where:

- $\tilde{\phi}^{t,m+1}_{i,j,k} - \phi^{t,m}_{i,j,k}$=first estimate of the head change for element $[i,j,k]$ at iteration $m+1$. It is approximately equal to $\phi^{t,m+1}_{i,j,k} - \phi^{t,m}_{i,j,k}$.

The equations constitute a system of n simultaneous linear equations (where n is the number of elements in a row) in n unknowns. As in most groundwater problems n is relatively small, the system is solved directly by means of a Gauss-Jordan elimination. The result is a set of values of $\tilde{\phi}^{t,m+1}_{i,j,k} - \phi^{t,m}_{i,j,k}$ in slice 1. The value $\phi^{t,m+1}_{i,j,k}$ can be calculated by the equation:

$$\phi^{t,m+1}_{i,j,k} = \phi^{t,m}_{i,j,k} + \omega\left(\tilde{\phi}^{t,m+1}_{i,j,k} - \phi^{t,m}_{i,j,k}\right) \quad (9.48)$$

where:

- ω=is an acceleration parameter, usually between 1 and 2.

The rest of the slices are handled in a similar manner. Terms in equations for slice I which involve heads in slice $I+1$ use heads of the preceding iteration m. At the end of each iteration $m+1$, the maximum head change for the iteration is compared to the closure criterion. The iteration loop is terminated if the maximum head change is smaller than the closure criterion.

9.3 Micro-Fem

Micro-Fem[7] (Hemker & Elburg, 1988: version 2.0; Hemker & Nijsten, 1996: version 3.1) is a computer code for groundwater modelling in saturated multiple hydrogeologic systems (confined, leaky and unconfined). From version 2.50 on, also transient groundwater flow can be modelled. Micro-Fem can be applied for single density regional groundwater flow. Micro-Fem simulates two-dimensional horizontal flow in multiple layers using the finite element approach, and one-dimensional vertical flow between the layers using a finite difference technique. It handles multiple time-varying sources and sinks, as well as spatially and temporally varying boundary conditions, including connected and unconnected streams, drains, and evapotranspiration linearly varying with depth to ground water. Micro-Fem can simulate drains, streams, evapotranspiration, heterogeneous aquifers and aquitards, and anisotropy.

The software supports mesh generation, input preparation, model computation, graphic postprocessing and plotting of results. The code, version 3.1 [Scientific Software Group, 1996]. is able to solve sixteen hydrogeologic systems (aquifers or sublayers). The domain

[7]Not public domain, thus quite expensive: complete version 3.1 US$ 2330 (march 1997). University discount is possible: a reduced-problem size, operational demonstration version is available.

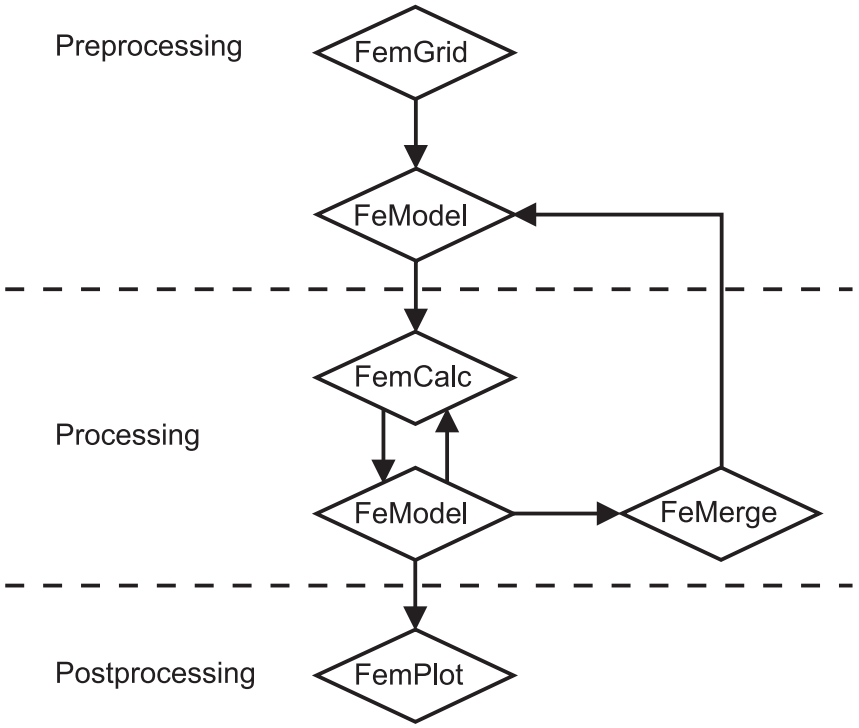

Figure 9.12: *Overview of the programmes which accompanies the Micro-Fem code, version 2.0*

is subdivided into triangular elements, interconnected through nodes (version 2.0: 3000 nodes, 6000 elements; version 3: 4000 nodes per aquifer for the 640 kB RAM version and 12,500 nodes for the Extended Memory RAM version). Waterbalances can be presented for each aquifer or subarea.

The code is based on the finite element method ('Fem') for calculating heads. Micro-Fem consists of a pre- and postprocessor for easy data handling. Its capacity, ease-of-use, and flexibility in representing complex field geometry has made Micro-Fem a widely used ground-water flow modelling package in the Netherlands. Figure 9.12 gives an overview of the programmes of the Micro-Fem code version 2.0:

- FemGrid
  to generate a triangular mesh for irregular geometries.
- FemCalc
  to calculate nodal heads and internal and external fluxes.
- FeModel
  -preprocessor: to modify the grid, to specify and to change aquifer and aquitard parameters, discharges and extractions and boundary conditions, and to provide a graphical representation of entered data.
  -postprocessor: to observe, to analyse, to present and to interpret model results, such as contour lines of heads, travel times.

- FemPlot
  to plot (hardcopy) the grid mesh, the distribution of heads, aquifer and aquitard model properties, flowlines and travel times.

- FeMerge
  to compile a new model based on an existing model and new mesh data.

- FemMesh (optional)
  to generate a grid for complex grids requiring gradually changing node-spacing to accomplish high contrasts in spacing.

- FemCat (optional)
  to calculate transient flow including display of time series of heads for selected nodes.

- FemPath (optional)
  to generate three-dimensional particle tracking with display of individual flow lines or a series of evenly distributed flow lines in two or three dimensions.

- FemInvs (optional)
  to automatically calibrate steady state Micro-Fem models with horizontal flow in up to 16 layers (based among others on nonlinear regression).

In version 2.50 (1995) and 3 (1996) of Micro-Fem, a few new programmes have been implemented: FemCat calculates transient situations, FemInvs automatically calibrates steady state Micro-Fem models, and F3Model traces three-dimensional flowlines.

During the computer workshop, the programmes FemGrid, FeModel and FemCalc will be used to examine the groundwater system, whereas FemPlot will be used for hardcopy output. Because the generation of the mesh, the input of parameters and boundary conditions, etc., is rather laborious, the regional model has already been completed during the computer workshop.

A few remarks on Micro-Fem

- The use of triangular -as compared to rectangular- elements has the advantage of an easy adaptation to the shape of the boundaries. Also the course of a river, the locations of wells or areas with fixed head can easily be taken into consideration.

- To each element individual parameters can be allocated, such as transmissivity and hydraulic resistance. The heads are defined at the nodes, the heads in an element are described by a linear interpolation function. The flow across the side of an element is allocated equally to the nodes to which it is connected. In case of vertical flow, the recharge or discharge is distributed over the nodes by a polygon through the centre of the triangle, as shown in figure 7.6.

- As far as boundary conditions are concerned, there are two possibilities: (1) a *fixed head boundary*: the program calculates the horizontal flow across the boundary of the node; and (2) a *no-flow boundary*, e.g. a water divide: the program calculates the head in the node.

- Rivers and canals can be introduced in the program, by allocating a fixed head to the nodal points. The relation with the underlying aquifer can be defined using a hydraulic entrance resistance. The in- or outflow is calculated from the difference in head between river and aquifer and the hydraulic resistance of the river bed.

9.4 MOC3D

The three-dimensional computer code MOC3D [Konikow *et al.*, 1996] is developed by the U.S. Geological Survey. The groundwater flow equation is solved by the MODFLOW module of MOC3D. The advection-dispersion equation is solved by the MOC module, using the method of characteristics. Advective transport of solutes is modelled by means of particle tracking and dispersive transport by means of the finite difference method. An advantage of applying the method of characteristics is that the condition of spatial discretisation is not strict (section 8.1).

Characteristics of MOC3D

MOC3D (in total some 15000 FORTRAN lines including remarks) consists of two robust modules which are fully integrated with each other. First, it comprises a solute transport module, here called the MOC module[8], to simulate ordinary solute transport. Second, it comprises a groundwater flow module, here called the MODFLOW module[9], to compute transient groundwater flow. Some characteristics of MOC3D are:

- the code takes into account hydrodynamic dispersion (molecular diffusion as well as mechanical dispersion) and chemical reactions such as adsorption (by means of a retardation factor) and radioactive decay,

- solute transport is modelled through splitting up the advection-dispersion equation into two components: (a) an advective component which is solved by means of a particle tracking technique (the so-called Method Of Characteristics: MOC), and (b) a dispersive component which is solved by the finite difference method. Due to the splitting up, numerical dispersion can be kept within bounds, even if coarse elements and small longitudinal dispersivities are used (see section 8.3, page 128). As such, numerical problems don't occur when elements are measured e.g. 250*250*10 m in combination with a longitudinal dispersivity of α_L=1 m. Especially in this characteristic MOC3D differs from codes which solve the partial differential equations with the standard finite element or finite difference methods. With these methods, severe numerical implications can occur when the spatial discretisation condition is not met. This spatial discretisation condition is characterized by the so-called grid-Peclet-number [Frind & Pinder, 1982; Daus *et al.*, 1985; Kinzelbach, 1987a and 1987b; Oude Essink & Boekelman, 1996].

[8]MOC3D [Konikow, Goode & Hornberger, 1996], version 1.1 of May 1997, is the 3D successor of MOC [Konikow & Bredehoeft, 1978].

[9]The MODFLOW module is just MODFLOW-96 [McDonald & Harbaugh, 1988; Harbaugh & McDonald, 1996], version 3.0 of December 1996, but now fully integrated in MOC3D.

- the variation of the pore volume of the elements should be relative small, as otherwise the demand of mass conservation of solute is violated too much. This numerical characteristic is related to the particle tracking technique; as a matter of fact, the 3D solute transport code MT3D [Zheng, 1990] suffers the same problem. The applied version of MOC3D uses a uniform grid.

- though numerical dispersion is limited, deviations in the mass balance of solute transport still occur. A substantial difference between the initial mass (in the appearance of the concentration distribution) and the mass after a large number of particle displacements can arise, in particular when discretisation of the elements is coarse or when time steps are large.

9.5 MOC, (2D) adapted for density differences

The original two-dimensional computer code MOC (Method Of Characteristics), which was developed in 1978 by Konikow & Bredehoeft for the United States Geological Survey, is a widely applied and widely accepted groundwater flow code throughout the world. The adaptation implies that the variations in fluid density now affect the velocity distribution. In order to obtain the adapted MOC code from the original MOC code, small adjustments due to density differences have been accomplished. As a consequence, the code is capable to simulate density dependent two-dimensional groundwater flow with solute transport.

As MOC applies the method of characteristics to solve advection through a particle tracking procedure, numerical dispersion is suppressed considerably. This property makes the adapted MOC code a very suitable groundwater flow code for simulating groundwater flow systems with Holocene and Pleistocene deposits of marine and fluviatile origin such as occur along the Dutch coast.

Note that a computer code similar to the adapted MOC code came on the market in 1985: MOCDENSE [Sanford & Konikow, 1985]. It is a modified version of the original MOC code. Whereas the original and the adapted MOC code are still based on (freshwater) heads, MOCDENSE is based on pressures. Although MOCDENSE was removed from the software-list of the IGWMC (International Ground Water Modeling Center) for a few years because of (small) errors in the computer code, it is gaining ground again. It is now beginning to enjoy a good reputation with respect to other solute transport codes such as SUTRA [Voss, 1984].

History

Originally, MOC was only applied as a horizontal two-dimensional groundwater flow code. It appeared that the code could easily be adapted in order to model groundwater flow systems with non-uniform density distributions. In August 1981, Lebbe [1983] was the first to adapt MOC for vertical groundwater flow and density differences. In 1986, van der Eem and Peters also adapted MOC for density differences. In March 1990, Oude Essink adapted the updated version 3.0 of MOC [1989]. He used documentation of Lebbe [1981, 1983] and van der Eem [1987].

9.5.1 Theoretical background of the groundwater flow equation

This paragraph comprises the fundamentals of the numerical algorithm to represent two-dimensional density dependent groundwater flow. The equation of motion is already described in subsection 6.1 (equation 6.14, page 71):

$$q_x = -\frac{\kappa_x}{\mu_i}\frac{\partial p}{\partial x} \qquad q_z = -\frac{\kappa_z}{\mu_i}(\frac{\partial p}{\partial z} + \gamma) \tag{9.49}$$

where γ=$\rho_i g$=the specific weight ($M\,L^{-2}\,T^{-2}$). The relation between the pressure and the so-called, *fictive*, *freshwater head* is as follows (if the atmospheric pressure equals zero):

$$\phi_f = \frac{p}{\rho_f g} + z \tag{9.50}$$

where

- ϕ_f = *fictive* freshwater head (L),
- $\frac{p}{\rho_f g}$ = pressure head, expressed in fresh water (L),
- ρ_f = density of fresh groundwater ($M\,L^{-3}$),
- z = elevation with respect to the reference level (L).

The horizontal and vertical hydraulic conductivities of fresh groundwater are defined as follows (see also equation 6.17):

$$k_x = \frac{\kappa_x \rho_f g}{\mu_f} \qquad k_z = \frac{\kappa_z \rho_f g}{\mu_f} \qquad (L\,T^{-1}) \tag{9.51}$$

The density distribution in the deep groundwater flow systems is assumed to be *non-uniform* and varies with depth. As the density ρ_i (γ in equation 9.49) varies with position, effects of density difference have to be considered. Henceforth, the Darcian specific discharge in vertical direction takes into account density differences. Inserting equation 9.50 into equation 9.49 gives:

$$q_x = -\frac{\kappa_x \rho_f g}{\mu_i}\frac{\partial \phi_f}{\partial x} \qquad q_z = -\frac{\kappa_z \rho_f g}{\mu_i}\left(\frac{\partial \phi_f}{\partial z} - 1 + \frac{\rho_i}{\rho_f}\right) \tag{9.52}$$

As the density varies with position, the intrinsic permeabilities κ_x, κ_z and the dynamic viscosity μ should be applied instead of the hydraulic conductivities k_x or k_z. However, small viscosity differences may be disregarded in case density differences are taken into account in groundwater problems in vertical profiles [Bear & Verruijt, 1987]. As such, the factor μ_f/μ_i, which is close to 1, is ignored in the development of the adapted MOC code from this point on, also because of the lack of accuracy by which the horizontal and vertical hydraulic conductivities are determined. Making use of equation 9.51, equation 9.52 becomes:

$$q_x = -k_x\frac{\partial \phi_f}{\partial x} \qquad q_z = -k_z\left(\frac{\partial \phi_f}{\partial z} + \Upsilon\right) \tag{9.53}$$

where $\Upsilon = (\rho_i - \rho_f)/\rho_f$ is the relative density difference, the so-called *buoyancy*[10] $(-)$. As can be seen, the vertical Darcian specific discharge has an *extra term* in comparison with groundwater flow with a uniform density: this term is called the *vertical density gradient velocity*.

Rewriting equation 6.28 gives the equation of continuity for density dependent groundwater flow in two-dimensions:

$$-\left[\frac{\partial q_x}{\partial x} + \frac{\partial q_z}{\partial z}\right] = S_s \frac{\partial \phi_f}{\partial t} + \frac{W'(x,z,t)}{\rho_i} \tag{9.54}$$

Through combining the equations 9.53 and 9.54, and multiplying the obtained equation by the thickness of the aquifer b, the *groundwater flow equation* can be defined:

$$\frac{\partial (T_{xx} \frac{\partial \phi_f}{\partial x})}{\partial x} + \frac{\partial (T_{zz} \frac{\partial \phi_f}{\partial z})}{\partial z} + \frac{\partial (T_{zz} \Upsilon)}{\partial z} = S \frac{\partial \phi_f}{\partial t} + W(x,z,t) \tag{9.55}$$

where

- $T_{xx}, T_{zz} = k_x b, k_z b =$ respectively horizontal and vertical transmissivities in the principal x and z-directions $(L^2\,T^{-1})$,
- $W(x,z,t) = (W'(x,z,t) \cdot b)/\rho_i =$ volume flux per unit area (positive sign for outflow, e.g. well pumpage or groundwater extraction; negative for inflow, e.g. well injection and natural groundwater recharge) $(L\,T^{-1})$.

Numerical algorithm

To solve the groundwater flow equation numerically, the derivatives are replaced in the finite difference approximation by values of the difference quotients of the function in separate discrete points, using Taylor series, see the equations 7.75 to 7.77, page 106. In addition, Υ is discretised as follows, see figure 9.13:

$$\Upsilon_{(i,j)} = \frac{\frac{\rho_{(i,j)} + \rho_{(i,j+1)}}{2} - \rho_f}{\rho_f} \tag{9.56}$$

where $\rho_{(i,j)}$ and $\rho_{(i,j+1)}$ are the densities of groundwater in respectively the elements $[i,j]$ and $[i,j+1]$. The Darcian specific discharges at the boundary of the element $[i,j]$, the so-called *boundary velocities* are given by the explicit finite difference formulations (see figure 9.13):

$$q^k_{x(i+1/2,j)} = k_{x(i+1/2,j)} \frac{\phi^k_{f(i,j)} - \phi^k_{f(i+1,j)}}{\Delta x} \tag{9.57}$$

and

$$q^k_{z(i,j+1/2)} = k_{z(i,j+1/2)} \left(\frac{\phi^k_{f(i,j)} - \phi^k_{f(i,j+1)}}{\Delta z} + \Upsilon_{(i,j)} \right) \tag{9.58}$$

where

[10] Dutch: 'drijfvermogen'.

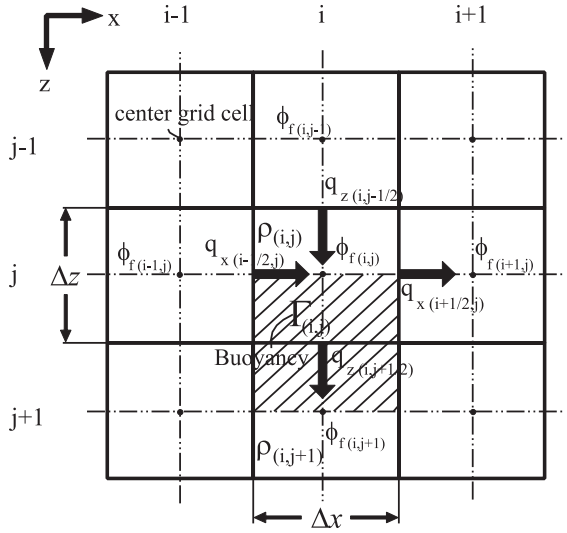

Figure 9.13: *Nodal array for development of finite difference expressions. The buoyancy of the vertical velocity $q_{z(i,j+1/2)}$ is determined over the hatched area.*

- $q^k_{x(i+1/2,j)}$ = boundary velocity in the x-direction at the k-moment in time on the boundary between the nodes $[i,j]$ and $[i+1,j]$ $(L\,T^{-1})$,
- $q^k_{z(i,j+1/2)}$ = boundary velocity in the z-direction at the k-moment in time on the boundary between the nodes $[i,j]$ and $[i,j+1]$ $(L\,T^{-1})$,
- $k_{x(i+1/2,j)}, k_{z(i,j+1/2)}$ = *weighted harmonic mean* of the hydraulic conductivity in respectively the x and z-direction:

$$k_{x(i+1/2,j)} = \frac{2k_{x(i+1,j)}k_{x(i,j)}}{k_{x(i+1,j)} + k_{x(i,j)}}, \qquad k_{z(i,j+1/2)} = \frac{2k_{z(i,j+1)}k_{z(i,j)}}{k_{z(i,j+1)} + k_{z(i,j)}} \tag{9.59}$$

Writing out equation 9.55 in terms of finite difference approximations (and applying equation 7.77) yields:

$$\begin{aligned} \tfrac{\partial}{\partial x}\left(T_{xx}\tfrac{\partial \phi_f}{\partial x}\right)^k_{(i,j)} + \tfrac{\partial}{\partial z}\left(T_{zz}\tfrac{\partial \phi_f}{\partial z}\right)^k_{(i,j)} + \tfrac{\partial}{\partial z}(T_{zz}\Upsilon)^k_{(i,j)} = \\ S\left[\tfrac{\phi^k_{f(i,j)} - \phi^{k-1}_{f(i,j)}}{\Delta t}\right] + W^k_{(i,j)} \end{aligned} \tag{9.60}$$

To solve equation 9.60, the first term in the x-direction should be rewritten:

$$\frac{\partial}{\partial x}\left(T_{xx}\frac{\partial \phi_f}{\partial x}\right)^k_{(i,j)} = T_{xx(i,j)}\frac{\partial^2 \phi_f}{\partial x^2} + \frac{\partial T_{xx(i,j)}}{\partial x}\frac{\partial \phi_f}{\partial x} \tag{9.61}$$

or, by applying the equations 7.75 and 7.76, after rearranging:

$$\begin{aligned} \tfrac{\partial}{\partial x}\left(T_{xx}\tfrac{\partial \phi_f}{\partial x}\right)^k_{(i,j)} = \left[\tfrac{T_{xx(i,j)}}{(\Delta x)^2} - \tfrac{1}{2\Delta x}\tfrac{\partial T_{xx(i,j)}}{\partial x}\right][\phi^k_{f(i-1,j)} - \phi^k_{f(i,j)}] \\ + \left[\tfrac{T_{xx(i,j)}}{(\Delta x)^2} + \tfrac{1}{2\Delta x}\tfrac{\partial T_{xx(i,j)}}{\partial x}\right][\phi^k_{f(i+1,j)} - \phi^k_{f(i,j)}] \end{aligned} \tag{9.62}$$

The expressions of the Taylor series in the form $(-\frac{1}{6}\Delta x^2\frac{\partial^3\phi_f}{\partial x^3})$, $(-\frac{1}{12}\Delta x^2\frac{\partial^4\phi_f}{\partial x^4})$, etc., are neglected. Similarly, the same procedure can be followed for the z-direction.

The transmissivity midway between $[i,j]$ and $[i-1,j]$ in the x-direction is given by the Taylor series:

$$T_{xx(i,j)} = T_{xx(i-1/2,j)} + \frac{\Delta x}{2}\frac{\partial T_{xx(i,j)}}{\partial x} - \frac{(\Delta x^2)}{8}\frac{\partial^2 T_{xx(i,j)}}{\partial x^2} + \ldots \tag{9.63}$$

and similarly

$$T_{xx(i,j)} = T_{xx(i+1/2,j)} - \frac{\Delta x}{2}\frac{\partial T_{xx(i,j)}}{\partial x} - \frac{(\Delta x^2)}{8}\frac{\partial^2 T_{xx(i,j)}}{\partial x^2} + \ldots \tag{9.64}$$

Substituting the equations 9.63 and 9.64 into equation 9.62, the finite difference approximation in the x-direction becomes[11]:

$$\begin{gathered}\frac{\partial}{\partial x}\left(T_{xx}\frac{\partial\phi_f}{\partial x}\right)^k_{(i,j)} = \\ \left[\frac{1}{(\Delta x)^2}\left(T_{xx(i-1/2,j)} + \frac{\Delta x}{2}\frac{\partial T_{xx(i,j)}}{\partial x}\right) - \frac{1}{2\Delta x}\frac{\partial T_{xx(i,j)}}{\partial x}\right][\phi^k_{f(i-1,j)} - \phi^k_{f(i,j)}] \\ + \left[\frac{1}{(\Delta x)^2}\left(T_{xx(i+1/2,j)} - \frac{\Delta x}{2}\frac{\partial T_{xx(i,j)}}{\partial x}\right) + \frac{1}{2\Delta x}\frac{\partial T_{xx(i,j)}}{\partial x}\right][\phi^k_{f(i+1,j)} - \phi^k_{f(i,j)}]\end{gathered} \tag{9.65}$$

or

$$\begin{gathered}\frac{\partial}{\partial x}\left(T_{xx}\frac{\partial\phi_f}{\partial x}\right)^k_{(i,j)} = \\ T_{xx(i-1/2,j)}\left(\frac{\phi^k_{f(i-1,j)} - \phi^k_{f(i,j)}}{(\Delta x)^2}\right) + T_{xx(i+1/2,j)}\left(\frac{\phi^k_{f(i+1,j)} - \phi^k_{f(i,j)}}{(\Delta x)^2}\right)\end{gathered} \tag{9.66}$$

To obtain the final finite difference approximation for the groundwater flow equation, the equation 9.66 and a similar equation for the situation in the z-direction are substituted into equation 9.60:

$$\begin{gathered}T_{xx(i-1/2,j)}\left(\frac{\phi^k_{f(i-1,j)} - \phi^k_{f(i,j)}}{(\Delta x)^2}\right) + T_{xx(i+1/2,j)}\left(\frac{\phi^k_{f(i+1,j)} - \phi^k_{f(i,j)}}{(\Delta x)^2}\right) \\ + T_{zz(i,j-1/2)}\left(\frac{\phi^k_{f(i,j-1)} - \phi^k_{f(i,j)}}{(\Delta z)^2} + \frac{\Upsilon_{(i,j-1)}}{\Delta z}\right) + T_{zz(i,j+1/2)}\left(\frac{\phi^k_{f(i,j+1)} - \phi^k_{f(i,j)}}{(\Delta z)^2} - \frac{\Upsilon_{(i,j)}}{\Delta z}\right) = \\ S\left[\frac{\phi^k_{f(i,j)} - \phi^{k-1}_{f(i,j)}}{\Delta t}\right] + W^k_{(i,j)}\end{gathered} \tag{9.67}$$

Alternating-direction implicit procedure

The iterative Alternating-Direction Implicit procedure (ADI)[12] is applied to solve the equations. This (backward difference in time) technique is unconditionally stable, and thus,

[11] Note that the Taylor series in the equations 9.63 and 9.64 have been truncated after the second term, so that expressions of the form $\frac{(\Delta x)^2}{8}\frac{\partial^2 T_{xx(i,j)}}{\partial x^2}$ have been neglected [Pinder and Bredehoeft, 1968].

[12] This procedure has intensively been used by the petroleum industry for predicting oil and gas reservoir behaviour.

there are no stability restrictions on the length of Δt as in an explicit (forward difference in time) technique [Pinder & Bredehoeft, 1968].

The piezometric heads ϕ_f in equation 9.67 are unknown in only one coordinate direction, the known piezometric heads are calculated at the time level k. During one complete cycle of $2N$ calculations, the entire matrix is solved twice, using the two equations 9.68 and 9.69:

column: implicit in $z-$direction, explicit in $x-$direction

$$\begin{aligned}
&\tfrac{T_{xx(i-1/2,j)}}{(\Delta x)^2}\left(\phi^{k-1}_{f(i-1,j)}-\phi^{k-1}_{f(i,j)}\right)+\tfrac{T_{xx(i+1/2,j)}}{(\Delta x)^2}\left(\phi^{k-1}_{f(i+1,j)}-\phi^{k-1}_{f(i,j)}\right)\\
&+\tfrac{T_{zz(i,j-1/2)}}{(\Delta z)^2}\left(\phi^{k}_{f(i,j-1)}-\phi^{k}_{f(i,j)}+\Upsilon_{(i,j-1)}\Delta z\right)\\
&+\tfrac{T_{zz(i,j+1/2)}}{(\Delta z)^2}\left(\phi^{k}_{f(i,j+1)}-\phi^{k}_{f(i,j)}-\Upsilon_{(i,j)}\Delta z\right)=\\
&S\left[\tfrac{\phi^{k}_{f(i,j)}-\phi^{k-1}_{f(i,j)}}{\Delta t}\right]+W^{k}_{(i,j)}
\end{aligned}\tag{9.68}$$

and

row: implicit in $x-$direction, explicit in $z-$direction

$$\begin{aligned}
&\tfrac{T_{xx(i-1/2,j)}}{(\Delta x)^2}\left(\phi^{k}_{f(i-1,j)}-\phi^{k}_{f(i,j)}\right)+\tfrac{T_{xx(i+1/2,j)}}{(\Delta x)^2}\left(\phi^{k}_{f(i+1,j)}-\phi^{k}_{f(i,j)}\right)\\
&+\tfrac{T_{zz(i,j-1/2)}}{(\Delta z)^2}\left(\phi^{k}_{f(i,j-1)}-\phi^{k}_{f(i,j)}+\Upsilon_{(i,j-1)}\Delta z\right)\\
&+\tfrac{T_{zz(i,j+1/2)}}{(\Delta z)^2}\left(\phi^{k}_{f(i,j+1)}-\phi^{k}_{f(i,j)}-\Upsilon_{(i,j)}\Delta z\right)=\\
&S\left[\tfrac{\phi^{k}_{f(i,j)}-\phi^{k-1}_{f(i,j)}}{\Delta t}\right]+W^{k}_{(i,j)}
\end{aligned}\tag{9.69}$$

The technique first calculates values by sweeping the matrix column by column (using equation 9.68), and then recalculates the matrix by sweeping row by row (using equation 9.69). For example, rewriting equation 9.68, the finite difference expression for any column gives:

column

$$\begin{aligned}
&\tfrac{T_{zz(i,j-1/2)}}{(\Delta z)^2}\phi^{k}_{f(i,j-1)}-[\tfrac{T_{zz(i,j+1/2)}}{(\Delta z)^2}+\tfrac{T_{zz(i,j-1/2)}}{(\Delta z)^2}+\tfrac{S}{\Delta t}]\phi^{k}_{f(i,j)}+\tfrac{T_{zz(i,j+1/2)}}{(\Delta z)^2}\phi^{k}_{f(i,j+1)}=\\
&-\tfrac{T_{xx(i-1/2,j)}}{(\Delta x)^2}\phi^{k-1}_{f(i-1,j)}+[\tfrac{T_{xx(i-1/2,j)}}{(\Delta x)^2}+\tfrac{T_{xx(i+1/2,j)}}{(\Delta x)^2}-\tfrac{S}{\Delta t}]\phi^{k-1}_{f(i,j)}-\tfrac{T_{xx(i+1/2,j)}}{(\Delta x)^2}\phi^{k-1}_{f(i+1,j)}\\
&-\tfrac{T_{zz(i,j-1/2)}}{\Delta z}\Upsilon_{(i,j-1)}+\tfrac{T_{zz(i,j+1/2)}}{\Delta z}\Upsilon_{(i,j)}+W_{(i,j)}(x,z,t)
\end{aligned}\tag{9.70}$$

Analogous expressions for these equations are of the form:

$$\begin{aligned}
B_1\phi_{f,1}+C_1\phi_{f,2} &= D_1 \\
A_j\phi_{f,j-1}+B_j\phi_{f,j}+C_j\phi_{f,j+1} &= D_j, \qquad \text{for } \; 2\le j\le \eta-1, \\
A_\eta\phi_{f,\eta-1}+B_\eta\phi_{f,\eta} &= D_\eta
\end{aligned}\tag{9.71}$$

where

- η is the length of the row or column under consideration,
- A_j, B_j and C_j are the coefficients of the unknown piezometric head values. A_j stands for the term that belongs to $\phi^{k}_{f(i,j-1)}$ in equation 9.70, B_j to $\phi^{k}_{f(i,j)}$ and C_j to $\phi^{k}_{f(i,j+1)}$.

- D_j is the sum of all known parameters, namely all terms on the right hand side of equation 9.70.

This matrix is solved by means of the Thomas algorithm, see section 7.3, page 102. The following *dummy variables*[13] w_j $(T^{-1})$and g_j (L) are defined:

$$\begin{aligned} w_j &= B_j - \frac{A_j C_{j-1}}{w_{j-1}} \\ g_j &= \frac{D_j - A_j g_{j-1}}{w_j} \end{aligned} \tag{9.72}$$

When the last node in the row or column is reached, the piezometric head is calculated in order of decreasing j as follows:

$$\begin{aligned} \phi_{f,j} &= g_j - \frac{C_j \phi_{f,j+1}}{w_j}; \\ \text{if} \quad j = \eta \quad &\text{then} \quad \phi_{f,j} = g_j \end{aligned} \tag{9.73}$$

To take into account the boundary conditions, some small adjustments must be executed. For example, if the edge is a *barrier boundary*, the reflection technique is employed: $\phi_{f,j-1} = \phi_{f,j+1}$ and $A_1 = C_1$.

9.5.2 Theoretical background of the solute transport equation

The applied two-dimensional advection-dispersion equation for solute transport in homogeneous isotropic porous media is similar to equation 6.68, page 87. Already since August 1985 (and modified again for more intensive chemical reactions by Goode & Konikow in 1989), MOC is suited to simulate non-conservative solute transport in saturated groundwater flow systems. The solution technique of the advection-dispersion equation in the adapted version of MOC does not differ from the solution technique in the original version. The solution technique, based on the method of characteristics, is summarized in section 7.8.

The advection-dispersion equation used in Konikow and Bredehoeft [1978] is as follows (somewhat simplified):

$$\frac{\partial C}{\partial t} = \frac{\partial}{\partial x_i}\left(D_{ij}\frac{\partial C}{\partial x_j}\right) - V_i\frac{\partial C}{\partial x_i} + \frac{(C - C')W}{n_e\, b} \tag{9.74}$$

where

- b= saturated thickness of the aquifer (L),
- W= volume flux per unit area (LT^{-1}).

[13] In MOC, additional terms are appended in the dummy variables. These terms represent iteration parameters, as the *iterative* version of the Alternating-Direction Implicit procedure *ADI* is applied. Iteration parameters are applied to compute rapidly the acceptable freshwater head ϕ_f. The determination of the iteration parameters is not discussed here. See for more information Trescott, Pinder & Larson [1976].

The changes in concentration caused by hydrodynamic dispersion, and fluid sources and sinks are solved by an explicit finite-difference approximation of equation 7.87:

$$\Delta C_{i,j}^{k} = \Delta t_s \left[\frac{\partial}{\partial x_i} \left(D_{ij} \frac{\partial C}{\partial x_j} \right) + \frac{(C - C')W}{n_e\, b} \right] \tag{9.75}$$

or

$$\Delta C_{i,j}^{k} = (\Delta C_{i,j}^{k})_I + (\Delta C_{i,j}^{k})_{II} \tag{9.76}$$

where

- $(\Delta C_{i,j}^{k})_I$ = change in concentration by hydrodynamic dispersion,
- $(\Delta C_{i,j}^{k})_{II}$ = change in concentration by sources and sinks.

As computation of the concentration gradient for a large number of particles appears to be laborious, equation 9.76 is solved in MOC at each node of the grid rather than directly at the location of each particle. The first right hand term in equation 9.76 can be rewritten as follows:

$$(\Delta C_{i,j}^{k})_I = \Delta t_s \left[\frac{\partial}{\partial x}(D_{xx}\frac{\partial C}{\partial x} + D_{xz}\frac{\partial C}{\partial z}) + \frac{\partial}{\partial z}(D_{zz}\frac{\partial C}{\partial z} + D_{zx}\frac{\partial C}{\partial x}) \right] \tag{9.77}$$

Substitution of spatial derivatives of the concentration gives an explicit finite-difference approximation. The second right hand term in equation 9.76 can also be rewritten by an explicit finite-difference approximation:

$$(\Delta C_{i,j}^{k})_{II} = \frac{\Delta t_s}{n_e\, b_{i,j}^{k}} \left[W_{i,j}^{k} (C_{i,j}^{k-1} - C'^{\,k}_{i,j}) \right] \tag{9.78}$$

The change in concentration is the sum of the following terms:

$$C_{i,j}^{k} = C_{i,j}^{k^*} + \Delta C_{i,j}^{k} \tag{9.79}$$

where

- $C_{i,j}^{k}$ = new nodal concentration at the end of time level k $(M\,L^{-3})$,
- $C_{i,j}^{k^*}$ = average of the concentration of all particles in cell $[i,j]$ for time level k after only advective transport $(M\,L^{-3})$,
- $\Delta C_{i,j}^{k}$ = change in concentration caused by hydrodynamic dispersion (dispersion term), sources and sinks $(M\,L^{-3})$.

The procedure to solve the advection-dispersion equation is as follows:

1. first, the concentration gradients at the previous time level $(k-1)$ are determined at each node,
2. second, based on equation 7.89 in the lecture notes, the particles are advected to new positions for time level k^*, which is a new time level k prior to the adjustments for concentration for dispersion and mixing (sources and sinks). The time index is distinguished with an asterisk $*$, because this temporarily assigned average concentration represents the new time level only with respect to advective transport,

3. after all particles have been moved, the concentration at each node is temporarily assigned the average of the concentration $C_{i,j}^{k^*}$ of all particles which are at that moment located within the area of that specific grid cell,

4. at the new positions of the particles, the concentration gradients are computed again at each node from concentrations at the time level k^*,

5. finally, since the concentration gradients are continuously changing with time, e.g. from the $k-1$ to the k time level, a two-step explicit procedure is applied to adjust the concentration distribution at each node: thus first based on concentration gradients at $k-1$, and second based on concentration gradients at k^*. Thus, the change in concentration due to dispersion and sources and sinks is determined by:

$$\begin{aligned}\Delta C_{i,j}^{k} &= 0.5\,\Delta t_s \left[\frac{\partial}{\partial x_i}(D_{ij}\frac{\partial C_{i,j}^{k-1}}{\partial x_j}) + \frac{W_{i,j}^{k-1}(C_{i,j}^{k-1}-C_{i,j}^{\prime\,k-1})}{bn_e}\right] \\ &\quad +0.5\,\Delta t_s \left[\frac{\partial}{\partial x_i}(D_{ij}\frac{\partial C_{i,j}^{k^*}}{\partial x_j}) + \frac{W_{i,j}^{k}(C_{i,j}^{k^*}-C_{i,j}^{\prime\,k})}{bn_e}\right] \end{aligned} \tag{9.80}$$

Stability criteria

A number of stability criteria determine the explicit numerical solution of the advection-dispersion equation in Konikow & Bredehoeft [1978]. These criteria may require that the flow time step Δt, applied to solve the groundwater flow equation, must be subdivided into a number of smaller solute time steps Δt_s to accurately solve the advection-dispersion equation. During such a solute time step, particles are moved to new positions. The distance over which a particle is moved is proportional to the length of that solute time step and the velocity at the location of that particle (see equation 7.89, page 113). The three stability criteria of the advection-dispersion equation, which must all three be satisfied in MOC, are:

1. The explicit solution of hydrodynamic part of the advection-dispersion equation 9.77 is stable, according to Redell and Sunada [1970] (see also section 8.1.1), if:

$$\frac{D_{xx}\Delta t_s}{(\Delta x)^2} + \frac{D_{zz}\Delta t_s}{(\Delta z)^2} \leq 0.5 \tag{9.81}$$

   This expression is called the Neumann-criterion. Solving equation 9.81 for Δt_s yields:

$$\Delta t_s \leq \min_{(\text{over grid})}\left[\frac{0.5}{\frac{D_{xx}}{(\Delta x)^2} + \frac{D_{zz}}{(\Delta z)^2}}\right] \tag{9.82}$$

   From equation 9.82 can be deduced that the maximum permissible time step in the simulation is the smallest Δt_s computed for any individual node in the entire grid. Thus, the smallest permissible time step Δt_s for solving the advection-dispersion equation occurs in the node that has the greatest value of $\frac{D_{xx}}{(\Delta x)^2} + \frac{D_{zz}}{(\Delta z)^2}$.

2. Consider the mixing of groundwater of one concentration $C_{i,j}$ with injected or recharged (surface) water of a different concentration $C'_{i,j}$. The change in concentration in that

specific source node is not allowed to exceed the difference between the concentration in the aquifer $C_{i,j}$ and the source concentration $C'_{i,j}$:

$$(\Delta C^k_{i,j})_{II} \leq C^{k-1}_{i,j} - C'^k_{i,j} \tag{9.83}$$

In combination with equation 9.78, equation 9.83 produces:

$$\Delta t_s \leq \min_{(\text{over grid})} \left[\frac{n_e \, b^k_{i,j}}{W^k_{i,j}} \right] \tag{9.84}$$

3. The last stability criterion for the maximum permissible time step Δt_s involves the particle movements to simulate advective transport. Equation 7.89 in the lecture notes shows that the distance a particle moves is a linear spatial extrapolation from one time level to the next. However, as the streamlines are curvilinear, an error is introduced into the numerical solution. In order to suppress the deviation of the particles from the streamline, the solute time step should be such that no critical distance is exceeded:

$$\begin{aligned} \Delta t_s V_{x\,[x^k_p, z^k_p]} &\leq \zeta \Delta x \\ \Delta t_s V_{z\,[x^k_p, z^k_p]} &\leq \zeta \Delta z \end{aligned} \tag{9.85}$$

where

- ζ = the maximum relative distance across a grid cell, in which a particle is allowed to move during one solute time step Δt_s. It is usually a fraction of the grid dimension ($0 < \zeta \leq 1$) in order to ensure that the particle movements are controlled within one solute time step.

Obviously, this criterion is based on the Courant number Co. Rewriting equation 9.85 gives:

$$\begin{aligned} \Delta t_s &\leq \frac{\zeta \Delta x}{(V_x)_{max}} \\ \Delta t_s &\leq \frac{\zeta \Delta z}{(V_z)_{max}} \end{aligned} \tag{9.86}$$

where

- $(V_x)_{max}, (V_z)_{max}$ = the maximum real velocity at a node or boundary of a grid cell respectively in the x and z-direction.

Finally, the smallest solute time step Δt_s is applied which is determined by the equations 9.82, 9.84 and 9.86. If the flow time step Δt is greater than the smallest solute time step Δt_s, then the flow time step Δt is subdivided into the appropriate number of smaller time steps Δt_s required to solve the advection-dispersion equation. It may occur that the stability criteria are not so strict that the smallest required solute time step Δt_s is greater than the flow time step Δt. Then, Δt_s must be equal to Δt.

Numerical dispersion

Numerical dispersion is caused by the numerical calculation process. Although the method of characteristics itself does not introduce numerical dispersion [Garder, Peaceman and Pozzi, 1964], solving the advection-dispersion equation generates numerical dispersion due to, among others, the movement and tracking of particles, the conversion from particles to elements and finite difference approximations. Examples of how numerical dispersion occurs in MOC are:

- solving the concentration gradient, e.g. $\frac{\partial C}{\partial x}$, by finite difference approximations. For example, the spatial derivatives of concentration in equation 7.87, $\frac{\partial}{\partial x_i} D_{ij} (\frac{\partial C}{\partial x_j})$, (representing the concentration by hydrodynamic dispersion) are approximated by the average (*weighted arithmetic mean*) of the concentration in adjacent elements,
- averaging the concentration $C_{i,j}^{k^*}$ in an element, based on all particles that are located within an element at the time level k^*,
- assigning concentrations at nodes of sources and sinks to the entire area of the element. Concentration variations within the area of the element are eliminated,
- eliminating concentration variations within individual elements. This occurs when too many grid cells have become void of particles (e.g. two percents of all participating elements). Then, a procedure (called GENPT) is executed that initiates again a uniform distribution of tracer particles throughout the entire grid. The procedure attempts to preserve an approximation of the previous concentration gradient within each element,
- calculating zero change in concentration due to advective transport (equation 7.89) at nodes which became void due to divergent flow, though the nodal concentration is still adjusted due to hydrodynamic dispersion, fluid sources and sinks (equation 7.87).

Some special problems associated with MOC, in particular moving and tracking of particles in the particle tracking procedure, are pictured only briefly here. See for further information Konikow & Bredehoeft [1978]. Some special aspects are:

- to prevent that groundwater or solute cross a no-flow boundary, particles have to be relocated within the aquifer by reflection across the boundary, see figure 9.14,
- in areas with fluid sources or sinks in grid cells, a special procedure is required to maintain a reasonably uniform and continuous spacing of particles,
- in order to maintain the total number of particles in the entire flow field at a nearly constant value, new particles have to be created at sources and old particles have to be removed at sinks or discharge boundaries.

Changes in the solute concentration of particles due to chemical reactions or physical processes may also cause problems in the particle tracking procedure. Finally, numerical dispersion also occurs in combination with numerical instabilities in the (vertical) velocity field due to, among others, density differences.

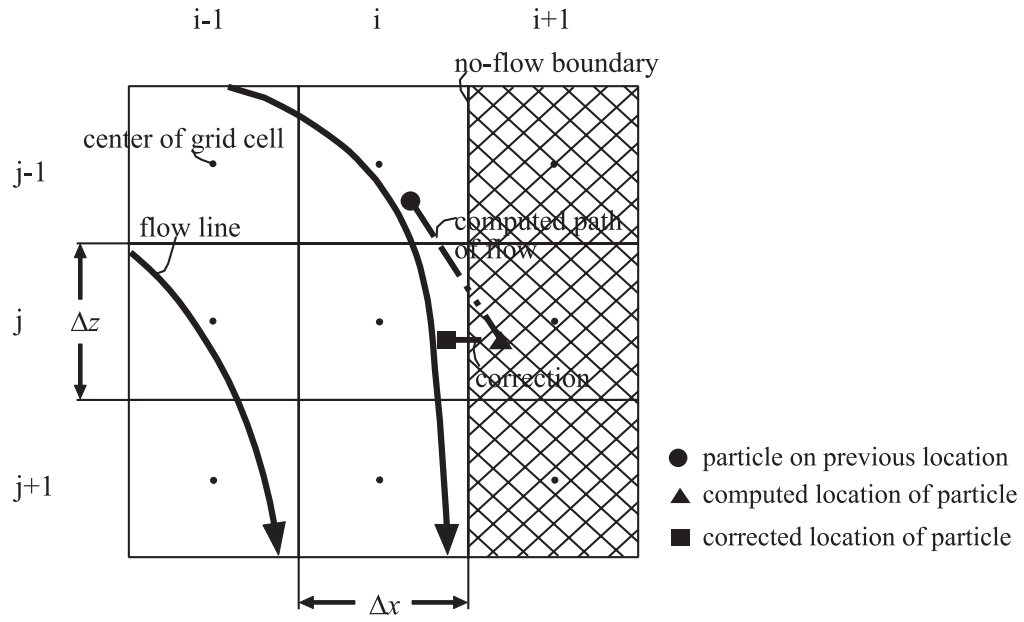

Figure 9.14: *Possible movements of particles near an impermeable (no-flow) boundary [after Konikow and Bredehoeft, 1978].*

Numerical instabilities in the velocity field

Numerical instabilities, which make the solution of the solute transport inaccurate, are caused by: (1) numerical approximations that already occur in the original MOC code; and (2) density flow that additionally arises in the adapted MOC code. The latter cause is discussed here (figure 9.15).

Numerical instabilities in the (vertical) velocity field can occur when particles from an element with a high solute concentration and thus a high density enter in an element with a low solute concentration. At the end of every flow time step, new solute concentrations and thus new densities are determined for both the elements. This may lead to abrupt differences in density between the two adjacent elements. Subsequently, the groundwater flow equation is solved again at the beginning of a new flow time step, and thus a new velocity field is calculated. The new vertical velocity field could have changed significantly, as it depends on the changed density distribution. Occasionally, the direction of the vertical velocity may even alter in some elements, at least if the initial vertical velocity was small. During that subsequent flow time step, the new computed velocity field may move particles in the opposite direction. This may, once again, lead to new abrupt changes in density of some adjacent elements, etc., and the velocity fluctuations in vertical direction can cause numerical instabilities. Under certain circumstances, these instabilities may get out of hand and could locally disturb the solute concentration to such an extent that the result of the simulation is not accurate anymore.

Numerical instabilities occur at those places where the densities in adjacent elements differ rapidly, for example at places where the transition zone between fresh and saline

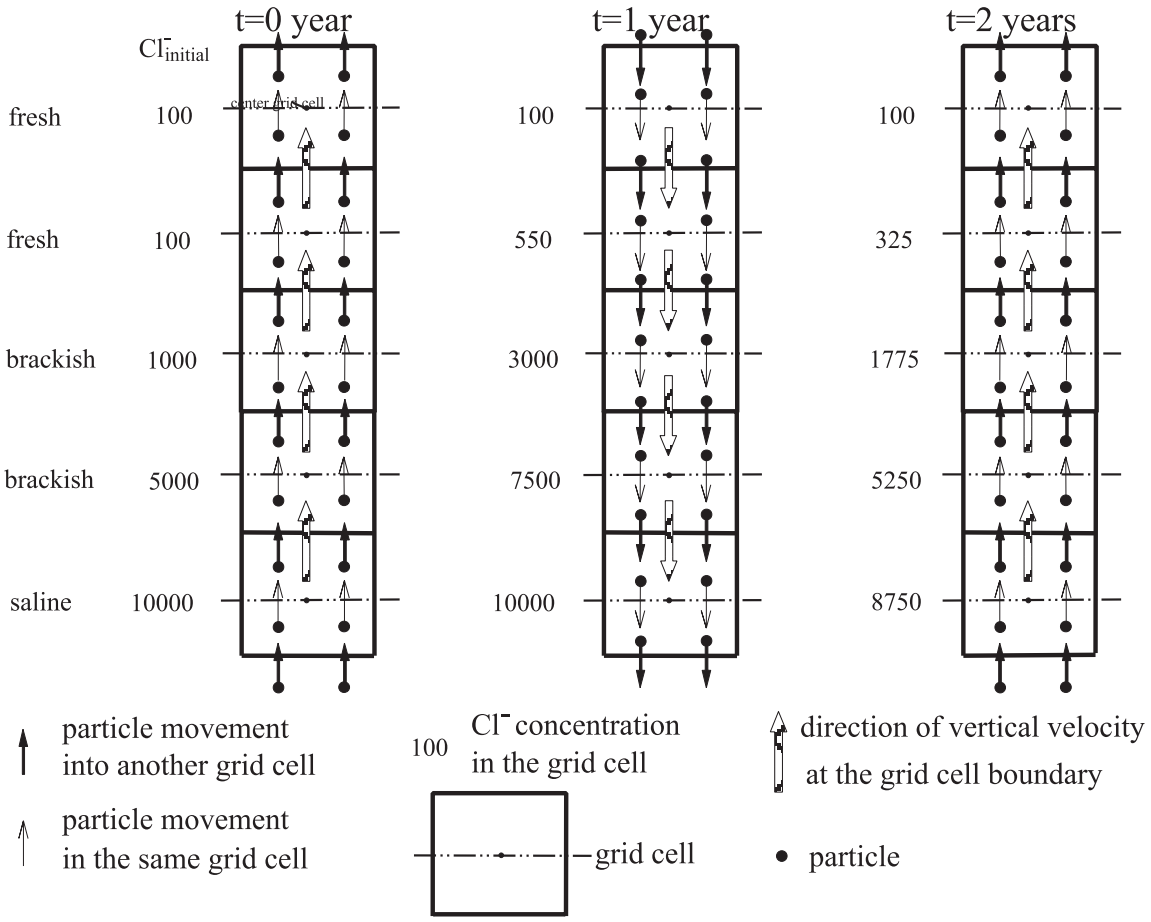

Figure 9.15: Schematisation showing how numerical instabilities due to density flow can occur. The solute and the flow time step have the same length of 1 *year*. Only the vertical groundwater flow is displayed. Because particles are moved to other grid cells, abrupt changes in solute concentration and thus in density in several grid cells can create fluctuations in vertical velocity.

groundwater is small or at places where surface water is injected with a density different from that of the original groundwater at that depth. It depends, among others, on the geometry of the hydrogeologic system whether the vertical velocities in the elements fluctuate in direction with approximately equally small amplitudes, or diverge to (unacceptable) strong amplitudes.

The causes of numerical instabilities in the velocity field due to density flow are closely connected with model and subsoil parameters. Numerical instabilities can be limited by adapting model parameters, such as by enlarging the number of particles per element, by shortening the length of the flow time step or smoothing the initial density differences in the vicinity of transition zones. Furthermore, by increasing the dispersivity, the numerical instabilities due to density flow can somewhat be reduced.

Parameters in MOC

In MOC, parameters are specified in the *input data file* to properly compute the freshwater head distribution, the solute concentration distribution and both horizontal and vertical velocities as a function of specific moments in time. They are subdivided into:

a. *model* parameters which determine the setup of the computation,

b. *subsoil* parameters which determine the geometry and hydrogeology of the schematised profile,

c. initial and boundary conditions.

ad a. Several model parameters are briefly discussed here, see for more information Oude Essink [1996]. In figure 9.16 the influence of different model parameters is illustrated with the model through the Gemeentewaterleidingen Amsterdam (see also figure 3.13 on page 41):

1. Number of elements

   MOC uses rectangular, block-centered elements, as the finite difference method is applied. Personal computers with only some Mb RAM can already accommodate a much larger number of elements than originally possible: e.g. 20,000=500·40 elements with 180,000 particles on a 8 Mb RAM computer instead of originally 400=20·20 elements with 3200 particles (in 1978), see also table 3.4, page 43.

   When vertical profiles are simulated, the number of elements in horizontal direction is usually greater than the number of elements in vertical direction. The ratio horizontal length Δx to vertical height Δz can range from 25 to 1 without numerical problems.

2. Number of particles

   In the original MOC code of 1978, 4, 5 and 9 particles per element could be inserted. Since June 1985, the computer code was adapted in order to specify 16 particles per element, as this could lead to an increase in numerical accuracy of the solution of the solute transport. Since August 1985, it is allowed to specify 1 particle per element in order to reduce the calculation time if input data files are only tested or if the interest is just focused on the groundwater flow equation.

3. Flow time step Δt

   After each flow time step, the buoyancy is deduced from the computed solute concentration, and a new freshwater head distribution as well as a new velocity field is calculated. The flow time step in the adapted MOC code should be chosen with care. The reason for this is that the groundwater flow equation depends on density differences, and thus the solute concentration also determines the solution. The salinity distribution changes after every solute time step Δt_s, while the velocity field is kept constant during that flow time step (see figure 9.17). It may happen that the salinity distribution changes so rapid during one flow time step (there is a number of solute time steps within one flow time step), that the velocity field does not closely match any more with the salinity distribution,

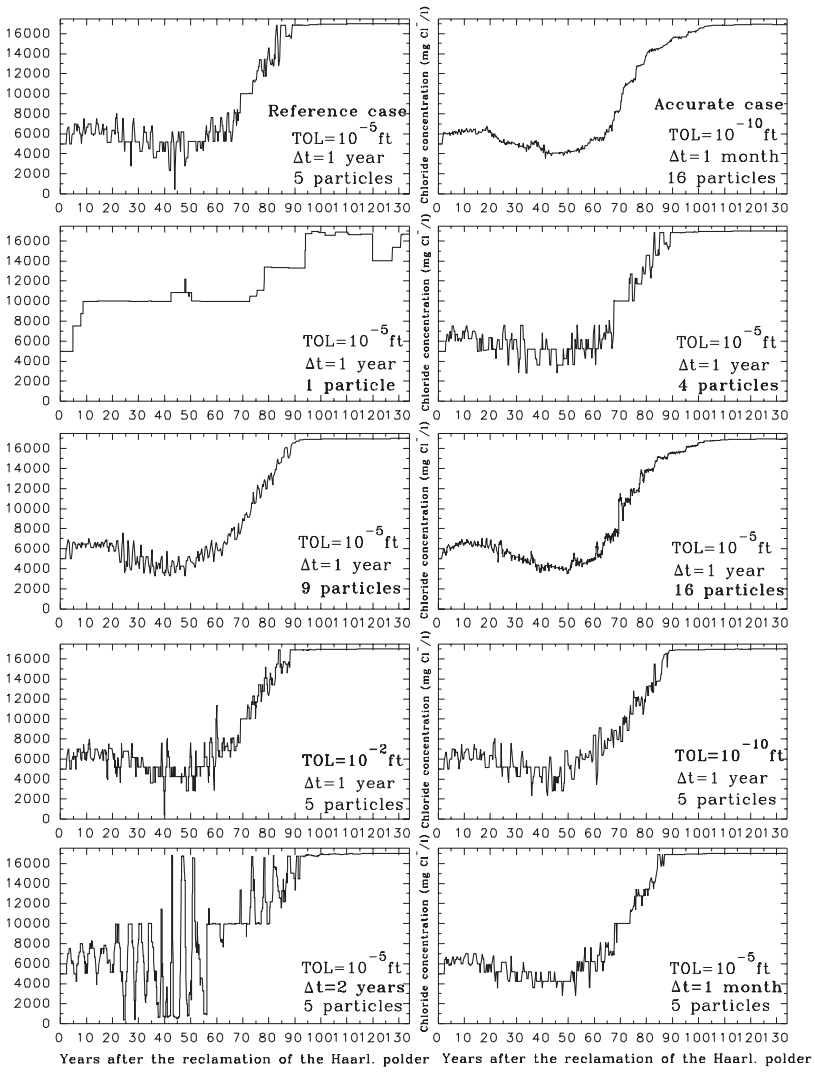

Figure 9.16: Chloride concentration as a function of time in the observation point at x=3475 m and z=-105 m *N.A.P.* The influence of different model parameters is shown.

and thus, with the current density. This could lead to numerical instabilities. In order to remedy this problem, the length of the flow time step should be shortened.

4. Convergence criterion TOL

   The convergence criterion TOL for the iterative calculation of the freshwater head in the groundwater flow equation is presented in ft. The criterion should range from about 10^{-4} to 10^{-6} ft, which seems to be rather strict. Nonetheless, the freshwater head should be given precisely, especially at the constant piezometric head boundaries of vertical profiles where hydrostatic conditions ought to apply. At those boundaries, small deviations in the fixed freshwater head could

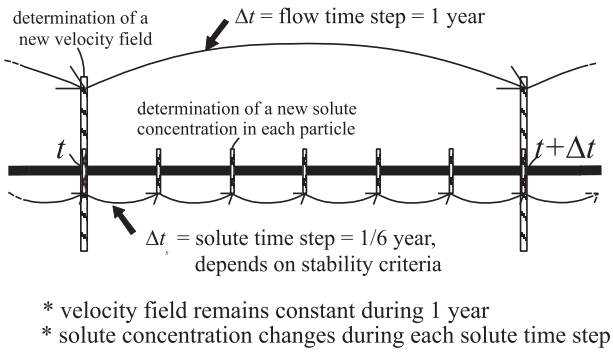

Figure 9.17: *Example of the relation between the flow time step and the solute time step.*

lead to significant (erroneous) velocities in vertical direction.

ad b. The conversion from the original *horizontal* code to the adapted *vertical* code has its effects on several subsoil parameters:

1. Saturated thickness of the aquifer

   As the adapted MOC code is applied, the saturated thickness b of the aquifer, which could vary spatially, represents the thickness of the aquifer *perpendicular* to the vertical profile. This parameter is set to the unit length of *one foot*, the so-called *stretched foot*. As a consequence, the hydraulic conductivity k_i corresponds with the transmissivities T_{ii} through:

   $$T_{ii} = bk_i \tag{9.87}$$

2. Specific storativity S_s

   The storage coefficient S which is applied in the original MOC code represents the specific storativity S_s in the adapted MOC code, as the saturated thickness b is equal to *one foot*: $S_s = S/1\ foot$. In some cases, it may occur that the time lag of solute transport is so great in relation to the time lag of groundwater flow that the transient component of groundwater flow can be neglected. As a consequence, the specific storativity S_s can be taken equal to zero. Note that a specific storativity S_s equal to zero significantly simplifies the calculations with the adapted MOC code.

The hydraulic resistance of aquitards, the extraction and injection wells, and the spatially varying (natural groundwater) recharge or discharge are simulated in the adapted MOC code by means of a conversion of certain subsoil parameters in the original MOC code. Discussion of these parameters goes beyond the scope of these lecture notes (for more information see Oude Essink [1996]).

ad c. The initial distribution of solute concentration of the entire hydrogeologic system must be known, as the density distribution is applied in the groundwater flow equation of

the adapted MOC code. The conversion from chloride concentration to density is given by equation 6.39.

Two different types of boundary conditions for the groundwater flow can be imposed in MOC:

- a *constant piezometric head* boundary, the so-called *Dirichlet problem*.
  As MOC computes freshwater heads, the constant piezometric head boundary has to be converted into a freshwater head boundary in case density differs from fresh groundwater (see equation 9.89).
- a *constant flow* boundary, the so-called *Neumann problem*.
  This type of boundary can be implemented in the adapted MOC code by means of two tools: (1) 'Extraction and infiltration' (e.g. lines of extraction and injection wells), and (2) 'Recharge and discharge' (e.g. natural groundwater recharge into the hydrogeologic system).

In the MOC code of 1989 an additional procedure is included to implement so-called *pumping periods* with different freshwater heads and salinity distributions during one complete simulation.

The density of groundwater

The density of groundwater should be considered to be a function of pressure, temperature of the fluid and concentration of dissolved solids. However, you must assure yourself whether or not the influence of pressure and the influence of temperature on the density is of minor importance with respect to the influence of dissolved solids concentration for the circumstances of your specific hydrogeologic system. Fortunately, this situation is true for many hydrogeologic systems. Under those circumstances, the density of groundwater can be related to the concentration of dissolved solids in the groundwater. For example, the conversion from chloride concentration to density, that can be applied in the adapted MOC code, is as follows:

$$\text{Equation of state:} \qquad \rho_{(i,j)} = \rho_f \cdot (1 + \frac{\rho_s - \rho_f}{\rho_f} \cdot \frac{C_{(i,j)}}{C_s}) \tag{9.88}$$

where

- $\rho_{(i,j)}$ = density of groundwater in element $[i,j]$ $(M\,L^{-3})$,
- ρ_f = reference density, usually the density of fresh groundwater (without dissolved solids) at mean subsoil temperature $(M\,L^{-3})$,
- ρ_s = density of saline groundwater at mean subsoil temperature $(M\,L^{-3})$,
- $(\rho_s - \rho_f)/\rho_f$ = relative density difference $(-)$,
- $C_{(i,j)}$ = chloride concentration or the so-called *chlorinity* in element $[i,j]$ $(mg\ Cl^-/l)$,
- C_s = reference chloride concentration $(mg\ Cl^-/l)$.

In equation 9.88, a linear relation exists between ρ_s and C_s. For more information, see section 6.1.8, page 81.

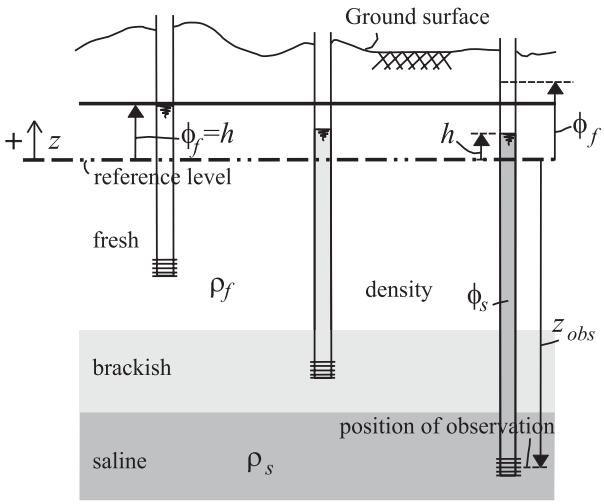

Figure 9.18: *Conversion from observed piezometric head to freshwater head.*

Conversion to freshwater head

As a non-uniform density distribution in the groundwater flow system is simulated with the adapted MOC code, the piezometric heads in fresh, brackish or saline groundwater must be converted into freshwater heads ϕ_f. The determination of the (fictive) freshwater head is as follows (see also figure 9.18):

$$\phi_f = (h - z_{obs})\frac{\rho_{obs}}{\rho_f} + z_{obs} \tag{9.89}$$

where

- ϕ_f = freshwater head of the observation well with respect to the reference level (L),
- h = observed piezometric head relative to the reference level (L),
- z_{obs} = elevation of the point of observation relative to the reference level (L),
- ρ_{obs} = density of the water column in the observation well ($M\,L^{-3}$).

For example, at a vertical boundary with a constant piezometric head the freshwater head configuration can be assessed assuming that no vertical groundwater movements occur. This means the situation is supposed to be *hydrostatic*. If the piezometric head in the upper element, $\phi_{f(i,2)}$[14], and the density distribution in vertical direction are known, the freshwater heads in all elements underneath the upper element in the same column can be determined. For each element at an increasing depth with respect to the reference level, e.g. *N.A.P.*, the freshwater head in the center of the element $[i, j]$ is as follows:

$$\phi_{f(i,j)} = \phi_{f(i,j-1)} + \Upsilon_{(i,j)}\Delta z \tag{9.90}$$

[14]MOC uses dummy elements around the finite difference grid, thus the upper row which participates has the index $j = 2$.

where

- $\phi_{f(i,j)}, \phi_{f(i,j-1)}$ = freshwater heads respectively in the elements $[i,j]$ and $[i,j-1]$ (L),
- $\Upsilon_{(i,j)}$ = relative density difference, the buoyancy between the elements $[i,j]$ and $[i,j+1]$ $(-)$, see equation 9.56.
- Δz = height of an element (L).

For more information on this computer code, see Konikow & Bredehoeft [1978] and Oude Essink [1996].

æ

Continuïteitsvergelijking: niet stationair

(uit: "Grondwatermechanica" [Verruijt, 1983])

In een afgesloten watervoerend pakket kan, alhoewel er geen freatisch (vrij) oppervlak is, toch enig water worden geborgen door expansie van de grond. Ruwweg gesproken: als de druk in het water toeneemt, dan neemt de gem. korrelspanning σ_k af. Hierdoor zal een vergroting van het poriënvolume optreden. In deze extra poriënruimte kan water worden geborgen. Door de beschouwingen te beperken tot de belangrijkste gevallen van niet-stationaire grondwaterstroming kan één en ander vereenvoudigd worden, waardoor de complexe vergelijkingen van deze zgn. consolidatietheorie behoorlijk simplificeren.

Volumeverandering ΔV van met water verzadigde grond wordt veroorzaakt door twee vormen van volumeverandering in de poriën: $\Delta V = \Delta V_1 + \Delta V_2$ (N.B.: samendrukbaarheid korrels te verwaarlozen):

- water uitzetten of comprimeren onder invloed van drukverandering Δp:

$$\Delta V_1 = -\beta V_w \Delta p$$

  waar

  - β=compressibiliteit of samendrukbaarheid van zuiver water (m^2/N): $\pm$ 0.5·10^{-9} m^2/N,
  - V_w=volume water=nV,
  - V=volume beschouwde grondelementje.

- verandering van hoeveelheid water in de poriën door netto stromingsverlies:

$$\Delta V_2 = -\left(\frac{\partial q_x}{\partial x} + \frac{\partial q_y}{\partial y} + \frac{\partial q_z}{\partial z} - Q^{'}\right) V \Delta t$$

  waar

  - $Q^{'}$=instroming per volume-eenheid, bijv. bron of put in het betreffende elementje ($1/T$),
  - Δt=beschouwde interval (T).

Combineren:

$$\frac{\Delta V}{V} = -n\beta\Delta p - \left(\frac{\partial q_x}{\partial x} + \frac{\partial q_y}{\partial y} + \frac{\partial q_z}{\partial z} - Q^{'}\right) \Delta t$$

Stel nu: dat $\frac{\Delta V}{V} = \Delta e$, waarin e de volumerek is. Met behulp van de wet van Darcy ($q = -k...$, enz.) wordt de vergelijking:

$$\frac{\partial e}{\partial t} = -n\beta\frac{\partial p}{\partial t} - \frac{k}{\rho g}\left(\frac{\partial^2 p}{\partial x^2} + \frac{\partial^2 p}{\partial y^2} + \frac{\partial^2 p}{\partial z^2}\right) + Q^{'}$$

Dit is de zgn. bergingsvergelijking.
Nu moet er een relatie worden gevonden tussen e en p, kijkend naar de vervorming van de grond. In sommige complexe gevallen wordt een ingewikkelde afleiding gebruikt die gebaseerd is op de 3D consolidatietheorie van Biot. Meestal gebruikt men echter een vereenvoudigde theorie (van Jacob en Terzaghi), dit is gebaseerd op vier min of meer redelijk lijkende aannamen:

1. in laag alleen vertikale deformaties (verandering in horizontale afmetingen te verwaarlozen t.o.v. vertikale):
$$e = \varepsilon_{zz}$$
2. zgn. korrelspanningsbegrip (Terzaghi): grondspanning=korrelspanning+waterdruk
$$\sigma_{gr} = \sigma_k + p$$
3. grondspanning constant, geen funktie van de tijd: spanningen worden voornamelijk veroorzaakt door gewicht bovenliggende lagen, hetgeen niet beïnvloed wordt door veranderingen in de grondwater randvoorwaarden:
$$\sigma_{gr} = \mathsf{const}, \qquad \frac{\partial \sigma_{gr}}{\partial t} = 0 \qquad \frac{\partial \sigma_k}{\partial t} + \frac{\partial p}{\partial t} = 0$$
4. lineair verband tussen vervorming en korrelspanning:
$$\varepsilon_{zz} = -\alpha \sigma_k$$

waar

- α=compressibiliteit van het korrelskelet (ook wel weergegeven in literatuur met m_v) (m^2/N):
- klei: 10^{-6}–10^{-8} m^2/N
- zand: 10^{-7}–10^{-9} m^2/N
- grind/gesteente met breuken: 10^{-8}–10^{-10} m^2/N
- massief gesteente: 10^{-9}–10^{-11} m^2/N
- water ($=\beta$): $4.4{\cdot}10^{-10}$ m^2/N ($\pm$ $0.5{\cdot}10^{-9}$ m^2/N)

Deze vergelijkingen combineren geeft:
$$\frac{\partial e}{\partial t} = \alpha \frac{\partial p}{\partial t}$$
Deze vergelijking combineren met de bergingsvergelijking en $\phi = z + \frac{p}{\rho g}$ geeft na enige omwerking:
$$S_s \frac{\partial \phi}{\partial t} = k \nabla^2 \phi + Q'$$

waar S_s=$\rho g(\alpha+n\beta)$= specifieke bergingscoefficient (L^{-1}): bijv. $5{\cdot}10^{-5}-5{\cdot}10^{-6}$ $1/m$. N.B.: $\alpha \gg n\beta$ als het zuiver water betreft, echter: als lucht in poriën, dan β vele malen groter. Als $S = S_s \cdot D$ (D=dikte van het watervoerend pakket en S=elastische bergingscoefficiënt ($-$), engels: storage coefficient); $T = k \cdot D$ (T=doorlaatvermogen van het watervoerend pakket (L^2/T) engels: transmissivity) en $Q^{'}D$ = instroming per dikte van het pakket (L/T), bijv. neerslag N (L/T) (!) dan:

$$S\frac{\partial \phi}{\partial t} = T\nabla^2\phi + N$$

- Specifieke bergingscoefficient S_s watervoerend pakket
  de verhouding tussen het volume water dat bij toe- of afname van de stijghoogte per eenheidsvolume watervoerend pakket extra wordt geborgen, resp. vrijkomt bij de betreffende stijghoogteverandering

$$S_s = (\alpha + n\beta)\rho g$$

- Elastische bergingscoefficient S afgesloten watervoerend pakket
  de verhouding tussen het volume water dat bij toe- of afname van de stijghoogte per eenheid van horizontale oppervlakte van het pakket extra wordt geborgen, resp. vrijkomt bij de betreffende stijghoogteverandering

$$S = S_s D$$

- Freatische bergingscoefficient μ freatisch watervoerend pakket
  de verhouding tussen het volume water dat bij toe- of afname van het freatisch vlak per eenheid van horizontale oppervlakte van het pakket extra wordt geborgen, resp. vrijkomt bij de betreffende verandering van het freatisch vlak

æ

References

Consulted literature

Althy, L.F. 1930. Density, porosity, and compaction of sediments. *Am. Ass. Petroleum Geol. Bull., 14, 1-24 p.*

Anderson, M.P. & Woessner, W.W. 1992. Applied groundwater modeling. Simulation of flow and advective transport. *Academy Press, Inc., San Diego. 381 p.*

Bear, J. 1972. Dynamics of fluids in Porous Media. *American Elsevier Publishing Company, Inc., New York. 764 p.*

Bear, J. 1979. Hydraulics of Groundwater. *McGraw-Hill Book Company, New York.*

Bear, J. & Verruijt, A. 1987. Modeling Groundwater Flow and Pollution. *D. Reidel Publishing Company, Dordrecht, the Netherlands. 414 p.*

Bethke, C. 1985. A numerical model of compaction-driven groundwater flow and heat transfer and its application to the paleohydrology of intracratonic sedimentary basins. *J. of Geophys. Res., 90B: 6817-6828.*

Boekelman, R.H. & Dijk, M.J., van. 1996. Geohydrologie, f15B. Lecture notes. (in Dutch). *Delft University of Technology, Faculty of Civil Engineering.*

Campbell, J.E., Longsine, D.E. & Reeves, M. 1981. Distributed velocity method of solving the convective-dispersion equation: 1. introduction, mathematical theory, and numerical implementation. *Adv. in Water Resour. 4: 102-108.*

Canter, L.W., Knox, R.C., Fairchild, D.M. 1987. Ground water quality protection. *Lewis Publishers, Inc., Michigan. 562 p.*

Carslaw, H.S. & Jaeger, J.C. 1959. Conduction of Heat in Solids. *Oxford University Press, London.*

CHO-TNO: Committee for Hydrological Research. 1986. Verklarende Hydrologische Woordenlijst. (in Dutch). *Rapporten en Nota's No. 16.*

Connor, J.J. & Brebbia, C.A. 1976. Finite element techniques for fluid flow. *Newnes-Butterwoths. 310 p.*

Cooper, H.H., jr., Kohout, F.A., Henry, H.R. & Glover, R.E. 1964. Sea water in coastal aquifers. *U.S.G.S. Water Supply Paper 1613-C, 84 p.*

CRC, Handbook of Chemistry and Physics. 1994. 75^{th} Edition. Lide, D.R. (ed). *Chemical Rubber Company Press, Boca Raton, Florida.*

Cotecchia, V., Fidelibus, M.D., Tadolini, T. & Tulipano, L. 1997. Karstic coastal aquifers. In: *Seawater intrusion into coastal aquifers. Guidlines for study, monitoring and control. Chapter 5, p. 57-66. Expert consultation on seawater intrusion into coastal aquifers in the Mediterranean Basin and the Near East, 10-13 Oct. 1993, Cairo, Egypt. Food and Agricultural Organization of the United Nations, Rome.*

Dam, J.C., van. 1976. Partial depletion of saline groundwater by seepage. *J. of Hydrol., 29: 315-339.*

Dam, J.C., van & Sikkema, P.C. 1982. Approximate solution of the problem of the shape of the interface in a semi-confined aquifer. *J. of Hydrol.,* **56***: 221-237.*

Dam, J.C., van. 1992. Geohydrology. Lecture notes. (in Dutch). *Delft University of Technology, Faculty of Civil Engineering, Section Hydrology, the Netherlands.*

Dam, J.C., van. 1993. Impact of sea-level rise on salt water intrusion in estuaries and aquifers. *Keynote lecture Session III of the International Workshop SEACHANGE'93: Sea Level Changes and their Consequences for Hydrology and Water Management. Noordwijkerhout, the Netherlands. April, 1993. UNESCO, IHP-IV Project H-2-2. pp. 49-60.*

Dam, J.C., van & Boekelman, R.H. 1996. Geohydrologisch Onderzoek, f15C. Lecture notes. (in Dutch). *Delft University of Technology, Faculty of Civil Engineering.*

Daus, A.D., Frind, E.O. & Sudicky, E.A. 1985. Comparative error analysis in finite element formulations of the advection-dispersion equation. *Adv. in Water Resour. 8: 86-95.*

Davis, S.N. & DeWiest, R.J.M. 1980. Hydrogeology. *John Wiley & Sons, New York. 463 p.*

Domenico, P.A. & Schwartz, F.W. 1998. Physical and Chemical Hydrogeology. *John Wiley & Sons, Inc. 506 p.*

Dooge, J.C.I. 1968. The hydrologic cycle as a closed system. *Bull. Int. Ass. Scient. Hydrol., 13 (1): 58-68.*

Eem, J.P., van der. 1987. Adaption Konikow-Bredehoeft for Density Differences. (in Dutch). *Interne notitie KIWA. Aug. 1987.*

Eem, J.P., van der. 1992. Rekenen aan de stroming van zoet, brak en zout grondwater. (in Dutch). *KIWA mededeling 121. 137 p.*

Eppink, L.A.A.J. 1993. Processes and models in erosion and soil and water conservation. Water erosion models: an overview. Lecture notes. *Wageningen.*

Fleming, G. 1979. Deterministic models in hydrology. *FAO Irrigation and Drainage Paper, no. 32.*

Frind, E.O. & Pinder, G.F. 1983. The principle direction technique for solution of the advection-dispersion equation. *Proc.* 10^{th} *IMACS World Congress on Systems Simulation and Scientific Computation, Concordia University, Montreal, Canada, Aug. 1982. pp. 305-313.*

Garder, A.O., Jr., Peaceman D.W. & Pozzi, A.L., Jr. 1964. Numerical calculation of multidimensional miscible displacement by the method of characteristics. *Soc. of Petroleum Eng. J., 4 (1): 26-36.*

Gelhar, L.W., Welty, C. & Rehfeldt, K.R. 1992. A Critical Review of Data on Field-Scale Dispersion in Aquifers. *Water Resour. Res., 28 (7): 1955-1974.*

Gerven, M.W., van & Lange, W.J., de. 1994. Experiences with the new variable density module of MLAEM in a well-defined test area. *Proc.* 13^{th} *Salt Water Intrusion Meeting, Cagliari, Italy, 5-10 June 1994. (in press).*

Goode, D.J. & Konikow, L.F. 1989. Modification of a method-of-characteristics solute-transport model to incorporate decay and equilibrium-controlled sorption or ion exchange. *U.S. Geological Survey Water-Resources Investigations Report 89-4030, Reston, Virginia.*

Haitjema, H.M. 1977. Numerical application of vortices to multiple fluid flow in porous media. *Delft Progress Report, Vol. 2: 237-248.*

Harbaugh, A.W. & McDonald, M.G. User's documentation for the U.S. Geological Survey modular finite-difference ground-water flow model, *U.S.G.S. Open-File Report 96-485, 56 p., 1996.*

Hassanizadeh, S.M., Mathematical modelling of hydro-geologic processes, lecture notes, *Utrecht University, Institute of Earth Sciences, 1997.*

Hassanizadeh, S.M. & T. Leijnse. 1988. On the modeling of brine transport in porous media. *Water Resour. Res., 24 (3): 321-330.*

Heide, P.K.M., van der & Boswinkel, J.A. 1982. The Fresh-saline Distribution of the Groundwater in the Netherlands. Part 2A. Theoretical Background. (in Dutch). *TNO Institute of Applied Geoscience.*

Heikens, D.L.J., Leeuwen, P.E.R.M., van & Bol, R. 1991. Komputermodellen in het waterbeheer. Het SAMWAT modellenbestand. (in Dutch). *Report no. 7.*

Heikens, D.L.J. 1995. Modelleren voor het waterbeheer. Lecture notes Delft University of Technology f15D. (in Dutch). *Nieuwegein. 25 p.*

Hemker, K. 1994. Hydrological models, f15D. Handouts. (in Dutch). *Delft University of Technology, Faculty of Civil Engineering.*

Hemker, C.J. & Elburg, H. van. 1988. Micro-fem. MicroComputer MultiLayer Steady State Finite Element GroundWater Modeling. Users's Manual, version 2.0. Amsterdam.

Holzbecher, E., Modeling density-driven flow in porous media, Principles, numerics, software, *Springer Verlag, Berlin Heidelberg, 286 p., 1998.*

Huyakorn, P.S. & Pinder, G.F., A pressure-enthalpy finite difference model for simulating hydrothermal reservoirs, *2nd Int. Symp. on Computer Meth. for Part. Diff. Eq. Lehigh Univ. Bethlehem, Pa., June 22-24, 1977.*

Huyakorn, P.S., Kretschek, A.G., Broome, R.W., Mercer, J.W. & Lester, B.H. 1984. Testing and validation of models for simulating solute transport in ground-water. Development, Evaluation, and Comparison of Benchmark Techniques. *International Ground Water Modeling Center, GWMI 84-13*

Huyakorn, P.S., Andersen, P.F., Mercer, J.W. & White, H.O., Jr. 1987. Saltwater Intrusion in Aquifers: Development and Testing of a Three-Dimensional Finite Element Model. *Water Resour. Res., 23 (2): 293-312.*

IGWMC. Ground-Water Software Catalog. Summer 1995. *International Ground Water Modeling Center. Colorado School of Mines, Golden, CO 80401-1887, USA.*

ILRI, International Institute for Land Reclamation and Improvement, *Veldboek voor Land- en Waterdeskundigen, (in Dutch), Wageningen, The Netherlands, 1972.*

INTERCOMP. 1976. A model for calculating effects of liquid waste disposal in deep saline aquifers. *Resource Development and Engineering, Inc. U.S.G.S. Water-Resources Investigations Report 76-96, 263 p.*

IWACO. 1987. SALINA. Computer code for a sharp salt/fresh water interface in a non steady groundwater flow system, developed by Consultants for Water & Environment IWACO Ltd.

Jensen, O.K. & Finlayson, B.A. 1978. Solution of the convection-diffusion equation using a moving coordinate system. *Second Int. Conf. on Finite Elements in Water Resour., Imperial College, London, July. pp. 4.21-4.32.*

Josselin de Jong, G., de. 1977. Review of vortex theory for multiple fluid flow. *Delft Progress Report, Vol. 2: 225-236.*

Kinzelbach, W.K.H. 1986. Groundwater Modelling. An introduction with sample programs in BASIC. *Developments in Water Science, 25. Elsevier Science Publishers, Amsterdam.*

Kinzelbach, W.K.H. 1987a. Numerische Methoden zur Modellierung des Transport von Schadstoffen im Grundwasser. (In German). *Schriftenreihe GWF Wasser-Abwasser. Band 21. R. Oldenbourg Verlag GmbH, Munchen.*

Kinzelbach, W.K.H. 1987b. Methods for the simulation of pollutant transport in ground water. A model comparison. In: *Proc. Solving Ground Water Problems With Models. Conference and Exposition. Vol. 1, Denver Colorado, USA, Feb. 1987. pp. 656-675.*

Kinzelbach, W.K.H. 1988. The random walk method in pollutant transport simulation. In: *Groundwater flow and quality modelling. Custodio et al. (eds), pp. 227-245. D. Reidel Publishing Company, Dordrecht, the Netherlands.*

Kipp, K.L. Jr. 1986. HST3D. A Computer Code for Simulation of Heat and Solute Transport in Three-dimensional Groundwater Flow Systems. *IGWMC, International Ground Water Modeling Center. U.S.G.S. Water-Resources Investigations Report 86-4095.*

Klemeš, V. 1986. Dilettantism in Hydrology: transition or destiny ? *Water Resour. Res., 22 (9): 177S-188S.*

Konikow, L.F. & Bredehoeft, J.D. 1978. Computer model of two-dimensional solute transport and dispersion in ground water. *U.S.G.S. Techniques of Water-Resources Investigations, Book 7, Chapter C2, 90 p.*

Konikow, L.F. & Bredehoeft, J.D. 1992. Ground-water models cannot be validated. *Adv. in Water Resour.* **15***: 75-83.*

Konikow, L.F., Goode, D.J. & Hornberger, G.Z. 1996. A three-dimensional method-of-characteristics solute-transport model (MOC3D); *U.S.G.S. Water-Resources Investigations Report 96-4267, 87 p.*

Kooiman, J.W. 1989. Modelling the salt-water intrusion in the dune water-catchment area of the Amsterdam Waterworks. *Proc.* 10^{th} *Salt Water Intrusion Meeting, Ghent, Belgium, May 1988. pp. 132-142.*

Kooiman, J.W., Peters, J.H. & Eem, J.P., van der. 1986. Upconing of brackish and salt water in the dune area of Amsterdam Waterworks and modelling with the Konikow-Bredehoeft program. *Proc.* 9^{th} *Salt Water Intrusion Meeting, Delft, the Netherlands, May 1986. pp. 343-359.*

Lange, W., de. 1996. Groundwater modeling of large domains with analytic elements. *Ph.D. thesis. Delft University of Technology. 237 p.*

Lantz, R.B. 1971. Quantitative Evaluation of Numerical Diffusion (Truncation Error). *Transactions AIME, Soc. of Petroleum Eng. J. 251: 315-320.*

Lebbe, L.C. 1981. The subterranean flow of fresh and salt water underneath the western Belgian Beach. *Proc.* 7^{th} *Salt Water Intrusion Meeting, Uppsala, Sweden, Sept. 1981. Sver. Geolog. Unders. Rap. Meddel.,* **27***, 193-219.*

Lebbe, L.C. 1983. Mathematical model of the evolution of the fresh-water lens under the dunes and beach with semi-diurnal tides. *Proc.* 8^{th} *Salt Water Intrusion Meeting, Bari, Italy. Geologia Applicata e Idrogeologia, Vol. XVIII, Parte II: 211-226.*

Lester, B. 1991. SWICHA. A Three-Dimensional Finite-Element Code for Analyzing Seawater Intrusion in Coastal Aquifers. *Version 5.05. GeoTrans, Inc., Sterling, Virginia, USA. IGWMC, International Ground Water Modeling Center, Delft, the Netherlands. 178 p.*

Liggett, J.A. & Liu, P.L-F. 1983. The boundary integral equation method for porous media flow. *George Allen & Unwin, London. 255 p.*

Maas, C. 1989. The origin of saline groundwater in the Netherlands. (in Dutch). Het vóórkomen van zout grondwater in Nederland. *H_2O (22), no. 7, 214-219.*

Maidment, D.R. (ed). 1993. Handbook of hydrology. *McGraw-Hill, Inc.*

Manning, C.E. & Ingebritsen, S.E., Permeability of the continental crust: implications of geothermal data and metamorphic systems, *Reviews of Geophysics,* **37***, no. 1, pp. 127-150, 1999.*

Marsily, G., de. 1986. Quantitative Hydrogeology. Groundwater Hydrology for Engineers. *Academic Press, Inc., Orlando, Florida. 440 p.*

McDonald, M.G. & Harbaugh, A.W. 1984. MODFLOW. A modular three-dimensional finite-difference ground-water flow model. *U.S.G.S. Open-File Report 83-875, 528 p.*

McDonald, M.G. & Harbaugh, A.W. 1988. A modular three-dimensional finite-difference ground-water flow model. *U.S.G.S. Techniques of Water-Resources Investigations, Book 6, Chapter A1, 586 p.*

Meinardi, C.R. 1973. The occurrence of brackish groundwater in the lower parts of the Netherlands. (in Dutch). Het zoutwatervoorkomen in de ondergrond van de lage gedeelten van Nederland. *H_2O (6), no. 18, 454-460.*

Ogata, A. & Banks, R.B. 1961. A solution of the differential equation of longitudinal dispersion in porous media. *United States Geological Survey, Professional Paper No. 411-A.*

OCV: Overleg Commissie Verkenningen. 1997. *Ruimte voor Aardwetenschappen. Toekomstverkenning Aardwetenschappelijk Onderzoek. Eindrapport. 152 p.*

Oude Essink, G.H.P. 1993. A sensitivity analysis of the adapted groundwater model MOC. *Proc.* 12^{th} *Salt Water Intrusion Meeting, Barcelona, Spain, Nov. 1992. pp. 407-420.*

Oude Essink, G.H.P. 1996. Impact of sea level rise on groundwater flow regimes. A sensitivity analysis for the Netherlands. *Ph.D. thesis. Delft University of Technology. 411 p.*

Oude Essink, G.H.P. & R.H. Boekelman. 1996. Problems with large-scale modelling of salt water intrusion in 3D. *Proc.* 14^{th} *Salt Water Intrusion Meeting, Malmö, Sweden, June 1996, 16-31.*

Oude Essink, G.H.P. 2000. Density Dependent Groundwater Flow: Salt Water Intrusion and Heat Transport. *Lecture notes Hydrological Transport Processes/Groundwater Modelling II, p. 120.*

Peaceman, D.W. 1977. Fundaments of numerical reservoir simulation. *Developments in Petroleum Science 6, Elsevier Scientific Publishing Company, Amsterdam.*

Peters, J.H. 1983. The movement of fresh water injected in salaquifers. *Proc. 8^{th} Salt Water Intrusion Meeting, Bari, Italy. Geologia Applicata e Idrogeologia. Vol. XVIII, Parte II: 145-155.*

Pinder, G.F. & Bredehoeft, J.D. 1968. Application of the Digital Computer for Aquifer Evaluation. *Water Resour. Res., 4 (***5***): 1069-1093.*

Pinder, G.F. & Gray, W.G. 1977. Finite element simulation in surface and subsurface hydrology. *Academy Press, Inc., New York. 295 p.*

Price, H.S., Varga, R.S. & Warren, J.E. 1966. Application of oscillation matrices to diffusion-convection equations. *J. Math. Phys. Cambridge Mass., 45, 301-311.*

Pulles, J.W. 1985. Policy Analysis for the Watermanagement in the Netherlands (PAWN). (in Dutch). Een beleidsanalyse van de waterhuishouding van Nederland. *Rijkswaterstaat, Hoofddirectie van de Waterstaat, Den Haag.*

Reilly, Th.E. 1990. Simulation of dispersion in layered coastal aquifer systems. *J. of Hydrol.,* **114***: 211-228.*

Sanford, W.E. & Konikow, L.F. 1985. A two-constituent solute-transport model for ground water having variable density. *U.S.G.S. Water-Resources Investigations Report 85-4279.*

Sauter, F.J., Leijnse, A. & Beusen, A.H.W. 1993. METROPOL. User's Guide. *Report number 725205.003. National Institute of Public Health and Environmental Protection. Bilthoven, the Netherlands.*

Scheidegger, A.E. 1961. General theory of dispersion in porous media. *J. of Geophys. Res., 66 (10): 3273-3278.*

Schulze-Makuch, D. & Cherkauer, D.S. Method developed for extrapolating scale behaviour, *EOS, 78 (1), Jan 7, 1997.*

Shamir, U. & Harleman, D.R.F. 1966. Numerical and analytical solutions of dispersion problems in homogeneous and layered aquifers. *M.I.T. Dept. Civil Eng., Hydrodynamics Lab. Rept. 89, May.*

Spaans, W. 1992. The groundwater system. Groundwater and numerical modelling. Additional lecture notes (f15B). *Delft University of Technology, Faculty of Civil Engineering.*

Sorey, M.L., Numerical modeling of liquid geothermal systems, *U.S. Geological Survey Prof. Pap. 16044-D, 1978.*

Souza, W.R. & Voss, C.I. 1987. Analysis of an anisotropic coastal aquifer system using variable-density flow and solute transport simulation. *J. of Hydrol.,* **92***: 17-41.*

Stelling, G.S. & Booij, N. 1996. Computational modelling in open channel hydraulics, b84. Lecture notes. *Delft University of Technology, Faculty of Civil Engineering.*

Strack, O.D.L. 1989. Groundwater Mechanics. *Prentice Hall, New Jersey, USA. 732 p.*

Strack, O.D.L. 1995. A Dupuit-Forcheimer model for three-dimensional flow with variable density. *Water Resour. Res., 31 (12): 3007-3017.*

Stuyfzand, P.J. 1986. Hydrochemistry and hydrology of dunes and adjacent polders between Zandvoort and Wijk aan Zee (map numbers 24F and 25A). (in Dutch). *KIWA SWE-86.016, 203 p.*

Stuyfzand, P.J. 1986b. A new hydrochemical classification of watertypes: principles and application to the coastal dunes aquifer system of the Netherlands. *Proc. 9^{th} Salt Water Intrusion Meeting, Delft, the Netherlands. pp. 641-655.*

Stuyfzand, P.J. 1988. Hydrochemistry and hydrology of dunes and adjacent polders between Noordwijk and Zandvoort aan Zee (map no. 24H and 25C). (in Dutch). *KIWA SWE-87.007, 343 p.*

Stuyfzand, P.J. 1991. Composition, genesis and quality variations of shallow groundwater in coastal dunes. (in Dutch). Samenstelling, genese en kwaliteitsvariaties van ondiep grondwater in kustduinen. *KIWA SWE-91.008, 175 p.*

Sudicky, E.A. 1989. The Laplace Transform Galerkin Technique: a time-continuous finite element theory and application to mass transport in groundwater. *Water Resour. Res., 25 (8): 1833-1846.*

Todd, D.K. 1980. Groundwater Hydrology. *John Wiley & Sons, New York.*

Trescott, P.C., Pinder, G.F. & Larson, S.P. 1976. Finite-difference model for aquifer simulation in two dimensions with results of numerical experiments. *U.S.G.S. Techniques of Water-Resources Investigations, Book 7, Chapter C1, 116 p.*

Uffink, G.J.M. 1990. Analysis of dispersion by the random walk method. *Ph.D. thesis. Delft University of Technology. 150 p.*

Ven Te Chow, Maidment, D.R. & Mays, L.W. 1988. Applied Hydrology. *McGraw-Hill Book Company, New York.*

Verruijt, A. 1970. Theory of Groundwater Flow. *Macmillan, London.*

Verruijt, A. 1980. The rotation of a vertical interface in a porous medium. *Water Resour. Res., 16 (1): 239-240.*

Verruijt, A. 1994. Numerical Geomechanics, b25. Lecture notes. *Delft University of Technology, Faculty of Civil Engineering.*

Volp, C. & Lambrechts, A.C.W. 1988. The SAMWAT database for computer models in water management. (in Dutch). *Report no. 2.*

Voss, C.I. 1984. SUTRA – A finite element simulation for saturated-unsaturated, fluid-density-dependent ground-water flow with energy transport or chemically reactive single-species solute transport. *U.S.G.S. Water-Resources Investigations Report 84-4369. 409 p.*

Voss, C.I. & Souza, W.R. 1987. Variable density flow and solute transport simulation of regional aquifers containing a narrow freshwater-saltwater transition zone. *Water Resour. Res., 23 (10): 1851-1866.*

Vries, M. de. 1977. Waterloopkundig onderzoek, b80. Lecture notes. (in Dutch). *Delft University of Technology, Faculty of Civil Engineering.*

Walraevens, K., Lebbe, L.C., *et al.* 1993. Salt/fresh-water flow and distribution in a cross-section at Oostduinkerke (Western Coastal Plain of Belgium). *Proc.* 12^{th} *Salt Water Intrusion Meeting, Barcelona, Spain, Nov. 1992. pp. 407-420.*

Ward, D.S. 1991. Data Input for SWIFT/386, version 2.50. *Geotrans Technical Report, Sterling, Va.*

Weast, R.C., Handbook of Chemistry and Physics, 63 rd ed., p. D261, *CRC Press, Boca Raton, Fla., 1982.*

Weiden, R.M., van der. 1988. Boundary integral equations for the computational modeling of three-dimensional steady groundwater flow problems. *Ph.D. thesis. Delft University of Technology. 253 p.*

Zoeteman, B.C.J. 1987. Soil pollution: an appeal for a new awareness of Earth's intoxication. In: *Vulnerability of soil and groundwater pollutants, pp. 17-27. Committee for Hydrological Research TNO. Proc. and Inform. No. 38.*

Zienkiewicz, O.C. 1971. The finite element method in engineering science. *McGraw-Hill, London. 521 p.*

Interesting textbooks

Ahlfeld, D.P. & Mulligan, A.E. 2000. Optimal management of flow in groundwater systems. *Academy Press, Inc., 185 p.*

Anderson, M.P. & Woessner, W.W. 1992. Applied groundwater modeling. Simulation of flow and advective transport. *Academy Press, Inc., San Diego, 381 p.*

Bear, J. 1972. Dynamics of fluids in Porous Media. *American Elsevier Publishing Company, Inc., New York, 764 p.*

Bear, J. & Verruijt, A. 1987. Modeling Groundwater Flow and Pollution. *D. Reidel Publishing Company, Dordrecht, the Netherlands, 414 p.*

Domenico, P.A. & Schwartz, F.W. 1998. Physical and Chemical Hydrogeology. *John Wiley & Sons, Inc. 506 p.*

Freeze, R.A. & Cherry, J.A. 1979. Groundwater, *Englewood Cliffs, N.J., Prentice Hall.*

Fetter, C.W. 1994. Applied Hydrogeology, *3rd ed. New York, Macmillan College.*

Huisman, L. 1972. Groundwater Recovery. *MacMillan Press, London.*

Kinzelbach, W.K.H. 1986. Groundwater Modelling. An introduction with sample programs in BASIC. *Developments in Water Science, 25. Elsevier Science Publishers, Amsterdam, p. 343.*

Maidment, D.R. (ed). 1993. Handbook of Hydrology. *McGraw-Hill, Inc.*

Marsily, G., de. 1986. Quantitative Hydrogeology. Groundwater Hydrology for Engineers, Academic Press, Inc., Orlando, Florida, p. 440.

Pinder, G.F. & Gray, W.G. 1977. Finite element simulation in surface and subsurface hydrology. *Academy Press, Inc., New York. 295 p.*

Strack, O.D.L. 1989. Groundwater Mechanics. *Prentice Hall, New Jersey, USA. 732 p.*

Todd, D.K. 1959. Groundwater Hydrology. *John Wiley & Sons, New York, p. 336.*

Ven Te Chow, Maidment, D.R. & Mays, L.W. 1988. Applied Hydrology. *McGraw-Hill Book Company, New York.*

Verruijt, A. 1970. Theory of Groundwater Flow. *Macmillan, London.*

Wang, H.F. & Anderson, M.P. 1982. Introduction to groundwater modeling, Finite difference and finite element methods, *Academy Press, Inc., 237 p.*

Distributors of computer codes

GeoTrans, Inc. *46050 Manekin Plaza, Suite 100, Sterling, Virginia 22170, USA. Fax: 1-703-444-1685. http://www.hsigeotrans.com/*

International Association of Hydrological Sciences. http://www.wlu.ca/˜wwwiahs/.

ITC. 1996. ILWIS. The Integrated Land and Water Information System. *International Institute for Aerospace Survey and Earth Sciences. Hengelosestraat 99, P.O. Box 6, 7500 AA Enschede, the Netherlands. Fax: 31-53-4874484. E-mail: ilwis@itc.nl; http://www.itc.nl.*

IGWMC. 1995. Ground-Water Software Catalog. Summer 1995. *International Ground Water Modeling Center. Colorado School of Mines, Golden, CO 80401-1887, USA. Fax: 1-303-273-3278; http://www.mines.edu/research/igwmc/.*

Scientific Software Group. 1996. Updated Product Guide. *P.O. Box 23041, Washington, D.C. 20026-3041, USA. Fax: 1-703-620-6793; http://www.scisoftware.com/.*

United States Geological Survey (U.S.G.S.). *Watstore Program Office, 437 National Center, Reston VA 22092, USA. Fax: 1-703-648-5295; http://water.usgs.gov/software/ground_water.html.*

Formula sheet for Groundwater Modellering I

$$\mathrm{Re} = \frac{\rho V R}{\mu} \qquad \text{(Reynolds number)}$$

$$\frac{\partial^2 \phi}{\partial x^2} + \frac{\partial^2 \phi}{\partial y^2} + \frac{\partial^2 \phi}{\partial z^2} = 0 \qquad \text{(Laplace equation)}$$

$$\phi_{i,j}^{n+1} = \frac{1}{4}\left(\phi_{i+1,j}^{n} + \phi_{i-1,j}^{n} + \phi_{i,j+1}^{n} + \phi_{i,j-1}^{n}\right) \qquad \text{(Jacobi iteration)}$$

$$\phi_{i,j}^{n+1} = \frac{1}{4}\left(\phi_{i+1,j}^{n} + \phi_{i-1,j}^{n+1} + \phi_{i,j+1}^{n} + \phi_{i,j-1}^{n+1}\right) \qquad \text{(Gauss-Seidel iteration)}$$

$$\phi_{i,j}^{n+1} = (1-\xi)\phi_{i,j}^{n} + \frac{\xi}{4}\left(\phi_{i+1,j}^{n} + \phi_{i-1,j}^{n+1} + \phi_{i,j+1}^{n} + \phi_{i,j-1}^{n+1}\right) \qquad \text{(Overrelaxation iteration)}$$

$$S\frac{\partial \phi}{\partial t} = T\nabla^2\phi + N \qquad S_s = (\alpha + n_e\beta)\rho g \qquad S = S_s D$$

$$S\frac{\partial \phi}{\partial t} = T\frac{\partial^2 \phi}{\partial x^2} \qquad \frac{T\Delta t}{S\Delta x^2} < 0.5$$

$$\phi_i^{t+\Delta t} = \phi_i^t + \frac{T\Delta t}{S\Delta x^2}\left(\phi_{i+1}^t - 2\phi_i^t + \phi_{i-1}^t\right) \qquad \text{(Explicit)}$$

$$\phi_{i+1}^{t+\Delta t} - \left(2 + \frac{S\Delta x^2}{T\Delta t}\right)\phi_i^{t+\Delta t} + \phi_{i-1}^{t+\Delta t} = -\frac{S\Delta x^2}{T\Delta t}\phi_i^t \qquad \text{(Implicit)}$$

$$\phi_{i+1}^{t+\Delta t} - \left(2 + 2\frac{S\Delta x^2}{T\Delta t}\right)\phi_i^{t+\Delta t} + \phi_{i-1}^{t+\Delta t} = -\frac{S\Delta x^2}{T\Delta t}\phi_i^t - \left(\phi_{i+1}^t - \left(2 - \frac{S\Delta x^2}{T\Delta t}\right)\phi_i^t + \phi_{i-1}^t\right) \qquad \text{(Crank-Nicolson)}$$

$$k_v = \frac{2k_1k_2}{k_1 + k_2} \qquad \text{(Harmonic mean)}$$

$$\frac{\kappa_e}{\rho' c'}\frac{\partial^2 T}{\partial x^2} - \frac{n_e \rho_f c_f}{\rho' c'} V \frac{\partial T}{\partial x} = \frac{\partial T}{\partial t} \qquad \text{(Heat transport)}$$

$$\kappa_e = n_e\kappa_f + (1-n_e)\kappa_s \qquad \rho' c' = n_e\rho_f c_f + (1-n_e)\rho_s c_s$$

$$i = \frac{I}{A} = -\frac{1}{\rho}\frac{\partial V}{\partial x} \qquad \Delta V = IR \qquad R = \rho\frac{\Delta l}{A}$$

$$\frac{D_x}{R_d}\frac{\partial^2 C}{\partial x^2} - \frac{V_x}{R_d}\frac{\partial C}{\partial x} - \lambda C = \frac{\partial C}{\partial t}$$

$$D_h = D + D_m \qquad D_L = \alpha_L |V| \qquad D_T = \alpha_T |V|$$

$$R_d = (1 + \frac{\rho_b}{n_e} K_d) \qquad (R_d\text{=retardation factor})$$

$$\lambda = \frac{\ln 2}{t_{1/2}} \qquad (\lambda\text{=decay rate; } t_{1/2}\text{=half-life time})$$

BIS=backwards in space: implicit; BIT=backwards in time: implicit
FIS=forwards in space: explicit; FIT=forwards in time: explicit
CIS=central in space: Crank-Nicolson

$$D\frac{C_{i+1}^k - 2C_i^k + C_{i-1}^k}{\Delta x^2} - V\frac{C_i^k - C_{i-1}^k}{\Delta x} = \frac{C_i^k - C_i^{k-1}}{\Delta t} \qquad \text{BIS and BIT}$$

$$D_{appearent} = D + D_{num}$$

$$D_{num} = V\frac{\Delta x}{2} + V^2\frac{\Delta t}{2} \qquad \text{BIS and BIT}$$

$$D_{num} = V^2\frac{\Delta t}{2} \qquad \text{CIS and BIT}$$

$$D_{num} = V\frac{\Delta x}{2} - V^2\frac{\Delta t}{2} \qquad \text{BIS and FIT}$$

von Neumann stability analysis:

$$V\frac{\Delta t}{\Delta x} + \frac{2D\Delta t}{\Delta x^2} \leq 1 \qquad \text{BIS and FIT}$$

$$\text{if } D_{appearent} = D - V\tfrac{\Delta x}{2} - V^2\tfrac{\Delta t}{2} \text{ then } \Delta t \leq \frac{2D}{V^2} \qquad \text{BIS and BIT}$$

MOC

$$\frac{\partial}{\partial x}\left(T_{xx}\frac{\partial \phi}{\partial x}\right)_{(i,j)}^k + \frac{\partial}{\partial y}\left(T_{yy}\frac{\partial \phi}{\partial y}\right)_{(i,j)}^k = S\left[\frac{\phi_{(i,j)}^k - \phi_{(i,j)}^{k-1}}{\Delta t}\right] + W_{(i,j)}^k$$

$$W_{(ij)}^k = N_{(ij)}^k + \frac{Q_{(ij)}^k}{\Delta x \Delta y} - \frac{k_z}{d}(P_{(ij)}^k - \phi_{(ij)}^k)$$

$$w_j = B_j - \frac{A_j C_{j-1}}{w_{j-1}} \qquad g_j = \frac{D_j - A_j g_{j-1}}{w_j} \qquad \phi_j = g_j - \frac{C_j \phi_{j+1}}{w_j} \qquad \text{(Thomas algorithm)}$$

Stability criteria:

1. $\Delta t_s \leq \min_{\text{(over grid)}}\left[\frac{0.5}{\frac{D_{xx}}{(\Delta x)^2} + \frac{D_{yy}}{(\Delta y)^2}}\right]$ 2. $\Delta t_s \leq \min_{\text{(over grid)}}\left[\frac{n_e\, b_{i,j}^k}{Q_{i,j}'^k}\right]$

3. $\Delta t_s \leq \frac{\zeta \Delta x}{(V_x)_{\max}} \qquad \Delta t_s \leq \frac{\zeta \Delta y}{(V_y)_{\max}}$

MODFLOW

$$\begin{gathered} CV_{i,j,k-1/2}\phi_{i,j,k-1}^m + CC_{i-1/2,j,k}\phi_{i-1,j,k}^m + CR_{i,j-1/2,k}\phi_{i,j-1,k}^m \\ +(-CV_{i,j,k-1/2} - CC_{i-1/2,j,k} - CR_{i,j-1/2,k} \\ -CR_{i,j+1/2,k} - CC_{i+1/2,j,k} - CV_{i,j,k+1/2} + HCOF_{i,j,k})\phi_{i,j,k}^m \\ +CR_{i,j+1/2,k}\phi_{i,j+1,k}^m + CC_{i+1/2,j,k}\phi_{i+1,j,k}^m + CV_{i,j,k+1/2}\phi_{i,j,k+1}^m \\ = RHS_{i,j,k} \end{gathered}$$

where:

- $HCOF_{i,j,k} = P_{i,j,k} - SC1_{i,j,k}/(t_m - t_{m-1})$,
  - $RHS_{i,j,k} = -Q_{i,j,k} - SC1_{i,j,k}\phi_{i,j,k}^{m-1}/(t_m - t_{m-1})$,
  - $SC1_{i,j,k} = SS_{i,j,k}\Delta r_j \Delta c_i \Delta v_k$.

External sources: $Q_{rch} = I_{i,j,k}\Delta r_j \Delta c_i \qquad Q_{eva} = EVTR\frac{\phi_{i,j,k} - EXEL}{EXDP}$

$Q_{dr} = C_{dr}\left(\phi_{i,j,k} - d_{i,j,k}\right) \qquad Q_{riv} = \frac{KLW\left(\phi_{riv} - \phi_{aquifer}\right)}{M} \qquad Q_{ghb} = C_{ghb}\left(\phi_{i,j,k}^{ext} - \phi_{i,j,k}\right)$

æ

Index

æ